

**ISOTHERMAL MICROWAVE BIOLOGY;  
CATALYSIS AND FERMENTATION**

**ALEXANDER JAMES STAVRINIDES**

Submitted in partial fulfilment of the requirements of  
**Liverpool John Moores University**  
for the degree of Doctor of Philosophy

**January 2012**

## ***Abstract.***

This thesis looks directly into the controversial subject of the microwave field effect by the production of a versatile prototype isothermal microwave reactor for the investigation of enzymatic and microbiological reactions. The observed results from the prototype reactor and experiments conducted conclude that there is a nonthermal, nonlinear response between the exposure microwave power and rate and yield of cellulose saccharification. The nature of the nonthermal response is controversial and may be dependent on the definition of “nonthermal,” leading to ambiguity of exact mechanism.

Enzymatic and microbial conversion of cellulosic material to ethanol is a highly desirable industrial process. Whether the demand is for the mitigation of climate change, political obligations or energy independence, the use of arable land for energy crops limits the available glucose carbon sources for conversion to bioproducts. To prevent this limitation, cellulose ( $\beta$ -1,4-linked glucose polymers) are touted as the “silver bullet” to prevent carbon exhaustion or impinging on food crops.

The technical constraint for the industrialization of cellulose based processing is the rate limitation in the cellulase enzymatic action on cellulose. The enzyme rate is limited by feedback cycles and limited mechanical freedom, therefore a relatively high enzyme concentration is required to speed up the process. To date, the associated enzyme production costs and infrastructure prevents bulk volume exploitation. Biomolecular advances (amino acid substitutions, recombination of expression vectors etc) have gone some way to increase either enzymatic rate or enzyme concentration. The work presented in this thesis differs by increasing the rate of the enzyme without molecular modification. Using a microwave field, the work presented shows that by separating the system into its base units, irradiation of the enzyme/substrate complex in an aqueous environment can increase both the initial enzyme rate and the saccharification yield without alteration of the temperature set point. This study shows that the rate increase is not proportional to the microwave field power. An optimal power in each study is either found or suggested. The results cited show that in the three systems (Endoglucanase and cellobiohydrolase with cellulose, endoglucanase and cellobiohydrolase and  $\beta$ -glucosidase with cellulose, and  $\beta$ -glucosidase with cellobiose) the initial rates can be increased by 201%, 65.5% and 69% respectively. In the total hydrolytic process (endoglucanase and cellobiohydrolase and  $\beta$ -glucosidase on a cellulose substrate) the final glucose yield was increased by 43% in comparison to the conventional thermal control reaction. This is shown in Figure 1.

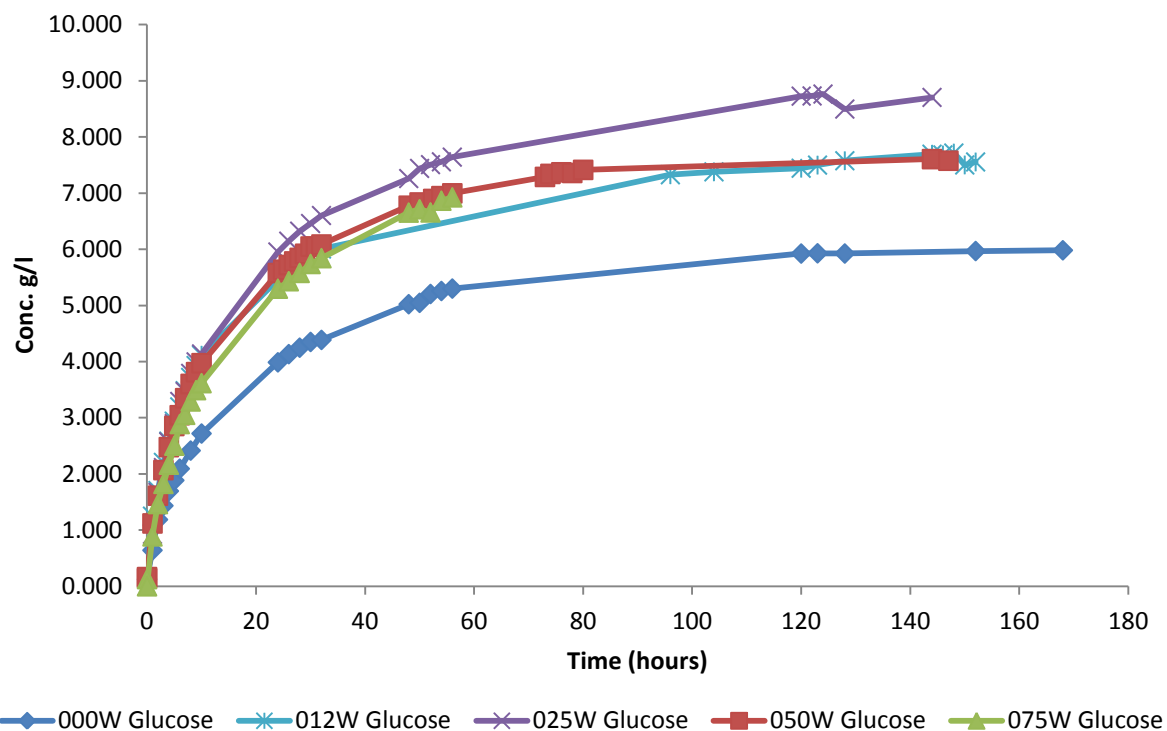


**Figure 1. Microwave irradiated "cellulase" enzymes with cellulose substrate**

For development into an industrial system and looking towards simultaneous saccharification and fermentation (SSF), the yeast *Saccharomyces cerevisiae* was subjected to irradiated microwave fermentations on a glucose substrate. Although inconclusive in terms of rate increase, cell density was comparable across the power range showing that the irradiation does not have a derogatory effect. The natural evolution of the conclusions drawn would be development of the system into a SSF or SSCF configuration for bio-product formation is possible with irradiation up to 50W.

The novelty of the experiments conducted is twofold. Firstly, the reactor has been designed to ensure that the microwave irradiation is independent of the bulk temperature therefore allowing the exploration of the microwave field effect independently to the thermal effect. Secondly, the microwave source is a continuous microwave irradiation (none pulse irradiation) ensuring that the reaction is subjected to the microwave field for the entire reaction.

## **Declaration**

This is to certify that;

1. The thesis comprises only of my original work towards the Ph.D. except where indicated
2. Due acknowledgment has been made in the text to all other material used
3. The thesis is less than 80,000 words in length, exclusive of tables, maps, bibliographies, appendices and footnotes

---

**Alexander James Stavrinos**

## **Acknowledgements**

The author would like to thank Liverpool John Moores University for the opportunity and financial support to conduct the following research.

I have been supported by a PhD supervision team of Professor Ahmed Al'shamma'a, Professor David A. Phipps, Dr. Montserrat Ortoneda-Pedrola, and Dr. Andrew Shaw, whom have made varying contributions in the development of hypothesis and aid of technical expertise. In development and advice in the theory behind the molecular mechanisms and detailed and critical review of the scientific principles, I would like to thank Dr. Phil Riby and Dr. Glyn Hobbs. In the development and production of the prototype microwave bioreactor, I have been aided by Mr. Steve Moran, Dr. Steve Wylie and Dr. Jeff Cullen for fabrication or advice.

For the completion of the written aspects, in addition to my supervision team, I have been aided by Mrs. Virginia Wigan and Mr. Andreas Stavrinides for grammatical accuracy and a non-scientific critical eye. They have also significantly aided me in overcoming my dyslexia. Thank you to all of the professional and industrial contacts that I have made and liaised with over the course of this project

My final acknowledgement is to my wife, Anna Stavrinides for her support throughout the project.

## Abbreviations

|                    |   |                    |  |
|--------------------|---|--------------------|--|
| Å                  | Angstrom  | LHW                | Liquid hot water   |
| ADH                | alcohol dehydrogenase   | LiP                | Lignin peroxidase  |
| AdoHcy             | S-adenosylhomocysteine hydrolase                                      | LJMU               | Liverpool John Moores University                                 |
| AFEX               | Ammonia fibre explosion   | LMEs               | lignin-modifying enzymes   |
| AO                 | aryl-alcohol  | LSU                | Louisiana State University                                       |
| ATP                | Adenosine-5'-triphosphate   | MCC                | Microcrystalline cellulose                                       |
| BEAN               | Built Environment and Natural Environment                             | MEC                | Microwave enhanced chemistry                                     |
|                    |   | MnP                | Manganese dependant peroxidase                                   |
| BEST               | Built Environment and Sustainable Technology (School of)              | MSW                | Municipal solid wastes   |
|                    |   | MTA                | 5'-methylthioadenosine phosphorlyase                             |
| BMCC               | Bacterial microcrystalline cellulose                                  | MW                 | Microwave  |
| BGL                | $\beta$ -glucosidase  | NC-E               | Negative control – Enzyme  |
| CBD                | Cellulose binding domain  | NC-MW              | Negative control – Microwave                                     |
| CBEL               | Cellulose-binding elicitor lectin                                     | NC-S               | Negative control – Substrate                                     |
| CBH                | Cellobiohydrolase   | NREL               | National Renewable Energy Laboratory (USA)                       |
| CBU                | Cellobiase units  | OD                 | Optical density  |
| CBP                | Consolidated BioProcessing  | ORNEL              | Oak Ridge National Energy Laboratory                             |
| CDH                | cellobiose dehydrogenase  |                    |  |
| CEM                | a Chemist, an Electrical engineer and a Mechanical engineer (company) | [P]                | Product concentration  |
|                    |   | PASC               | Phosphoric acid swollen  |
| CESA               | Cellulose synthase  | PEP                | Phosphoenolpyruvate  |
| CFU                | Colony forming units  | PERA               | The Production Engineering Research Association of Great Britain |
| CHP                | Combined Heat and Power   | PDC                | pyruvate decarboxylase   |
| CMB                | Cosmic microwave background   | PDC-ADH            | Pyruvate decarboxylase-alcohol dehydrogenase                     |
| CSC                | Cellulose synthase complex  | PEG                | Polyethylene glycol  |
| CSL                | Corn Steep Liquor   | PFK                | phosphofructokinase  |
| dBm                | Decibel   | PGI                | phosphoglucose isomerase   |
| DCW                | Dry cell waste  | PG                 | phosphoglycerate kinase  |
| DP                 | Degree Polymerisation   | pNPGU              | p-Nitrophenyl- $\beta$ -D-glucoside                              |
| [E]                | Enzyme concentration  | PY                 | pyruvate kinase  |
| EC <i>n.n.n.n.</i> | Enzyme commission number  | PWM                | Pulse width modulation   |
| ED                 | Entner-Doudoroff  | RasMol             | (Program) <b>R</b> aster <b>M</b> olecules                       |
| EGL                | Endoglucanase   | RF                 | Radio frequency  |
| EH                 | Enzyme hydrolysis   | RFM                | Radio Frequency and Microwave group (LJMU)                       |
| EMP                | Embden-Meyerhof-Parnas  |                    |  |
| <i>ENO</i>         | enolase   | RLK                | Receptor like kinases  |
| EP                 | Experimental Package  | RMS                | Root mean square   |
| EV                 | Electric vehicle  | RSE                | Relative standard error  |
| FBA                | fructose-1, 6-bisphosphate aldolase                                   | [S]                | Substrate concentration  |
| FBP                | fructose-1, 6-bisphosphatase  | SAR                | Specific absorption rate   |
| FPU                | Filter paper units  | SC-CO <sub>2</sub> | Supercritical carbon dioxide                                     |
| GARS               | GERI Annual Research Symposium  | SHF                | Separate hydrolysis and fermentation species                     |
| GERI               | General Engineering Research Institute                                | Spp.               | Simultaneous saccharification and co-fermentation                |
| GHG                | Green House Gas   | SSCF               | Simultaneous saccharification and fermentation                   |
| GLK                | glucokinase   |                    |  |
| GLOX               | glyoxal oxidase   | SSF                | Simultaneous saccharification and fermentation                   |
| GPD + GUT2         | glycerol-3-phosphate dehydrogenase                                    | SuSy               | Sucrose synthase   |
| GPM                | glycerolphosphate mutase  | TMV                | Tobacco mosaic virus   |
| GPP1, HOR2         | glycerol-3-phosphatase  | TPI                | triphosphate isomerase   |
| GPS                | Global positioning satellite  | TSB                | Technology Strategy Board  |
| GRAS               | Generally Regarded As Safe  | TWT                | Travelling Wave Tube   |
| GT                 | glycosyltransferases  | U/I                | User interface   |
| GUT1               | glycerol kinase   | VAN                | Vanillin   |
| HERI               | UK Health and Environmental Research Institute                        | WAK                | Wall associated kinases  |
|                    |   | UDP                | Uridine 5'-diphosphate   |
| HFSS               | High Frequency Structural Simulator                                   | VP                 | versatile peroxidase   |
| HMF                | 5-hydroxymethylfurfural   | VPN                | Virtual Private Network  |
| HXK                | hexokinase  | WHO                | World Health Organisation  |
| HPLC               | High Performance Liquid Chromatography                                | XDH                | Xylitol dehydrogenase  |
|                    |   | XK                 | Xylulosekinase   |
| HSP                | Heat shock proteins   | XR                 | Xylose reductase   |
| ISM                | Industrial, Scientific and Medicinal frequencies                      |                    |  |
| ITU                | International Telecommunications Union                                |                    |  |
| KGPG               | 2-keto-3-deoxy-6-phosphogluconate                                     |                    |  |
| K                  | Kelvin  |                    |  |
| K <sub>L</sub>     | mass transfer coefficient   |                    |  |
| K <sub>1,a</sub>   | volumetric mass transfer coefficient                                  |                    |  |
| LAP                | Laboratory protocol   |                    |  |
| Lcc                | Laccase   |                    |  |

Italicised abbreviations highlight gene code identification

## Units of measurement

All units of measurement are either in SI units or derived from SI units.

| Unit                 | Symbol | Definition  |                   |
|----------------------|--------|---|-------------------|
| <b>Power</b>         | W      | Watts   | Joules per second |
|                      | dBm    | Power ratio in decibels (used where original work has been quoted in dBm) |                   |
| <b>Frequency</b>     | Hz     | Hertz   | Cycles per second |
| <b>Concentration</b> | [x]    | Mass of reagent per unit volume   | g/l               |

## Figures

|  |    |
|--|----|
| Figure 1. Microwave irradiated "cellulase" enzymes with cellulose substrate .....  | ii |
| Figure 2. Thesis construction.....   | 8  |
| Figure 3. Simplified illustration of carbon transformation (Renewable vs. non-renewable).....  | 12 |
| Figure 4. Block diagram of bioproduct formation from biomass .....   | 15 |
| Figure 5. Conversion of solar energy to biofuels through biological means .....  | 16 |
| Figure 6. From sunlight and CO <sub>2</sub> to bioproducts.....  | 17 |
| Figure 7. Lignin proximity to cellulose fibre.....   | 18 |
| Figure 8. Three dimensional microstructure of plant cell walls. ....   | 19 |
| Figure 9. Amorphous and crystalline morphology of cellulose fibres.....  | 20 |
| Figure 10. Aldehyde and ketone functional groups .....   | 24 |
| Figure 11. Biological degradation of biomass .....   | 28 |
| Figure 12. A simplified model of the plant cell wall and its loosening by indigenous expansins. ....   | 30 |
| Figure 13. Cellulose degradation through the use of enzyme cocktails and gene expression feedback. .   | 32 |
| Figure 14. RASMOL image of CE112A. ....  | 35 |
| Figure 15. Cellobiohydrolase II in complex with cellulose .....  | 36 |
| Figure 16. CBH processing .....  | 37 |
| Figure 17. CBM of a CBH family 1 in complex with cellulose .....   | 38 |
| Figure 18. Alternative mechanism of CBM behaviour.....   | 39 |
| Figure 19. Orientation and spacing of CBM-CD linker sequence .....   | 40 |
| Figure 20. Proposed Cel7A progression as hypothesised by Zhao <i>et. el.</i> .....   | 41 |
| Figure 21. Catalytic domain of CBHI in complex with cello oligomer.....  | 41 |
| Figure 22. RASMOL images of Cel7A catalytic domain. ....   | 42 |
| Figure 23. Water ingress into the cellulose cleft in fibre lifting .....   | 43 |
| Figure 24. Comparison on Michaelis Menten and proposed minimal theoretical model .....   | 45 |
| Figure 25. Physical catalysis constraints .....  | 47 |
| Figure 26. Mechanistic hydrolysis of cellulose by CBH .....  | 48 |
| Figure 27. Bioproduct processing train. ....   | 49 |
| Figure 28. From Upstream to downstream processing in a biomass based biorefinery.....  | 51 |
| Figure 29. Comparative overview of four cellulosic ethanol processing methods. ....  | 51 |
| Figure 30. Schematic representation of Separate Hydrolysis and Fermentation .....  | 52 |
| Figure 31. Schematic of Simultaneous Saccharification and Fermentation .....   | 54 |
| Figure 32. Schematic of Simultaneous Saccharification and Co-Fermentation (SSCF).....  | 55 |
| Figure 33. Schematic of Consolidated Bioprocessing (CBP) fermentation.....   | 56 |
| Figure 34. Conceptual scheme of consolidated bioprocessing .....   | 57 |
| Figure 35. Establishment of evolutionary relationship between <i>Saccharomyces</i> species <i>S. uvarum</i> , <i>S. cerevisiae</i> , <i>S. paradoxus</i> , <i>S. bayanus</i> and <i>S. pastorianus</i> ..... | 62 |
| Figure 36. Glycolysis and gluconeogenesis.....   | 64 |
| Figure 37. Pathways for the formation of products of a mixed acid and 2,3-butanediol fermentations ..  | 66 |
| Figure 38. Magnetrons - original 1940 Randall and Boot and a modern counterpart.....   | 68 |

|   |     |
|---|-----|
| Figure 39. The electromagnetic spectrum ( $3 \times 10^1$ to $>3 \times 10^{24}$ ).....                                 | 69  |
| Figure 40. Typical microwave equipment.....   | 70  |
| Figure 41. Continuous microwave (CW) vs. pulsed power with the same energy (the same time-average power).....           | 72  |
| Figure 42. Microwave power, reaction temperature and pressure using a CEM Explorer.....                                 | 74  |
| Figure 43. Monomode and multimode cavity principles.....  | 75  |
| Figure 44. Chronological order of key microwave developments.....   | 76  |
| Figure 45. Modern horn antenna.....   | 77  |
| Figure 46. Research microwave reactors.....   | 78  |
| Figure 47. Industrial microwave reactor.....  | 78  |
| Figure 48. Dielectric excitation of water molecules.....  | 78  |
| Figure 49. Comparison of microwave irradiation-free hydrolysis and intermittently treated by microwave irradiation..... | 86  |
| Figure 50. Suggested rate and temperature profiles for work conducted by Zhu <i>et. al.</i> ....                        | 87  |
| Figure 51. Effect of varying power and frequency settings on the microwave response.....                                | 88  |
| Figure 52. Experiment design by major unit tasks.....   | 96  |
| Figure 53. Microwave reaction vessel design.....  | 99  |
| Figure 54. Benchtop research bioreactor.....  | 100 |
| Figure 55. Simplified schematic of microwave bioreactor.....  | 101 |
| Figure 56. Microwave generators.....  | 103 |
| Figure 57. Sairem microwave generator user interface.....   | 103 |
| Figure 58. Schematic of prototype system.....   | 105 |
| Figure 59. Complete system overview.....  | 106 |
| Figure 60. Microwave bioreactor.....  | 107 |
| Figure 61. Microwave bioreactor (Profile view).....   | 108 |
| Figure 62. Submerged elements of the STR.....   | 109 |
| Figure 63. Experimental Package 2. Enzymatic catalysis in a microwave field.....  | 113 |
| Figure 64. Experimental Package 3. Fermentation.....  | 113 |
| Figure 65. Proposed Experimental packages 4 and 5. Cellulytic fermentation.....   | 114 |
| Figure 66. Example standard curves.....   | 121 |
| Figure 67. EGL, CBHI, CBHII and BGL degradation of cellulosic material.....   | 123 |
| Figure 68. Contextualised illustration of Experimental Package 2.1 -2.3.....  | 124 |
| Figure 69. Example of a REZEX ROA HPLC Chromatogram.....  | 124 |
| Figure 70. Calculation of cell density through the use of a haemocytometer.....   | 135 |
| Figure 71. Sampling time frames for the microwave negative control.....   | 137 |
| Figure 72. Heating profiles of the microwave bioreactor under different microwave powers.....                           | 146 |
| Figure 73. Microwave power in relation to heating rate.....   | 147 |
| Figure 74. Section of thermal profile from experimental data.....   | 149 |
| Figure 75. Thermal image of reactor in operation.....   | 150 |
| Figure 76. Enzymatic hydrolysis (CBH/EGL on cellulose) in the absence of microwave irradiation (NC-MW).....             | 152 |
| Figure 77. Enzymatic hydrolysis (CBH/EGL +BGL on cellulose) in the absence of microwave irradiation (NC-MW).....        | 154 |
| Figure 78. Comparison of percentage saccharification with EGL/CBH and EGL/CBH/BGL.....                                  | 155 |
| Figure 79. Cellobiose catalysis with BGL - Initial and repeated values for glucose and cellobiose.....                  | 156 |
| Figure 80. Overlay of HPLC traces for 33 hour exposure of alpha-cellulose in 100W microwave field.....                  | 158 |
| Figure 81. Determination of enzyme activity after microwave exposure determined by a modified NREL/TP-510-42628.....    | 159 |
| Figure 82. Glucose production in varying microwave power (full plot).....   | 161 |
| Figure 83. Cellobiose production in varying microwave power (full plot).....  | 162 |
| Figure 84. Comparison of microwave power rates to MW-NC.....  | 163 |

|   |     |
|---|-----|
| Figure 85. Initial rates for glucose and cellobiose production in varying microwave power .....   | 164 |
| Figure 86. Summary of results – Percentage saccharification by microwave irradiation (+EGL/CBH - BGL).....                                      | 165 |
| Figure 87. Percentage difference in initial rates to MW-NC .....  | 166 |
| Figure 88. Percentage saccharification against microwave power based on initial rates.....  | 167 |
| Figure 89. Initial rates for EGL/CBH -BGL on cellulose with variable microwave irradiation (Constituents and percentage saccharification) ..... | 168 |
| Figure 90. Glucose:Cellobiose ratio in comparison to Vanillin concentration .....   | 170 |
| Figure 91. Glucose production at substrate loadings of 10g/l and 50g/l cellobiose at 50W and NC-MW at 10g/l.....                                | 172 |
| Figure 92. Cellobiose production at substrate loadings of 10g/l and 50g/l cellobiose at 50W and MW-NC at 10g/l .....                            | 173 |
| Figure 93. Initial rates for glucose production at substrate loadings of 10g/l and 50g/l cellobiose with 50W and NC-MW at 10g/l .....           | 174 |
| Figure 94. Comparison of 10g/l and 50g/l substrate loading with 50W irradiation by initial rates of percentage saccharification.....            | 175 |
| Figure 95. Percentage difference in initial rates of 10g/l and 50g/l at 50W to 10g/l MW-NC.....   | 176 |
| Figure 96. Glucose production in varying microwave power (full plot) .....  | 177 |
| Figure 97. Cellobiose production in varying microwave power (full plot) .....   | 178 |
| Figure 98. Initial rates for Glucose production in varying microwave power .....  | 179 |
| Figure 99. Percentage saccharification of cellulose with EGL, CBH and BGL with variable microwave irradiation (EGL/CBH/BGL).....                | 179 |
| Figure 100. Curve fit data for CBH/EGL/BGL catalysis of cellulose with microwave irradiation .....  | 180 |
| Figure 101. Percentage difference in initial rates .....  | 181 |
| Figure 102. Percentage saccharification rate against microwave power .....  | 182 |
| Figure 103. 50W comparison of EGL/CBH -BGL and EGL/CBH +BGL.....  | 184 |
| Figure 104. Glucose evolution through the hydrolysis of cellobiose by BGL with variable microwave irradiation .....                             | 185 |
| Figure 105. Cellobiose degradation through the hydrolysis of cellobiose by BGL with variable microwave irradiation.....                         | 186 |
| Figure 106. Percentage difference in initial rates .....  | 187 |
| Figure 107. Glucose evolution rate against microwave power.....   | 187 |
| Figure 108. Light microscope determination of cell density .....  | 189 |
| Figure 109. Relating optical density to cell density.....   | 190 |
| Figure 110. Fermentation profiling by pH, gas exchange and temperature.....   | 191 |
| Figure 111. Fermentation negative control. Profile by glucose, ethanol and optical density .....  | 191 |
| Figure 112. Comparison on ethanol production with no irradiation in repeat data sets and fit modelling .....                                    | 192 |
| Figure 113. Optical density under varying microwave power against time .....  | 195 |
| Figure 114. Change in optical density during exponential growth. ....   | 195 |
| Figure 115. Percentage difference to thermal negative control .....   | 196 |
| Figure 116. Data plot of glucose uptake with varying microwave irradiation.....   | 197 |
| Figure 117. Glucose uptake - curve fit .....  | 197 |
| Figure 118. Glucose uptake rate - gradient determination.....   | 198 |
| Figure 119. Percentage difference to thermal negative control .....   | 199 |
| Figure 120. Ethanol formation under varying microwave powers (raw data) .....   | 200 |
| Figure 121. Ethanol formation under varying microwave powers (curve fitting) .....  | 201 |
| Figure 122. Ethanol formation rate.....   | 201 |
| Figure 123. Ethanol production rate as percentage of MW-NC against microwave power .....  | 202 |
| Figure 124. Comparison of fermentation indicators by rate .....   | 203 |
| Figure 125. Alternative method of direct microwave launching .....  | 209 |
| Figure 126. Illustration of localised heat distribution versus thermal bulk recording .....   | 218 |

## Tables

|   |     |
|---|-----|
| Table 1. Biofuel production estimations/targets for the USA and EU by directive .....   | 11  |
| Table 2. Biofuel technology generations .....   | 12  |
| Table 3. Cellulose polymorphs .....   | 19  |
| Table 4. Hemicellulose subunits.....  | 21  |
| Table 5. Plant sugar subunits.....  | 22  |
| Table 6. Lignin degrading enzymes and mediator compounds. ....  | 29  |
| Table 7. Three key enzymes in cellulose depolymerisation .....  | 31  |
| Table 8. Enzyme accession numbers of previously described CAZymes that occur in clustered area....  | 33  |
| Table 9. CBH structures .....   | 36  |
| Table 10. Progression of cellulase action .....   | 37  |
| Table 11. Comparison of Consolidated Bioprocessing methods. ....  | 56  |
| Table 12. Comparisons of enzymatic hydrolysis and fermentation process configurations .....   | 59  |
| Table 13. Kinetic parameters for <i>Zymomonas mobilis</i> and <i>Saccharomyces uvarum</i> on 250g/L-1 glucose media in non-aerated batch culture (30°C, pH 5.0). .... | 67  |
| Table 14. Microwave band frequency identification .....   | 69  |
| Table 15. ISM band availability in accordance to ITU-R in 5.138, 5.150, and 5.280 of the Radio Regulations.....   | 70  |
| Table 16. Variables in microwave research.....  | 71  |
| Table 17. Quantum energy values by frequency and bond energy. ....  | 79  |
| Table 18. Effect of microwave irradiation on enzyme activity in aqueous solutions. ....   | 84  |
| Table 19. Microwave bioreactor design parameters .....  | 98  |
| Table 20. List of experiments conducted.....  | 115 |
| Table 21. Nomenclature of published protocols .....   | 116 |
| Table 22. Comparison of HPLC columns for Saccharide detection .....   | 118 |
| Table 23. Calibration curve data analysis.....  | 120 |
| Table 24. EP 2.1.0. Variable focus; Microwave power (000W-200W).....  | 127 |
| Table 25. EP 2.1.1. Variable focus; BGL inhibition.....   | 128 |
| Table 26. EP 2.1.1. Experimental design for BGL inhibition.....   | 129 |
| Table 27. EP 2.1.2. Variable focus; Biomass loading .....   | 130 |
| Table 28. EP 2.2.0. Variable focus; Enzyme addition (EGL and BGL).....  | 131 |
| Table 29. EP 2.3.0. Variable focus; Carbohydrate with BGL .....   | 132 |
| Table 30. EP 3.1.0. Variable focus; Microwave power on yeast growth.....  | 138 |
| Table 31. Results summary .....   | 142 |
| Table 32. Overview and summary of experiments conducted.....  | 145 |
| Table 33. Heating profiles with different microwave powers .....  | 147 |
| Table 34. Table of microwave influence on product formation and rate alteration.....  | 163 |
| Table 35. Summary of initial rates for CBH/EGL on cellulose with varying microwave irradiation ...  | 165 |
| Table 36. Summary of initial rates for biomass variation (10 and 50g/l at 50W irradiation) against MW-NC (10g/l).....   | 176 |
| Table 37. Summary of initial rates for CBH/EGL + BGL on cellulose with varying microwave irradiation .....  | 181 |
| Table 38. Comparison of addition of BGL with and without microwave irradiation.....   | 183 |
| Table 39. Summary of initial rates for BGL on cellobiose with varying microwave irradiation .....   | 186 |
| Table 40. Comparison of gradients in two curve fit models.....  | 193 |
| Table 41. Summary of exponential growth phase by optical density .....  | 196 |
| Table 42. Summary of glucose uptake rates where biomass growth is exponential .....   | 198 |
| Table 43. Summary of ethanol formation rate by HPLC analysis and curve fitting.....   | 202 |
| Table 44. Summary of project contribution to knowledge .....  | 208 |
| Table 45. Comparison of energy exposure between this study and <i>Zhu et. al.</i> .....   | 211 |
| Table 46. Summary of results (Catalysis).....   | 214 |
| Table 47. Thermal heat flow through the microwave bioreactor system.....  | 216 |

## ***Equations***

|   |     |
|---|-----|
| Equation 1. Fractal kinetics as per product concentration .....         | 47  |
| Equation 2. Correction for water hydration .....                        | 122 |
| Equation 3. Calculation of % saccharification.....                      | 122 |
| Equation 4. Calculation of concentration .....                          | 122 |
| Equation 5. Catalysis curve fitting .....                               | 122 |
| Equation 6. Calculation of fermentation inoculum.....                   | 133 |
| Equation 7. Conversion for cell counting (Small to large squares) ..... | 134 |
| Equation 8. Calculation of cell number .....                            | 134 |
| Equation 9. Exponential curve fit .....                                 | 136 |
| Equation 10. Empirical determination of [S].....                        | 153 |
| Equation 11. Cellobiose : Glucose correlation .....                     | 157 |

|   |            |
|---|------------|
| <b>ABSTRACT.</b>  | <b>I</b>   |
| <b>Declaration</b>  | <b>iii</b> |
| <b>Acknowledgements</b>   | <b>iv</b>  |
| <b>Abbreviations</b>  | <b>v</b>   |
| Units of measurement  | vi         |
| Figures   | vi         |
| Tables  | ix         |
| Equations   | x          |
| <br>  |            |
| <b>CHAPTER 1 – INTRODUCTION</b>   | <b>1</b>   |
| <b>1.1. Defining the problem</b>  | <b>2</b>   |
| <b>1.2. The proposed solution</b>   | <b>3</b>   |
| <b>1.3. Thesis chapters.</b>  | <b>4</b>   |
| <br>  |            |
| <b>CHAPTER 2. - BACKGROUND</b>  | <b>9</b>   |
| <b>2.1. The need for biofuels</b>   | <b>10</b>  |
| 2.1.1. Biotechnology principles for biofuels and bioproducts                        | 15         |
| <b>2.2. Ligno-cellulosic feedstocks</b>   | <b>18</b>  |
| 2.2.1. Cellulose, hemicellulose and lignin.   | 19         |
| 2.2.2. Lignin   | 21         |
| 2.2.3. Cellulosic materials as fermentation feedstocks.                             | 21         |
| 2.2.4. Hexose sugars  | 23         |
| 2.2.5. Pentose sugars   | 23         |
| 2.2.6. Comparison to hydrocarbons   | 25         |
| 2.2.7. Inhibitory elements  | 25         |
| <b>2.3. Biological degradation of post pre-treatment ligno-cellulosic materials</b> | <b>26</b>  |
| 2.3.1. Lignase  | 29         |
| 2.3.2. Swollenin  | 30         |
| 2.3.3. Cellulases   | 31         |
| 2.3.3. Endoglucanases (EGL)   | 34         |
| 2.3.4. Exoglucanase / Cellobiohydrolases (CBH)                                      | 36         |
| Cellulose Binding Module (CBM)  | 38         |
| Linker sequence   | 39         |
| Catalytic core  | 41         |
| Water location and action in the CBH system   | 42         |
| 2.3.5. $\beta$ -glucosidases (BGL)  | 44         |
| 2.3.6. Cellulase enzyme quantification/qualification                                | 44         |
| <b>2.4. The ethanol biorefinery</b>   | <b>49</b>  |
| 2.4.1. Separate Hydrolysis and Fermentation (SHF)                                   | 52         |
| 2.4.2. Simultaneous Saccharification and Fermentation (SSF)                         | 54         |
| 2.4.3. Simultaneous Saccharification and Co-Fermentation (SSCF)                     | 55         |
| 2.4.4. Consolidated BioProcessing (CBP)   | 56         |
| 2.4.5. Product recovery   | 58         |
| 2.4.6. Industrial adoption  | 58         |

|   |            |
|---|------------|
| <b>2.5. Developing bioethanol production processes - Ethanogenic micro-organisms</b>                              | <b>60</b>  |
| 2.5.1. Ethanogenic micro-organisms  | 60         |
| 2.5.1.1. Yeast  | 60         |
| Saccharide metabolism   | 63         |
| 2.5.1.2. Bacteria   | 65         |
| 2.5.2. Yeast versus bacteria for glucose based ethanol fermentations  | 67         |
| <b>2.6. Microwave irradiation</b>   | <b>68</b>  |
| 2.6.1. Microwaves and magnetrons  | 68         |
| 2.6.2. Microwave cavity designs and development   | 70         |
| Frequency   | 71         |
| Power/microwave source  | 71         |
| Thermal   | 72         |
| EM wave propagation (Mode)  | 74         |
| 2.6.3. Application of microwave energy to chemical/biochemical reactions and biological systems.                  | 76         |
| 2.6.4. Microwave/chemical interactions  | 78         |
| 2.6.5. Microwave chemistry and applications in biochemistry, catalysis and fermentation                           | 80         |
| 2.6.6. Microwave and biofuel/cellulase research   | 85         |
| <b>Conclusion</b>   | <b>90</b>  |
| <br>  |            |
| <b>CHAPTER 3. RESEARCH METHODOLOGY: MATERIALS AND PROTOCOLS</b>   | <b>91</b>  |
| <br>  |            |
| <b>3.0.0. Literature, theoretical and mathematical methods</b>  | <b>92</b>  |
| 3.0.1. Literature searching   | 92         |
| 3.0.2. Referencing methods and database compilation   | 93         |
| 3.0.3. Modelling and mathematical tools   | 93         |
| 3.0.4. Digital imagery  | 94         |
| 3.0.5. Digital data management  | 94         |
| 3.0.6. Experimental design  | 95         |
| Aim   | 95         |
| Objectives  | 95         |
| Null hypothesis   | 95         |
| <b>3.1. Practical work - Microwave</b>  | <b>98</b>  |
| 3.1.1. Prototyping, design, operation and testing.  | 98         |
| 3.1.2. Isothermal microwave bioreactor overview   | 99         |
| 3.1.3. Stirred tank reactor   | 99         |
| 3.1.4. Microwave cavity, waveguide, tuning section and launcher   | 101        |
| 3.1.5. The microwave source   | 102        |
| 3.1.6. Variation by microwave power (including thermal stability)   | 103        |
| 3.1.7. Sampling   | 104        |
| 3.1.8. Schematics and images of the prototype system  | 105        |
| 3.1.9. Thermal profiling  | 110        |
| <b>3.2. Practical work - Catalysis</b>  | <b>112</b> |
| 3.2.0.0. EP 2.0 – Microwave irradiation of cellulase systems  | 112        |
| Microwave enzymatic saccharification – validation, experiments conducted, reaction protocols, analytical methods. | 112        |
| 3.2.0.1. Experiment validation  | 116        |
| References to published protocols   | 116        |

|   |            |
|---|------------|
| Protocol development  | 117        |
| HPLC analysis of breakdown products (NREL/TP-510-42628)   | 117        |
| Standardisation of reactor substrates   | 119        |
| Standardisation of enzyme preparations  | 119        |
| Standardisation of substrate and enzyme loading   | 119        |
| Standard curves for determination of constituents   | 120        |
| Data processing   | 121        |
| Standardisation by internal standard.   | 121        |
| Correction for water hydration.   | 122        |
| Calibration by standard curve.  | 122        |
| Curve fitting data  | 122        |
| Exposure time periods   | 122        |
| Qualification by saccharification by-products.  | 123        |
| 3.2.0.2. Negative controls  | 125        |
| Hydrolysis under standard thermal condition (Microwave negative control (NC-MW))  | 125        |
| Influence of microwave power on substrate (Substrate negative control (NC-S))   | 125        |
| Influence of microwave on enzyme degradation (Enzyme negative control (NC-E))   | 125        |
| 3.2.1.0. EP. 2.1.0. – Cellulose hydrolysis by CBH/EGL – BGL with varying microwave irradiation                          | 127        |
| 3.2.1.1. EP. 2.1.1. - Investigation for inhibition of residual BGL through the addition of vanillin                     | 128        |
| 3.2.1.2. EP. 2.1.2. - Variation of cellulose loading with hydrolysis by CBH/EGL –BGL with varying microwave irradiation | 130        |
| 3.2.2.0. EP. 2.2.0. – Cellulose hydrolysis by CBH/EGL +BGL with varying microwave irradiation.                          | 131        |
| 3.2.3.0. EP 2.3.0. – Cellobiose hydrolysis by BGL with microwave irradiation  | 132        |
| 3.3.0.0. EP. 3.0 - Fermentation   | 133        |
| Stain culture, frozen stock culture and inoculum preparation.   | 133        |
| Relating optical density to cell density  | 134        |
| Fermentation  | 135        |
| Fermentation profiling  | 135        |
| HPLC analysis of fermentation products  | 136        |
| Standard curves for determination of fermentation products  | 136        |
| Data processing   | 136        |
| Negative controls   | 136        |
| Sampling frequency and structure  | 136        |
| Fermentation under thermal conditions (Microwave negative control (NC-MW))  | 137        |
| 3.3.3.1. EP 3.1.0. – Anaerobic glucose fermentation with varying microwave irradiation                                  | 138        |
| <b>Conclusion</b>   | <b>139</b> |

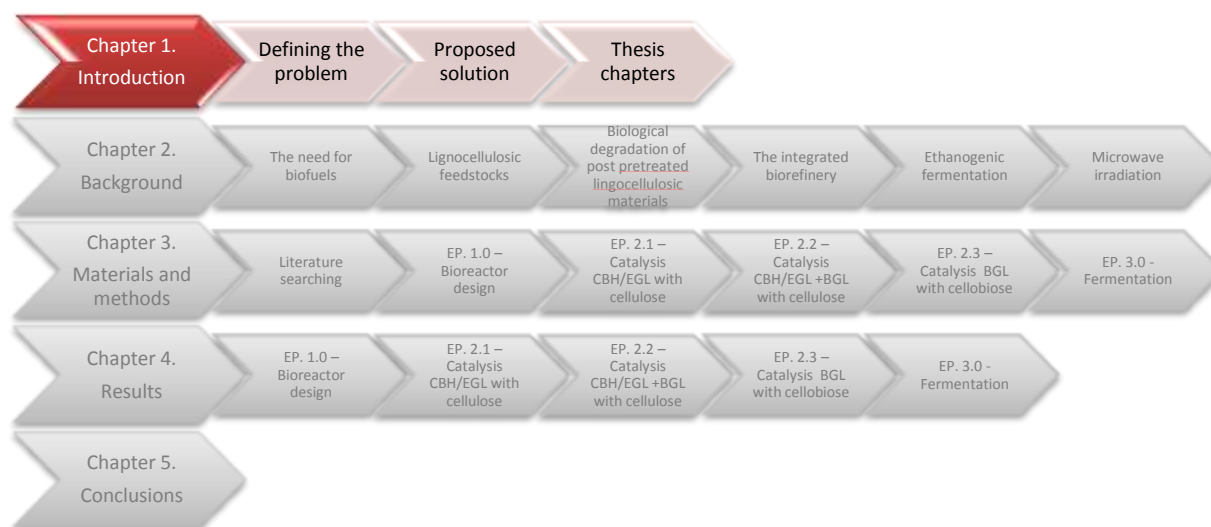
## **CHAPTER 4. RESULTS AND CRITICAL ANALYSIS** **140**

|   |     |
|---|-----|
| 4.1. EP 1.0. – Bioreactor thermal profiling   | 146 |
| 4.2.0. EP 2 – Saccharification of cellulosic materials                                  | 151 |
| Negative Controls   | 151 |
| Hydrolysis under standard thermal condition (Microwave negative control (NC-MW))        | 151 |
| 4.2.0.1. NC-MW – EGL/CBH without BGL  | 152 |
| 4.2.0.2. NC-MW – EGL/CBH with BGL   | 154 |
| 4.2.0.3. Comparison of NC-MW – EGL/CBH with and without BGL                             | 155 |
| 4.2.0.4. NC-MW – BGL with cellobiose  | 156 |
| 4.2.0.5. Influence of microwave energy on substrate (substrate negative control (NC-S)) | 158 |
| 4.2.0.6. Influence of microwave on enzyme degradation (Enzyme negative control (NC-E))  | 159 |
| 4.2.1.0. EP 2.1.0. – Cellulase hydrolysis by CBH/EGL – BGL with microwave irradiation   | 161 |

|  |            |
|--|------------|
| 4.2.1.1. EP 2.1.1. –Investigation for inhibition of residual BGL through the addition of vanillin            | 169        |
| 4.2.1.1. EP 2.1.2. - Variation by biomass  | 172        |
| 4.2.2.0. EP 2.2.0. – Cellulose hydrolysis by CBH/EGl +BGL with varying microwave irradiation                 | 177        |
| 4.2.2.1. Comparison of reference reactions (+BGL and –BGL) to 50W microwave irradiated (+BGL and –BGL)       | 183        |
| 4.2.3.0. EP. 2.3.0. – Cellobiose hydrolysis by BGL with varying microwave irradiation                        | 185        |
| 4.3.0.0. EP 3 – Fermentation of <i>Saccharomyces cerevisiae</i> as a model eukaryotic system                 | 189        |
| Negative control (thermal conditions) and data analysis  | 189        |
| Relating optical density to cell density   | 189        |
| Fermentation profiling   | 190        |
| HPLC analysis of fermentation products   | 191        |
| 4.3.1.0 EP 3.1. – Investigation of variable microwave power on the growth of <i>Saccharomyces cerevisiae</i> | 194        |
| Biomass by optical density.  | 194        |
| Substrate utilisation  | 197        |
| Ethanol formation  | 200        |
| <b>Conclusion</b>  | <b>204</b> |
| <br>   |            |
| <b>CHAPTER 5. CONCLUSIONS</b>  | <b>206</b> |
| The microwave bioreactor   | 209        |
| Achievement of study objective;  | 209        |
| Scientific significance:   | 212        |
| Industrial acceptance;   | 212        |
| <br>   |            |
| <b>Bibliography</b>  | <b>223</b> |

# *Chapter 1 – Introduction*

# Chapter 1 – Introduction



## 1.1. Defining the problem

The problem being addressed in this research project is the need for preparation technologies for combustible liquid fuels (bio-alcohols) from renewable sources, using lower grade biomass that is not suitable as food crops. The carbon sources being considered are energy crops, such as grasses and short rotation herbaceous crops on set-aside land<sup>1</sup> and land unsuitable for food crops [1-4]. The current limitations in the conversion of lignocellulosic plant biomass through to liquid biofuels are:

1. Delignification - removal of phenolic polymers (see page 21)
2. Enzymatic catalysis is seen as the route to cellulose hydrolysis but it needs
  - a. Improvement of efficiency
  - b. Coupling to the fermentation process
3. Technology scaling feasibility and cost

1) **Delignification** is problematic due to the protective lignin fraction of the biomass causing steric hindrance to enzymatic digestion. Many different and varied chemical and physio-chemical delignification processes have been developed or are currently under development (for an overview, see Alvira *et. al.*, [5], Balat *et. al.*, [2] and Godfrey [6]). As the industrial delignification process is mainly physical or non-biological, it is considered to be outside the scope of this study.

---

<sup>1</sup> Land left fallow between crop rotations from soil recovery.

2) **Enzymatic catalysis** is accepted as the most efficient hydrolytic process for the conversion of cellulose and hemicellulose fibres to glucose and other monosaccharides. The difficulty in processing occurs with multiple end product and intermediate product feedback systems which retard the catalytic rate. This has led to long reaction residence times, yield limitations, and mismatching of rates in combined saccharification and fermentation. Many different (predominantly molecular biology based) approaches have been taken to increase the catalytic rate through modification of the enzymes being used, or the expression of enzyme in higher concentration to reduce enzyme production cost [2, 7, 8].

As enzymatic hydrolysis precedes the fermentation process, the two processes are coupled and it is necessary to assure the prevention of saccharide loss due to microbial contamination (opportunistic colonisation). Thus, modifications of the hydrolytic process are required to be compatible with the fermentation process to reduce processing restraints.

3) **Feasibility** is the final consideration. For technology adoption, the cost associated with the current process compared to the cost of the new process developed in this study has to be favourable. The current process is cost dependent on the enzyme for hydrolysis and facilities cost. Any processes developed that can be retrofitted to a current system, developed quickly and cheaply to a commercial scale (scalable through either scale up or scale out) have benefit to the end user. For this study, the importance of economic feasibility is acknowledged, although largely outside of the technical scope of this thesis. For detail on cost economics, reviews by Avinash Kumar (2007), An *et. al.*, (2011), and Escobar (2009) [9-11]

## **1.2. The proposed solution**

The technology being developed in this study involves;

- 1) **The design of a novel microwave reactor on a 1-2 litre scale, capable of continuously irradiating liquid reactions at varying microwave powers, under thermally steady state conditions (isolation of the microwave effect from the thermal effect). Optimisation of its operation with the aim to maximise to use of the microwave field.**
- 2) **Increasing the rate of the enzymatic rate digestion of cellulosic materials to monomeric saccharides. The hydrolytic rate increases with temperature until thermal denaturing of the enzyme where the protein loses its tertiary structure and loses function. Using microwave irradiation under isothermal conditions, the effect of microwaves on the hydrolytic rate can be investigated in isolation from the temperature effect.**

**3) The consolidation of fermentation and catalysis into a single unit operation is a major factor in the streamlining of the process pathway. If the enzyme is irradiated in the presence of a ethanogen, how will the ethanogen respond?**

The aim of using these methods is to potentially alleviate the choke point caused by hydrolysis. This will be done by microwave irradiation of the enzyme system with frequency, power and electromagnetic (EM) wave propagation (the “mode”) as variables. Microwave radiation is known to accelerate chemical reactions and enzymes in non-aqueous environments, therefore it was considered worthy of investigation within the organic system. As consolidation of hydrolysis and fermentation is the natural processing progression, the effects of irradiation will be examined on a fermentation system.

### **1.3. Thesis chapters.**

**Chapter 1 – Introduction**, introduces the notion of a problem that requires a technical solution with a high degree of innovative and novel approaches, a proposed solution to the problem and the structure of the thesis in which the technology developed is explained.

In **Chapter 2 – Background**, an investigation of microwave technologies and explanation the mechanisms of cellulose breakdown is described in detail.

The research is divided into two sections;

- 1) Microwave technology and the effects observed in chemical/biochemical processing
- 2) Biochemistry and biotechnology of cellulose hydrolysis and fermentation to ethanol rich media.

The main subject areas covered are;

- 1) What is the biofuel need?
- 2) What is cellulose and why ferment it?
- 3) Understanding cellulases – a prerequisite to optimisation
- 4) Fermentation practices
- 5) The microwave effect
- 6) Previous microwave enhanced reactions

**Chapter 3 – Materials and methods** introduces the methods used in both the literature and practical studies. The first section of the chapter details the research methods used for literature searching, data mining and software based processing. This includes reference evaluation, citing peer texts, reference database compilation, interactions with academic and

industrial leaders, the use of standard reporting software and the use of bespoke modelling software.

The middle section of Chapter 3 describes the process taken in the development of the microwave bioreactor, its design, fabrication and operation for isothermal conditions. It also includes sampling methods and process developments that are applicable across all the reactions undertaken in the reactor.

The final section to Chapter 3 describes the materials and methods, equipment, reagents and experimental protocols. The methods section is divided into subsections: the methods for the sample analysis; and a description of each experiment (including negative controls) and their significance to the overall study.

**Chapter 4 – Results and critical analysis** looks at the performance of the microwave reactor and the results for both the catalysis and fermentation experiments. As the reactor is of a new and novel design, reactor testing is evaluated for the ability to maintain isothermal conditions, design limitations and microwave performance. For catalysis and fermentation, each data set has been analysed in accordance to its own negative control.

For catalysis (where applicable), there has been a comparison of results against relevant data sets from other experimental groups. In each catalysis experiment, the data have been analysed by two analyte profiles and two metrics (initial rate and yield). As glucose is the desired product, glucose is the primary product of interest. Where applicable, cellobiose formation has been quantified for  $\beta$ -glucosidase (BGL) activity. Percentage saccharification to show how much of the original material has been saccharified into the range of mono to tetrasaccharide has been used to show total process progression through initial rate and total yield in each experiment.

For fermentation, microwave irradiation has been compared to the thermal negative control by glucose uptake, ethanol production and cell density.

As each experiment requires substantial quantification and analysis, each experiment is summarised and concluded individually. Complete representations of the highlighted graphs are shown in the appendices.

**Chapter 5 - Conclusions** summarises the thesis. Due the multiple aspects of the project in previous chapters, this chapter is split into the three research themes that run throughout the thesis.

- 1) The production of a microwave bioreactor with independent thermal and microwave controls.
- 2) The effects of microwaves on the hydrolysis of a cellulose substrate by “cellulase” enzymes.
- 3) The irradiation of a eukaryotic fermentation under 12 to 50W resulted in a subtle alteration of fermentation progress, with slight retardation of microbial growth in comparison to the thermal negative control.

The three themes are evaluated by the criteria of:

- 1) Critical evaluation - attaining the research object; novelty or inventive step
- 2) “Blue skies” research - relationship to scientific significance
- 3) Real World research - industrial relevance

The fourth criterion of evaluation is the potential development, and potential lead-on work from this research. This is discussed within the evaluation points 1 to 3.

The conclusions chapter is a summary and analysis of the key scientific contributions to knowledge. As proven within the methods and results section, a novel microwave reactor that is capable of operating isothermally and static microwave power set points and thus capable of isolating the thermal and microwave field effects on catalysis and fermentation, has been designed, developed and operated. Using this reactor it has been proven that the increase in initial rates and yield observed in the industrially important cellulase catalysed reactions can be achieved by microwave irradiation without the genetic modification of the protein structure. The implication of this research supporting the “microwave effect” is discussed.

The results of varying microwave power at constant temperature are novel. The greatest effect occurred at lower powers with decline as power increased, dropping the rate to below the negative control (no microwave power). A number of possible explanations are hypothesised for future study. The process studied is critiqued in terms of how far the conclusions drawn can be applied to other systems, and the implications of a quantifiable microwave field on organic systems.

The final section of the conclusion highlights the importance of the work to both the biofuels and pharmaceutical industries and the work that can and will be built upon these findings.

Postscripts to the thesis are the bibliography and appendices. The bibliography is compiled by the standard formats and covers the thesis text. As there has been a considerable amount

of data and research generated over the course of the PhD, materials that are relevant to the understanding of the study although not considered core to thesis are compiled in the appendix. This material includes expansion on background research sections, complete protocols against which the materials and methods section was developed, further detailed pictorial representations of the bioreactor from various observation angles, expanded graphs from those used in Chapter 4 and additional tables and figures.

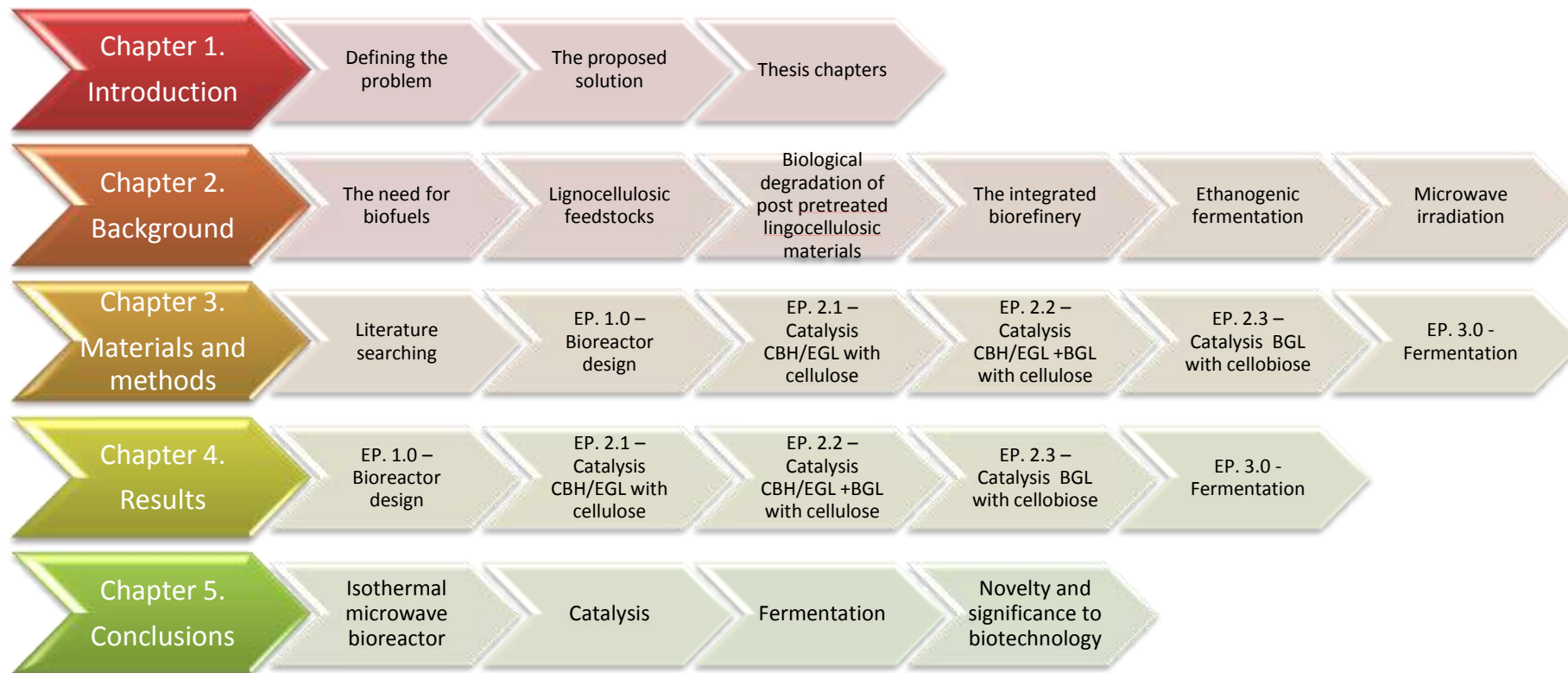
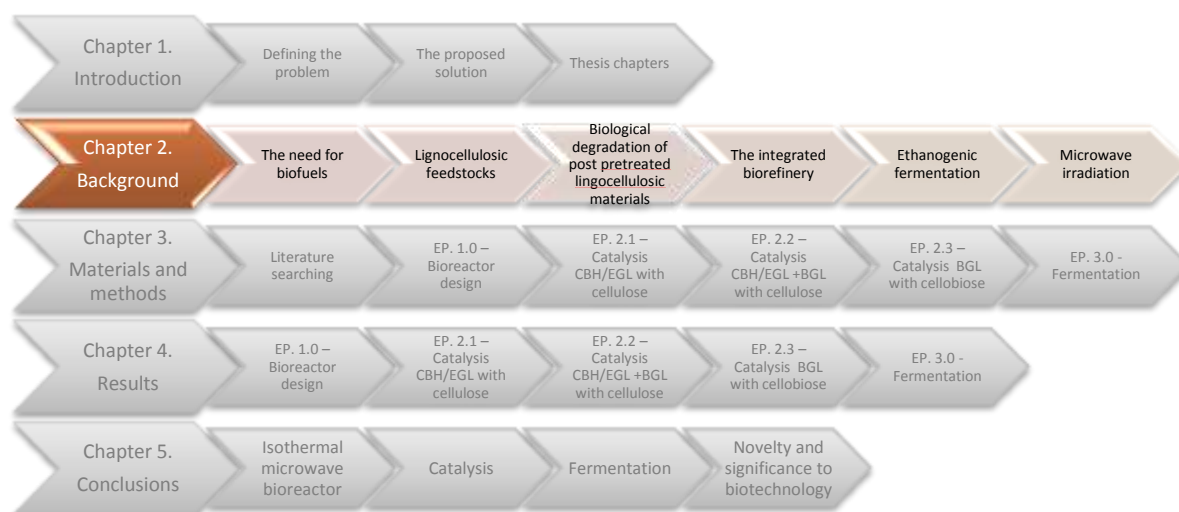


**Figure 2. Thesis construction.**

Each chapter is highlighted with the main subsections extended from each chapter root. Further sub-levels are used below the major subsections where further detail is required.

## ***Chapter 2. - Background***

## Chapter 2. - Background



### 2.1. The need for biofuels

The global drivers for the substitution, or supplementation of hydrocarbon based combustion cycle fuels with bioethanol and other renewable energy sources is very much based on the topical argument of choice. As this thesis is a study of technology development and not of biofuel policy, a selection of common drivers is simply listed below;

Global community/multinational level drivers;

- Peak oil without foreseeable energy economy or energy substitute at suitable maturity
- Energy independence from oil producing states where energy price or volume restrictions may threaten global community stability
- The mitigation of climate change by reduction of Green House Gases (GHG)
- Public health considerations – reduction of NO<sub>x</sub> gases and soot
- Development of high technology/low carbon industries and economies
- Prevention of resource diversion of landmasses from food production to fuel production
- Agricultural/environmental factors such as biodiversity, arable land run off, herbicide/pesticide use associated to an increase in biofuel crops.

On the basis of adopting alternative energy sources, liquid biofuel substitutes (bioethanol, biobutanol, biodiesel etc) have the lowest barriers to use, as the established mechanism of storage and distribution is through the pumping, storage and combustion of liquid fuels. Transportation fuels have been evaluated by Safaei Mohamadabadi *et. al.* (2009) by the criteria of fuel type, economics and environmental parameters [12].

Although motivations for adoption are governed by economic and national/international politics, the mitigation of climate change has eclipsed all other arguments with the overriding consensus that not addressing anthropogenic green house gas (GHG) emission will cause significant hardship for all global inhabitants. As such the development of biofuels and clean energy has been seen as imperative [13].

Bioethanol is an alternative liquid fuel source to the mineral oil derived petrochemicals used in combustion engines. Approximately 96% of global and 98% of EU transport fuels were mineral derived in 2006. In 2011 figures for the USA point towards a 2% contribution from bioethanol [1, 14]. With mandates in place and the continual maturing of current research practices, a series of targets have been set with varying degrees of compliance depending on food and fuel prices. Fuel production targets are highlighted in Table 1.

| <b>Geographical location</b> | <b>Target as percentage of combusted fuel</b> | <b>Year of compliance/forecasted data</b> |
|------------------------------|---|---|
| <b>EU-25</b>                 | 2%  | 2005                                      |
| <b>EU-25</b>                 | 5.75%   | 2010                                      |
| <b>USA</b>                   | 20%   | 2017                                      |
| <b>EU-25</b>                 | 10%   | 2020                                      |

**Table 1. Biofuel production estimations/targets for the USA and EU by directive**  
Table adapted from [1] and [15].

The appeal of bioethanol and biobutanol over mineral petrol consists of the reduction in carbon emissions over complete well-to-wheel/field-to-wheel carbon cycle comparison [16-19] (Figure 3). In terms of differentiation of fuels, bioethanol/biobutanol is seen as the partial alternative to petrol with petrol accounting for around 80% of global automotive fuel consumption by volume. Biodiesel is seen as the alternative to diesel (remaining 20% of fuel consumption by volume) [18]. Performance characteristics are dependent on ethanol/petrol blend and car design. Flexi-fuel cars, common in areas of high ethanol usage (Brazil, South American and part of US), show adaptability between different fuel grades [20]. In contrast, biobutanol in some respects is more analogous to petrol in combustion thermodynamics and physical properties and is therefore termed a “drop in” substitute to petrol [21]. The use of ethanol, either blended or as a sole fuel source, is shown to increase octane number, reduce MTBE (methyltertiarybutyl ether) requirements, reduce toxicity impact on environmental release and reduce emissions of combustion by-products [22-27].

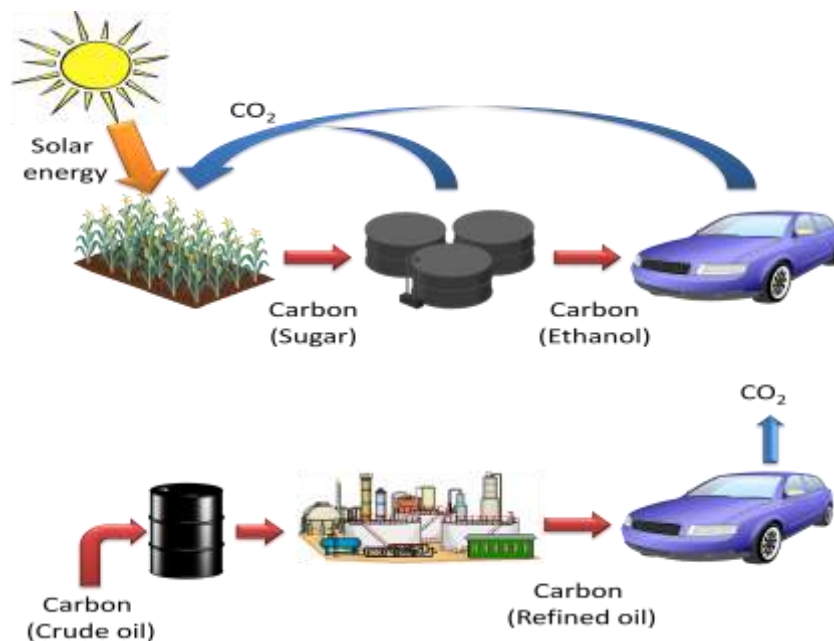


**Figure 3. Simplified illustration of carbon transformation (Renewable vs. non-renewable)**

Top; Ethanol cycle where solar energy is captured by biomass, conversion through bioprocessing and fermentation and then used in transport based combustion. Released carbon dioxide is used as feed in biomass formation.

Bottom; Mineral oil based combustion where crude oil is mined from geological source, refined for a cleaner combustion product and combusted in transport. Carbon dioxide released to the atmosphere.

The development of bioethanol has been split into three phases or generations (see Table 2).

| Generation  | Description   |
|---|---|
| 1 <sup>st</sup> generation                        | Fermentation of free mono-saccharides and starch from cereal crops.   |
| 2 <sup>nd</sup> generation                        | Fermentation of polysaccharide complexes from non-food crops and waste residues – cellulosic and ligno-cellulosic   |
| 3 <sup>rd</sup> generation or “Advanced biofuels” | Conversion of the saccharides directly to electrical energy, commercialisation of butanol and bio-battery development (also known as “Advanced” biofuels) |

**Table 2. Biofuel technology generations**

For bioethanol use, the predominant end user is the internal combustion engines in road based motor vehicles. Secondary to this is the markets of recreational vehicles (outboard motors and gardening equipment) and small scale static electricity generators. Of notable emergence is micro generation or backup/redundancy generators at specific commercial sites where solid-oxide fuels cells are becoming more popular (such as the collaboration of Bloom Box with the Google server centres [28]). For all these applications, the production of bioethanol is almost exclusively through the fermentation of free monosaccharides derived from cereal crops. These cereals have the dual potential of edible sustenance for humans and domestic animals as well as fuel production, therefore constraints on availability are observed [29].

Production constraints include -

- Availability of agricultural land
- Crop pricing
- Biodiversity impact
- Socioeconomic practices

The implementation of the UK RTFO (Road Transport Fuel Obligation), EU 2003/30/EC (Directive on the Promotion of the Use of Biofuels and Other Renewable Fuels for Transport) and the US EISA (Energy and Independence Security Act of 2007), the requirement for fuel ethanol is greater than the total potential yield obtainable from first generation fermentative technologies. To meet a 5% biofuel protocol in the UK under the UK RTFO, 1.2Mha of land is required with an expansion to 1.75Mha for the 5.75% target achieved by the end of 2010 based predominantly on 1<sup>st</sup> generation processing. In reality, available agricultural land set aside for biofuel production is limited to 1.72Mha without impinging on food production. With the target of 20% by 2020, a clear constraint is observed in the use of 1<sup>st</sup> generation technologies [3, 16, 19, 30-32].

Progression towards the mandated biofuel requirements foresees the impending choke point where arable land is incapable of delivering sufficient material for processing into fuels. To achieve the required volumes, saccharide sources which do not contribute to foodstuffs are required. Complex polysaccharide sources (ligno-cellulose, hemicellulose and cellulose) which are high in saccharide content but technically difficult to unlock, requiring advanced technologies to release the mono-saccharides may provide an answer. They also address the total processing carbon balance and satisfy the current legislative demand [22]. The US has an obligation to produce a total of  $36 \times 10^9$  US gal ( $136 \times 10^9$  litres)<sup>2</sup> per annum derived from biomass by 2020. Of this,  $31 \times 10^9$  US gallons ( $117.3 \times 10^9$  litres) per annum (86% to total) is expected to come from cellulosic bioethanol. Therefore, there is a large technological potential due to the limitations of arable land required to meet the EISA requirements [16].

The employment of ligno-cellulosic based materials has the advantage of using base materials that would otherwise be regarded as waste. Source materials under consideration are:

- Fuel crops from non-arable lands, marginal lands and brown field sites
- Spent distillers' grain from spirit production
- Municipal solid wastes (MSW) where the organic fraction maintains a high cellulose content
- Waste materials and bioremediation from the paper pulping and recycling industries
- Lint materials from the textile industries

---

<sup>2</sup>  $\times 10^9$  = billion (short)

- Plant materials from the remediation and reclamation of contaminated lands with heavy and/or low radioactive metals by the growth of contaminant accumulating crops [33-36].

The production process for biologically derived fuels is through the use of metabolic pathways expressed in both prokaryotic and eukaryotic micro-organisms. Microbial metabolism for product formation reduces the processing cost; therefore the production of the bio-product is limited by the management of the fermentative micro-organisms metabolic rate, tolerance to product feedback inhibition and substrate availability. Although biobutanol is superior to bioethanol as a straight hydrocarbon replacement (due to ethanol forming azeotropes in the presence of moisture), the production volumes of ethanol are easier to achieve due to greater end product tolerance in ethanogens in comparison to butanogens [37].

With a focus on the production of ethanol, the technological movement from monosaccharide sources (sugar cane) through simple polysaccharide sources (starch) to complex polysaccharide sources (cellulose, hemicellulose and lignocellulose) has been driven by the limitation of biomass feedstocks. With the increase in the degree of polymerisation per unit mass, the amount of monosaccharide freely available decreases due to increased complexity of saccharide recovery. Therefore more novel and innovative ways of extracting the saccharides are required in the research stage for progression to the development stage before final industrial adoption.

For the release of the fermentable sugars from the ligno-cellulosic materials, two limitations are noted:

- Delignification; accessing the polysaccharides in the complex carbohydrates, by removal of steric hindrance of lignin from the larger ligno-cellulose complex.
- Hydrolytic rate; the amorphous and crystalline cellulose fractions require depolymerisation to reduce the hetero- and homopolysaccharides into their constituent monosaccharides.

Fermentation inhibitors will be either released or produced according to the method of degradation, with a mixed saccharide hydrolysate requiring fermentation to ethanol. With the heterologous-saccharide hydrolysate containing a mixture of pentose and hexose mono- and disaccharides, either a co-/sequential fermentation method or microbe capable of fermenting both pentose and hexose sugars will be required to obtain the maximum yield [22, 35, 38-40].

Current methods of monosaccharide release from lignocellulosic complexes are based on a unit operation system shown in Figure 4 where the units consist of;

- 1) Material handling     Material size reduction through physical/mechanical destruction
- 2) Pretreatment        Chemical and/or physical pretreatment for lignin removal and/or initial hydrolysis
- 3) Hydrolysis            Enzyme based catalytic process used for the reduction of polymerisation and hydrolysis of the cellulosic materials
- 4) Fermentation         Production of the bioproduct through microbial fermentation
- 5) Product recovery     Separation of desired product from the spent fermentation media

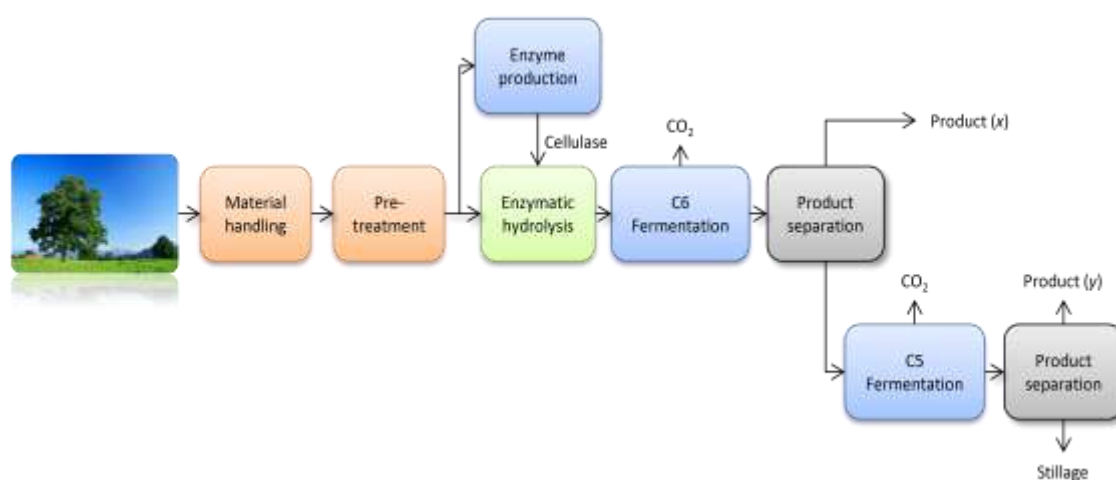
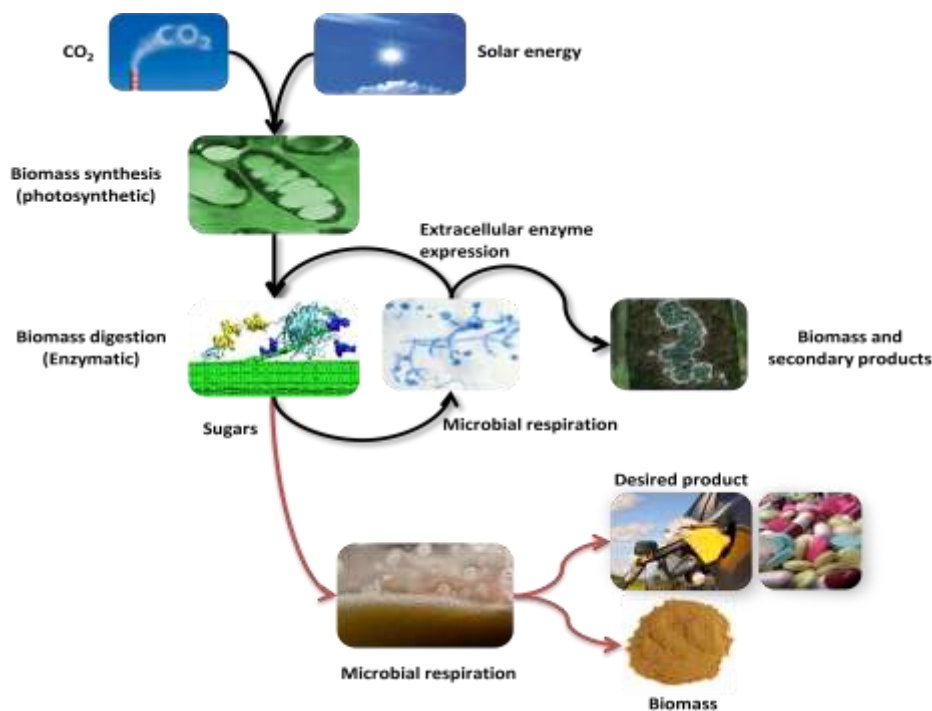


Figure 4. Block diagram of bioproduct formation from biomass

### 2.1.1. Biotechnology principles for biofuels and bioproducts

Energy for biological systems predominantly comes from one of two sources; photon energy in the form of light (phototrophic life) or the planet's internal heat source (chemolithotrophic life). Plant based biomass can be viewed as “solar energy collectors and thermochemical energy stores” [41] where solar energy is converted into a physical energy store (see Figure 5 and Figure 6, page 16). Once energy is acquired, all other biological products abundant today can be derived. In simplistic terms this can be through the combustion of fuel pellets or the metabolism of foodstuffs in human nourishment. Examples of more advanced derived energy conversions include fermentation for alcohols, hydrogen or direct production of electrical current in biobatteries [42]. For the perspective of biological exploitation for human benefit, this is in the context of enzymatic catalysis and fermentation - a sunlight-to-product sequence (see Figure 5).



**Figure 5. Conversion of solar energy to biofuels through biological means**

Illustration of the bioconversion of solar energy through the intermediate of plant biomass. Solar energy is captured through the process of photosynthesis for the production of plant saccharides. Saccharides are used in respiration, stored in the insoluble form of starches or converted to polysaccharide complexes for plant wall structural elements. For fuel conversion, processes are required to reduce the degree of polymerisation, releasing the monosaccharide before a fuel-producing micro-organism is used in the fermentative conversion of the sugars to ethanol. Exploitation of a biomass degrading microbe is used with a sugar shunt for selection of desired product. Adaption of [41].

The energy required for microbial growth and product formation can come from a number of origins. Predominantly these are either; the oxidation of media components (chemo-organotrophs); or from a light source (auto-organotrophs) [43]. Dark fermenters (exclusively chemo-organotrophs) utilise carbon sources of carbohydrates, lipids and proteins from other biological entities (symbiotic), or mineral sources within the immediate surroundings. Depending on the fermentation kinetics, microbe selection and carbon/nitrogen/oxygenation control, the formation of a desired product can be influenced to push the fermentation towards a defined primary or secondary metabolite for the greater yield. As the energy required in dark fermentations has come from another biological entity, the upstream organism has significance on the total process (Figure 6).

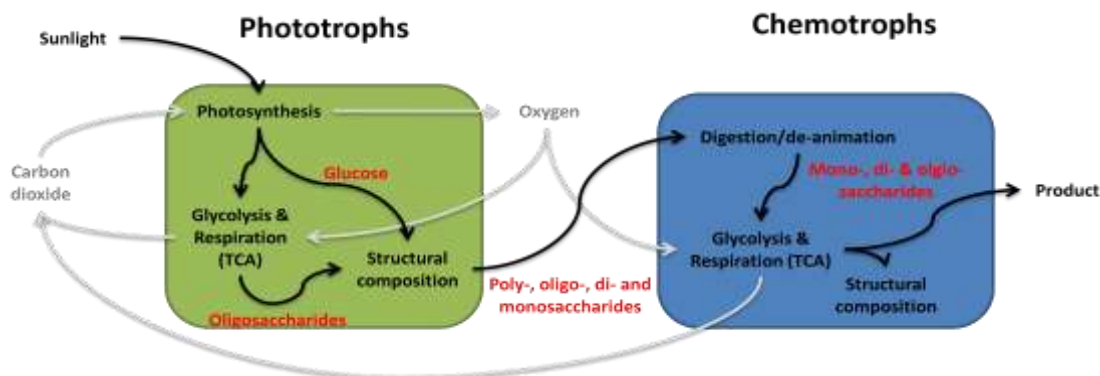


**Figure 6. From sunlight and CO<sub>2</sub> to bioproducts**

Schematic showing the process of bioconversion of sunlight and carbon dioxide through to a bioproduct. This simplified diagram highlights the relationship between phototrophs and chemotrophs with the dependency link in saccharide exchange between the two orders. Areas highlighted within the coloured boxes are representative of an organism level, with the chemotroph expressing an extracellular product. Amino acid and water utilisation is omitted to enhance simplicity

For the synthesis of biologically derived materials, the common mechanism across all biological species is the utilisation of carbon (predominantly in the form saccharides) in conjunction with a nitrogen source for the provision of energy and materials for growth. The coupled reactions seen in this mechanism are the glycolysis of a saccharide based carbon source and the citric acid cycle (TCA cycle) for the production of intermediates in the synthesis of all other biological derivatives. These mechanisms are seen as the common system across all autotrophs and chemotrophs and across all six biological kingdoms. As such, the availability and utilisation of mono to oligosaccharides are seen as a common limiting point in any biological system. With the example of the plant Kingdom or autotrophic bacteria, saccharide synthesis is a native, autonomous system through the photosynthetic pathway. In the case of nearly all other biological entities, securing a saccharide source is coupled to the consumption of plant or algal material.

Metabolic manipulation of pathways in the microbial systems allow a single micro-organism to be selected, or modified, to produce multiple products through either the alteration of the culture conditions, or through genetic manipulation. Thus, the process of hydrolysing polymeric sugars is not limited to the exclusive production of bioethanol. As bioethanol is a low value bulk commodity, the financial return is marginal and current industrial production is heavily dependent on governmental subsidies. Monosaccharide availability and cost is a common issue across all materials linked to food production costs. As such, polysaccharide conversion technology has significant advantages across the whole biotechnology industry. Investment in pre-fermentation technologies for both high and low value products has shown significant interest, especially in high value products where the percentage saving in processing on a small scale is substantially more beneficial than on large scale productions.

Through the development of biotechnology in the enhancement of human life, nearly every field of biotechnology has focused on the principle of generating greater product yield either

directly from light or from the saccharide intermediate. This has been seen in blue biotechnology through aquaculture and the development of marine species with the increased expression of oils; green biotechnology with the development of C4 photosynthetic pathway in C3 phototrophs, transgenic and crossbred crops for increased polysaccharide content; red biotechnology through the increased expression of medicinal products and white biotechnology through the increased production of industrially commercial volumes of synthetic materials. The use of industrial bioprocessing has enhanced and greatly increased the number of compounds available from the basic saccharide carbon sources. With the development of both the white and red biotechnology streams, the exploitation of microorganisms has led to the production of increasingly sophisticated biopharmaceuticals and biosynthetic materials far removed from the original source microorganism's original biochemical pathway.

## 2.2. Ligno-cellulosic feedstocks

Lignocellulosic, hemicellulosic and cellulosic materials are the products of plant cell wall fabrication, with lignocellulose predominantly found in secondary cell walls [44]. Common across all plants, the generalised structure is conserved across the whole kingdom, with variations depending on species, biotic and abiotic factors. Lignocellulosic materials contribute to the complex structures found within the plant kingdom, determining the plant's shape and architecture, and has a major role in pathogen defence and cellular growth. With the dynamic abilities of the ligno-cellulosic plant scaffolding, the production of the biomaterial has to be coordinated through a complex system and be able to carry out multiple functions without excessive resource demands [6].

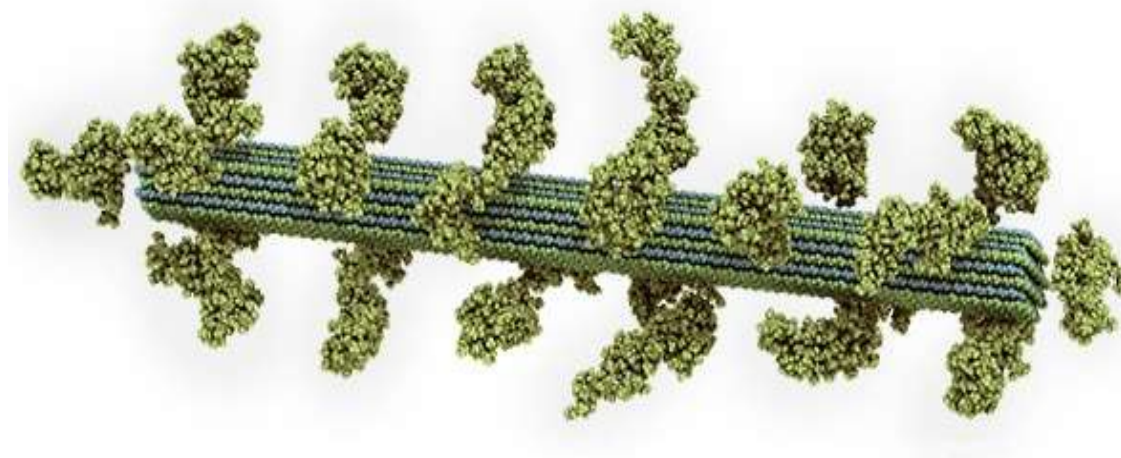


**Figure 7. Lignin proximity to cellulose fibre**

Polymeric fibres seen in the central structure (blue/green). Lignin residues observed surrounding the cellulose fibre (green). <http://www.nccs.gov/wp-content/uploads/2009/04/cellulose.jpg>

Lignocellulose contains of three key elements; lignin, hemicellulose and cellulose. The configuration of the three elements and the constituents of the lignin and hemicellulose fractions show variation between plants due to biotic and abiotic factors. A summary of plant species by constituent variation is shown in the Appendix (see page 7). The accepted model of lignocellulose is that the cellulose fibres are in a chain form, embedded within a matrix of other polysaccharides, pectins, glycoproteins and proteins [44]. To protect the whole assembly, lignin is bound onto the outside of the fibre bundles (see Figure 7 and Figure 8).

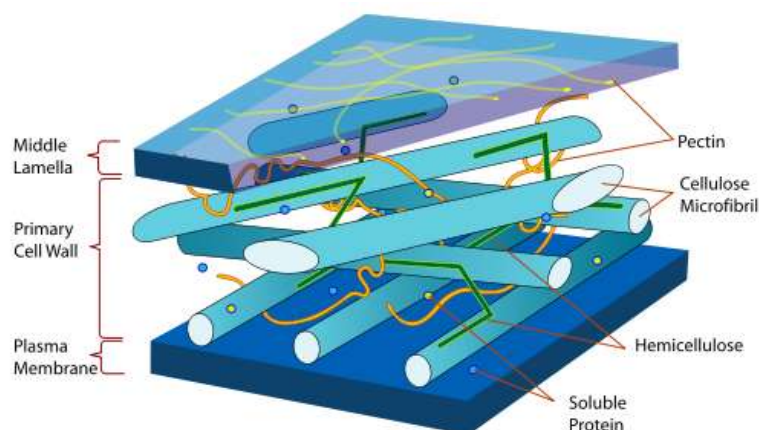


**Figure 8. Three dimensional microstructure of plant cell walls.**

Diagram illustrates the associations between the constituents of a plant cell wall where the middle lamella is the out side of the plant cell, descending through the primary cell wall with the loci of the cellulosic material sited within the pectin adhesion molecules and the plasma membrane prior to cell cytoplasm. [45, 46]

### 2.2.1. Cellulose, hemicellulose and lignin.

Whereas cellulose is often used in a generalised term for post pre-treated biomass, cellulose is specifically a chain of unbranched anhydroglucose ( $C_6H_{10}O_5$ )<sub>n</sub> linked by  $\beta$ -glycosidic bonds. Cellulose is highly stable and resistant to enzymatic hydrolysis due to the high number of inter- and intra-molecular hydrogen bonds. Consisting of  $\beta$ -1,4 linked glucose monomers, six polymorphs are known to exist (see Table 3). Of the six polymorphs, only cellulose I is seen in nature while the derived polymorphs are frequently seen as the result of thermo-chemical pre-treatments [47].

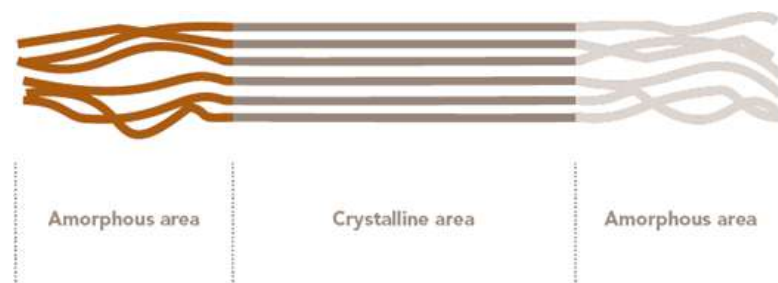
| Cellulose         | Characteristic  |
|-------------------|---|
| I                 | Only form found in nature. Parallel chain arrangement   |
| II                | Thermodynamically greater stability. Anti-parallel arrangement of strands. Some inter-sheet hydrogen bonding. |
| III <sub>I</sub>  | Obtained from I through pretreatment with ammonia or some amines  |
| III <sub>II</sub> | Obtained from II through pretreatment with ammonia or some amines   |
| IV <sub>I</sub>   | Obtained from III <sub>I</sub> through treatment with glycerol at 206°C                                       |
| IV <sub>II</sub>  | Obtained from III <sub>II</sub> through treatment with glycerol at 206°C                                      |

**Table 3. Cellulose polymorphs**

Characteristics of native cellulose and cellulose polymorphs. Adapted from [47]

Within the cellulose fibre, two distinct regions of cellulose organisation are observed. These are the crystalline and amorphous sections, defined by chain orientation. In the crystalline

sections, the cellulose fibrils are aligned parallel to each other and linked through hydrogen bonding. In the amorphous regions, the chain organisation is separated with water molecules between the micro-fibre bundles leading to a disorganised orientation (see Figure 9) [22, 48, 49].

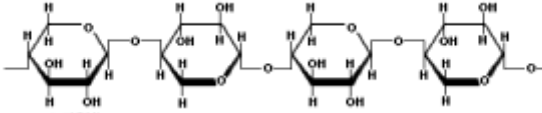
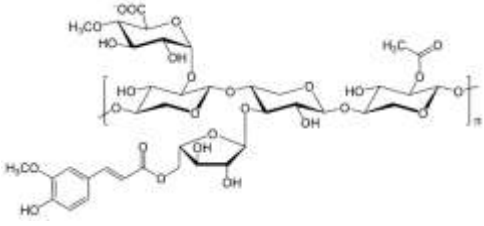
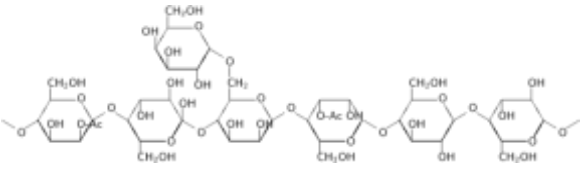
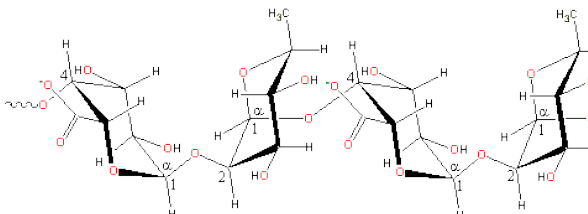


**Figure 9. Amorphous and crystalline morphology of cellulose fibres.**

In the regions of amorphous cellulose, the regular crystalline structure is disrupted by the inclusion of water molecules between the sheets, disrupting the regular hydrogen bonding. [48, 49]

With cellulose being solely polymeric glucose, the exploitation of cellulose is the key driving factor in the use of lignocellulose as a carbon source for fermentation processing.

In contrast to cellulose, hemicellulose is a heteropolysaccharide consisting of multiple saccharide species, and varies widely according to species and abiotic factors. Hemicellulose consists of both C5 and C6 monosaccharides and generally falls under four subgroups (see Table 4). Hemicellulose structurally has greater similarity to cellulose than lignin, with the variation of monosaccharide building blocks governing the efficiency of each method of degradation. Hardwood hemicelluloses are mainly comprised of highly acetylated heteroxylans (classified as 4-O-methyl glucuronoxylans) with low hexoses (in the form of glucomannans). Hardwoods contain a greater degree of acidic characteristics, leading them to have a higher liability to acidic hydrolysis and auto-hydrolysis in high temperature and/or pressure pretreatment processes. Conversely, softwood hemicelluloses are less liable to acidic hydrolysis due to having a higher proportion of partially acetylated glucomannans and (1-4-) linked galactoglucomannans and xylans [26, 50]

| Type | Description   | Notes   | Typified structure   |
|------|---|---|--|
| 1    | unbranched chains such as (1-4-) linked xylans or mannans | Repetitive pentose polymer                                    |  |
| 2    | helical chains such as (1-3-) xylans                      |   |  |
| 3    | branched chains such as (1-4-) galactoglucomannans        | Consisting of glucose, galactose, and mannose. Water soluble. |  |
| 4    | pectic substances such as polyramnogalacturonans          |   |  |

**Table 4. Hemicellulose subunits.**  
[50].

### 2.2.2. Lignin

Structurally, lignin is involved in the repulsion and hindrance of destructive mechanisms trying to access the cellulose fibre, limiting enzyme mobility and preventing chemical attack [6]. Lignin is a complex macromolecule. Comprising of free radical polymerisation of *p*-hydroxyl cinnamyl alcohol units with varying methoxyl contents, the monolignols give rise to syringyl (S), guaiacyl (G) and *p*-hydroxyphenyl (H) units in the lignin polymer which in turn are responsible for the hydrophobic nature of the external plant walls and internal xylem structure, and give structural strength to the plant fibres [6, 50].

For the exploitation of biomass saccharides for fermentation, lignin is a hindrance to saccharide liberation. Delignification (or pretreatment) has been addressed through a broad spectrum of physical-chemical pretreatment methods, out of the scope of this study. An overview of current pretreatments is presented in the Appendix (pages 8 to 17).

### 2.2.3. Cellulosic materials as fermentation feedstocks.

All microbial fermentations require a carbon source for cellular respiration and product formation. The carbon source has a direct effect on product yield and product formed depending on the metabolic pathway used. In pharmaceutical fermentations where substrate

specificity has direct correlation to product formation (for example, in antibiotic production where primary carbon exhaustion and switching to secondary metabolite triggers product production), a defined carbon media has to be used [43, 51]. In contrast, for ethanol (with specific focus on ethanol for non-human consumption), the specification has to be that product is formed from whatever carbon source is cheaply available and plentiful.

The mono-saccharides used are defined as five carbon (pentose) and six carbon (hexose) sugar, both of which are available from hemicellulose and lignocellulose (see Table 5).

| Carbon Number of Basic Subunit | Type of basic subunit | Saccharide                      | Basic Unit            | Degree of polymerisation (DP) |
|--------------------------------|-----------------------|---------------------------------|-----------------------|-------------------------------|
| 6 carbon                       | Aldoses               | Glucose                         | Glucose               | 1                             |
|                                |                       | Maltose                         | Glucose               | 2                             |
|                                |                       | Maltotriose                     | Glucose               | 3                             |
|                                |                       | Cellobiose                      | Glucose               | 2                             |
|                                |                       | Trehalose                       | Glucose               | 4                             |
|                                |                       | Galactose                       | Galactose             | 2                             |
|                                |                       | Mannose                         | Mannose               | 1                             |
|                                |                       | Lactose                         | Glucose and galactose | 2                             |
|                                |                       | Melibiose                       | Glucose and galactose | 2                             |
|                                | Ketoses               | Fructose                        | Fructose              | 1                             |
|                                |                       | Sorbose                         | Sorbose               | 1                             |
|                                | Aldoses and ketoses   | Sucrose                         | Glucose, fructose     | 2                             |
| Raffinose                      |                       | Glucose, fructose and galactose | 3                     |                               |
| Deoxy-sugars                   | Rhamnose              | 6-deoxymannose                  | 1                     |                               |
|                                | Deoxyribose           | 2-deoxyribose                   | 1                     |                               |
| 5 carbon                       | Aldoses               | Arabinose                       | Arabinose             | 1                             |
|                                |                       | Xylose                          | Xylose                | 1                             |
|                                |                       | Ribose                          | Ribose                | 1                             |
|                                |                       | Lyxose                          | Lyxose                | 1                             |
|                                | Ketose                | Ribulose                        | Ribulose              | 1                             |
|                                |                       | Xylulose                        | Xylulose              | 1                             |

**Table 5. Plant sugar subunits**

Summarisation of the basic subunits of plant derived carbohydrates. Adapted from [52]

Cellulose as a carbon source is a polymeric carbohydrate rather than a monomeric feedstock as seen in hexameric and pentameric fermentations. As the hydrolysis of cellulose produces a large abundance of C6 saccharides (predominantly dextrose), post hydrolysis the fermentation is treated much in the same way as a hexasaccharide fermentation, with theoretical yield matching the fermentation yield and kinetics of the C6 metabolites.

The hemicellulosic amorphous regions consist of a mixture of C5 and C6 saccharides. Complete hydrolysis of the feedstock results in a heterosaccharide mixture in the fermentation media. Once the primary carbon sources of hexasaccharides are exhausted (in mono-culture fermentations), the pentasaccharides are left remaining, reducing potential yield [2, 53]. Co-fermentations of *Saccharomyces* spp. with *Zymomonas* spp. or other microbes with the

capability of pentose metabolism are being trialled to increase the yield to be closer to the theoretical maximum. This is seen in the application of simultaneous saccharification and fermentation (SSF) with a mono-culture microbial content that can carry out C5 and C6 metabolism, and in the co-cultures seen in simultaneous saccharification and co-fermentation (SSCF). Importantly, this process is used as a parallel system as product inhibition from the primary micro-organism frequently prevents production from the secondary micro-organism. The examples observed are where the ethanogen with the greatest turnover rate and resilience quickly causes necrosis in the secondary microbe through permeation of the cellular membranes [54].

#### **2.2.4. Hexose sugars**

Hexose sugars are the most common saccharides used in fermentation and used in the majority of research, commercial and industrial applications. The scope for hexose fermentation is well documented and common practice. Hexasaccharides commonly found in plant cell walls are highlighted in Table 5.

Glucose has been the hexose with most exploitation due to abundance in freely available saccharide deposits in the form of sucrose<sup>3</sup> from sugar cane and other sucrose rich biomass sources. Cultivation of sugar cane and sugar beet has been the predominant sources of glucose although many fruiting bodies from various plants have also been used. Glucose is the predominant saccharide in metabolism due to the glycolysis/TCA pathway therefore the saccharide with greatest biological compatibility.

All other hexose sugars have only been used for either defined product formation (due to the triggering of specific metabolic pathways) or as a secondary feed in an impure fermentation feedstock. In the presence of other hexose saccharides within the fermentation media, fermentative organism may go through a diauxic shunt to other hexose saccharides. Microorganisms incapable of fermenting the additional saccharides will leave un-metabolised saccharides in the fermentation media.

#### **2.2.5. Pentose sugars**

Pentose sugars are divided into two groups dependant on the presence of either an aldehyde functional group in position one (aldopentoses of D-Ribose, D-Arabinose, D-Xylose and D-Lyxose) or a ketone functional group in position one (ketopentoses of D-Ribulose and D-Xylulose) (see Figure 10).

---

<sup>3</sup> Glucose-fructose compound

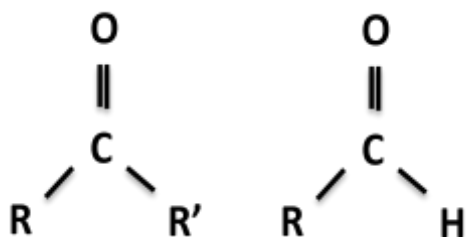


**Figure 10. Aldehyde and ketone functional groups**  
 Left; Ketone functional group. Right; Aldehyde functional group.

In microbial metabolism, pentose metabolisers are found among yeasts, fungi and bacteria, with the yeasts *Pichia stipitis*, *Candida shehatae* and *Pachysolen tannophilus* being the most promising naturally occurring species for industrial exploitation in the context of biofuel processing.

For the exploitation of the pentose monosaccharides, pentose metabolising yeasts take advantage of the pyruvate decarboxylase-alcohol dehydrogenase (PDC-ADH) pathway along with a handful of bacterial species (most notable of which is *Zymomonas mobilis*) to convert pentose substrates directly to ethanol. However, two alternative routes to ethanol production are present, these being through xylose isomerase → xylulokinase and xylose reductase → xylitol dehydrogenase → xylulokinase pathways.

With primarily xylose used in pentose metabolism, the xylose is reduced to xylitol through the aid of xylose reductase (XR). As xylitol is an accumulating intermediate compound that reduces the yield through feedback inhibition, it is converted to xylulose, catalyzed by xylitol dehydrogenase (XDH). Following conversion, the xylulose is then phosphorylated with xylulosekinase (XK) to xylulose-5P for further catabolism via the pentose phosphate pathway and the Embden-Meyerhof-Parnas (EMP) pathway in eukaryotes or the Entner-Doudoroff (ED) pathway in prokaryotic organisms such as *Zymomonas mobilis* [51]. This is shown in Figure 11 (see page 28).

The use of pentose saccharides as a sole carbon source has never been commercially viable due to the lack of high pentose concentrations in plant materials. Except for a small number of products with a specific metabolic pathway where synthetically prepared high xylose media are used, pentose fermentations has only had implications in the ethanol industry through being a secondary metabolite in co-fermentations. With the advent of cellulysis of cellulose sources, the liberation of pentose sugars has become of greater interest as a way of increasing yield through removal of xylose repression in *Sacch.* spp. and secondary metabolism rather than liberation as a primary metabolite.

### **2.2.6. Comparison to hydrocarbons**

Fermentation carbon sources have focussed on the available carbon sources of the time. With the majority of microbes capable of fermenting hexose sugars, glucose has been the primary feedstock of choice in many industrial applications. With monomeric and some polymeric saccharides being of use in human (and animal) nourishment and price fluctuations due to crop yield and climate, alternative carbon sources have been used. For petrochemical derived carbon sources, historically this had been hexadecane due to the low cost of production at times of low oil prices. Price sensitivity has now reduced its use to only specific high value fermentations or as an addition to saccharide based fermentations [55]. Regardless of microbial capability, exploitation of hydrocarbon based fermentations is accepted as either niche product formation or of limited scope. Where advances have been made, has been for toxin remediation where microbial biodegradation has been used for oil spills to aid the clearing of contaminated soils and sands. As hydrocarbon fermentations do not address the problems of availability, price acceptance, climate change or energy independence, no further comment is required.

### **2.2.7. Inhibitory elements**

In the degradation of lignocellulose to its base components, a number of inhibitor elements are released into the media that can act either as catalyst inhibitors or exhibit toxicity to the fermentative micro-organism. The common lignin derived inhibitors are grouped into two functional groups of furan aldehydes (furfural ( $C_5H_4O_2$ ) and 5-hydroxymethylfurfural (HMF,  $C_6H_6O_3$ )), aliphatic acids (acetic ( $C_2H_4O_2$ ), formic ( $CH_2O_2$ ) and levulinic acid ( $C_5H_8O_3$ )) compounds [56, 57]. Without inhibitor removal the inhibition of microbial fermentation will reduce yields below theoretical maximum. The inhibitors produced vary in composition and abundance depending on prior processing methods. In the instance of acid derived hydrolysates (including auto hydrolysis through liquid hot water pretreatment), a high degree of acidic inhibitors are produced (formic, acetic, levulinic acids for example) [58].

Of particular notice is the feedback system of vanillin on BGL. At vanillin ratio of 4 mg to 1 mg protein (0.5FPU), BGL activity is retarded by 50% [59]

In the hydrolysis of cellulosic materials (post pretreatment and washing), the hydrolysis of cellulose itself produces end product feedback pathways upon the cellulase enzymes. Cellobiose is known to a cause of cellulase inhibition and can be alleviated by excess BGL addition [60].

### 2.3. Biological degradation of post pre-treatment ligno-cellulosic materials

Many billions of tons of cellulosic material are reduced to their constituent parts annually through natural microbial metabolism. In this section, the natural process of enzymatic degradation is examined from the excretion of lignin degrading lignases and associated mediators through to BGL action on cellobiose for glucose production. The conclusion drawn from this section shows that although important, the mineralisation from lignases is not sufficient for rapid biomass conversion. Cellobiohydrolase (CBH) and BGL are the rate limitation points in white rot fungi and are therefore of most interest in enhancement [51, 52, 61-63].

Post pre-treatment, lignocellulosic materials require hydrolysis of the hemicellulose and cellulose fibres for complete depolymerisation. Cellulose is a homopolyglucan chain producing a high yield of glucose monomers ( $(C_6H_{10}O_5)_n + nH_2O \rightarrow nC_6H_{12}O_6$ ) post lysis. Hemicellulose is a heteropolyglucan structure yielding a heterogeneous monosaccharide hydrolysate, (predominantly xylose, with arabinose, galactose and mannanm). Biological degradation of cellulosic materials through enzyme hydrolysis (EH) is accepted as a low energy process in the biotechnology industry. The required enzymes are CBHI and CBHII (endo- and exo-glucanases), and BGL [2, 51, 52, 61].

In contrast to chemical and physical processing, the addition of biological based agents to the media is desirable due to the milder conditions required, therefore reducing the overall production cost. As such, industrial scale production of cellulolytic preparation on a bulk scale has been achieved through two methods. These are;

- Development of hypercellulytic fungal strains (site-directed and random mutagenesis)
- Recombinant bacterial strains (fungal gene expression in recombinant *E. coli*)

To date the commercialisation of a number of enzyme preparations have been shown to be economically viable, specifically marketed at the biofuel industry by the biotechnology companies Danisco A/S and Novozyme A/S. In addition to the current product catalogue of enzymes, there are a large number of enzymes in development stages with greater thermal stability and  $K_m$  values, from a wide range of biological sources due to strain improvement, site-directed and random mutagenesis and bioprospecting.

In this section, the focus will be on the enzymes that are primarily from fungal origins that have an active role in the reduction of cellulosic materials to glucose. To show complete fungal processing, the upstream biological process of lignin degradation is included. Due to

glucose being the primary carbon source in metabolism, the process of glycolysis (glucose through to pyruvate) is the primary focus. Also illustrated is the xylose feed in for the utilisation of hemicellulose.

Enzymatic interactions with lignocellulosic mass are shown in Figure 11. Although the process is present in the natural environment as part of carbon metabolism, the process, even in the most favourable conditions, is slow.

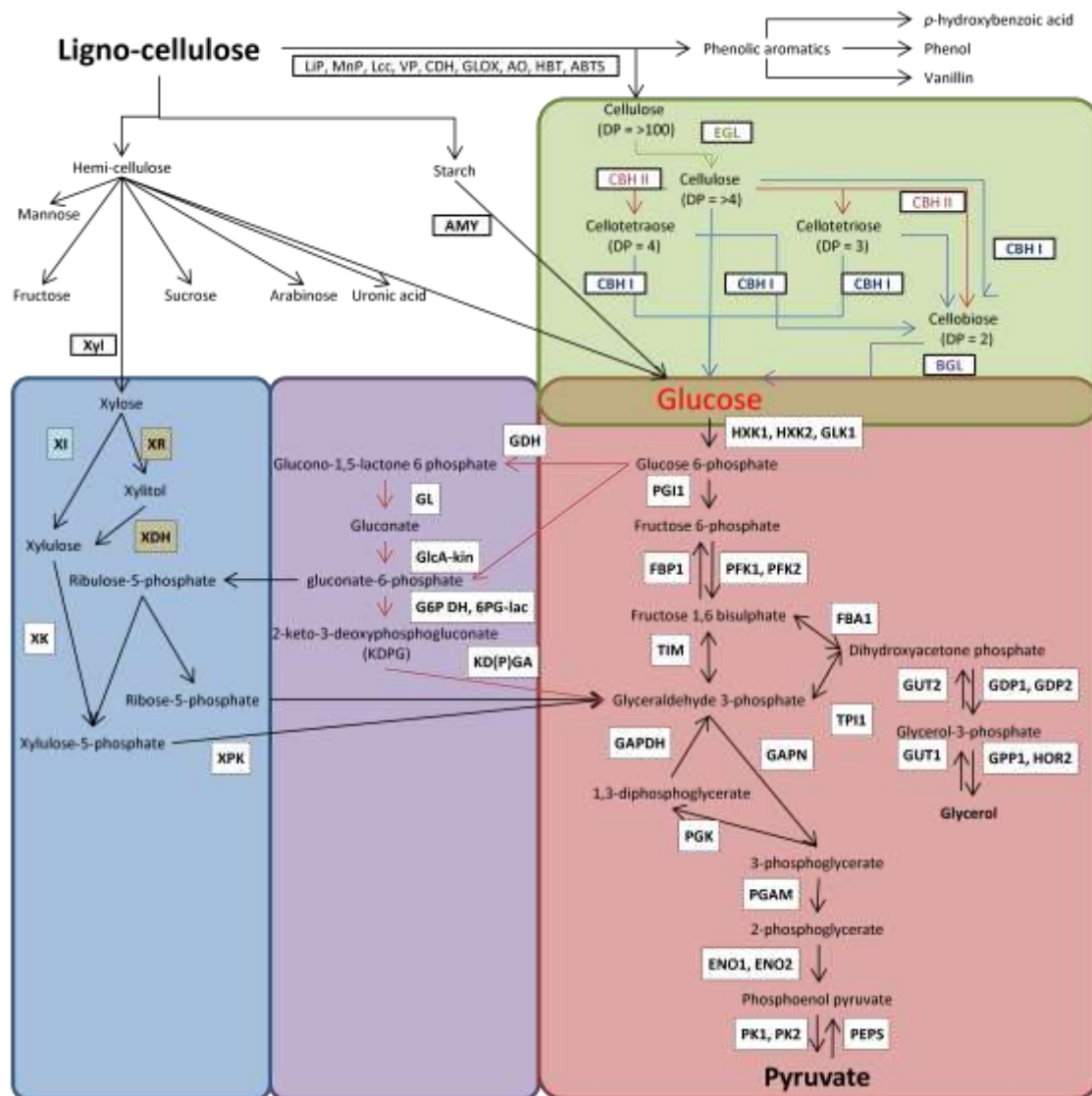


**Figure 11. Biological degradation of biomass**

Overall pathways. NOT representative of a mechanistic system, but of all possible scenarios. Green area shows the degradation of cellulose through the cellulase pathways. Blue box shows pentose pathway with xylose shown as the example. Enzyme box in blue shows prokaryote pathway, green shows eukaryotic pathways. Purple box highlights Entner-Doudoroff pathway (glucose to GL6P and G3P to pyruvate not highlighted but included). Red box shows Glycolysis. Diagram shows the enzymatic sequence of degradation from a biological mass through to pyruvate. All boxes indicate the enzyme require for that particular conversion. Double ended arrows indicate reversible reactions. Reaction pathway is ceased at pyruvate for indication of inclusion into the Calvin cycle. Final conversion of pyruvate to ethanol omitted due to absence of evidence as a viable pathway in native microbial species (eukaryotes). Primary focus is on the conversion of glucose. Additional sugars are illustrated although conversion is not included. Abbreviations; ABTS - 2,2'-azino-bis-3-ethylbenzothiazoline-6 sulphonic acid (mediator); AMY - amylase (EC 3.2.1.1); AO - Aryl-alcohol oxidase (EC 1.1.3.7); BGL -  $\beta$ -glucosidase (EC 3.2.1.21); CBH - cellobiohydrolase (EC 3.2.1.91); CDH - cellobiose dehydrogenase (EC 1.1.99.18); EGL - endoglucanase (EC 3.2.1.4); ENO - enolase (EC 4.2.1.11); FBA - fructose-1,6-bisphosphate (EC 4.1.2.11); FBP - fructose-1,6-bisphosphatase (3.1.3.11); G6P DH - glucose-6-phosphate dehydrogenase (EC; 1.1.1.49); 6PG-lac - 6-phosphogluconoalctonase (EC 3.1.1.31); GAPN - non-phosphorylating GAP dehydrogenase (EC 1.2.1.9); GAPDH - glyceraldehydes-3-phosphate dehydrogenase (EC 1.2.1.12/13); GLK - glucokinase (EC 2.7.1.2); GLOX - Glyoxal oxidase (EC 1.15.11); GUT - glycerol-3-phosphate dehydrogenase (EC 1.1.5.3); HBT - 3-hydroxyanthranilate 1-hydroxybenzimidazole (mediator); HOR - glycerol-3-phosphate (EC 1.1.1.8); HXK - hexokinase (EC ; 2.7.1.1); KD(P)GA - KD(P)G aldolase (active on KDG as well as KDPG; EC 4.1.2.-); Lcc - Laccase (EC 1.10.3.2); LiP - Lignin peroxidase (EC 1.11.1.14); MmP - manganese dependent peroxidase (EC 1.11.1.13); PEPS - Phosphoenolpyruvate carboxykinase (EC 4.1.1.32); PGAM - phosphoglycerate mutase (EC 5.4.2.1); PGI - glucose-6-phosphate isomerase (EC 5.3.1.9); PGK - phosphoglycerate kinase (EC 2.7.2.3); PK - pyruvate kinase (EC 2.7.1.40); PKF - phosphofructokinase (EC 2.7.1.11); TIM - triosephosphate isomerase (EC 5.3.1.1); TPI - triphosphate isomerase (EC 3.5.1.1); VP - versatile peroxidase; XYL - xylase (EC 3.5.1.5). Diagram self produced using references from [64-66]

### 2.3.1. Lignase

Although strictly not involved in the depolymerisation of cellulose, biological degradation of lignin by lignase action complements industrial pretreatment exploration, so is included for the context of complete biological action. Ligninolytic organisms have the ability to degrade lignin in plant structures through the use of enzymatic and non-enzymatic lysis. In the biosphere, ligninolytic action is carried out by a small number of white-rot fungi. Lignin degradation is necessary for the alleviation of steric hindrance, to allow the access to the polysaccharide structures and not as a carbon source itself. As a result, the energy balance of ligninolytic interactions is neutral however the competitive advantage the microbe gains is the access to a metabolite source that would otherwise be inaccessible [64].

The degradation of lignin in the ligno-cellulosic complex comes from the aerobic oxidative process. The process of degradation involves one or more of the three extracellular enzymes, combined with other non-enzymatic processes for complete lignin mineralisation. The three key lignases found are; lignin peroxidase (LiP); Manganese dependent peroxidase (MnP); and laccase (Lcc). Together the three enzymes are often referred to as lignin-modifying enzymes (LMEs) [64]. Additional enzymes which have been studied in the complete degradation of cellulose have been versatile peroxidase (VP), cellobiose dehydrogenase (CDH), glyoxal oxidase (GLOX), aryl-alcohol (AO) and other H<sub>2</sub>O<sub>2</sub> generating enzymes [67]. These are summarised in Table 6.

| Enzymes   | Abbreviation | Enzyme recognition code. |
|---|--------------|--------------------------|
| Lignin peroxidase                                       | Lip          | E.C. 1.11.1.14           |
| Manganese dependent peroxidase                          | MnP          | E.C. 1.11.1.13           |
| Laccase   | Lcc          | E.C. 1.10.3.2            |
| Versatile peroxidase                                    | VP           | E.C. 1.11.1.16           |
| Cellobiose : Quinone oxidase                            |              | E.C. 1.1.5.1             |
| Cellobiose dehydrogenase                                | CDH          | E.C. 1.1.99.18           |
| Glyoxal oxidase   | GLOX         | E.C. 1.2.3.5             |
| Superoxide dismutase                                    |              | E.C. 1.15.11             |
| Glucose oxidase   | GO           | E.C. 1.1.3.4             |
| Aryl-alcohol oxidase                                    | AO           | E.C. 1.1.3.7             |
| <b>Mediators</b>  |              |                          |
| 3-hydroxyanthranilate                                   |              |                          |
| 1-hydroxybenzotriazol                                   | HBT          |                          |
| 2,2'-azino-bis-(3-ethylbenzothiazoline-6 sulfonic acid) | ABTS         |                          |

**Table 6. Lignin degrading enzymes and mediator compounds.**

Adapted from Pointing [64]

For lignin mineralisation, LiP is believed to be a major factor in the rate determination. The production of LiP deficient strains through gene knockout has shown the rate of lignin breakdown vastly decreases in laboratory based studies, indicating the importance of LiP [67].

### 2.3.2. Swollenin

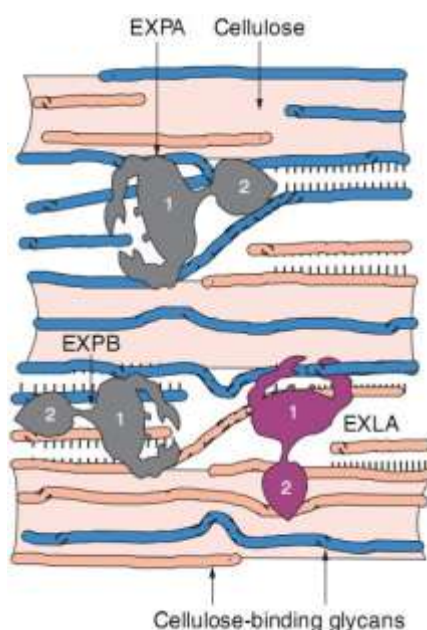


**Figure 12. A simplified model of the plant cell wall and its loosening by indigenous expansins.**

The cell wall consists of a scaffold of cellulose microfibrils (shaded areas) to which are bound various glycans such as xyloglucan or xylan (thin strands); together these polysaccharides form a strong, flexible, load-bearing network based on hydrogen bonds (indicated by rows of short lines). Extension of the cell wall entails movement and separation of the cellulose microfibrils by a process of molecular creep.  $\alpha$ -Expansins (EXPA) may promote such movement by inducing local dissociation and slippage of xyloglucans on the surface of the cellulose, whereas  $\beta$ -expansins (EXPB) work on a different glycan, perhaps xylan, for similar effect. Expansin-like A (EXLA) and expansin-like B (EXLB) proteins are predicted to be secreted to the cell wall, but their zactivity has not yet been established. Taken from [68]

Native to the plant material and embedded in the cellular structure, expansins are an often neglected mechanism in cellulose research. Expansins are a group of four protein subgroups ( $\alpha$ -expansin,  $\beta$ -expansin, expansin like-A and expansin like-B) that have been found in a range of plant cell walls. Shown to be the cell expansion mechanism for cell growth, expansins are hypothesised to have a role in the loosening the hydrogen bonds between cellulose chains to allow the expansion of the cellulose bundle for cell growth (the acid-growth response) (see Figure 12). Experiments carried out by McQueen-Mason, Durachko and Cosgrove on cucumbers have shown that with the addition of expansins to cucumber material subjected to tensional stress (extensometer methodology), an increase in span is observed over the negative control. With the same experimental procedures applied to tomato, pea, radish, lily, onion, maize and barley, extension is observed to varying degree depending on species suggesting a common action across the plant domain [69].

The mode of action in the fibre disruption is considered to be through the disturbance of the hydrogen bonds between cellulose microfibrils, or between cellulose and other cell wall polysaccharides. As a disruptive element, the protein appears to lack cellulytic activity, suggesting cellulose fibre expansion and alteration of plant morphology (seen in the ripening of fruits) over degradation for material recycling. Gene sequencing of expansins from a wide range of plant species implies protein sequence homology across the plant kingdom [70].

Investigation of cellulytic fungal and bacterial proteins has elucidated proteins with mechanisms homologous to the plant expansins. By expression, purification and concentration of the expansin analogues, the subjecting of cotton fibres to the protein preparation has demonstrated similarities in the alteration of fibre morphology (elongation and swelling of the fibre) without releasing reducing sugars, leading to the proteins being named swollenin. In sequence determination, unlike the plant expansins, swollenin has a modular structure with an endoglucanase domain and an expansins like sequence with an N-terminal cellobiose binding module (CBM). This suggests evolutionary commonality to the cellulase class of enzymes [70, 71]

Through gene sequencing, the swollenin proteins have shown distinct family classification and are now classified as  $\alpha$ -expansins [72]. Although thought to be exclusive to the plant kingdom, the expansin swollenin (SWO) has been identified in *Trichoderma reesei* along with another unknown homologous protein. In experimental work carried out by Saloheimo *et. al.*, gene knock out and suppression of the *Swo1* gene for SWO expression has shown that lack of SWO has no effect on the growth of the expressing micro-organism (*Trichoderma reesei* in this case). This has indicated that the expression of swollenin in the process of cellulose degradation is for the purpose of degradation, and not the cellulytic organism's cell growth [70].

### 2.3.3. Cellulases

In microbial digestion ligninolytic action occurs in conjunction with cellulytic action of the cellulase class of enzymes. "Cellulase" enzymes catalyse the hydrolysis of cellulose to the monosaccharide constituents through the use of a cocktail of cellulase enzymes. For fungal degradation, saprophytic filamentous fungi produce three classes of secreted glycoprotein cellulases, based on hydrolytic activity [51, 52]. These are shown in Table 7.

|   | Common abbreviation  | Name                          | Cleaving position and product formed.   |
|---|--|-------------------------------|---|
| 1 | EGL  | Endoglucanases                | Random cleavage of $\beta$ -1,4-glucosidic bonds, away from the chain ends        |
| 2 | <br>CBHI<br>CBHII | Cel7A or cellobiohydrolase I  | Cleaves disaccharide cellobiose from the non-reducing end of the cellulose chain. |
|   |  | Cel6A or cellobiohydrolase II | Cleaves disaccharides from the reducing end of the cellulose chain                |
| 3 | BGL  | $\beta$ - glucosidase         | Hydrolysis of the cellulose and other short cello-oligosaccharides to glucose     |

**Table 7. Three key enzymes in cellulose depolymerisation**

Table generated by the author. Information sourced from [51, 60, 73-75].

or complete cellulose degradation all three enzymes are required, although protein structure and expression rates vary between microbial species. A schematic showing an illustration of the enzyme actions is shown in Figure 13 indicating swollenin action location, CBH family action, and the mechanism of induction feedback of cellulase expression. Table 8 contains full details of the enzymes discussed with accession numbers and EC codes.

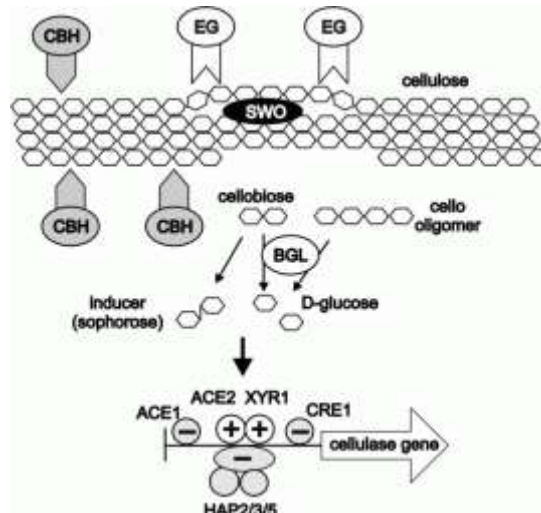


**Figure 13. Cellulose degradation through the use of enzyme cocktails and gene expression feedback.** Basic structural diagram of cellulose degradation by the four key enzyme complexes. Swollenin (SWO) disrupts the crystalline cellulose structure. Endoglucanase (EG) is seen as the mid chain cutter, cellobiohydrolase (CBH) acts on the reducing and non-reducing ends of the cellulose fibre releasing cellobiose. For the complete mineralisation of the cellobiose, β-glucosidase lyses cellobiose and cello oligomers to glucose. In the process, sophorose (β1-2 linked glucose dimer), cellobiose and lactose present induce the transcription of the cellulase genes. [76, 77].

| Gene        | Enzyme         | CAZy Family | Function             | Length * | Molecular mass, kDa | pI value (range) | Km value (range) | Accession Number | EC code  | CAS registration number | Ref      |
|-------------|----------------|-------------|----------------------|----------|---------------------|------------------|------------------|------------------|----------|-------------------------|----------|
| cbh1/cel7a  | CEL7A (CBHI)   | GH7         | Cellobiohydrolase    | 513      | 59-68               | 3.8 – 6          | 0.46 – 543       | P00725           | 3.2.1.91 | 37329-65-0              | [78]     |
| cbh2/cel6a  | CEL6A (CBHII)  | GH6         | Cellobiohydrolase    | 471      | 50-58               |                  |                  | M16190           | 3.2.1.91 | 37329-65-0              | [79]     |
| egl1/cel7a  | CEL7B (EGI)    | GH7         | Endo-1,4-glucanase   | 459      | 50-55               | 7.5 – 3.7        | 0.19 - 15.4      | M15665           | 3.2.1.4  | 9012-54-8               | [80]     |
| egl2/cel5a  | CEL5A (EGII)   | GH5         | Endo-1,4-glucanase   | 418      | 48                  |                  |                  | M19373           | 3.2.1.4  |                         | [81]     |
| egl3/cel12a | CEL12A (EGIII) | GH12        | Endo-1,4-glucanase   | 234      | 25                  |                  |                  | AB003694         | 3.2.1.4  |                         | [82, 83] |
| egl4/cel61a | CEL61A (EGIV)  | GH61        | Endo-1,4-glucanase   | 344      | 34                  |                  |                  | Y11113           | 3.2.1.4  |                         | [84]     |
| egl5/cel45a | CEL45A (EGV)   |             | Endo-1,4-glucanase   | 242      | 23                  |                  |                  | Z33381           | 3.2.1.4  |                         | [85]     |
| bgl1/cel3a  | CEL3A (BGL1)   | GH3         | $\beta$ -glucosidase | 744      | 75                  | 3 - 8.5          | - 200            | U09580           | 3.2.1.21 | 9001-22-3               | [86, 87] |

**Table 8. Enzyme accession numbers of previously described CAZymes that occur in clustered area**

\* Length of the protein including signal peptide and amino acid residues. Molecular mass determined from amino acid sequence [88, 89]

### 2.3.3. Endoglucanases (EGL)

$\beta$ -1,4-D-glucan glucanohydrolase, the endo-enzyme endoglucanase (EGL, EG or  $C_x$ ), cleaves the disordered amorphous region of the cellulose fibres. There are at least five known endoglucanases secreted by fungi - EGI to EGV. The lack of particular EGs are known to greatly reduce EG activity. EG enzymes hydrolyse glycosidic bonds mid-chain allowing quick fragmentation along the length of the polysaccharide chains, rapidly decreasing the degree of polymerisation (DP) of the substrate. In the process, the enzyme produces cellulose chains with varying length from  $2n$  through to  $>5000n$  (where  $n$  is the number of monomers), with the products themselves acting as inhibitors to cellulose hydrolysis [49].

In nomenclature,  $\beta$ -1,4-D-glucan glucanohydrolase is abbreviated to *egl* (gene) and EG for the enzyme. EG(n) is used to highlight the difference between the five accepted EG enzymes. In this document, the annotation of EG is through the use of the Roman numeral where EGI is synonymous with EG1, EGII is synonymous with EG2 etc. In published data and references, convention uses the systems of Roman numeral annotation, although the use of numeric is also seen.

With the example of *Trichoderma reesei*, EG1 represents around 5 – 10% of the total secreted protein. Whereas a lack of EGI will reduce total EG activity by around 25%, the lack of EGII is seen to reduce activity by around 55%. This has supported the account that the EGII is accountable for the majority of EG activity in *Trichoderma*. Within the industrial context of cellulase exploitation in the biofinishing of denim materials, the use of EGII has been seen to be the most effective on a enzyme rate basis [90].

The EGI protein has homology to the CBH protein, with 70% conservation at the C terminus, 45% total homology and with 437 amino-acid (aa) residues and a 22-aa long signal peptide. This indicates that the two enzymes have arisen from common ancestry. As the two proteins conserve homology in the C terminus region, EGI contains six suggested *N*-glycosylation sites and a suggested *O*-glycosylation site that show a similarity to the orientation of the CBH-1 protein, implying evolutionary divergence. Penttilä *et. al.* illustrate how it is suggested that the EGI sequence is derived from the CBHI sequence through the deletion of four separate 10-20 aa deletions [75].

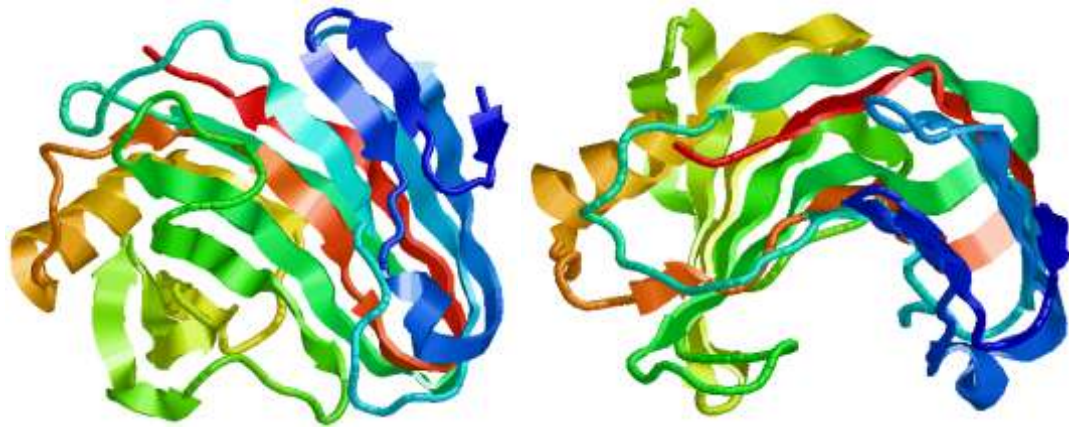


**Figure 14. RASMOL image of CEI12A.**

Left image shows the protein as seen across the beta-sheets. Right images viewed along the binding domain. Colours signify group [91].

### 2.3.4. Exogluconase / Cellobiohydrolases (CBH)

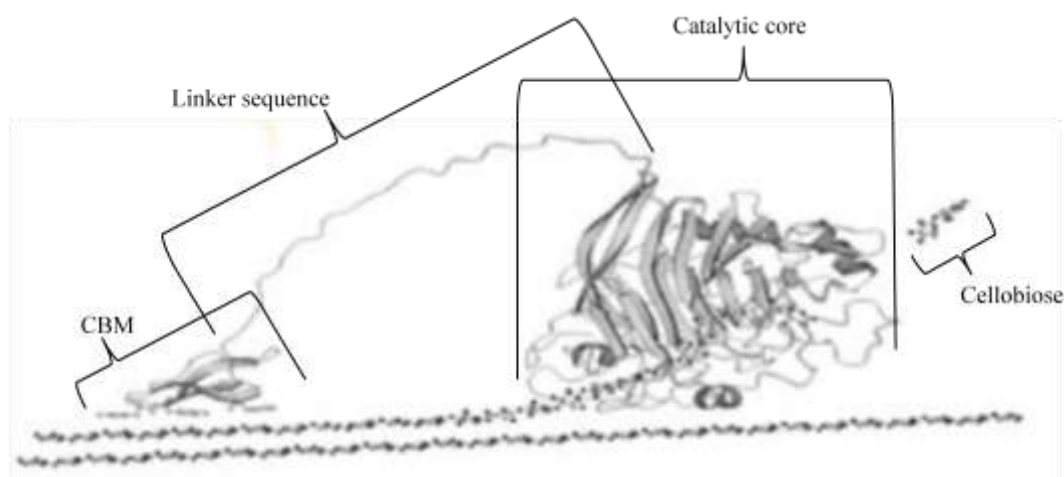


**Figure 15. Cellobiohydrolase II in complex with cellulose**

Cellobiohydrolase (CBHII) in complex with cellulose, showing the three-dimensional configuration of the enzyme and substrate. Two cellulose fibres are shown with the lower chain as native, while the upper chain is hydrolysed. The Cellulose Binding Module (CBM) is observed bound to the cellulose fibre on the left of the image. The peptide linker sequence is observed bridging between the CBM and the catalytic core domain (seen on the right). With the CBM involved in the adhesion to the chain, it is also hypothesised that the CBM is involved in the partial lifting of the chain from the fibre bundle. Once the chain is directed into the catalytic domain, the catalytic head cleaves the chain into cellobiose for the instance of CBH II. Image adapted from [92]

The two cellobiohydrolases used in the degradation of cellulose are  $\beta$ -1,4-glucan glucohydrolase (CBHI) and  $\beta$ -1,4-D-glucan cellobiohydrolase (CBHII). CBHI sequentially cleaves one glucose molecule from the non-reducing end. CBHII cleaves two bound glucose molecules (cellobiose) from the reducing end [49, 74]. Working in synergy with EG, the increased shearing caused by EG hydrolysis allows a greater number of cellulose chain ends to be reduced by CBHI and CBHII. In cellulase inducing conditions, around 80-85% of the total protein expressed extra-cellular are cellobiohydrolases, with CBHI accounting for between 50-60%, and CBHII accounting for around 25% of the total secreted protein from the wild type *Trichoderma reesei* [2, 93].

Structurally, the CBHI family of enzymes have three structural features and two key functional domains, summarised by Table 9 and Figure 15.

| Structure                       | Function   |
|---------------------------------|--|
| <b>Cellulose binding module</b> | Binding of the CBH enzyme to the cellulose fibre. Hypothesis raised of possible lifting through “wedging.” Suggestion of lifting a single fibre into the catalytic core. |
| <b>Linker</b>                   | Peptide link between the CBM and catalytic core  |
| <b>Catalytic core</b>           | Contains the catalytic tunnel – position of hydrolysis   |

**Table 9. CBH structures**

As cellulose hydrolysis requires a multiple enzymatic approach, there are more intermediate steps than the classical enzyme kinetic model. The major steps are shown in Table 10

| Step | Process   | Ref      |
|------|---|----------|
| 1    | Adsorption of cellulases onto the substrate via the binding domain  | [94]     |
| 2    | Location of a bond susceptible to hydrolysis on the substrate surface (chain end if CBH, cleavable bond if endoglucanase)   | [95]     |
| 3    | Formation of enzyme-substrate complex (by threading of the chain into the catalytic tunnel if CBH, to initiate hydrolysis)  | [96, 97] |
| 4    | Hydrolysis of $\beta$ -glycosidic bond and simultaneous forward sliding of the enzyme along the cellulose chain.  | [96, 97] |
| 5    | Desorption of cellulases from the substrate or repetition of step 4 or step 2/3 if only the catalytic domain detaches from the chain  |          |
| 6    | Hydrolysis of cellobiose to glucose by $\beta$ -glucosidase (if present in the enzyme mixture). In addition, product inhibition and substrate changes in properties along the course of the hydrolysis effects the above steps. |          |

**Table 10. Progression of cellulase action**

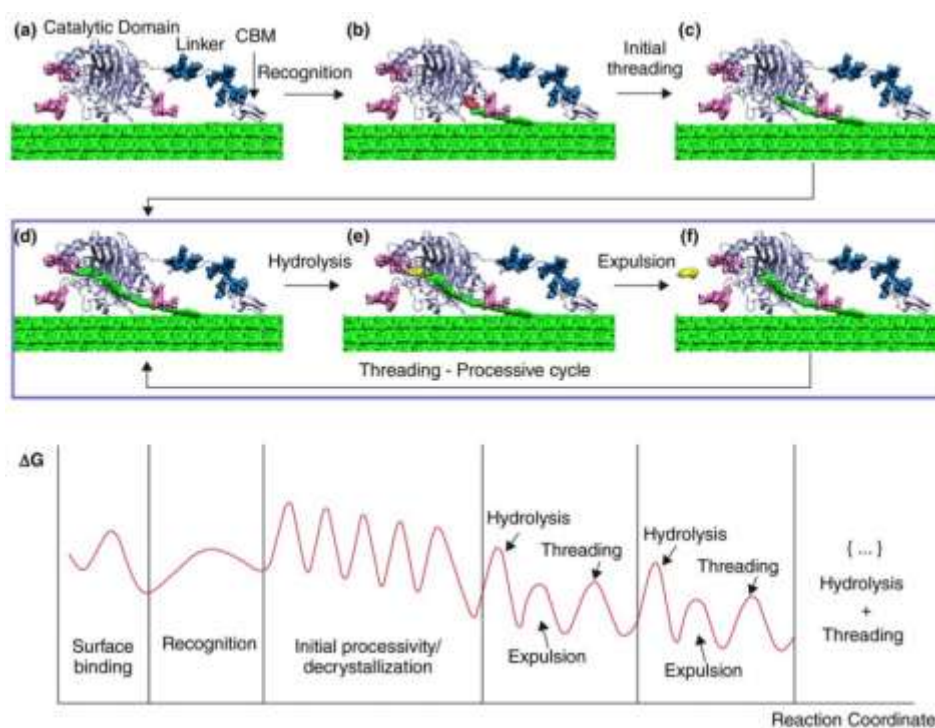


**Figure 16. CBH processing**

The *Trichoderma reesei* Family 7 cellobiohydrolase (Cel7A) acting on cellulose. Cel7A is comprised of a 36-aminoacid CBM, a linker domain with O-glycan (dark blue), and a large catalytic domain with N-linked glycan (pink) and a 50-Å tunnel for processing cellulose chains (green). The cellobiose product is shown in yellow (e) and (f). Here we show the putative steps that Cel7A takes to deconstruct biomass and the hypothesized free energy surface for each elementary step. Taken from [98]

## Cellulose Binding Module (CBM)

The CBM's role in hydrolysis is the binding to the substrate and disruption of the cellulose chain and promoting the association of the enzyme with the substrate (therefore lifting the effective enzyme concentration) (see Figure 15, Figure 17 and Figure 18)[99]. Three current hypotheses for the mode of action are discussed, although acceptance of each theory varies. Common to each theory is the substrate binding through three aromatic amino acid side groups located on a relatively planar surface. The total spread of the attractive sites equates to approximately 1.1nm, or 1 cellobiose unit in length. With the three aromatic side chains oriented in a linear plane and being hydrophobic on a hydrophobic cellulose chain, the dehydration of the cellulose/CBM binds without the aid of hydrogen bonding as seen in Figure 17 [99].

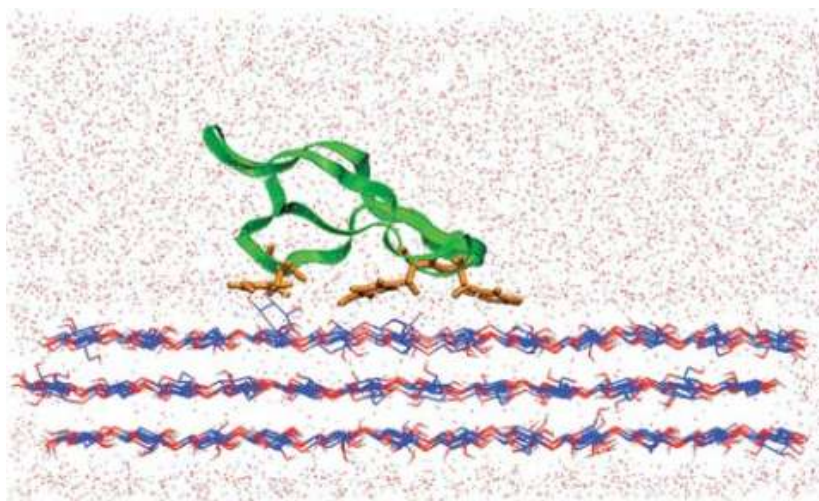


**Figure 17. CBM of a CBH family 1 in complex with cellulose**

View of the molecular components of a typical MD simulation of CBM acting on cellulose. The binding domain, shown as a green ribbon with the tyrosine residues in orange, is placed  $\sim 3$  Å above a three sheet slab of cellulose in a box of water molecules (dots) CBH direction of travel would be progressive left to right in this rendering. [99].

Once bound, the affinity of the cellulose to the binding site is hypothesised to lift the cleaved chain away from the bulk surface and towards the CD (Figure 15). In both of these models, a similar mode of action is seen described as the “shaving” or “planing” of the bulk surface. Contrary to the description given by Hahn-Hägerdal *et. al.* and Minlos *et. al.* and many others and as seen in Figure 15, Mulakala and Reilly propose an alternative hypothesis where the CBM acting as a wedge placed below the chain being hydrolysed directs the fibre upwards, away from the cellulose surface, and into the catalytic domain. The energy required for forward movement and into the cleft is derived from the free energy available from the hydrolysis of the glycosidic bond. This is shown in Figure 18. [92, 97, 99]

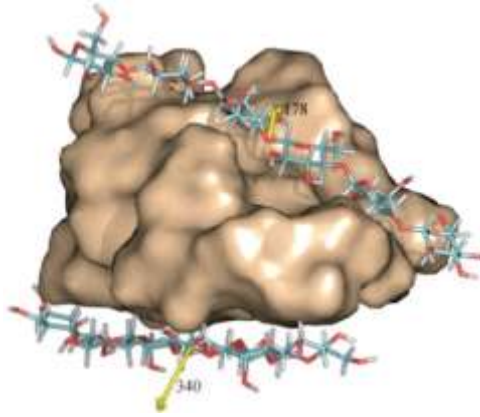


**Figure 18. Alternative mechanism of CBM behaviour**

Alternative hypothesis for CBM mode of action. Surface rendering of the CBM with wire structure rendering of the cellulose chain in the process of hydrolysis (upper chain) and chain still adhered to the cellulose fibre surface (lower chain) [97]

Another mechanism of action suggested by Arantes and Saddler has looked at the possibility of CBM migration into the cellulosic material. Suggested to occur at the initiation of CBH hydrolysis, the term amorphogenesis has been coined to describe a method of fibre disruption through CBM disruption other than that seen in the more generally accepted “shaving” or “planing” mechanisms. In the hypothesis put forward, the CBH CBM has loose association to the cellulose bulk. In recognition of micro-cracks in the microfibre, the CBM penetrates the cellulose fibre and becomes lodged within the interfibrillar space. The bulk of the CBH mass within the fibre causes mechanical pressure on the pore wall leading to water molecule ingress into the interfibrillar space, cleaving hydrogen bonds and forming free chain ends [100]. Although some plausibility is seen in the theory, the quantity of research built upon this hypothesis has not gained significant acceptance. In comparison with other mechanisms modelled, the mechanism appears less intuitive.

### **Linker sequence**

Consisting of a 27 amino acid sequence and maintaining the positional relationship between the catalytic core and the CBM, the Cel linker sequence is used for cellulase motion. The linker is considered to be an intrinsically disordered protein allowing flexibility for movement of the whole molecule [98, 101-103]. For progression, discussion has focussed on three hypothesis of movement. These are summarised as;

- The CBM moves at a rate higher than the CD therefore the linker acts as a “pulling” mechanism to drag the CD. CBM leading acts a ratchet mechanism preventing two directional movement
- The linker is inflexible and the system moves in accordance to the slowest constituent as a rigid molecule
- Molecular movement originates from the feeding of the cellulose fibre through the catalytic tunnel. The linker sequences “pushes” the CBM along the fibre

Through the sequencing of the linker sequence and computational analysis of the structure by the likes of Beckham *et. al.* [98] and Zhong *et. al.* [101] the hypothesis of the inflexible system is discounted immediately as there is insufficient mechanical rigidity to prevent linker folding. Work conducted by Zhong *et. al.* used computation methods to investigate flexibility of the linker system. In the modelling that they conducted, repetitive iterations of molecular movement based on free energy calculations, suggesting that the CBM lags the CD therefore inducing a “push” on the CBM with the force originating from the progressive threading of cellulose fibre through the catalytic tunnel [101]. This results in a creeping system where the total protein size varies between 2.5 and 5.5nm correlating to linker compression and extension (length by distance between domain centres is shown in Figure 19). These two stable states of the linker position are separated by a free energy difference of 10.5kcal/mol. The switching between to the two states is suggested to be through energy storage and release similar to a spring mechanism.

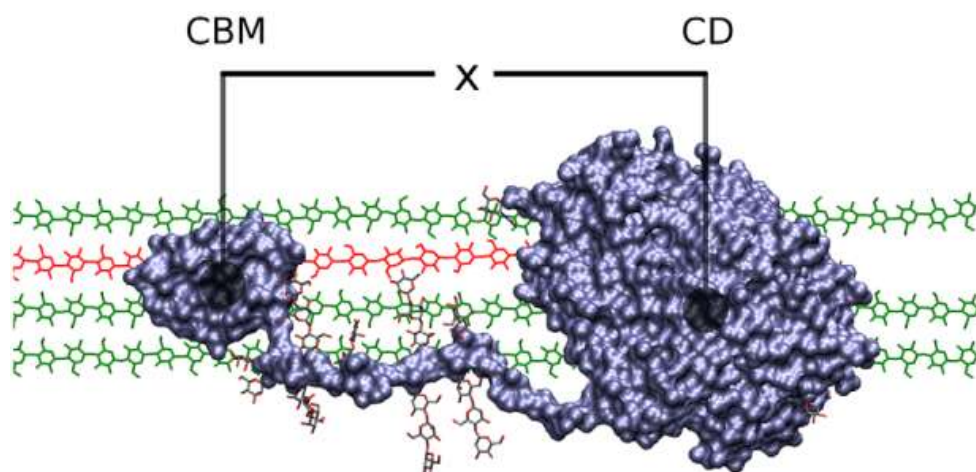


**Figure 19. Orientation and spacing of CBM-CD linker sequence**

Determination of cellulase movement by distance between domain centres. CBM – Cellulase binding module; CD – catalytic domain; X – distance between domain centres where molecule is at rest. Green fibre indicates fibres within a cellulose bundle. Red fibre is the cellulose fibre in the process of catalysis [104].

The mechanism described is shown in Figure 20, and works through a repetitive sequence. In the images reproduced, Cel7A with cellulose catalysis occurs within the catalytic tunnel (1). The total length at this point will equate to 5.5nm. The expulsion of cellobiose from the CD (2) allows further fibre threading, causing linker sequence to flex due to CD movement, compressing the linker into its compressed state. The total length of the molecule reduces to 2.5nm (3) with energy stored within the linker sequence. Upon exceeding the free energy barrier of 10.5kcal/mol, the linker returns to the extended position, pushing the CBM along the cellulose fibre. Once completed, the sequence is repeated along the length of the cellulose chain.

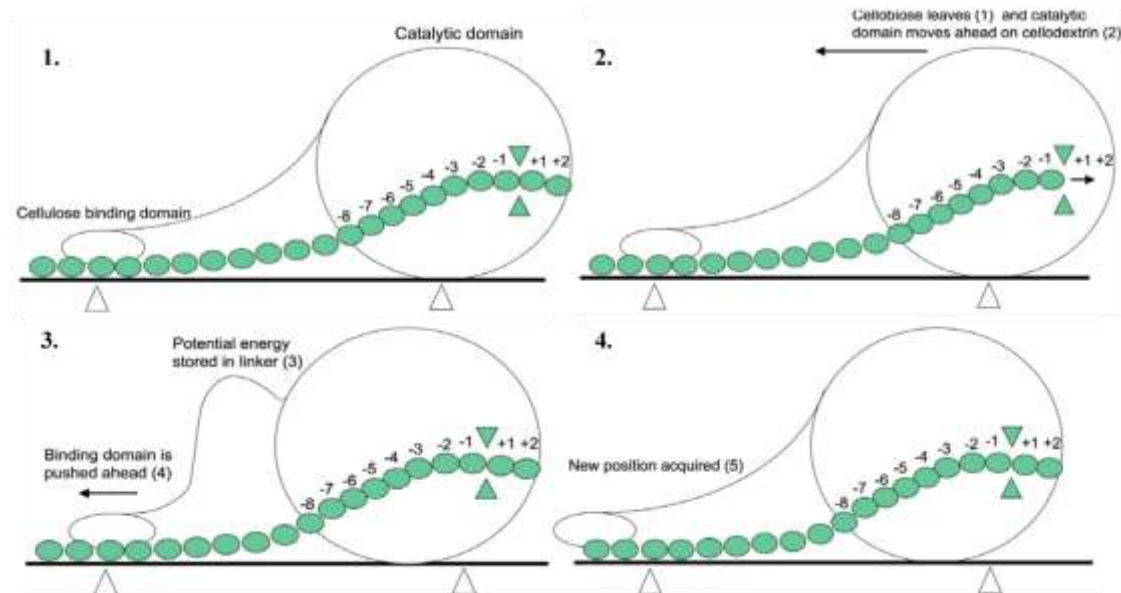


**Figure 20. Proposed Cel7A progression as hypothesised by Zhao *et. al.***

Illustration of Cel7A progression. Adapted from [105]. Cel7A with catalysis occurring within the catalytic tunnel (1). Total length = 5.5nm. Expulsion of cellobiose from the CD (2) allows further fibre threading, causing linker sequence to flex due to CD movement to a compressed state. Total length reduces to 2.5nm (3) with energy stored within the linker sequence. Upon exceeding the free energy barrier of 10.5kcal/mol, the linker returns to the extended position, pushing the CBM along the cellulose fibre (Adapted from [105]).

## Catalytic core

Regardless of the three previous models suggested, hydrolysis of the cellulose chain occurs within the catalytic tunnel continued in the catalytic domain. Following the lifting of the fibre away from the bulk, the cellulose chain is fed into catalytic tunnel consisting of a 50Å tunnel in CBHI and 20Å tunnel in CBHII. The cellulose fibre is held within the tunnel by residues -7 through to +4 where 0 represents where cleavage occurs. This is seen in complex in Figure 21 and from two differing faces in Figure 22 [62, 96],

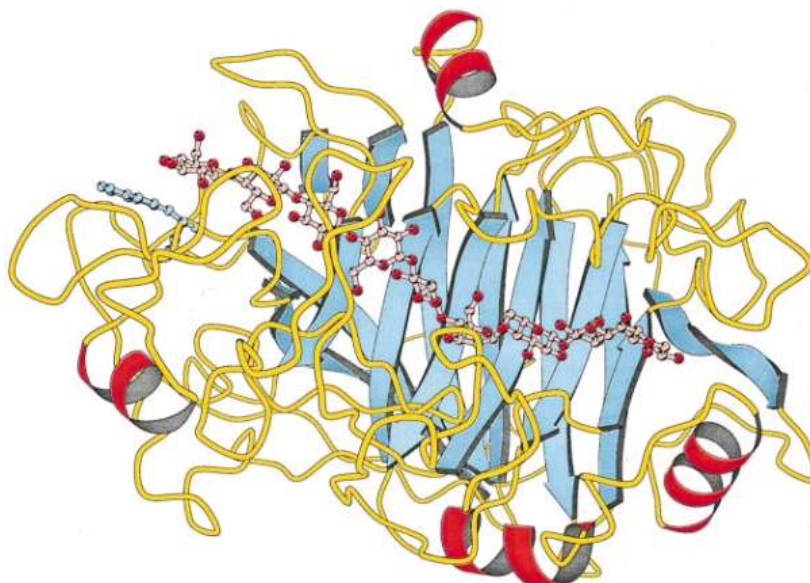


**Figure 21. Catalytic domain of CBHI in complex with cello oligomer**

Figure 1. Schematic representation of the CBHI catalytic domain with a cello oligomer bound in sites -7 to +2. Secondary-structure elements are coloured as follows:  $\beta$  strands, blue arrows;  $\alpha$  helices, red spirals; loop regions, yellow coils. The cello oligomer is shown in pink as a ball-and-stick object. The illustration was created with MOLSCRIPT [96]

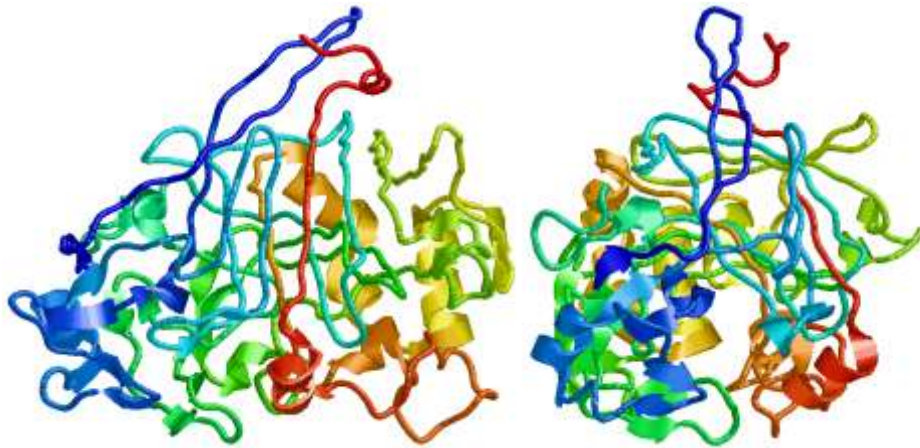


**Figure 22. RASMOL images of Cel7A catalytic domain.**

Left image showing three-dimensional orientation of amino-groups. Cellulose chain feeding is orientated left to right through the cleft with lysis product expelled to the right of the CD. Right image showing active site cleft orientated looking along the axis of the cellulose fibre. Forefront structures show fibre tunnel. Lysis products would be expelled to the rear of the CD in this rendering with the CD progressing towards the reader [106].

Work carried out by the Oak Ridge National Laboratory using 1,000-2,000 processors of “Jaguar” on the Laboratory Cray XT3 supercomputer has studied the induced fit adhesion of the enzyme to the cellulose fibre with a rate determination of one glucose molecule release per 100 nanoseconds. The method of progression shown in Table 10 and imagery produced by the ORNL study is shown in Figure 16 [99].

With the adhesion of the CBM to the cellulose chain, the pre-hydrolysis sequence of recognition and initial threading can proceed. Once threaded, the repetitive sequence of hydrolysis, threading and expulsion can be maintained for the length of the freely available chain.

### **Water location and action in the CBH system**

In the hydrolysis of cellulose by cellulase enzymes, water molecules play a crucial role in a number of locations. These are predominantly;

- Water movement into the catalytic domain for hydration in the hydrolytic event
- Hydrophobic nature of the CBM in relation to the cellulose fibre
- Movement of water molecules into the cleft created by the lifting of the cellulose fibre being cleaved
- Water molecules in association with the linker sequence

In the cleavage of the glycosidic bonding, the water molecule in close proximity to the hydrolytic event provides the hydroxyl group and the hydrogen ion for bond stability. The water is sourced from the aqueous media and moves through the catalytic domain to within the

catalytic tunnel, migrating into the catalytic domain via a channel positioned below the core [99]

The hydrophobic nature of the CBM causes an adhesion pocket around the CBM to form a loose association with the cellulose fibre. The affinity of the bonding is dependent on the hydrostatic pressure of the water molecules keeping the CBM in close proximity [99, 101, 107].

The cellulose fibre between the CBM and catalytic core is lifted from the bulk fibril and threaded into the catalytic core. In the process, water molecules move in to the cleft left by the lifted fibre (see Figure 23). For every four glucose molecules lifted, five water molecules move into the cleft [101].

In the proximity of the linker, a large number of molecules are held in association to the peptide chain. In addition to this, o-linked glycosylation of the peptide sequence incurs additional side chains, increasing the abundance of hydroxyl groups in this area [70].

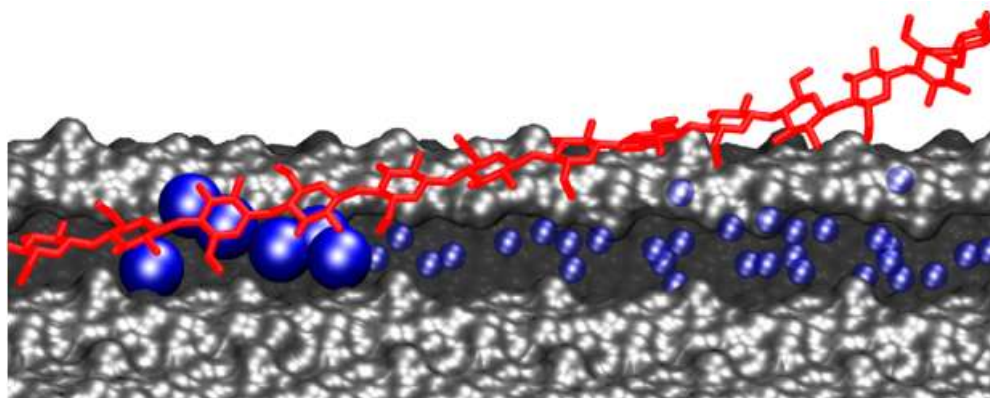


**Figure 23. Water ingress into the cellulose cleft in fibre lifting**

Blue spheres represent water molecules in the groove from which the cellobiose chain was pulled up. The large blue spheres represent the water molecules which are displaced when four glucose monomers reanneal. As presented in [101]

### **2.3.5. $\beta$ -glucosidases (BGL)**

$\beta$ -glucosidases (BGL) is not directly required in the digestion of cellulose material; however it is required in the hydrolysis of the cellobiose intermediate to glucose. For utilisation of the glucose in the TCA cycle, the dimeric glucose molecule of cellobiose cannot be used, therefore to metabolise the cellulose fully, BGL has to be present to release the glucose monomers.

Although BGL is not directly essential for metabolism as CBH will liberate glucose for glycolysis, its inclusion in metabolic pathways prevents a significant feedback product inhibition choke point caused by the accumulation of cellobiose [74].

Capable of hydrolysing both di- and oligosaccharides, the enzyme has significance in the lifting of feedback repression of the CBH/EGL system.

### **2.3.6. Cellulase enzyme quantification/qualification**

In the catalysis of cellulose by cellulase enzymes, the reaction rate and yield limitations have been subjected to a number of studies in practical and computational terms. Of relevance to this study is the understanding of the termination of catalysis, possible mechanisms for stopping, and a method of modelling the affect seen.

Activity loss in the cellulase system has been hypothesised to have been the result of a number of mechanisms. Chiefly, these have been implicated to be;

- the CBHs becoming stuck on the substrate surface due to a crystalline effect defect, or when surrounding cellulose chains prevent further processive action [108]
- Enzyme jamming on the substrate surface resulting in hydrolysis rate reduction [109]
- negligibly reversible cellulase binding [110]
- non-productive binding in of absorbed cellulase [111].

Additional speculative (and studied) areas of retardation are highlighted by Nidetzky and Steiner [112] as possibly from;

- Thermal instability of the cellulases
- Strong product inhibition by cellobiose and/or glucose
- Inactivation of the absorbed enzyme due to diffusion into the cellulose fibrils
- Transformation of the substrate into a less digestible form
- The heterogeneous structure of the substrate itself



catalytic cleft. Assuming that the CBH progression will occur along the length of the chain until cleavage ends with disengagement at the end residue, the substrate length will vary from polysaccharides in the order of  $DP_n = 20$  through to  $DP_n = >4000$ . As concluded by Xu and Ding [109], when an immobilised reactant or enzyme has restriction of diffusion and collision on an inert carrier, the system can be described with a “fractional” (fractal) dimension, rendering a more peculiar behaviour.

Väljamäe *et. al.* explore the fractal exponent of the catalysis through a relationship to the rate coefficient,  $k$ . Where  $k$  is time dependant and related to the rate constant  $k_1$  by  $k = k_1 t^{-h}$  where  $h$  is the fractal exponent. In normal, non-fractal systems,  $h$  is assumed to be 0, therefore  $k$  is constant. For fractal kinetics,  $h = \sim 0.3$  [102].

As the solubility of cellulose varies with time course, the  $[S]$  term is dynamic in accordance to  $t$ . As such, the process can be considered as the sum of two or more pseudo-first-order reactions due to the presence of oligomers of various sizes, enzyme inactivation and adsorption parameters. Work carried out by Jervis *et. al.* (using fluorescence-labelled substrate with Cel7A) showed that the 2-D diffusion of the enzyme on the cellulose surface was not the rate limitation [95].

In terms of physical parameters, a number of indicators of fractal behaviour can be indicated. As the protein sizes in CBH cleavage is considerably larger than the chain dimension, in a one dimensional system the CBH geometry leads to the opportunity of “jamming” whereby CBH content has insufficient degree of movement for passing (see Figure 25, top) [109].

In light of CBH working synergistically with EGL, the number of free ends for threading has significance over rate. With the CBH CBM having affinity for free substrate adhesion, specificity of location is not mechanistically mediated. As such, CBH CBM is not homogeneously distributed on cellulose surfaces (see Figure 25). By having a varying  $[S]$ , the opportunity for incorrect CBM affinity increases as  $[S]$  reduces, consequently  $[E]$  decreases with increased E inactivation. At lower  $[E]$  values, this will lead to yield limitations once all E is immobilised, inactivated or jammed.

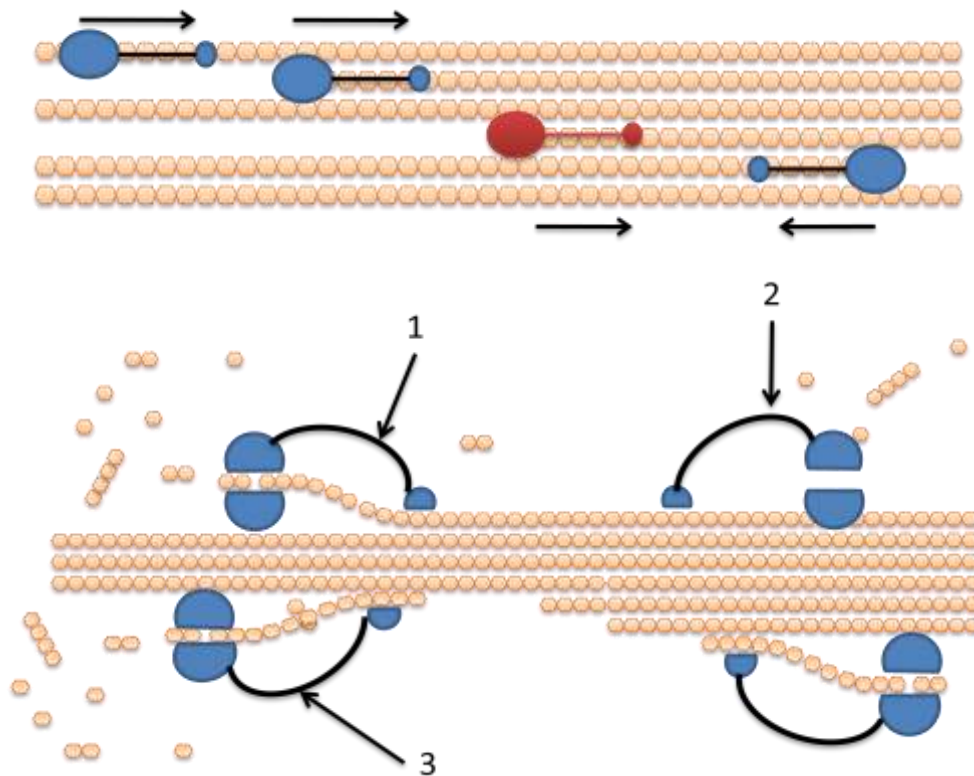


**Figure 25. Physical catalysis constraints**

Illustration of physical limitations in cellulase affinity to substrate catalysis. Blue objects represent the cellulase (CBH) enzymes in proximity to the cellulose fibre.

Top; Fractal jamming from protein obstruction and inactivation. “Aerial view” of enzyme and substrate. Red CBH highlights where jamming will occur with CBH catalysing from the opposite end, reducing catalytic rate by a half.

Bottom; Enzyme inactivation by substrate jamming. “Portrait view” of enzyme and substrate (cellulose). Enzyme 1 shows the expected threading of the cellulose chain through the catalytic core with progression towards enzyme two. Enzyme two shows the CBM affinity to the cellulose fibre without free chain end for catalytic core threading, rendering the enzyme inactive in catalysis. As the enzyme 2 affinity will prevent enzyme 1 progression by physical objection, enzyme 1 and 2 will be inactivated. Enzyme 3 shows catalysis nearing completion of polymer chain. As such, release and adhesion will govern successive rate progression.

For empirical determination of rate considering catalysis as a fractal like kinetic analogue of pseudo first order reactions, the product concentration ( $p(t)$ ) can be expressed as Equation 1.

$$p(t) = [S]_0 \cdot [1 - \exp(-k \cdot t^{(1-h)})]$$

**Equation 1. Fractal kinetics as per product concentration**

where  $p(t)$  is the concentration of released cellobiose ( $\mu\text{M}$ );  $[S]_0$  is the initial concentration of cellulose represented as cellobiose units ( $\mu\text{M}$ );  $t$  is time,  $k$  and  $h$  are empirical constants [102].

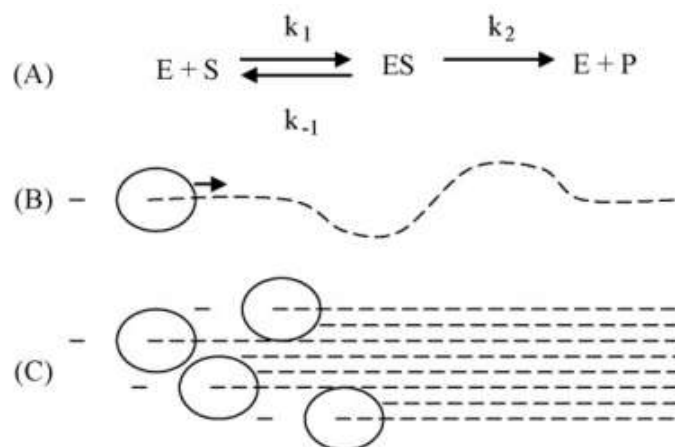


**Figure 26. Mechanistic hydrolysis of cellulose by CBH**

Schematic Michaelis, fractal, and “jammed” reactions. (A) Michaelis scheme. E, enzyme; S, substrate; ES, Michaelis intermediate; P, product. (B) Fractal scheme for an enzyme (ellipsoid) acting on chained substrates (dashed curve). The enzyme binds to the chain through its active site tunnel. After cleaving off a substrate unit (bar), the enzyme slides along the chain (in the  $\rightarrow$  direction) for the next catalytic cycle. (C) “Jammed” scheme for enzymes (ellipsoids) acting on substrate chains (dashed lines) that are packed orderly with defined spacing. Being “oversized” in comparison to the inter-chain space, the enzymes anchored on adjacent chains may jam each other [109].

## 2.4. The ethanol biorefinery

Exploitation of the technologies discussed in this thesis is dependent on both the raw feedstocks used and integration into the process chain (raw feedstock preparation, pretreatment, hydrolysis, fermentation, product recovery and dispatching). For illustration of the process train and where this research project relates to the total process, Figure 27 is shown. The streamlining of the system into the minimal number of unit operations, or conjoining the process to other product streams, is paramount for commercialisation. In light of this, the development of the biorefinery concept as a model system has been developed with the all-new build facilities having the concept integrated from planning. In existing facilities, the biorefinery concept is often adopted with facility expansion, upgrades and modification. In this chapter, the four key systems (separate hydrolysis and fermentation, simultaneous hydrolysis and fermentation, simultaneous saccharification and co-fermentation and consolidated bioprocessing) are set out from the established and implemented SHF, through to the target process of CBP.

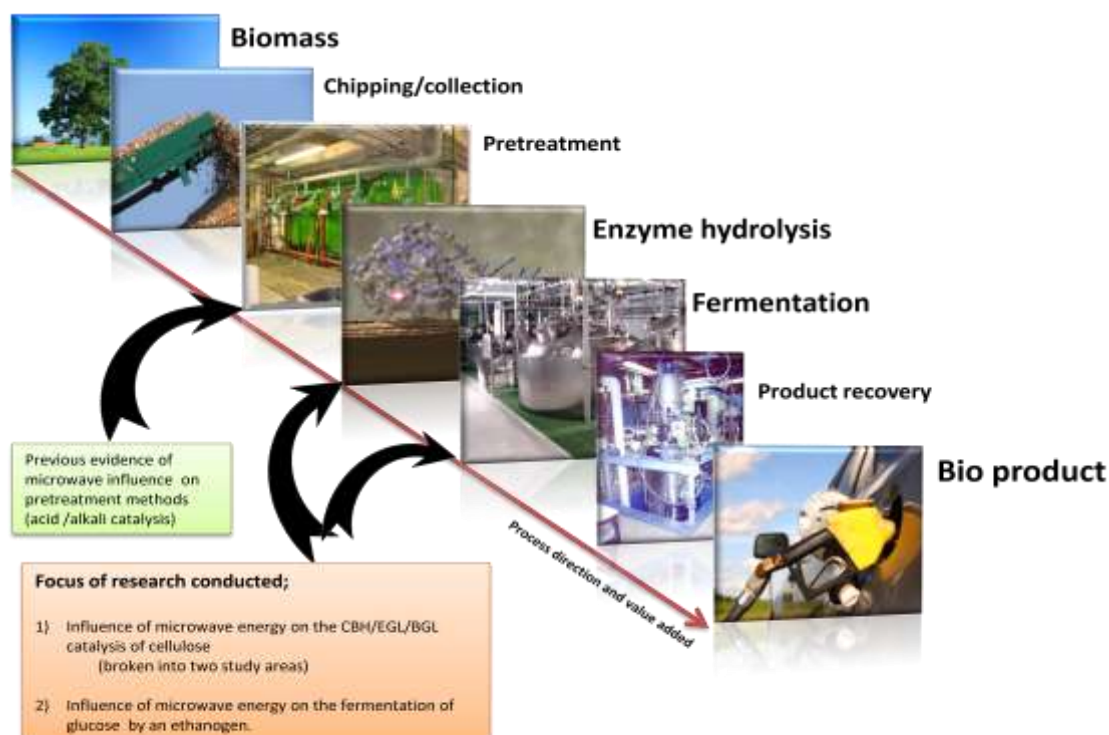
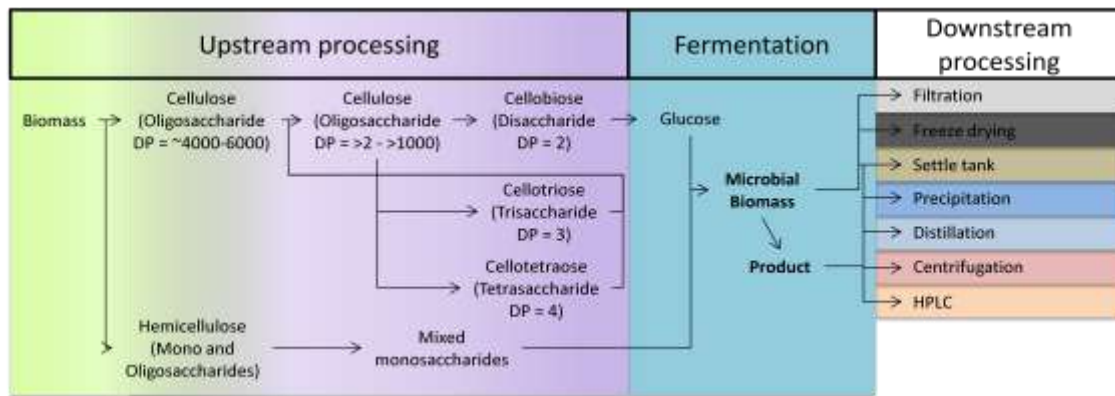


Figure 27. Bioproduct processing train.

A biorefinery concept is analogous to the mineral refining model widely adopted by both the petrochemical and commercial chemical industry. The biorefinery is an infrastructure facility which uses various conversion methods for the production of higher value commodities from lower value biological feedstocks [22, 118, 119]. The products formed vary depending on the refinery design and particular target market. Products range from high value niche fine chemicals and pharmaceuticals to mass-produced commodities such as liquid fuels, organic materials and bioplastic precursors [120]. The process will involve the bioconversion using a fermentative micro-organism or cell line. The term biorefinery is commonly used as generalised term for the place of biofuel production although this is not exclusively the case [120-122].

The majority of biorefinery production plants use either a single low-value/high-volume product process or multiple high-value/low-volume processing methods depending on infrastructure. The current motivation in biorefining is the production of facilities that are akin to mineral oil refineries where a single low value feedstock is used for multiple products of varying value. Within the whole series of processes, minimal waste is produced. By employing integrated cascade of processing methods, secondary products and wastes can be used as primary feeds in subsequent product processing. This process integration brings increased efficiencies and reduces capital, production and product cost across the bioprocessing industries (a prime example for this minimal waste and cascade processing is the British Sugars refinery in Wisington, UK).

By means of reference to feedstock cost and commercial competitiveness with mineral analogues, the Brazilian method of refining sugar cane for processing to either bioethanol or succinic acid is typified, showing how plant flexibility accommodates market fluctuations. Linking feedstock constraints to commodities prices, switching product to a more profitable product with common equipment when the operating margin prevents profitability makes greater economic sense. For the processing of biomass to product, the pre-treatment processes upstream of fermentation may be seen as a common system with multiple carbon feed-in points depending on feedstock availability or price. During fermentation, the value added product is formed before final downstream processing is used for product purification. When pretreatment and fermentation systems can be common to a product range, the process cost is reduced. This is illustrated in Figure 28.



**Figure 28. From Upstream to downstream processing in a biomass based biorefinery**  
 Illustration of the biorefinery principle. Biomass input is pretreated by physical and thermo-chemical means (green) prior to enzymatic saccharification (purple). All processes undertaken (green and purple areas) are under the classification of “Upstream processing.” Once glucose liberation has occurred, fermentation is carried out for biological product formation (turquoise). For product recovery from the spent fermentation media, the common methods of liquid and solid mass recovery are shown in varying colours. All processes post fermentation are termed “Downstream processing.”

With the upstream and fermentation processes for final product preparation a commonality, method developments in these areas have been considerable. The processing methods of separate hydrolysis and fermentation (SHF), simultaneous saccharification and fermentation (SSF), simultaneous saccharification and co-fermentation (SSCF) and consolidated bio-processing (CBP) are illustrated in Figure 29 and discussed in the subsequent sections. For complete process block diagrams, see Appendix pages 18 –22.

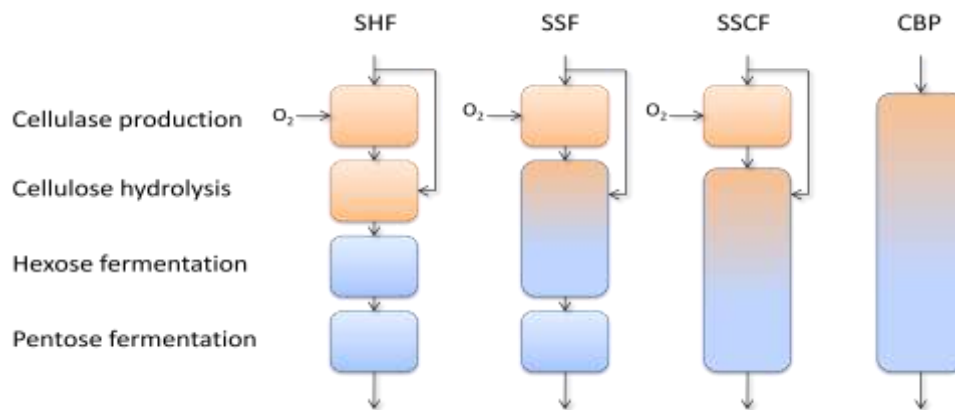


**Figure 29. Comparative overview of four cellulosic ethanol processing methods.**  
 Each block represents a unit operation of physical processing. Abbreviations; SHF - separate hydrolysis and fermentation; SSF - simultaneous saccharification and fermentation; SSCF - simultaneous saccharification and co-fermentation; CBP - consolidated bioprocessing. Although based on unit operations, the procedure of each individual unit may not signify a separate infrastructure or physical unit. Colour representation indicates degree of polymerisation of the cellulosic material; peach colour illustrating high degrees of polymerisation; blue illustrating mono- to oligo- saccharides.

### 2.4.1. Separate Hydrolysis and Fermentation (SHF)

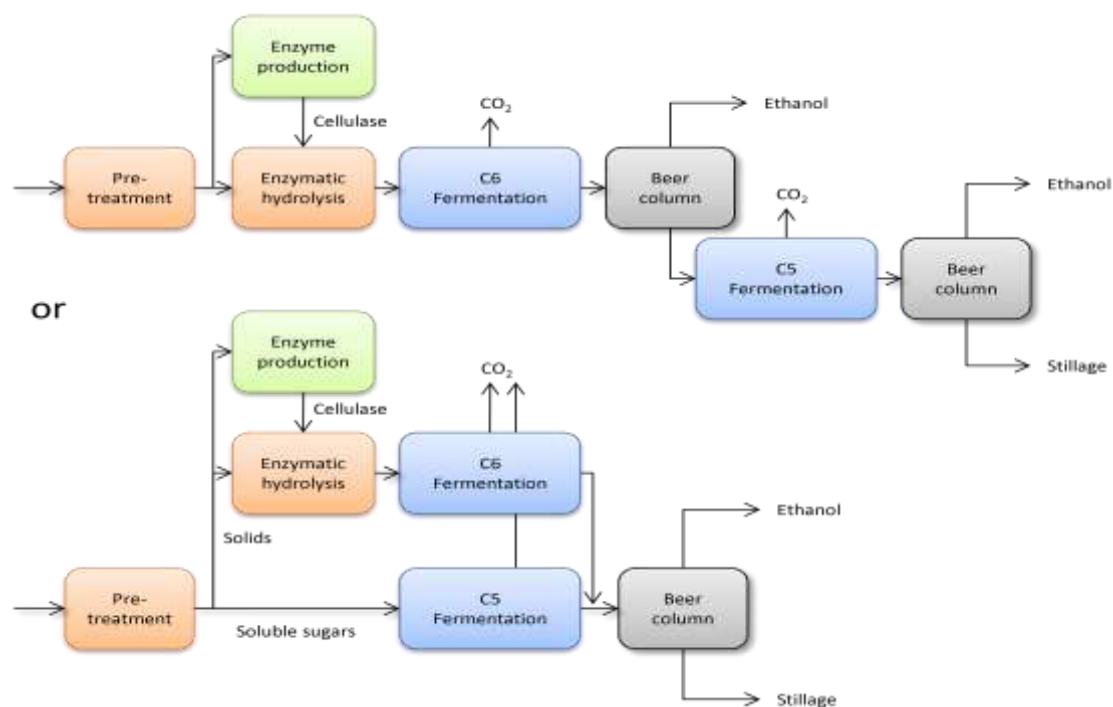


**Figure 30. Schematic representation of Separate Hydrolysis and Fermentation**

Top diagram represents a serial fermentation approach while the lower illustrates a parallel approach. Colour key; Orange/Pink; Pre-treatments and depolymerisation processes, Blue; Fermentation processes, Grey; Product recovery. Images adapted from [2]

Separate Hydrolysis and Fermentation (SHF) is defined as a two step process conducted as sequential unit operations. Post pre-treatment, the cellulosic substrate is hydrolysed with the addition of complementary enzymes followed by a fermentative stage. The actual practicalities of carrying out SHF are often less distinct in physical processing as the hydrolysis carried out in the same vessel in which fermentation will occur is still seen as two distinct steps (see Figure 29) [2]<sup>4</sup>.

Cellulase enzymes have a temperature range of  $>1^{\circ}\text{C} - \sim 70^{\circ}\text{C}$  with an optimal temperature of between  $25$  and  $70^{\circ}\text{C}$  depending on origin. Peak efficiency is observed at around  $55$ - $62^{\circ}\text{C}$  and pH  $4$  to pH  $5$  depending on enzyme source [123]. By having a two stage consecutive process, the primary reaction vessel can heat the substrate and enzyme mixture to the enzyme's optimal temperature. With the exception of thermophilic bacteria, this temperature is significantly higher than the tolerance of common fermentation cultures'. Variations within the system at this point also include filtration to remove insoluble fractions prior to fermentation and/or chemical measures to re-optimize the solution for fermentation [2, 123].

For complete hydrolysis, the vessel will be held at between  $60^{\circ}\text{C}$  and  $65^{\circ}\text{C}$  for a pre-determined time period depending on enzyme concentration, substrate type and particle size,

<sup>4</sup> For expanded and total process illustrations, see Appendix pages 19 and 20

and desired yield. The vessel and lysate is then cooled, or the hydrolysate is pumped to a further reactor via a heat exchanger to achieve the optimal fermentation temperature. Addition of an ethanogen starter culture begins the fermentation process.

Post hydrolysis, one of two methods will be employed for fermentation with respect to the hexose and pentose sugars contained within the hydrolysate. Currently in order to achieve close to maximum theoretical yield, the pentose and hexose mono- and disaccharides will be fermented with two different ethanogens either in a serial or parallel system (dual C5/C6 ethanogens may do this in a single fermentation although solvent production is less favourable) [2, 51, 52].

Common practice in SHF where serial fermentation methods are used, the liberated sugars will be initially fermented using a *Saccharomyces* spp. for C6 fermentation. Following fermentation, the spent media will undergo downstream processing for product recovery before a C5 fermentation, followed by a second product recovery procedure. In a parallel system, both C5 and C6 ethanogens will be used prior to a single distillation or recovery process (see Figure 30).

Advantages gained through using a SHF process are; increased yield associated through the hydrolysis being carried out at the enzyme's optimal temperature and the ability to reduce the time required for complete hydrolysis. Hydrolysis is commonly accepted as the rate limiting step. The energy required in processing is reduced due to a high yield being obtained. However, the deficiency of the process is the solubilisation of excessive amounts of glucose and cellobiose in the media causing end-product inhibition of cellulolytic enzymes reducing efficiency with yield [2]. Additionally, the intermediate saccharide rich hydrolysate produced requires sterile handling to prevent opportunistic colonisation prior to ethanogen inoculation. This limitation has led to the consolidation of SHF in to SSF, analogous to the principle seen in nature where metabolism is coupled to the hydrolytic rate

## 2.4.2. Simultaneous Saccharification and Fermentation (SSF)

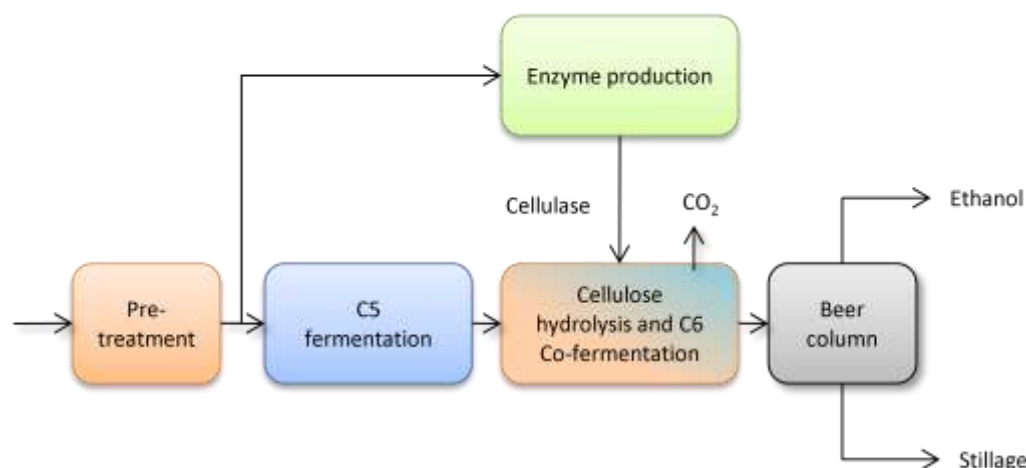


**Figure 31. Schematic of Simultaneous Saccharification and Fermentation**

Schematic highlights the sequential unit operations of hemihydrolysis through various means prior to C5 fermentation, and utilization of the free C6 monomers and cellulose for biomass increase in cellulytic enzyme production. Protein recovery of the cellulytic enzymes media is used in the subsequent cellulose fermentation downstream of the initial C5 fermentation. Ethanol recovery from the beer column is undertaken with standard methods. Simultaneous in this instance refers to the application of cellulytic enzymes being used in the same unit operation as the C6 fermentation. Schematic adapted from [2]

Simultaneous Saccharification and Fermentation (SSF) refer to combined unit operations of enzyme hydrolysis and C6 fermentation within the same vessel and time frame. In contrast to the SHF, enzymatic hydrolysis in concurrent fermentation removes product inhibition by alleviating cellobiose build up in the reactor vessel [26, 124]. With glucose being liberated at a similar speed to fermentation rate, glucose inhibition is removed (see Figure 29 and Figure 31). The advantages gained by using a SSF approach is the increased yield obtained in a short time period due to the prevention of feedback loops. As such, the enzyme requirement is reduced and the process does not require as stringent conditions due to the reduced prospect for opportunistic colonization. The disadvantage of the process is the incompatibility of the enzyme and microbial optima, although solvent and thermotolerant microbial strains are being developed to reduce the temperature difference. In this process it is worth noting that the enzyme production can be considered an offline fermentation in parallel to the desired product formation. As SSF is derived from SHF, two fermentation methods (serial and parallel) can be exploited [124]<sup>5</sup>.

<sup>5</sup> For expanded and total process illustrations, see Appendix page 21

### 2.4.3. Simultaneous Saccharification and Co-Fermentation (SSCF)

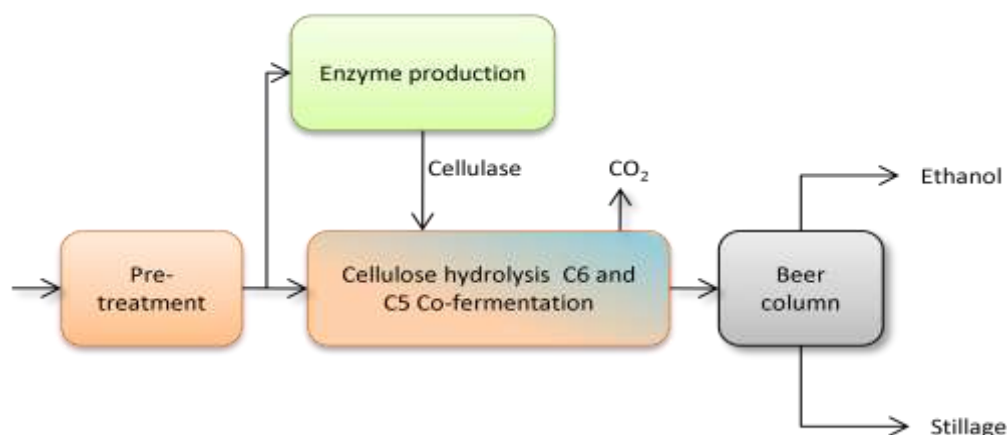


**Figure 32. Schematic of Simultaneous Saccharification and Co-Fermentation (SSCF)**

Schematic highlights the sequential unit operations of hemihydrolysis, cellulose hydrolysis and combined C5 and C6 fermentation. Ethanol recovery through the beer column is conducted under standard methods. Schematic adapted from [2]

SSCF is a development of SSF through the co-fermentation of both the C5 and C6 saccharides in the same fermentation media at the same time as saccharification (Figure 32)<sup>6</sup>. Through the co-fermentation method, the enzymatic hydrolysis continuously releases hexose sugars which increases rate of glycolysis to promote increased pentose fermentation rate. This increases the total production yield [2]. Processing difficulties arise in the balancing of C5 and C6 fermentations with hydrolytic rate.

A number of research lead groups have attained SSCF as a process in principle with a variety of feedstocks and microbial combination, each with their own merits and high yields of conversion. The review paper published by Cardona and Sanchez gives details of several research groups which have shown promise [125].

For development of the SSCF system, thermal compatibility in the process mechanisms is a significant problem. To address this issue, the research focus has been in the consolidated of product expressions within the microbes used, and the increase in thermal tolerances to unify elevated processing temperature.

<sup>6</sup> For expanded and total process illustrations, see Appendix page 21

## 2.4.4. Consolidated BioProcessing (CBP)

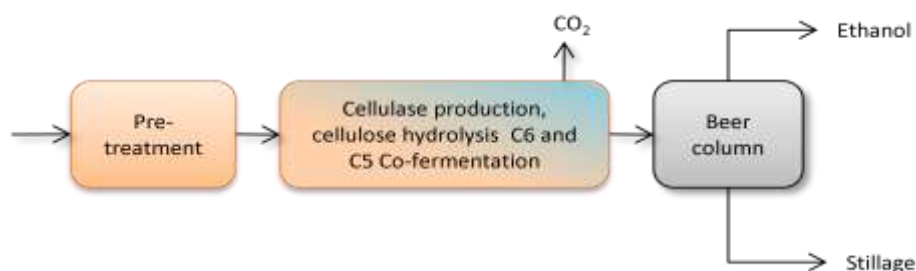


**Figure 33. Schematic of Consolidated Bioprocessing (CBP) fermentation**

Schematic highlights the consolidation of both the saccharification and fermentation processes into a single unit operation. Variation on CBP depends on the method of process combination.

CBP has the greatest opportunity for commercial feasibility through the consolidation of enzyme production into the fermentation method (see Figure 33)<sup>7</sup>. The exploitation of thermophilic bacteria, co-fermentations or recombinant yeast and/or bacteria, the method of CBP has seen feasibility abate currently at low yields. Due to the methods of manipulation and optimization that are becoming available, multiple analogues of CBP are being developed on the same principle (see Table 11).

| Methodology  | Comments  | Development point   | Ref            |
|--|---|---|----------------|
| <b>Thermophilic bacteria</b>                               | High temperature fermentation. Continuous process with simultaneous saccharification, hexose and pentose fermentation. Low ethanol yield. Ineffective in batch operations.  | Pilot scale   | [51, 126-128]  |
| <b>Cellulytic yeast co-fermentation</b>                    | Near ambient temperature fermentation with consolidated cellulytic enzyme production with C6 fermentation into a single yeast species. Co-fermentation with C5 fermentative yeast for increased yield. Greatest yield per unit substrate per unit time with batch fermentations. Possibility of continuous fermentation with development of ethanol selective filtration/membrane technologies. | Research based only, missing experimental proof of concept. No success to date. Technical difficulties with expression stability. | [51, 129, 130] |
| <b>Cellulytic yeast with combined C5 and C6 metabolism</b> | Development of above. Currently theoretical due to issue with genetic manipulation of the number of genes required. Theoretically highest yield at lowest operation cost.   | Extremely complex process. So far, limitations have prevented success.  | [131-134]      |

**Table 11. Comparison of Consolidated Bioprocessing methods.**

Table showing a comparison between the three platform technologies expected to be at the core of the CBP commercial exploitation.

<sup>7</sup> For expanded and total process illustrations, see Appendix page 22

In the implementation of CBP, reactor conditions are varied depending on the microorganism(s). In the instance of an ethanogenic thermophile, the reactor vessel is maintained at between 60-70°C for both optimal hydrolysis and fermentation. In contrast, recombinant yeast reactor vessels will be maintained between ambient and 35°C prior to ethanol recovery.

The advantages associated with CBP focus on the simplicity of the design (see Figure 33) and the movement towards the “one-pot” solution where minimal processing costs are associated. Through enabling enzyme secretion to be coupled to biomass density and product formation, the regulation of inhibition feedback is reduced to a level where inhibitor intermediates within the metabolic reaction sequence are metabolized before they have time to accumulate in the media. Additional advantages are the reduced contamination threats due to very strict media selection pressure. This allows only microbial content capable of respiring in the vessel being cellulolytic or capable of pentose metabolism.

CBP has the highest potential yield of each system due to the minimal inhibitor products produced. The process can be controlled with minimal input requirements, exploiting the anaerobic/aerobic pathways used in ethanogens. Microbial cell density can be optimised with partial aeration used to extend fermentation in a fed batch manner. A fermentation process using CBP may consist of staging the fermentation in a single vessel and controlling growth, respiration and product formation through aeration ( $K_{La}$ ). Though the process of complete respiration, the cellulolytic ethanogen would be promoted to produce cellulolytic enzymes through the substrate inducing expression, therefore increasing microbial biomass. With the increase in microbial biomass, extra cellular enzyme expression is increased. On reaching a specified cell density, oxygen repression would create anaerobic conditions causing a diauxic shift in cell metabolism, leading to ethanol formation.

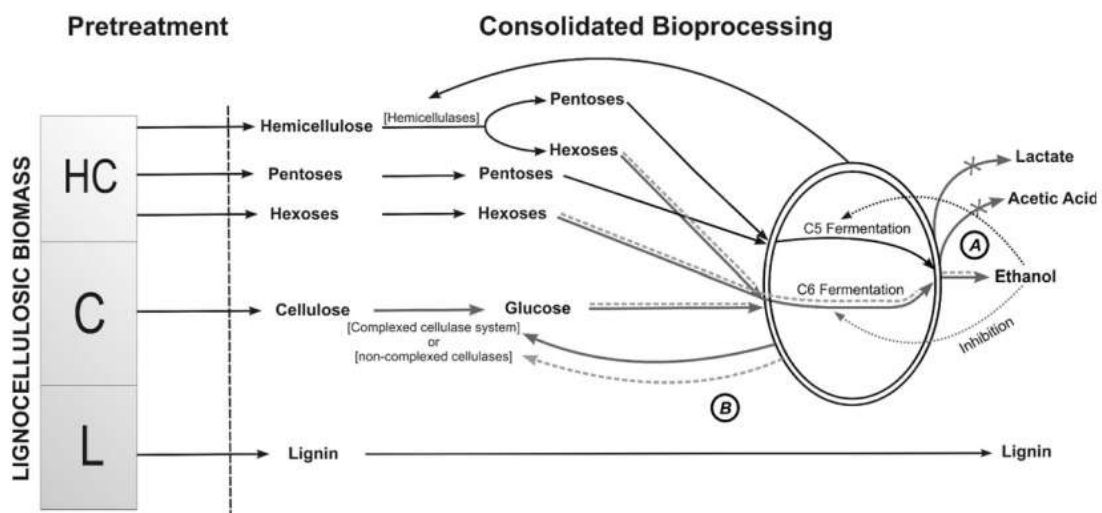


**Figure 34. Conceptual scheme of consolidated bioprocessing**

(a) Native cellulolytic strategy. (b) Recombinant cellulolytic strategy. HC, hemicellulose; C, cellulose; L, lignin. Processing pathway for a thermoanaerobic microorganism (e.g. *Clostridium thermocellum*) is indicated by continuous gray lines. Processing pathway for an ethanogenic microorganism (e.g. *Zymomonas mobilis*) is indicated by dotted lines.

### 2.4.5. Product recovery

As all processes describe produced an ethanol rich spent media, recovery of the ethanol content will be dependent on the product concentration. Downstream solvent recovery would be conducted through standard industry practices or through zeolite recovery, microwave volatilisation, low pressure distillation or selective membrane filtration. Lewandowicz *et. al.* [135] have developed a novel and promising method of membrane distillation, Chen *et al.* [136] highlight a number of classical and developing separation methods while Dias *et. al.* [137] review a number of established methods. These technologies are well documented and out of the scope of this project report.

### 2.4.6. Industrial adoption

The methods of SHF, SSF, SSCF and CBP have all been proven at the bench scale. For commercial purposes, only SHF has had scaled success. For acceptance as an industrial practice, as number of key parameters are considered.

- Scalability
  - Scale up (vertical scaling) in comparison to scale out (horizontal scaling). What are the volumetric limitations incurred and how does this balance unit operation residence times?
- “Bad batch” impact
  - What is an affordable volume loss in a single worst case scenario? Does increase in complexity to achieve sterility outweigh benefit from optimal unit conditions for hydrolysis?
- Infrastructure cost
  - How flexible is the system on product or is it “locked in” in processing? If process complexity increases, how does this reflect in both hardware and software development for control?
- Operation complexity
  - Through the consolidation of unit operations, associated complexity and operational risk increases. With the operational complexity (also related to infrastructure complexity) comes the greater risk of “bad batch” loss or down time due to integration to reduced infrastructure.

For a comparison of operational complexity in the various process modes, complete system configuration for SHF, SSHF, SSCF and CBP are illustrated with processing schematics assuming completion of a pretreatment stage prior to input in the appendix. Key side chain processes and material recycling are shown. An empirical comparison is shown in Table 12.

| Process           | Micro-organism                     | Consumed/Lost <sup>a</sup> | Conversion efficiency               |                      |                     |  |
|-------------------|------------------------------------|----------------------------|-------------------------------------|----------------------|---------------------|--|
|                   |                                    |                            | Cellulose <sup>b</sup> →<br>Ethanol | Glucose →<br>Ethanol | Xylose →<br>Ethanol | Mannose, Galactose,<br>Arabinose → Ethanol |
| SHF <sup>c</sup>  | <i>S. cerevisiae</i> (recombinant) | Cellulose 6%               | 75%                                 |                      | 85-90%              |  |
| SSF <sup>d</sup>  | <i>S. cerevisiae</i> (recombinant) | Cellulose 6%               | 80%                                 | 92.5%                | 80-92%              |  |
| SSCF <sup>e</sup> | Cellulase <sup>f</sup>             | Cellulose 5%               | 88%                                 |                      |                     |  |
|                   |                                    | Sugars 5%                  |                                     |                      |                     |  |
|                   | <i>Z. mobilis</i> <sup>g</sup>     | Glucose 4%                 |                                     | 92%                  |                     |  |
|                   |                                    | Xylose 3%                  |                                     |                      | 85%                 |  |
|                   |                                    | CSL                        |                                     |                      |                     | 90%  |
| All sugars 7%     |                                    |                            |                                     |                      |                     |  |
|                   |                                    |                            |                                     |                      |                     |  |
| CBP <sup>h</sup>  | As yet unknown                     | Cellulose 4%               | 90%                                 |                      | 92-95%              |  |

**Table 12. Comparisons of enzymatic hydrolysis and fermentation process configurations**

<sup>a</sup> Cellulase producing organisms consume (2–6% of the) cellulose (6% of the ‘‘feedstock’’). Fermenting organisms (‘‘ethanologen’’) consume sugars and a small amount of nutrients. A certain fraction of the sugars may also be lost to other products (contamination)

<sup>b</sup> Enzymatic hydrolysis gives high yields, which will show a gradual increase from 75–85% now (SHF) to 85–95% in future (CBP). The effective yield also depends on the pre-treatment method. The presented numbers hold for dilute acid pre-treatment and will be slightly higher for steam explosion and liquid hot water.

<sup>c</sup> The fermentation yield (85–90% of the theoretical maximum) is low due to enzyme inhibition by the products of the hydrolysis and is comparable with the starch hydrolysis and fermentation process. Fermentation by *Saccharomyces cerevisiae* may achieve 90% of theoretical.

<sup>d</sup> In SSF fermentation with *Saccharomyces cerevisiae* (yeast), ethanol yields are 92.5% for glucose and 80–92% for xylose. However, on the short term, xylose and arabinose fermentation may remain low, 59% was achieved by Sonderegger and Sauer.[131]

<sup>e</sup> Wooley et al. consider 7% of all fermentable sugars to be lost to contamination.

<sup>f</sup> Glucose yield holds for dilute acid pre-treatment. The most common organism used to produce cellulase industrially is *T. Reesei* (fungus). It grows in aerobic conditions and consumes both soluble sugars and holocellulose. 5% of the clean hydrolysate is directed to the cellulase reactor, where 100% of the sugars is consumed, 0% of the sugar oligomers, 0% of the CSL, 100% of the cellulose, 0% of the hemicellulose, 0% of the lignin. The total of cellulase (77%) and biomass (23%) produced equals 26% of the cellulose and sugar consumed, furthermore CO<sub>2</sub> is produced at 107% of the mass of cellulose and sugar consumed. Cellulase productivity on hardwood is significantly higher than on softwood. Productivity increases with increasing cellulose concentration, but the yield per gram cellulose decreases due to mass transfer limitation. Reaction time is 5–7 days. The costs associated with dedicated cellulase production are 0.5 US\$/gal ethanol, or 50 US\$/tonne dry biomass hydrolysed. Through time, less cellulase will be necessary, because of increased specific enzyme activity: three-fold in 2005, and ten-fold in 2010.

<sup>g</sup> Wooley et al. model hydrolysis, fermentation (*Zymomonas mobilis* bacterium) and seed production to take place in both seed reactor and SSCF reactor. For hydrolysis and fermentation, numbers are taken from the SSCF reactor. For sugar consumption, the number is taken from the seed reactor. SSCF fermentation of glucose yields 93% (of the theoretical maximum). Only conversion yields for glucose and xylose were found, the other sugars are assumed to convert at 90% (average of other configurations). The nutrient Corn Steep Liquor (CSL) (actually a 0.25wt% dilution) is a necessary nitrogen source (7.7% of the mass of entering cellulose).

<sup>h</sup> The fermentation yield of the bio ethanol production is 92–95% (of the theoretical maximum). In aerobic situation, cellulase yield is much higher than in anaerobic situations. On the other hand, fermentation gives higher yields in anaerobic situation. In SHF, SSF and SSCF these reactions take place in separate reactors. In CBP, where cellulase production and fermentation are combined in one reactor, an anaerobic microorganism culture will be used.

## 2.5. Developing bioethanol production processes - Ethanogenic micro-organisms

The conversion of any saccharide feed to product will be dependent on the microbe employed. For bioethanol, this will be through an ethanogen. In the production of biobutanol, the butanogens would be exploited. Equally, the microbe of choice for the myriad of biologically products we have been accustomed to would be exploited. For the conversion of saccharides, the majority of metabolic pathways employed are conserved across both eukaryotes and prokaryotes, therefore the product formation pathways, rates and tolerances become of greatest interest. In this section, the Embden-Meyerhof-Parnas and Entner-Doudoroff pathways are explored, as are the fermentation yields from the common *Saccharomyces* fermentation systems and pilot *Zymomonas* systems [51, 138].

### 2.5.1. Ethanogenic micro-organisms

Ethanol is a fermentation by-product in the culturing of certain microbes. Through the metabolism of a carbon source, the reforming of the carbon is predominantly into forms that are beneficial for the maintenance of the organism's homeostasis, storage, or excretion as wastes from respiration. In a number of organisms, the carbon can be formed into ethyl alcohol (ethanol) through anaerobic respiration, with which yeasts have had the most widespread commercial success. In microbiology, production of ethanol from a carbon source can occur through a number of biosynthetic pathways. Predominantly, production is initiated by glycolysis where pyruvate is formed prior to conversion to acetaldehyde by the enzyme pyruvate decarboxylase, with carbon dioxide as a by-product. The acetaldehyde is further converted to ethanol by alcohol dehydrogenase before being excreted into the fermentation media [61]. For a complete system wide overview of a number of selected pathways, Figure 11 (see page 28) shows the initial conversion steps from a lignocellulosic source, through cellulolysis and glycolysis to pyruvate.

Individual species of bacteria and yeasts have been long known to secrete ethanol as an intermediate metabolic carbon store to prevent carbon exhaustion at times of inter-species competition through the Crabtree effect. Tables included in the Appendix (pages 23 to 26) show the common ethanogens by taxonomic domains; eukaryotes (namely yeasts) and prokaryotes (bacterial, with differentiation by mesophilic and thermophilic).

#### 2.5.1.1. Yeast

Yeasts - unicellular fungi - have the ability to degrade carbohydrates (principally C<sub>6</sub>) molecules to two-carbon (C<sub>2</sub>) compounds, without complete oxidation to carbon dioxide. This is observed across a broad spectrum of yeast, with examples such as *Saccharomyces cerevisiae*, *Kluyveromyces lactis* and *Candida albicans* [139]. Other notable yeast, *Schizosaccharomyces pombe*, *Kluyveromyces*

*fragilis* and *Candida tropicalis*, have all been isolated for ethanol production to varying degrees of commercialisation. Yeasts are preferable for fermentations due to being able to utilize a variety of substrates, ability to grow and efficiently ferment ethanol at pH values of around 3.5 – 6.0, and temperatures of between 28 and 35 °C [52].

*Saccharomyces cerevisiae* is used in the majority of ethanol fermentations due to being Crabtree-negative, having a relative high rate of ethanol production, ethanol and osmotic tolerance, and using mild fermentation conditions. Able to metabolise a wide range of mono and disaccharides, the *Saccharomyces* genus has been well documented and studied. In addition, the use of *Saccharomyces* spp. for other commercial and pharmaceutical importance is due to its classification of GRAS<sup>8</sup>, established methods of recombination and the ability to perform post-translational modifications. The multitude of review articles and dedicated journals such as the “Yeast,” “Journal of Yeast and Fungal Research” and “Yeast Research” show the depth and spread of the yeast development.

In the production of ethanol, two species of the *Saccharomyces* species are frequently used. *Saccharomyces cerevisiae* is widely used for the fermentation of ale-type beer and wines, whereas *Saccharomyces carlsbergensis* or *pastorianus* (a cross between *bayanus* and *cerevisiae*) is used in the fermentation of lager-type beers [125, 140]. Phenotypical differentiation between the two species originated in the observation of the fermentation characteristics, either top or bottom fermentation. Top fermenting yeasts such as *S. cerevisiae* flocculate in the process of fermentation due to the hydrophobic flocculate adhesion to CO<sub>2</sub> producing the characteristic foam on top of the fermentation media (or wort in brewing terminology). This is not present in bottom fermenting strains such as *S. carlsbergensis* and *pastorianus*.

For a number of decades there has been debate over the taxonomy and nomenclature of *S. carlsbergensis*, as for many years the two *Saccharomyces* were considered as two distinct species [141]. With work carried out by Kreger-van Rij [142] based on genome homology studies, *S. carlsbergensis* was moved into the *S. cerevisiae* species and renamed *S. uvarum*. Subsequent studies by Vaughan-Martini and Kurtzman [143] and Vaughan-Martini and Martini [144] have pushed the view towards two distinct species, which has kept the differentiation between the two microbes [145]. *S. uvarum* is believed to be a hybridization of *S. cerevisiae* and *S. monacensis* due to its allopolyploid genome.

---

<sup>8</sup> Generally Regarded As Safe

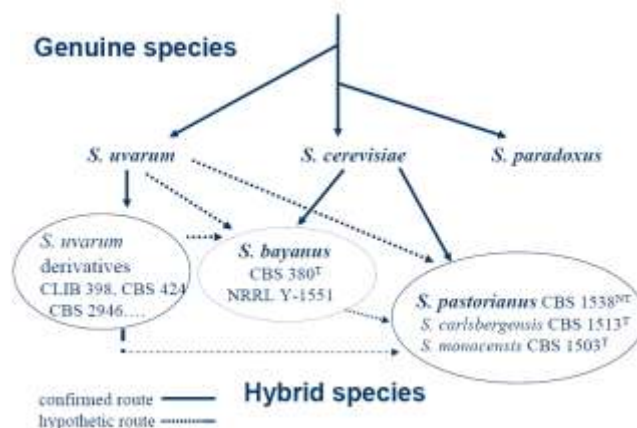


**Figure 35. Establishment of evolutionary relationship between *Saccharomyces* species *S. uvarum*, *S. cerevisiae*, *S. paradoxus*, *S. bayanus* and *S. pastorianus***  
 Reinstatement of *S. uvarum* abolished by synonym status.

Yeast has the ability to express ethanol under both aerobic and anaerobic conditions (see Figure 36) but predominantly under anaerobic conditions through the Embden-Meyerhof-Parnas (EMP) pathway [139]. The net reaction yields two molecules of ethanol, one molecule carbon dioxide and one molecule ATP per molecule of glucose fermented. This gives rise to a theoretical yield of 0.51 g of ethanol per gram of glucose under normal conditions. Cell maintenance, synthesis and secondary products (glycerol and succinate) limitations mean fermentations usually do not exceed 90-95% of the theoretical maximum. Through the production of glycerol and succinate deficient strains, a further 2.7% product yield may be gained [52].

Ethanogenic yeasts stems from the ability to use energy from glycolysis and fermentation pathways rather than the oxidative respiration pathways, allowing the yeast to maintain cell viability while producing ethanol [139]. In terms of fermentation practices, to maintain the stability of biomass population in yeast fermentations, a small supply of O<sub>2</sub> is required to ensure cell maintenance, as O<sub>2</sub> is required for biosynthesis of polyunsaturated fats. Typical amounts maintained in the broth are between 0.05-0.10 mm Hg oxygen tension. With values greater than 0.10mm Hg, cell growth is promoted at the expense of ethanol production. The nutritional requirements for ethanol production are based on cell maintenance. Components required in the nutrient source are solely used in the production of cell structures and cell synthesis pathways [52].

As yeasts are the predominant ethanogens, ethanol tolerance is a significant factor in industrial uses. Yeasts are susceptible to ethanol inhibition, with growth retardation observed in strains fermented with ethanol concentrations of 1-2% (w/v). Growth is completely halted by concentrations greater than 10% (w/v). Variation in tolerance is observed across a broad range of strains that have been developed through strain improvements. Tolerance is dependent upon the fatty acyl composition of the plasma membrane [52].

With commercially available home brewing kits, a strain of *S. cerevisiae* with the ethanol tolerance of 23% is available through the Alcotec brand, as well as fast yielding strains (for example Alcotec Turbo yeast with 12% in a 24hr period) [146].

In the testing of strains with ethanol tolerance, the nature of the ethanol tolerance is in relation to the microbial strain has shown variation through being either autogenous or exogenous fermentations. As exogenous additions of ethanol to a strain do not accumulate within the cell, growth is observed at higher concentrations than autogenous ethanol concentrations indicating the inhibitory mechanism is propagated through an internal cell signalling sequence from an ethanol build up in intracellular areas [52].

### **Saccharide metabolism**

*Saccharomyces cerevisiae* has the ability to utilise specific mono-, di-, oligo-, and polysaccharides. The method of utilisation has an influence on the potential yields that may be obtained and the characteristics of the fermentation. *S. cerevisiae* has the transporters required for trans-membrane transportation of the disaccharides maltose and trehalose, with two transport mechanisms understood for trehalose; a high affinity H<sup>+</sup>-trehalose symporter ( $K_m = 4\text{mM}$ ) that is repressed by glucose and a low affinity constitutive transporter ( $K_m = 100\text{mM}$ ) [147].

The utilisation of maltose is important in the beverage brewing industry due to the use of malts in the production of beer. *S. cerevisiae* has the ability to metabolise maltose due to the five *MAL* genes that are found in unlinked but homologous loci on different chromosomes. The five *MAL* genes (*MAL1-MAL4* and *MAL6*) consist of three genes containing a maltose permease, maltase and transcriptional activator sequences at each gene locus. Down regulation of the genes is brought on through constitutive activation of the Ras-cAMP pathway inhibiting maltose metabolism through the reduction of maltose permease activity and transcription. Induction of maltose metabolism is through the lifting of glucose repression and induction through maltose arising to specificity in carbon source order of preference [147].

Sucrose metabolism is dependent on the six *SUC* genes encoding the two versions of invertase. The genes (*SUC1-SUC5* and *SUC7*) are located on different chromosomes with the major form of invertase secreted subject to glucose repression and responsible for extracellular hydrolysis of sucrose to glucose and fructose [147].

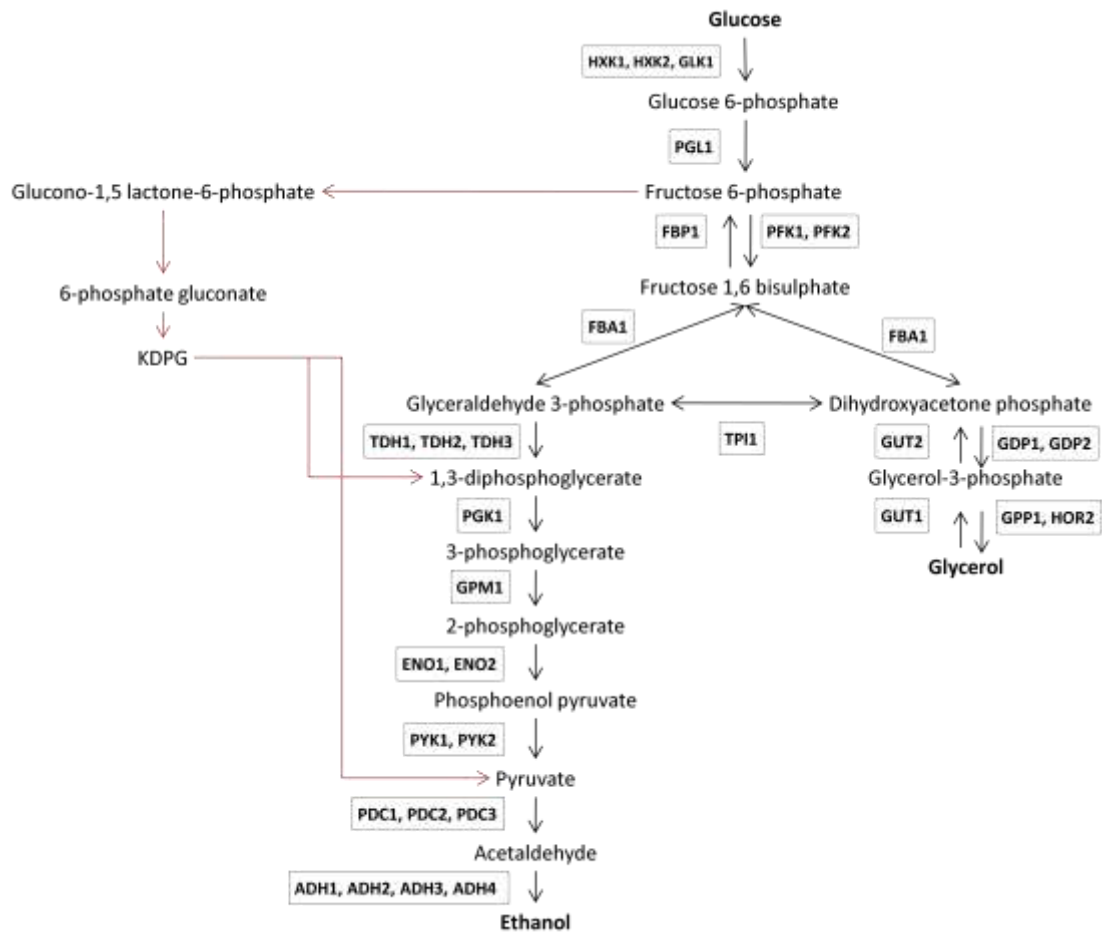


**Figure 36. Glycolysis and gluconeogenesis**

The Embden-Meyerhof-Parnas pathway (EMP). Double headed arrows indicate reversible reactions. Arrows in opposing directions indicate usage of separate enzymes for reverse process. Abbreviations; *ADH* – alcohol dehydrogenase (EC 1.1.1.1); *ENO* – enolase (EC 4.2.1.11); *FBA* – fructose-1,6-bisphosphate (EC 4.1.2.11); *FBP* – fructose-1,6-bisphosphatase (3.1.3.11); *G6P DH* – glucose-6-phosphate dehydrogenase (EC; 1.1.1.49); 6PG-lac – 6-phosphogluconoalctonase (EC 3.1.1.31); *GAPN* – non-phosphorylating GAP dehydrogenase (EC 1.2.1.9); *GAPDH* – glyceraldehydes-3-phosphate dehydrogenase (EC 1.2.1.2/13); *GLK* – glucokinase (EC 2.7.1.2); *GUT* – glycerol-3-phosphate dehydrogenase (EC 1.1.5.3); *HBT* – 3-hydroxyanthranilate 1-hydroxybenzimidazole (mediator); *HOR* – glycerol-3-phosphate (EC 1.1.1.8); *HXK* – hexokinase (EC ; 2.7.1.1); *KD(P)GA* – KD(P)G aldolase (active on KDG as well as KDPG; EC 4.1.2.-); *Lcc* – Laccase (EC 1.10.3.2); *PDC* – pyruvate dehydrogenase complex (EC 2.7.11.2); *PEPS* - Phosphoenolpyruvate carboxykinase (EC 4.1.1.32); *PGAM* – phosphoglycerate mutase (EC 5.4.2.1); *PGI* – glucose-6-phosphate isomerase (EC 5.3.1.9); *PGK* – phosphoglycerate kinase (EC 2.7.2.3); *PK* – pyruvate kinase (EC 2.7.1.40); *PKF* – phosphofructokinase (EC 2.7.1.11); *TIM* – triosephosphate isomerase (EC 5.3.1.1); *TPI* – triosephosphate isomerase (EC 5.3.1.1); *VP* – versatile peroxidase; *XYL* – xylase (EC 3.5.1.5). Diagram self produced using references from [64-66]

### 2.5.1.2. Bacteria

Many bacteria are capable of producing ethanol at low concentrations through the possession of either the EMP or Entner-Doudoroff (ED) pathway. Bacteria capable of expressing greater than 1 mol ethanol per mol of glucose are listed in the appendix in conjunction with strains known for potential strain enhancement and development (see Tables 2 to 5 on Appendix pages 23 to 26). Unlike eukaryotes, prokaryotes have the ability to express multiple end products, such as additional alcohols (butanol, isopropyl alcohol and 2,3-butanediol), organic acids (acetic, butyric, formic and lactic acid), polyols (arabitol, glycerol and xylitol), ketones (acetone) and/or various other gases (methane, carbon dioxide and hydrogen) in addition to ethyl alcohol. The ethanol yield in comparison to yeasts has demoted bacteria to a secondary role rather than as a preferential ethanol fermenter [52].

Prokaryotes have a low solvent tolerance, with interruption of cell membrane structures and integrity seen at low concentrations leading to necrosis [148]. Bacterial cells are susceptible to degradation from alcohols with reducing cell viability relating to increasing alcohol chain length and hydrophobicity. Production limitation is quickly reached with dose dependant inhibition seen between 1% and 10% ethanol concentrations depending on strain/species. At concentrations of 15% ethanol, immediate inactivation is observed in the majority of vegetative bacteria cells. The extreme of bactericidal ethanol tolerance is seen in the genus *Lactobacillus* where *L. heterohiochii* and *L. homohiochii* are seen to grow in concentrations up to and over 20% ethanol. However, whilst *L. heterohiochii* and *L. homohiochii* have high ethanol tolerance, neither species has the ability to ferment ethanol at commercial volumes [25, 149].

As with yeasts, many bacteria can produce ethanol through the EMP pathway, however in bacteria, the ED pathways may also be used. Here, glucose is phosphorylated and then oxidised to 6-phosphogluconate before dehydration occurs to form 2-keto-3-deoxy-6-phosphogluconate (KDGP). The KDGP is cleaved by KDGP-aldolase, yielding 2 mol of pyruvate from 1 mol glucose and 1 mol ATP [52]. The phosphoenolpyruvate (PEP) generated in the EMP pathway may be catabolised in different ways within the fermentation process, especially in facultative anaerobes resulting in many diverse product formations. This can lead to the formation of formate, acetate, succinate, lactate and 2,3-butanediol in addition to ethanol. This is shown in Figure 37. Only *Zymomonas mobilis* can be regarded as a strict ethanol producer due to the primary metabolic product being ethanol in a much higher concentration than other potential products [22, 26, 150].

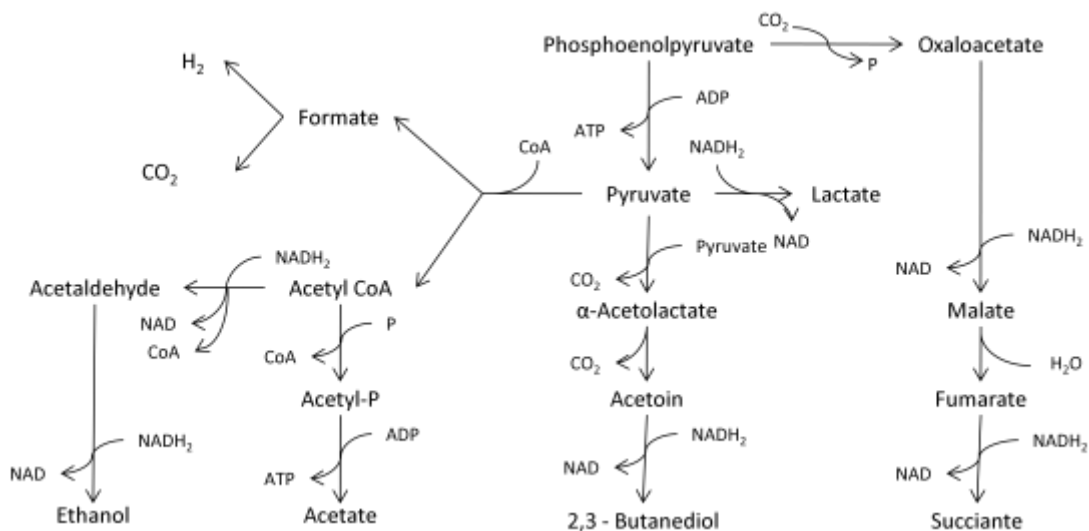


**Figure 37. Pathways for the formation of products of a mixed acid and 2,3-butanediol fermentations** [151]

The bacterium *Zymomonas mobilis* is regarded as a strict ethanologen. Much of the commercial interest in bacterial ethanol production has focused on this particular microbe due to its high product formation without inhibition and fermentation under aerobiosis conditions without restrictions due to the Pasteur effect [52]. Optimal fermentation conditions (30-40°C and a pH 4.0-5.0), *Z. mobilis* appears comparable to yeast in fermentation. However, the bacterium has sub-optimal usage of sucrose, additional by-product formation (excessive organic acids, e.g. acetic acid, lactic acid) in the fermentation with detrimental effects on ethanol recovery in down-stream processing. In fermentations based on sucrose, secondary products of the polysaccharide levan (made up of fructose units) increase the viscosity of the fermentation media, and sorbitol (a product of fructose reduction) decreases ethanol production [26]. This disadvantage has limited the commercialisation of the mesophilic bacteria in cellulosic fermentations due to the excessive sucrose liberated in hemicellulose hydrolysis.

*Z. mobilis* expresses a high ethanol production capacity and relative tolerance (~8% w/v with maximal strain tolerance seen at 12%,) due to the high levels of vaccenic acid seen in the plasma membrane [148]. Further genetic modification work has been carried out to enhance the bacterium's abilities.

## 2.5.2. Yeast versus bacteria for glucose based ethanol fermentations

Microbial choice is based on performance parameters and ease of use. For a kinetic comparison between bacterial and yeast fermentations, it is worth considering ethanol fermentation based on a monosaccharide glucose substrate (see Table 13).

| Kinetic parameter   | <i>Z. mobilis</i> | <i>S. uvarum</i>  |
|---|-------------------|-------------------|
| Specific growth rate, $\mu$ [ $\text{h}^{-1}$ ]                           | 0.13              | 0.055             |
| Specific glucose uptake rate, $q_s$ [ $\text{g g}^{-1}\text{h}^{-1}$ ]    | 5.5               | 2.1 <sup>c</sup>  |
| Specific ethanol production rate $q_p$ [ $\text{g g}^{-1}\text{h}^{-1}$ ] | 2.5               | 0.87 <sup>c</sup> |
| Cell yield, $Y$ [ $\text{g g}^{-1}$ ] <sup>a</sup>                        | 0.019             | 0.033             |
| Ethanol yield, $Y_{p/s}$ [ $\text{g g}^{-1}$ ] <sup>a</sup>               | 0.47              | 0.44              |
| Relative ethanol yield [%] <sup>a,b</sup>                                 | 92.5              | 86                |
| Maximal ethanol concentration [ $\text{g L}^{-1}$ ]                       | 102               | 108               |

**Table 13. Kinetic parameters for *Zymomonas mobilis* and *Saccharomyces uvarum* on 250gL<sup>-1</sup> glucose media in non-aerated batch culture (30°C, pH 5.0).**

<sup>a</sup> based on the difference between initial and residual glucose concentrations.

<sup>b</sup> a molar reaction stoichiometry of 1 glucose  $\rightarrow$  2 ethanol + 2 CO<sub>2</sub> has been assumed for a theoretical yield.

<sup>c</sup> kinetic parameters calculated for a fermentation run between 16 and 22 hours, the culture growing fully anaerobically [52].

Of specific interest for fermentation are; specific growth rate ( $\mu$ ); specific ethanol production rate ( $q_p$ ); and specific glucose uptake rate ( $q_s$ ). In comparing the two microbes in relative fermentations, *Z. mobilis* has the greater production capacity. With  $\mu$  2.4 times greater,  $q_p$  2.9 times greater and  $q_s$  2.6 times greater than those of *S. uvarum*, *Z. Mobilis* has a greater production potential [52]. With ethanol production greater in the bacterium than the yeast counterpart, fermentation method variation has been explored for maximal ethanol yield. In a continuous system, the bacterium has the greater efficiency even with the application of cell recycle with a negative atmospheric pressure.

For SSF, SSCF and CBP (see previous sections), further parameters have to be considered for optimal conditions (temperature range, pH range, alcohol tolerance, specific growth rate, productivity, osmotic tolerance, specificity, yield, genetic stability and inhibitor tolerance) [2].

## 2.6. Microwave irradiation

The development of microwave biology has been defined by three areas.

- 1) The development of the physical microwave system and the expansion of research from the radio frequency wavelengths (specifically microwave wavelengths)
- 2) The implications of microwave irradiation on public health and biology.
- 3) The microwave effect in chemical synthesis and organic systems.

For the understanding of the process described in the research proposal, the three elements are discussed with relevance to the PhD aims.

### 2.6.1. Microwaves and magnetrons

The term “microwave” defines a section of the electro-magnetic spectrum with frequencies between 300 MHz and 300 GHz, where the wavelength ranges from 1m to  $1 \times 10^{-3}$ m (see Figure 39). For operational use, the frequency range is segmented into frequency bands (see Table 14). To exploit the frequency bands, a microwave generator and aerial is required for transmission, and either an antenna for reception or an absorptive material to receive the microwave energy. The key technical innovation that has enabled the use of microwave technologies was the invention of the magnetron in 1940 by John Randall and Harry Boot, allowing the easy generation of wavelengths in the centimetre and millimetre range (see Figure 38). Originally developed as a signal generator with military applications in range detection during the Second World War, the magnetron has enabled the exploitation and commercialisation of the of the microwave spectrum, opening up the field of radio frequency science and engineering. Applications with mature exploitations include range finding and guidance, medical diagnostics, domestic cooking and long range telecommunications.



**Figure 38. Magnetrons - original 1940 Randall and Boot and a modern counterpart**

Left; original 1940 Randall and Boot cavity magnetron held in the London Science Museum. The cavity is the cylindrical object to the right [Science Museum/Science and Society Pictures].

Right; Modern 2.45GHz magnetron [152]

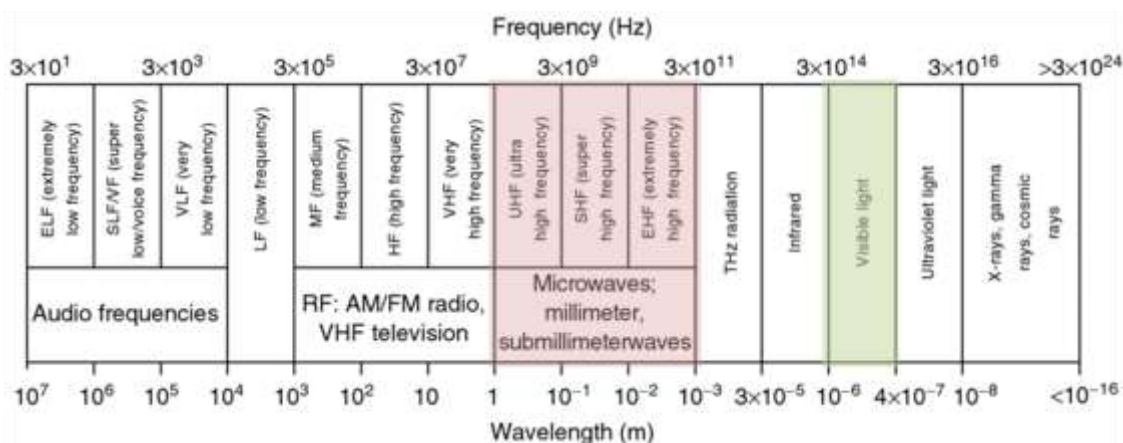


**Figure 39. The electromagnetic spectrum ( $3 \times 10^1$  to  $>3 \times 10^{24}$  Hz)**  
 Area in red highlights the microwave region. The visible light frequency band (green) is highlighted for reference. [153]

|  |               |          |          |          |           |          |                |
|--|---------------|----------|----------|----------|-----------|----------|----------------|
| <b>Band identification letter</b>        | <b>L</b>      | <b>S</b> | <b>C</b> | <b>X</b> | <b>Ku</b> | <b>K</b> | <b>Ka.....</b> |
| <b>Frequency range (GHz)</b>             | 1 - 2         | 2 - 4    | 4 - 8    | 8 -12    | 12 - 18   | 18 -26.5 | 26.5 - 40      |
| <b>Band identification letter (cont)</b> | <b>.....Q</b> | <b>U</b> | <b>V</b> | <b>E</b> | <b>W</b>  | <b>F</b> | <b>D</b>       |
| <b>Frequency range (GHz) (cont)</b>      | 33 - 50       | 40 - 60  | 50 - 75  | 60 - 90  | 75 - 110  | 90 - 140 | 110 - 170      |

**Table 14. Microwave band frequency identification**  
 Identification shown by Radio Society of Great Britain nomenclature for the region of 1 – 170GHz.

The application of interest in this study is the effect microwave energies have on biochemical and biological pathways, and how the energy source can be applied to a reaction vessel in a controlled manner. Work carried out in RF and microwave research post 1970 has been limited by two key interlinked parameters; cost and frequency availability. The majority of commercial scale microwave applications developed (where transmission of a generated signal is required), are at 2.45 GHz (S band).

At low power outputs, small signal generators ( $\sim 1\text{mW}$  -  $<10\text{W}$ ) are used for a broader spectrum of frequencies for signal sweeping (typically for signal transmissions, material science and medical diagnostics). In larger applications, the production of specific frequencies requires dedicated signal amplifiers such as Travelling Wave Tubes (TWTs), magnetrons and klystrons with much narrower operating frequency ranges.

Commercial frequency restrictions apply to avoid frequencies reserved for communications. Termed Industrial, Scientific and Medicinal (ISM) frequencies and with particular focus on 2.45GHz (12.2 cm), 900 MHz (33.3cm) and 27.12 MHz (11.05m) are reserved for research and commercial exploitation. A summary of all ISM frequencies available is shown in Table 15. As 2.45GHz is near the resonance frequency of water (depending on temperature), 2.45GHz has been extensively used where dielectric heating is required. Where an application has to use a source with the possibility of

interference, cost escalation is inevitable due to the production of a specific frequency generator, and the shielding required ensuring the prevention of signal leakage [10, 154, 155]

| Frequency range |             |                   | Availability                                  |
|-----------------|-------------|-------------------|---|
| Lower limit     | Upper limit | Central frequency |   |
| 6.765 MHz       | 6.795 MHz   | 6.780 MHz         | Subject to local acceptance                   |
| 13.553 MHz      | 13.567 MHz  | 13.560 MHz        |   |
| 26.957 MHz      | 27.283 MHz  | 27.120 MHz        |   |
| 40.660 MHz      | 40.700 MHz  | 40.680 MHz        |   |
| 433.050 MHz     | 434.790 MHz | 433.920 MHz       | Region 1 only and subject to local acceptance |
| 902.000 MHz     | 928.000 MHz | 915.000 MHz       | Region 2 only                                 |
| 2.400 GHz       | 2.500 GHz   | 2.450 GHz         |   |
| 5.725 GHz       | 5.875 GHz   | 5.800 GHz         |   |
| 24.000 GHz      | 24.250 GHz  | 24.125 GHz        |   |
| 61.000 GHz      | 61.500 GHz  | 61.250 GHz        | Subject to local acceptance                   |
| 122.000 GHz     | 123.000 GHz | 122.500 GHz       | Subject to local acceptance                   |
| 244.000 GHz     | 246.000 GHz | 245.000 GHz       | Subject to local acceptance                   |

**Table 15. ISM band availability in accordance to ITU-R in 5.138, 5.150, and 5.280 of the Radio Regulations**  
[154, 156]

## 2.6.2. Microwave cavity designs and development

The basic design premise of any microwave system has to be the controlled irradiation of a sample by a microwave source with even field distribution throughout the sample or reagents. The infrastructure requirements for any microwave reactor are; a power source; a filter for signal generation; a magnetron (or equivalent) for radiation source; a waveguide for waveform propagation; mode stirrer (optional) for radiation distribution; and the cavity or waveguide for containing the microwave field. The domestic oven typifies the system elements common across all applications (Figure 40) Variation on the basic parameters, particularly for research and industrial use, has caused a number of key parameters to show variation. These are shown in Table 16.

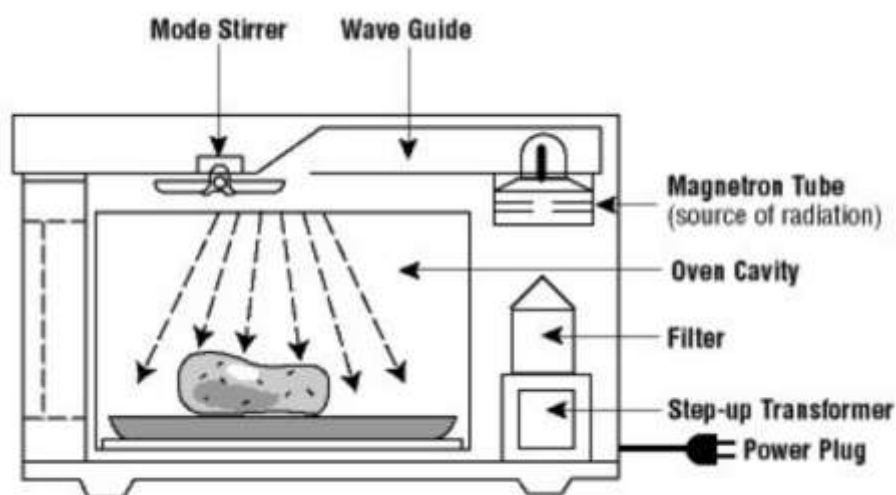


**Figure 40. Typical microwave equipment**  
[157]

| <b>Factor</b>           | <b>Options</b>                | <b>Note</b>  |
|-------------------------|-------------------------------|--|
| <b>Frequency</b>        | Typically UHF, S and X band   | 900MHz, 2.45GHz and 8-12GHz used in research for production. Complete range used in materials research |
| <b>Power</b>            | mW to KW or MW                | mW used in material analysis. kW to MW used for commercial production.                                 |
| <b>Microwave source</b> | Continuous vs. pulsed         |  |
| <b>Mode</b>             | Monomode or multimode         | Dependent on cavity physical structure. Mono used in research and small scale.                         |
| <b>Thermal</b>          | Static set point vs. variable |  |

**Table 16. Variables in microwave research**

### **Frequency**

Due to cost limitations for novel microwave sources in large scale use, and the restriction to ISM frequencies (particularly 2.45GHz and 900 MHz), industrial use has focused on the L and S bands. L, S and X band have been used in research, sample analysis and small scale production. Higher frequency waveguides for industrial and commercial use are less widespread due to the size limitations incurred by the restrictive dimensions of the wave guide (see “2.6.2. Microwave cavity designs and development” on page 74). For propagation, the waveguide has to be matched to the frequency desired, according to the international standards for frequency response and waveguide fabrication.

Frequency tuning to the resonant frequency of the molecule under investigation can significantly reduce to the energy requirement by focusing the energy in a more efficient manner. Work carried out within the LJMU research group has used this method for sample analysis with low power, whole spectrum sweeping for resonant frequencies for different materials (300MHz – 12GHz). By then applying the resulting frequency to the sample, preferential heating can be attained with a lower power input.

### **Power/microwave source**

Domestic oven based microwave sources operate by Pulse-Width Modulation (PWM). The irradiation is a function of the time (the Duty Cycle) when the microwave source is emitting. With the magnetron working as an on/off source, the percentage of time emitting compared to resting period will define the power output. This decreases the irradiation exposure time of the reaction compared to the total reaction time. As such, quotations of powers in the PWM mode are not representative of the peak irradiation power or time, but the RMS of the exposure (see Figure 41 for illustration). Where the source has been used a t less than 100% of the maximum output, the actual emitted radiation will be a function of the duty cycle duration and the number of cycles per unit time. Where the cycle is long and irradiation times are short, the quoted power setting can be significantly different from the actual energy supplied [11].

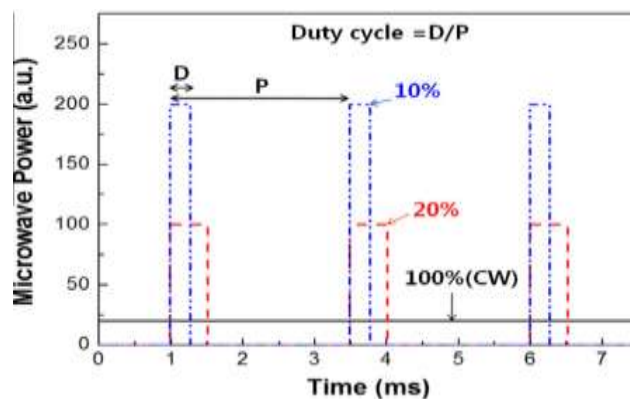


Figure 41. Continuous microwave (CW) vs. pulsed power with the same energy (the same time-average power) [11]

## Thermal

As quoted by Swicord *et. al.*, [158] the thermal features of microwave exposure can be characterised as;

- “Thermal - temperature increase greater than  $>1^{\circ}\text{K}$
- Nonthermal - a temperature change of  $<1^{\circ}\text{K}$
- Athermal - no measurable temperature increase”

By looking at the terminology in energy transfer terms, the phrase “thermal” implies a system where supplied energy equates to an increase in bulk temperature, regardless of thermal efficiency. Therefore  $\Delta T = >0$ , and  $Q = >0$  (where  $Q$  is heat exchange with the surroundings). This is considered to be an adiabatic system. By contrast, “non-thermal” or “athermal” implies a system where the bulk temperature has negligible temperature change with differentiation only defined by linguistic terminology.

A more accurate term used is the “isothermal” terminology of reactions concerned with thermodynamics where the bulk temperature is maintained at a controlled set point. The assumed conditions is where  $\Delta T = 0$  across the whole experiment. This can be maintained where the thermal energy (or induced thermal) input is balanced by a heat sink for energy removal. As such, the  $\Delta T = 0$  but  $Q \neq 0$  while in an adiabatic process,  $\Delta T \neq 0$  while  $Q = 0$ . As such, the term “isothermal” is used in preference throughout the study.

The parameter dominant in thermally controlled reactions is temperature control independent of microwave power. In experiments where the reagents or reactant has a thermostability optimum, to maintain the optimal temperature the microwave source is often used as the controlled variable, where pulsing or modulation of the microwave source is used to maintain a constant temperature. Without a cooling system for sample thermal stability, the microwave operating in the pulse mode will not represent the power setting selected. In addition, many temperature controlled systems use an initial heating ramp to attain the desired temperature, (depending on the sample size and control system

used). Overshooting the desired temperature is a common limitation, particularly at temperature ramping, and has been observed through experience using CEM Explorer devices, which use a fuzzy logic control system. In the CEM system, the initial ramp is through a high microwave power output until the heating gradient can be determined before reduction of power through duty cycle variation until a continuous power level can be achieved for temperature stability. In systems where temperature set point is the controlled variable, determination of microwave power variable can be difficult, misleading or impossible without a separate isolated thermal control [159].

The three plots shown in Figure 42 show an experiment progression in a CEM explorer, where the desired reaction is the maintenance of 150°C for a hold period of 10 minutes. Pressure build up is a result of fluid expansion in the sealed vessel. The reactant used in this example is pure water for determination of heating curves and CEM performance. Noticeable in the plots is the expected heating of the water, controlled by fuzzy logic feedback on the microwave source. Initial ramping is achieved by the application of approximately 200W power before reduction of power once the heating rate could be determined. Temperature maintenance is seen at a lower power level (100 – 130W), with variation through nearly the whole experiment exposure period. As the temperature is a function of microwave power, the fuzzy logic controller would continually adjust the irradiance until a low power variation could maintain the temperature set point. In this experiment, the exposure time is too short for determination.

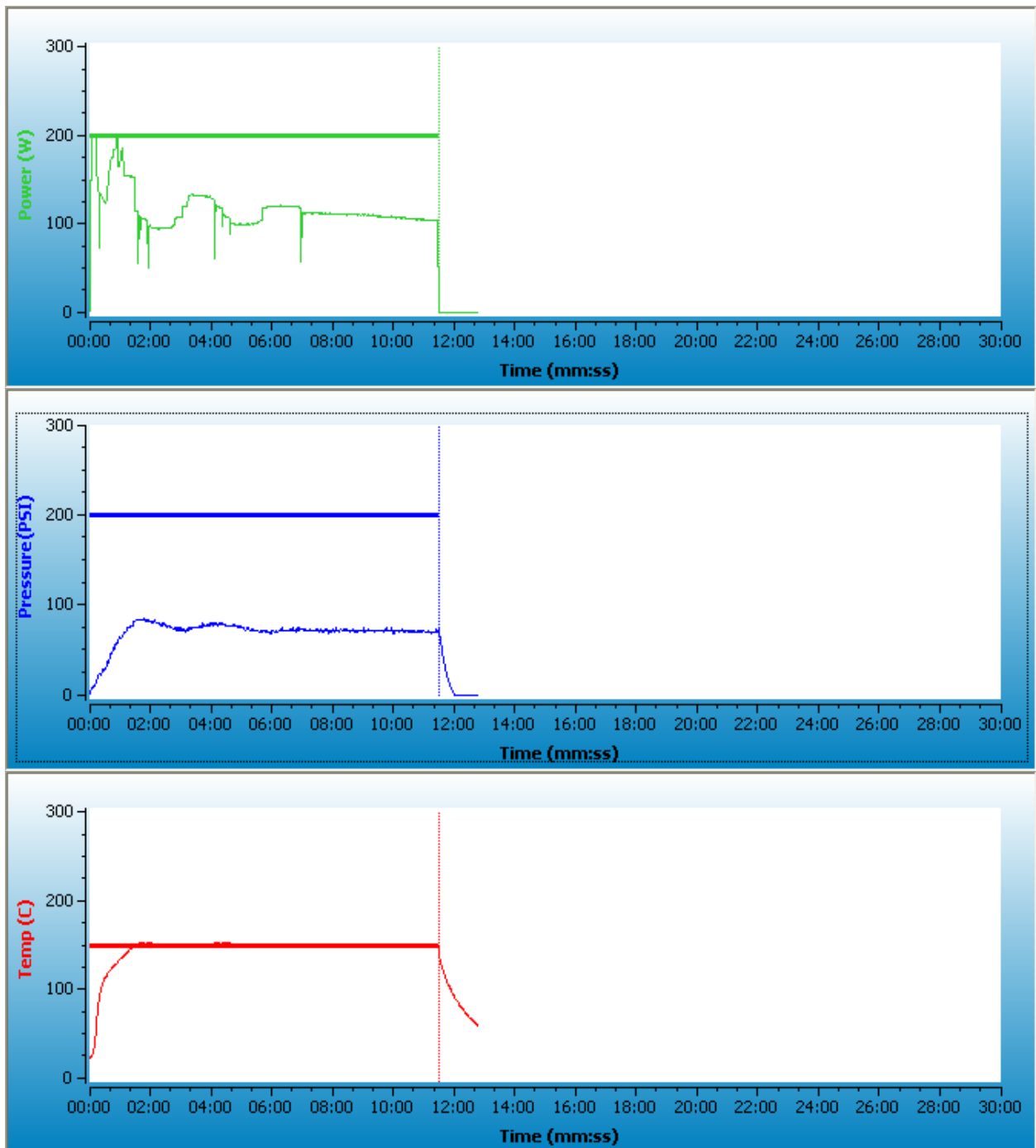


**Figure 42. Microwave power, reaction temperature and pressure using a CEM Explorer**

Data provided by Professor D. Phipps as part of a complimentary project to this study. Data is not shown as analogous to the study conducted but to show variation of microwave power in an isothermal reaction. [160]

### EM wave propagation (Mode)

The electromagnetic wave propagation down through the physical waveguide section is termed “mode,” where the mode describes the degree of freedom the microwave wave has within a waveguide/cavity system. In both monomode and multimode configurations, the wave is formed at the aerial and propagates along a waveguide of defined dimensions, set by the required frequency. These dimensions correspond to the bands as identified in Table 14.

In monomode configuration, the waveguide dimension is consistent with the wavelength to form uniform wave patterns within the waveguide. The sample is placed entirely inside, or transverse to, the waveguide with the sample for exposure concentrated within the microwave field at a location where the intensity is at its greatest. The advantage of monomode operation is the focusing of the wave beam at a particular location or sample. This is ideal for exploratory work where samples are typically small or a high field density is required. The disadvantage is scalability. As the frequency used is related to waveguide size (where a higher frequency relates to a small cross sectional dimension) the sample size has a physical limitation. A number of companies (CEM Corporation, Milestone S.r.l, Anton-Paar GmbH and others) have specialised in the production of microwave reactors in the monomode operation for research and refined high value small scale product manufacturing [161].

The alternative to monomode is multimode, where materials being irradiated can have larger dimensions than the size of the waveguide. This is done by using resonant cavities. The principle mechanism in multimode is the scattering of the microwave beam around the cavity through the use of a mode stirrer or by cavity design. The scattering dissipates the microwave energy throughout the cavity, reflecting off the cavity walls allowing energy extinction and/or amplification. Although energy density decreases per unit volume, operation of larger or complex reaction vessels can be achieved [161]. For illustration, see Figure 43.

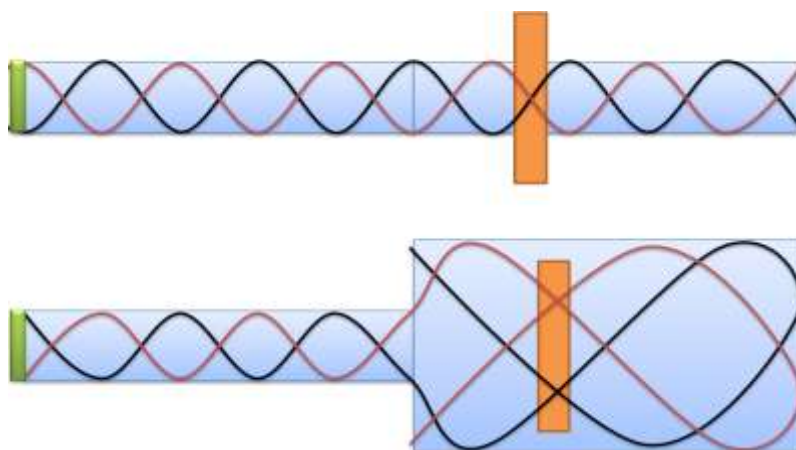


**Figure 43. Monomode and multimode cavity principles.**

Simplified rendering of a monomode (top) and multimode (bottom) cavity design. The block coloured green is the microwave source. Block coloured orange is the sample being investigated. Sample is shown is transverse to the waveguide axis.

Due to the nature of each cavity incurring “hot spots” and “cold spots” caused by constructive and destructive interference of the microwave field, uniform distribution is achieved by either movement of the sample through the field (liquid agitation or rotation of the solid) or by the use of a mode stirrer to disrupt the microwave irradiation and scatter the beam around the cavity. Figure 40 (page 70) shows what would be a domestic oven with a mode stirrer placed within the waveguide above the solid being heated, inferring that the cooking plate would be static. The alternative mode of operation

(and frequently seen in modern domestic ovens) would be by rotation of the cooking plate. For industrial and commercial use, the movement of the subject may be undesirable (for example in curing, irradiation of liquids which have to maintain phase separation, or where shearing forces would be derogatory to the sample) therefore the use of a mode stirrer may be preferable.

### 2.6.3. Application of microwave energy to chemical/biochemical reactions and biological systems.

| Time frame     | Technical innovation  | Scientific development (chemical/biological interactions)   |
|----------------|---|---|
| 1890's - 1940  | Pioneering work in the application of RF and microwave work. Demonstration of public radio (Tesla, 1893), commercialisation of RF. Blue sky research of MICROWAVE. Limitations of high cost and refined manufacturing of microwave sources. | Microwave detonation of gunpowder (Bose 1894).  |
| 1940 – 1970's  | 1940 – Development of the magnetron (Randall and Boot). Predominantly military research for the applications of telecommunications and electronic warfare, based on the development of the magnetron.                                       | Earliest examples of alternating field research on biological systems from the 1950's onwards. First human death attributed to microwave irradiation – 1957. Research into public health with high power microwave transmitters. Research based on bespoke cavities or horn transmitters. Analytical research into microbial spore viability, frequency/power/dose correlation to CFU viability   |
| 1975 onwards.  | Commercialisation of the domestic microwave oven. Reduction of cost of magnetrons and control systems   | First published peer reviewed paper of the use of a domestic microwave as a laboratory tool (1975). Domestic microwave ovens, modification of a domestic microwave oven, or laboratory microwave ovens based on domestic oven construction used extensively due to low cost. Increased commercial and industrial adoption of microwave irradiation in the food industry as bulk sterilisation and cooking methods.<br><br>Start of chemical synthesis with microwave energy |
| 1980's onwards | Applications in domestic communications. Advent of cellular telephone networks, WiFi and wireless technologies.   | Impact of mobile phone radiation with human tissue.   |
| Recent years   | Movement way from modified microwave ovens to bespoke scientific microwave reactors.  | Continued research into the microwave enhancement of synthetic chemistry. Isolation of the microwave field effect from the thermal effect. Cavities designed for specific applications.   |

**Figure 44. Chronological order of key microwave developments**  
[162-166]

Experimentation prior to the availability of commercial microwave ovens was through the use of either a horn antenna (Figure 45) or bespoke experimental microwave cavities. Post commercialisation, an early adoption of the domestic microwave oven in the laboratory was as a tool for the dehydration of biological samples. The drying of samples that would have taken many hours on a hot plate could be achieved within an hour through the use of the microwave oven [167]. This low cost entry point for analytical use has been based on the availability of cheap domestic

microwave ovens. Much of the domestic ovens' fabrication and controls have been adapted for research purposes. Experiments have been conducted in conventional domestic fixed size cavities, with either the rotational plate used for even field distribution throughout the sample, or a modification for either a magnetic or coupled shaft agitator. Power settings have been based on the original arbitrary microwave power setting of defrost, low medium and high [168].



**Figure 45. Modern horn antenna**

Broadband microwave horn antenna. Its bandwidth is 0,8 – 18 GHz. The coaxial cable feed line is attached to the connector visible at top. This type is called a *ridged horn*; the curving metal ridges or fins visible inside the mouth of the horn reduce its cut off frequency, increasing the bandwidth. Taken from [169].

For research into microwave applications, multidisciplinary approaches have only gained momentum in recent decades (1970's onwards). The majority of chemical reactions conducted in early microwave investigations by chemistry departments were dependent on the modification of available equipment for use (particularly at 2.45GHz). An early development for microwave enhanced chemistry (MEC) was the closing of reaction vessels allowing rapid temperature rises to pressures above atmospheric. This reduced the reaction times of many thermobaric dependent reactions and has gained wide spread adoption into R&D and commercially [170].

As the use of microwave has moved into both the food production and fine chemical production processes, larger and more advanced microwave designs have evolved, all based on the same basic components. Applications frequently exploit the resonance of water for thermal effects, with temperature rise (either heating or thermal sterilisation) or volatilisation being the desired effect. In the fine chemicals industry, temperature control is the desired parameter in addition to the reduced production times observed under microwave influence. Figure 46 and Figure 47 shows the diversity of microwave currently microwave designs with both research and commercial examples seen. With critical evaluation of the work being conducted, a niche market for research high quality, tuneable and controllable microwave reactors and waveguides was established allowing greater control.



**Figure 46. Research microwave reactors**  
Mono-mode microwave ovens from (a) CEM, (b) Biotage and multi-mode microwave ovens from (c) Milestone and (d) Anton Paar [161]



**Figure 47. Industrial microwave reactor**  
Left; industrial microwave irradiation (900MHz) for food production (cheese manufacturing shown) [171]  
Right; Industrial conveyer belt oven (2.45GHz) by Sairem for multiple applications (Bacon cooking shown) [172]

## 2.6.4. Microwave/chemical interactions

Microwave irradiation of chemical (and by extension biological) reactions have been credited to either the thermal or non-thermal effect, where the boundaries between the two mechanisms are often debated and contradictory. As a method of inducing dielectric heat, the microwave influence occurs through the application of an oscillating electromagnetic field, inducing rotation of dipolar molecules. As the microwave oscillation is much greater than the rotational speed of the dipole, the resulting intermolecular friction converts some of the electromagnetic energy into thermal energy (Figure 48).

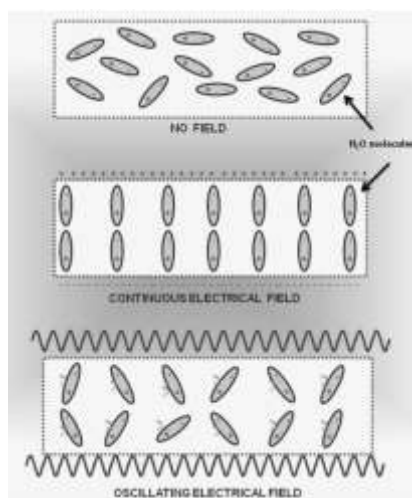


**Figure 48. Dielectric excitation of water molecules.**  
Effects of microwave energy on the reaction mixture in aqueous media [173].

The dielectric properties are correlated with the molecules' ability to absorb microwave energy, increasing the dielectric by substituting the solvent of choice affects the microwave influence. Of particular interest in this study is the basis of an aqueous system where water has the dielectric constant of  $\epsilon_s$  80.1 at 20°C. In this instance, water is being used as the fluid of choice due to the solvent volume required and used throughout the process [174]. In microwave engineering, this is termed dielectric heating, whereas in the natural sciences, it is often referred to as diathermy (heating induced by electric fields).

The energy provided through a microwave source at 2.45GHz corresponds to a microwave photon energy of  $10^{-5}$ eV. As the energy required to disrupt hydrogen bonds is between ~0.04 – 0.44eV, the energy provided is well below what is required. For comparison covalent bonds require ~3.82eV and ionic bonds require ~7.6eV, showing that microwave energy applied directly to the substrate or reagents lacks sufficient energy to cause direct bond disruption [161]. Table 17 shows the quantum energy transmitted by frequency in comparison to bond energy.

| <b>Radiation type</b>           | <b>Frequency (GHz)</b> | <b>Quantum energy (eV)</b> | <b>Bond type</b> | <b>Bond energy (eV)</b> |
|---------------------------------|------------------------|----------------------------|------------------|-------------------------|
| <b><math>\gamma</math>-rays</b> | $>3.0 \times 10^{19}$  | $1.24 \times 10^6$         | C-C              | 3.61                    |
| <b>X-rays</b>                   | $3.0 \times 10^{11}$   | $1.24 \times 10^5$         | C=C              | 6.35                    |
| <b>ultraviolet</b>              | $1.0 \times 10^6$      | 4.1                        | C-O              | 3.74                    |
| <b>Visible light</b>            | $6.0 \times 10^5$      | 2.5                        | C=O              | 7.71                    |
| <b>Infrared light</b>           | $3.0 \times 10^3$      | $1.2 \times 10^{-2}$       | CH               | 4.28                    |
| <b>Microwave irradiation</b>    | 2.45                   | $1.6 \times 10^{-3}$       | OH               | 4.8                     |
| <b>Radiofrequencies</b>         | $1 \times 10^{-3}$     | $4.0 \times 10^{-9}$       | Hydrogen bond    | 0.04 – 0.44             |

**Table 17. Quantum energy values by frequency and bond energy.**

In the instance of microwave heating through excitation of a polar molecule, the application is an exploitation of specific heating mechanism and not directly alteration of any physical parameters. Any alterations observed would be accounted for through thermal energy lowering the activation in the reaction. Where the original application used thermal heating, requiring a conventional heat source and a method of heat exchange, the use of microwaves has been seen as a method of direct heating with higher efficiency and reduced operating cost.

Contrary to the thermal application is the non-thermal effect, also referred to as isothermal, the microwave effect or specific effect. Although a controversial area of research due to the different schools of thought (a qualifiable, discernibly different mode of action compared to a specific application of the thermal effects), an observation that solvents have the ability to be heated in excess of their boiling points without phase transition (supercritical) has pointed to an alternative mechanism. Due to the retardation of nucleation, this has suggested a non-thermal mechanism where the molecular temperature can vary from the bulk temperature (localised microthermal effect in comparison to the

macro or bulk thermal temperature observed). Where microwaves are employed at subcritical temperatures, investigations have indicated an increase in reaction rate at temperature points that cannot be attributed to the microwave system superheating reagents. This has led to the idea a field effect distinct from the thermal effect exists. In chemical interaction, the non-thermal effect is likely to be considered through localised amplification of Fickian motion and localised thermodynamically driven collisions, whereas in biochemical reactions, it is likely to be through the modification of ligand interactions (see subsequent sections for description).

### **2.6.5. Microwave chemistry and applications in biochemistry, catalysis and fermentation**

RF and microwave interaction with chemical, biochemical and biological systems has grown in the past 50 years. In respect of biological interactions, in excess of 1700 peer-reviewed papers have been published according to the World Health Organisation (WHO) research database, predominantly with focus of consumer and domestic uses. The studies compiled in the database comprise of epidemiological, human, *in vivo* and *in vitro* studies in the English language. The database does not include non-English language publication to which a large number of papers should be included [158, 175]. Restricting the search to ISM frequencies results in 254 published reports with varying relevance to this study.

The ignition of gunpowder by J. C. Bose (in either 1894 or 1895) is the earliest cited example of mm range microwave chemistry, shortly after the first public demonstration of radio by Nikola Tesla in 1893 [162]. Between the 1890s and the 1940s, microwave interactions with chemical and biological systems became a niche research area in comparison to research in the radio frequency range ( $3 \times 10^3 - 3 \times 10^8$  Hz) due to RF's lower technical barriers to research. Post Second World War, the mass production of the magnetron and the post war surge in research associated with both ionising and non-ionising radioactive and irradiating source prospered. Prior to 1950, biological interactions were being investigated in the radio frequency range with notable early published work done by Ingram and Page in 1953, with the irradiation of *S. cerevisiae*, *E. coli*, tobacco mosaic virus (TMV) and bacteriophage T<sub>4</sub> in high frequency voltage fields (10 or 20MHz, up to 12 minute exposure) [163]. The review paper written by Chipley in 1980 outlines a comprehensive inventory of experiments carried out through the early advent of microwave and RF research on biological system. Although the review gives a detailed list of the species irradiated in each experiment, the conclusions drawn can be misleading due to the variability of irradiation methods, compromising comparisons between experiments [164].

One of the crucial areas of note is the observation of microwave heating in each microbial or biological experiment. Where each organism has been exposed to the energy field, the heating effect

may or may not have been nullified, suggesting exposure through the use of a horn antenna or cavity system over an aqueous, temperature controlled system (details are frequently omitted or equipment references are no longer supported). Following short exposure periods (for the prevention of sample dehydration and/or over heating), the organisms are typically cultured onto a media for the determination of colony forming units (CFU). On the culturing, the quoted CFU value is given as a response to the exposure [164].

The detrimental effects of microwave irradiation at 2.45GHz at high powers are well known, and subject of many investigations due either to the prevention of death (human safety) or the promotion of death (microbial sterilisation). An intermediate position has also developed of mutagenesis through microwave exposure, used as a method of selection pressure for microbial strain development.

The effects of RF and microwave energies on the human body gained particular attention through the development of increasingly powerful military applications through the 1930's to the 1950's and beyond. In 1957, the medical doctor John T. McLaughlin of Glendale California cited the first case of human mortality directly attributed to exposure to microwave radiation. The case study cited is of a 42 year old American microwave technician, who stood directly in the beam of a military radar transmitter, within 2 meters of the antenna face for less than one minute exposure. The frequency and power of the transmitter are not disclosed due to military security, however from the publicly known data it can be surmised that the power was in the 2.5 megawatt range. By comparison of the injuries to those observed in the test sample provided by animal experimentation on rabbits, death was attributed to the heating effect of the water molecules within high water content tissues causing an inflammatory response leading to shock and ultimately death [165].

From increased research in the biological interactions with 2.45GHz microwave sources, the exact molecular mechanisms discussed later underpin the potential mechanisms seen in this study. The mechanism of death is likely to be through internal heating causing biological stress, triggering heat shock proteins (HSPs) to start the inflammatory response. Work carried out by Laurence *et. al.* looking into the conformation of proteins in pulsed microwave fields. Their work describes the mechanism in detail, by the application of theoretical modelling to support their conclusions based on the HSP response. Of greatest significance is their description of the atypical lack of linear dose response [166]. Many further non-fatal incidents have been reported with the widespread use of domestic microwave ovens.

A beneficial development of the human-microwave exposure has been microwave frequency radio therapy methods for the destruction of surface tumours. Microwave radiotherapy has the ability to induce HSP stimulation in tumour cells by hyperthermia and localised cell necrosis without

toxicological side effects. Studies conducted by Giombini *et. al.* [176] has shown the effectiveness of 434 and 915MHz in conjunction with conventional radio and chemotherapy. With the application to human tissue, the dielectric properties of muscle and connective tissue favour microwave adsorption over the fatty tissues. This is due differences in moisture content between tissues, allowing targeting of the cancerous mass without excessive damage to surrounding tissues. The treatment has also been shown to increase circulation in the immediate treatment area aiding the clearing of cell debris in combined chemo and radiotherapy treatments

With the reduction of technical cost, the range of frequencies and powers investigated has increased. Whereas previous focus was on high power transmitters and their implications on human health, there has been increasing interest in the localised effects from low powered microwave sources due to the prevalence of mobile phones and wireless communications. A particular concern has been the proliferation of mobile phone use where a RF system is in close proximity to biological tissues for long exposure periods. A comprehensive review by Moulder *et. al.* in 2005 showed;

“Extensive *in vitro* studies have found no consistent evidence of genotoxic potential, but *in vitro* studies assessing the epigenetic potential of RF energy are limited. Overall, a weight-of-evidence evaluation shows that the current evidence for a causal association between cancer and exposure to RF energy is weak and unconvincing. However, the existing epidemiology is limited and the possibility of epigenetic effects has not been thoroughly evaluated, so that additional research in those areas will be required for a more thorough assessment of the possibility of a causal connection between cancer and the RF energy from mobile telecommunications [177].”

*In vivo* and *in vitro* laboratory based studies and statistical analysis of epidemiological studies have drawn similar conclusions. At the time of writing this thesis, the recent report published by Frei *et. al.* in the BMJ concludes evidence consistent with the claims held by Moulder *et.al.* and a whole host of others [9]

One of the crucial areas of note is the observation of microwave heating in each microbial or biological experiment. Where each organism has been exposed to the energy field, the heating effect may or may not have been nullified, suggesting exposure through the use of a horn antenna or cavity system over a temperature controlled system (details are frequently omitted or equipment references are no longer supported). Following short exposure periods (for the prevention of sample dehydration and/or overheating), the organisms are typically cultured onto a media for the determination of colony forming units (CFU). On the culturing, the quoted CFU value is given as a response to the exposure [164].

With the development of refined controllable microwave control systems and cavities, it is only in recent years that the investigation of the microwave field effected isolated from the thermal effect has come to the fore.

At a sub-cellular level, the investigation of enzyme interactions has been divided into two categories:

- (i) enzyme activity measured after microwave exposure (i.e. the enzyme buffered solution was exposed to the microwave irradiation at a fixed temperature and periodically, enzyme samples were taken and reacted with a substrate out of the microwave field) or
- (ii) enzyme activity was measured during microwave irradiation (i.e. the enzyme reaction is carried out with substrate within the microwave field and samples withdrawn for progress analysis).

A range of experiments on enzyme catalysis are shown in Table 18 on page 84 [174].

| Enzyme  | Frequency (GHz) | Microwave power (W/g)       | T (°C)          | Microwave effect  | Ref   |
|---|-----------------|-----------------------------|-----------------|---|-------|
| Lactate dehydrogenase, acid phosphatase and alkaline phosphatase  | 2.8             | 400-100 mW cm <sup>-2</sup> | 37 – 50 (fixed) | No non-thermal effect, but thermally induced inactivation                                     | [178] |
| Glucose-6-phosphate dehydrogenase, adenylate kinase, cytochrome c reductase   | 2.45            | 0.042                       | 25 – 60         | No effect   | [179] |
| Horseradish peroxidase  | 2.45            | 62.5 to 375                 | 25 (fixed)      | No effect at low power density, but inactivation at higher power density                      | [180] |
| Lysozyme and trypsin  | 2.45            | 0.1 – 0.6                   | 30 – 95         | No effect   |       |
| Acetylcholinesterase  | 2.45            |                             | 37              | No direct effect unless thermal inactivation  | [181] |
| Lactate dehydrogenase   | 3.00            | 30 – 1800                   | 25 – 60         | No direct but thermal activation  | [182] |
| Alcohol dehydrogenase   | 40 to 115       | 10mW cm <sup>-2</sup>       |                 | No effect   | [183] |
| Lactate dehydrogenase, glutamic oxaloacetic transaminase, and creatine phosphokinase  | 2.45            | 0.004 – 0.0162              | 37.5            | No effect   | [184] |
| Acetylcholinesterase, creatine kinase   | 2.45            | 0.001 – 0.1                 | 37 (fixed)      | No effect   | [185] |
| Acetylcholinesterase  | 2.45            |                             | 25              | No effect   | [186] |
| Cellulase from <i>penicillium funiculosum</i>   | 2.45            |                             | 35              | No effect   | [187] |
| Beta-galactosidase from <i>Bacillus acidocaldarius</i>  | 10.4            | 1.1 – 1.7                   | 70 (fixed)      | Inactivation at low enzyme concentration but no effect at higher enzyme concentration         | [188] |
| <i>Trichoderma reesei</i> cellulose   | 2.45            | 3                           | 45 – 55         | Higher initial rate, but lower yield under microwaves   | [189] |
| Thermophilic (S)-adenosylhomocysteine hydrolase and 5'-methylthioadenosine phosphorylase  | 10.4            | 1.5 – 3.1                   | 70 – 90         | Non-thermal, irreversible and time-dependent inactivation of both enzymes                     | [190] |
| $\alpha$ -amylase from <i>Rhizopus</i> mould  | 2.45            | 0 – 0.75                    | 60 (fixed)      | Higher enzyme activity under microwaves   | [191] |
| Thermophilic alcohol dehydrogenase from <i>Sulfolobus solfataricus</i>  | 2.45            |                             |                 | Non-thermal effect  | [192] |
| Thermophilic beta-galactosidase from <i>Bacillus acidocaldarius</i>   | 10.4            | 1.1 – 1.7                   | 70 (fixed)      | Irreversible inactivation at low enzyme concentration, but no effect at higher concentrations | [188] |
| Lactate dehydrogenase   | 2.45            |                             |                 | Non-thermal effect  |       |
| Several lipases   | 2.45            |                             |                 | Faster reaction rates under microwave irradiation (30s at 1.35KW) then the pH stat method     | [193] |
| <i>Aspergillus carneus</i> lipase   | 2.45            |                             | 38 – 40, 90     | Faster enzymatic hydrolysis under microwaves  |       |
| Hyperthermophilic enzymes; <i>Pyro-coccus furiosus</i> beta-glucosidase (Pfu CelB), alpha-galactosidase from <i>Thermotoga maritima</i> (Tm GalA), carboxylesterase from <i>Sulfolobus solfataricus</i> P1 (SsoP1 CE) | 2.45            | 83 - 500                    |                 | Enzyme activation and non-thermal effect under microwaves                                     | [179] |

Table 18. Effect of microwave irradiation on enzyme activity in aqueous solutions.

[174]

## 2.6.6. Microwave and biofuel/cellulase research

Research into the interaction of microwaves and biofuel production has been pretreatment centric. In addition to this, the terminology used has been misleading. The literature search conducted has focused on the terminology of microwave degradation, microwave enhanced and their application to biological systems (whole cell and protein alteration) and biofuels.

### Definitions

|                              |   |
|------------------------------|---|
| Enhanced;                    | an intensification or amplification of an effect already observed                   |
| Degradation;                 | the breakdown of a material or substance  |
| Pretreatment;                | Any process applied to the biomass prior to the addition of enzymes for hydrolysis. |
| Hydrolysis/saccharification; | the process of reducing the degree of polymerisation of the cellulose fibre.        |

The use of microwave energy as an alternative to thermal energy is desirable due to the specificity of the energy used. Microwave energy has the consequence of increasing specificity of heating by fluid tuning to the selected fluid, thus reducing operating costs. With simplistic application, this has led to a surge of research looking at the effects of classical chemical methods of de-lignification under microwave irradiation with favourable results. This approach has been seen extensively in pre-treatment although no adoption in industry has been seen. From work done at LJMU in a comparable technology, scalability of the complex microwave/thermal/fluid dynamics have shown to be the limiting factor.

The focus of this research is in the enhancement of cellulose hydrolysis. Specific information into research of cellulase enzymatic enhancement is scarce, therefore other microwave irradiated enzyme systems have to be considered and evaluated.

One frequently referenced experiment with direct relevance to this research project is the work conducted by Zhu *et. al.* on the effect of microwave irradiation on enzymatic hydrolysis of rice straw. In this study, both the rice straw and the enzyme were subjected individually to microwave irradiation, although the experiment (particularly the enzymatic irradiation) is fundamentally flawed. In the protocol described, the enzyme hydrolysis is conducted in 300ml flasks with 100ml working volume, maintained within a water bath at a steady state temperature of 45°C for 7 days. Microwave irradiation was conducted through the removal of the flask, cooling and irradiating through placement in a 300W microwave oven for 15 seconds before return to the water bath every 2 hours [189]. The result of the experiment was an observed increase in cellulolytic rate with a lower total yield - Figure 49.

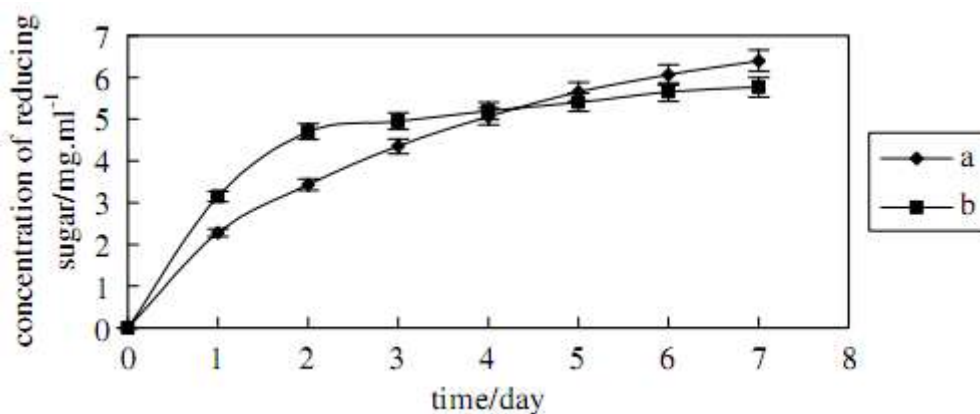


**Figure 49. Comparison of microwave irradiation-free hydrolysis and intermittently treated by microwave irradiation** (a) control (microwave irradiation free hydrolysis), (b) hydrolysis intermittently treated by microwave irradiation [189]

In the quoted figures, Zhu does not quote the initial rates; therefore the assumption has to be made over the first integer of a day. Using an approximation of the initial rate by reading the data from the graph, the apparent reaction rates of  $0.133\text{g l}^{-1}\text{hr}^{-1}$  and  $0.1\text{g l}^{-1}\text{hr}^{-1}$  for the control and irradiated experiments can be suggested. If this is correct, the influence of the microwave irradiation (total of 3 minutes over the first 24 hours) will have increased the initial reaction rate by 33%. On an energy balance, this would equate to  $15\text{Whr}^{-1}$ .

On the assumption that the experiment was conducted with a continuous sampling method, repetitive sampling would equate to a total exposure time of 21 minutes over the entire time period of 168 hours. As a percentage of total reaction time, this is equal to 0.21% within the microwave field. Zhu goes some way to control thermal profile through the use of a water bath. Cooling prior to microwave irradiation allows for a greater  $\Delta T$  increase in the microwave field. By conducting the experiment in this manner, Zhu tries to address the issue of diathermy and preventing the denaturation of the cellulase enzymes.

As a critical assessment of the experiment, the conducting of the experiment in the microwave oven and thermal control through the cooling of the reaction prior to microwave heating is insufficient to draw qualified conclusions against a thermal analogue. The temperature profile of the experiment will not be linear, therefore the reaction rate will vary with temperature, causing artefacts in the data. The negative control used is assumed to be a comparative hydrolysis experiment conducted on a thermal basis parallel to the irradiated experiment. As the negative control would not be able to be conventionally heated at the same rate as a true thermal analogue of the microwave heating (and the authors do not qualify how they controlled the negative control thermal profile), the reference values will naturally at variance from the irradiated experiment.

As an example of a possible mode of action in relation to rate and temperature, Figure 50 shows a suggested profile. For the representation with minimal data from the research group, the assumed  $\Delta T$

for 15 seconds irradiation is 15°C where cooling reduces the temperature by  $\Delta T$  10°C and return to 45°C is through natural cooling. On the assumption that irradiation does increase rate, the rate curves have been shown with a -5% rate alteration for cooling and an increase of 10% above baseline for irradiation with a return to base line within 5 minutes post irradiation. From the graph shown, it can illustrate how small amplification may accumulate to an overall increase in rate.

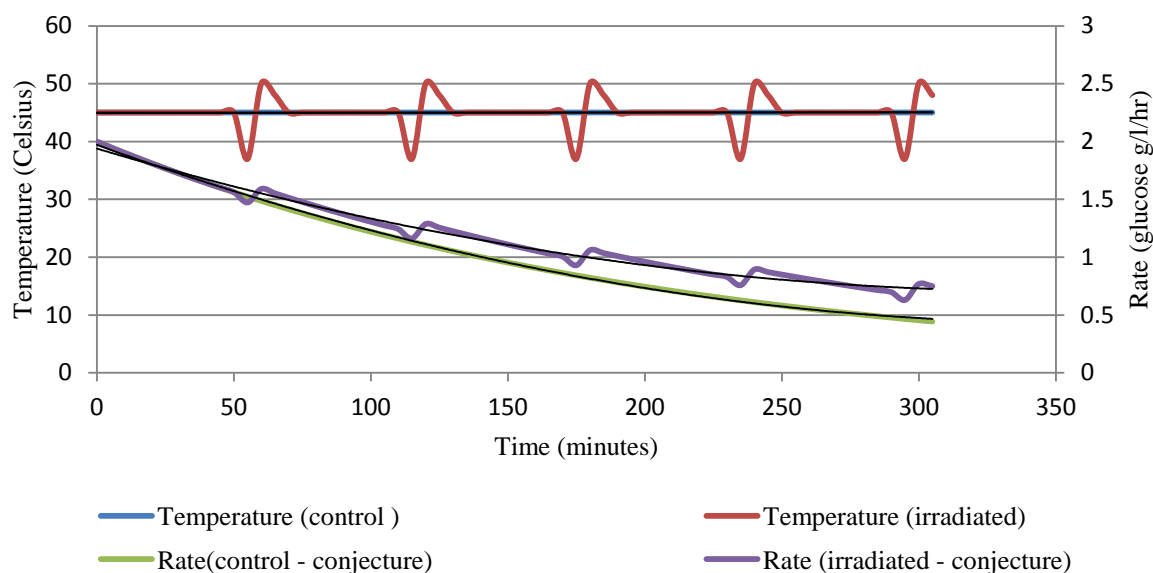


**Figure 50. Suggested rate and temperature profiles for work conducted by Zhu *et. al.***

Further to the intermittent nature of the exposure, the oven used is likely to be pulsed. The microwave quoted (a WD700 (MG-5062T) from LG Electronics Tianjin Appliances Co., Ltd, Tianjin, PR China) is not documented online for cross referencing.

Research conducted by Laurence *et.al.* has investigated the effect of pulsed microwaves in an electromagnetic field on the conformation of proteins, and has proposed a nonlinear response scenario. As stated previously microwaves at 2.45GHz does not have the energy required for the breakage of hydrogen bonds (see Table 17); however the paper presented describes how the electromagnetic field can alter the structural conformation in athermal conditions. The model is based on the principle that the heat shock protein is triggered via transient heating of the protein and its close environment under irradiated conditions.

The research was a response to the findings by Daniells *et. al.* [194] showing that using a pulsed microwave at 750MHz, heat shock genes were activated. Of more significance was the general trend of increased activation at lower power levels, contrary to the expected activation from a thermal stimulus. Daniells' paper alludes to the idea of a response correlating to a protein structural alteration by a mechanism other than heating. Based on the stress-inducible reporter gene  $\beta$ -galactosidase from *E. coli*, the response curve presented shows an activity peak at 750MHz and 24dBm (250mW) over

values reported at 21dBm (125mW) and 27dBm (500mW), where all conditions are thermally identical. Where the frequency applied is 300MHz, the trend presented is of the greatest amplification at 21dBm and a decrease through to 27dBm where the rate has returned to the normalised control (see Figure 51).

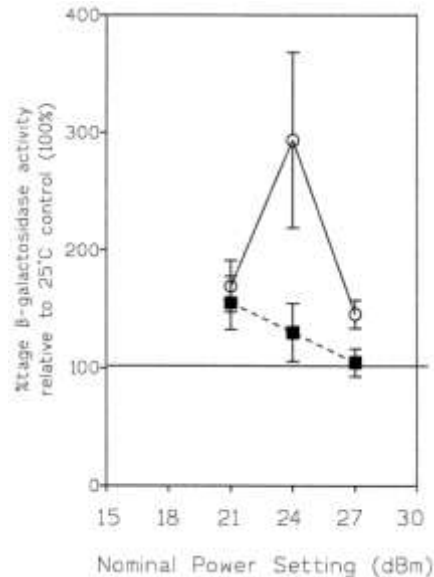


**Figure 51. Effect of varying power and frequency settings on the microwave response**

“Replicate Petri dishes (9cm) were exposed overnight (16hrs) to either 300MHz or 750MHz at power settings of 27, 24 or 21dBm. Because of variation in the 25°C control values following different exposure regimes (possibly reflecting temperature fluctuations in the incubator), each set of microwaves-exposed dishes has been compared against its own set of 20°C controls, arbitrarily normalised to 100% (solid horizontal line). The variance in each control set has been taken into account in the statistical analysis. Each point represents the mean  $\pm$ S.E.M. from 8 replicate assays in 2 separate runs. Open circles, solid lines: response at 750MHz. Filled squares, dashed lines: response to microwaves at 300MHz.” [194]

Daniells’ conclusion draws on the stimulation of the HSP gene without the temperature increase, where the normal trigger threshold is 28°C, and with the use of lower frequency away from the resonance frequency of water. The research shows that by removal of direct and accountable thermal parameters, activation is accomplished, holding strong evidence of the athermal microwave effect.

The nonlinear response shown in Daniells’ study is theorised by Laurence to be related to the protein folding and relaxing under different microwave powers and the pulse response time related to the speed of protein folding/unfolding. The hypothesis offered by Laurence states;

“At *low power levels*, a partial unfolding of specific target protein(s) occurs, which will be insufficient to induce the stress response, but sufficient to alter protein function.

At *higher power levels*, a more unfolded (molten globule) conformation is induced. The stress response will be activated, protecting the protein, and preventing an observable biological effect.

At very high power levels protein aggregation and precipitation occurs, and despite the activation of the entire stress response, a catastrophic biological effect (eg. Cell death) will be observed [166].”

Extending this hypothesis to other proteins is very subjective as each protein will respond in different manners according to a variety of factors, including; hydrophobicity, protein size, number of posttranslational modifications (PTMs), amino acid composition, conformation rigidity, resonant frequency (macro and micro structural), surrounding solvent environment, temperature and pH.

Looking at work beyond the field of cellulases but into the field of protein behaviour under irradiation in general, work conducted by Porcelli *et. al.* [190] looked at the non-thermal effects of microwave irradiation of thermotolerant enzymes as a model system and has taken precautions to remove the thermal effect. The enzymes investigated were S-adenosylhomocysteine (AdoHcy) hydrolase and 5'-methylthioadenosine (MTA) phosphorylase, purified from *Sulfolobus solfataricus* and irradiated at 10.4GHz for a varied time periods with  $T_{\max} = 39^{\circ}\text{C}$ . For separation of the thermal and microwave effects, the system used employs what is assumed to be an X band waveguide with the sample tube loaded along the waveguide's axis and surrounded by a water jacket at  $30^{\circ}\text{C}$ . Irradiation of the samples and thermal negative controls were conducted at a temperature range of  $70\text{-}90^{\circ}\text{C}$  where the microwave is also used as the heating source. There is no reference to the microwave mode of operation. From the research conducted, the observations noted the deactivation of both enzymes with increasing microwave exposure time and microwave power. Through fluorescence and circular dichroism measurements the research group concluded that the microwave irradiation had induced protein structural rearrangements not related to temperature.

## Conclusion

From the background research conducted, there is an apparent cross over between biological and microwave fields that have given glimpses of an alteration of a biological system by irradiation. Work by Zhu *et. al.* [189], the irradiating of cellulase enzymes in a semi-controlled manner, has shown particular prominence. The research conducted has shown a great variability in irradiative methods without any prominent method of separating the microwave effect from the thermal effect.

The discussion of biofuel and fermentation saccharide demand, the requirement for technologies to unlock the saccharides contained within biomass that are ordinarily only available to a selection of fungal, bacterial and plant species has been explained. With these feedstocks, the obligations of second generation biofuels can be addressed without impinging on food stuffs for nourishment. This has led to the deeper understanding of both the lignocellulosic feedstock and the enzymes that naturally degrade the substrate.

Of significance is the mode of action of the CBH, EGL and BGL enzymes, with acknowledgement of the SWO protein within the plant fibres. Due to the unusually nature of the enzymes being bound to the substrate they hydrolyse, the low yield and slow rate has been explained as the key sticking point in hydrolysis efficiency.

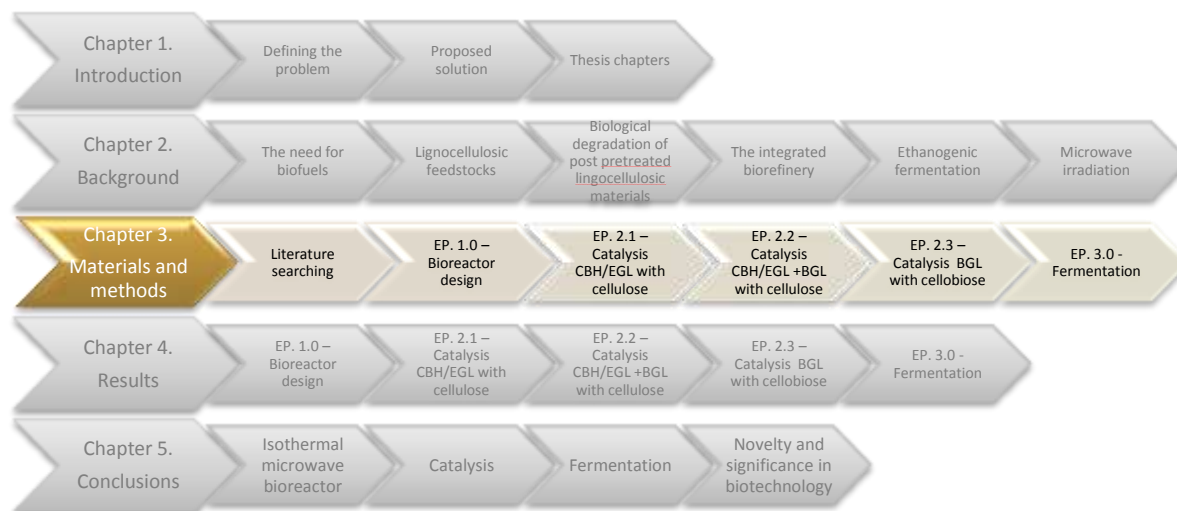
As saccharification is only a unit operation in the production of fermentation products, the coupling of the saccharification to the fermentation system has been described through the processes of SHF, SSHF, SSCF and CBP.

With consolidation of processing and with the dominance of the *Saccharomyces* spp. in fermentation, the choice of ethanogen and merit of each system are explained by biochemical pathways.

With respect to microwave technologies, the background research shows the development of the microwave system from a biological perspective and where microwave technologies have been studied for either biological enhancement or destruction.

***Chapter 3. Research methodology:  
Materials and Protocols***

## Chapter 3. Research methodology: Materials and Protocols



### 3.0.0. Literature, theoretical and mathematical methods

An extensive literature search using a selection of tools was undertaken to provide a background upon which the practical work could be constructed and directed. The task undertaken can be broken down into its constituent parts. Expanding on the traditional journal literature search, the use of database-driven websites designed for user input and interaction has allowed not only information searching and recall but also exchange, development and recording.

#### 3.0.1. Literature searching

For the research discussed, peer reviewed journals from reputable publishers are used for the justification of the discussion points raised or referenced in this document. For journal access, the Universities' licences for Elsevier were utilised through the ScienceDirect portal. Other journal databases periodically used were; arXiv, Biological Abstracts, Information Bridge: Department of Energy Scientific and Technical information; JournalSeek; PubMed; Science Accelerator; Scirus; Scopus; SpringerLink and Web of Knowledge. Generic searching through the Google Scholar as well as Google books and various open access portals was also used.

Due to the publication field being limited by university subscriptions, many papers were sourced through various means and search parameters returning results that weren't necessarily available online. Inter library loan requests were used for access to specific papers that were behind pay walls.

Selections of journals with key research focus in the remit of this thesis were quickly identified. Through accessing these journals directly, further relevant research papers were identified and the journals revisited. Citation notification has been used for a number of key texts where newly

published reports are alerted to through email notification. Searching with the use of MESH options, tags and meta data has also increased literature search efficiency.

Due to the rapid expansion of the biofuels research area and the social-eco-political issues surrounding it, key operator terms were used when searching outside the usual journal access portals. Due to bias potentially present in Blog entries and the uncertainty of the author's authenticity, citing Blog entries was avoided except where authenticity can be assured – such as domain names registered to reputable entities, or with the educational/research domains such as .ac.uk. Where possible, the journals highlighted in any given Blog were recalled and cited as a primary source over the Blog entry itself.

In addition to the literature searching conducted, other methods have been used, including the submission of conference papers, completion of the patent based on this research and numerous seminars, workshops, project presentation, site visits and industrial collaborations. These are summarised in the Appendix (pages 28 to 30).

### **3.0.2. Referencing methods and database compilation**

The reference database was compiled exclusively with Thomson Reuters Endnote X4, and organisation of a PDF journal database on an external hard drive for portability between work locations. Downloading of PDF documents from the majority of database portals generated file names of little relevance to the document title. Therefore, at the point of download each file was renamed with the document title. Nearly every journal database now offers a citation management option (.ris, .cif, .txt or .enw file extensions). Loading into EndNote, automatic citation compilation was quick and efficient. Only a minority of citations required manual entry. EndNote has the option of linking the citation entry to the PDF location allowing for journal database searching through author, tag, key term, key word or date.

In addition to the use of EndNote, Copernic Desktop Search Utility was used on personal computers. By indexing of hard drives with the Copernic Desktop search utility, quick searching of file systems, emails and documents by key terms of all files within the index was achievable.

### **3.0.3. Modelling and mathematical tools**

For the development of the microwave bioreactor, a conceptual prototype was produced from the materials available within the university. In trials using the reactor and with limited development, the prototype showed that microwave propagation into the reactor was being efficiently achieved with little modification. A limited amount of modelling was completed through the use of HFSS (High Frequency Structural Simulator, by Ansys Corp.) for the cavity design to ensure efficient microwave

propagation. Although the software package allows for the modelling of field, heat and fluid dynamics, only microwave field dynamics were of consideration in this study. Retrospective analysis of the system has been limited by the nature of the system due to the HFSS model assuming a 'perfect' condition. The complexity of the bioreactor internal furniture is prohibitive to modelling at any degree of resolution due to both processing power and man-hours needed. Therefore this has been identified for further development.

### **3.0.4. Digital imagery**

Although not a main research tool, digital imagery has been used to record the reactor design, fermentation progression and cell density studies. Digital cameras used have been appropriate for their point of use; a mobile phone camera has been sufficient for daily lab based observations; a compact camera has been used for presentation imaging; and a dSLR used for microscopic and presentation images. Image compilation has been through exporting all images to a central file system for storage. Where image manipulation has been required, either Adobe Photoshop or Jasc PaintShop Pro has been used depending on computer system used.

### **3.0.5. Digital data management**

To manage all digital resources, a hierarchical file management tree was constructed. A consistent filing nomenclature was used of date and file name (yyyy-mm-dd – title) with date altered according to file saving date. The exceptions to the rule were the compilation of the journal databases (by journal title) and Excel sheets where Macros links were dependent on file name/location.

HPLC data was transferred from the HPLC system computer over the University network through the use of WinSCP to a personal server space with data flow only away from the HPLC PC. From the server and through the use of WinSCP, HPLC data could then be studied and manipulated at other terminals. Data from stand alone computers were transferred through the use of memory pens.

A portable HDD acted as the central repository of all data to prevent multiple copies of the same sheet being accessed simultaneously. Where access was required while away from the PC connected to the HDD, remote access was conducted through Windows Remote Desktop within the VPN. LogMeIn was used outside the VPN. To ensure data security, the disk was regularly backed up for archiving with periodical DVD backups burned. For cloud based data storage, the combined use of Google Docs and WinSCP transfer to the University M drive ensured a non-geographical based secure storage.

### **3.0.6. Experimental design**

#### ***Aim***

For the development of this research project the follow questions were posed:

- 1) Can the separation of thermal and nonthermal effects be observed through the development of a reaction vessel with the capability to expose 1 litre of working fluid to microwave irradiation, where the exposure time, frequency, mode and power are variable and the bulk fluid temperature is isolated?
- 2) Can the use of the system developed in 1 be used to increase the enzymatic hydrolysis of cellulose where lysis is through a combination of cellulase enzymes?
- 3) Can the use of the system developed in 1 be used to investigate the effect of microwave exposure on the cellular systems of a fermentative micro-organism?

#### ***Objectives***

- 1) Design an isothermal microwave reactor with thermal stability of  $\Delta T \leq 1^\circ\text{C}$ .
- 2) Conduct cellulose catalysis with cellulase enzymes under isothermal conditions under a range of microwave powers.
- 3) Conduct fermentations in isothermal conditions in the same power range as seen in 2 for determination of compatibility when combined for SSF

#### ***Null hypothesis***

- 1) The null hypothesis in each instance is the conclusion that there is no relationship between microwave power and product formation.
- 2) Microwave irradiation of the cellulase enzymes CBHI, CBHII, EGL and BGL has no significant effect.
- 3) Microwave irradiation of a fermentation system has no significant effects.

For the development of the experiment practical work, the overall objectives were subdivided into experimental packages with three focal points; isothermal bioreactor prototyping, catalytic investigations, and fermentative investigations at controlled thermal and microwave set points. The key units are shown in Figure 52.

Following the results of the literature research (seen in Chapter 2. – Background, page 9), the prototyping of an isothermal microwave bioreactor system was conducted, followed by the development of protocols for reactor operation and adaption of NREL protocols to the vessel for validated and comparative studies. With Figure 52 used as the frame work of experiment development, each section is investigated as unit operations.

The Experimental Packages (EP) are shown in progression using the highlighting bar seen at the top of each subsection.

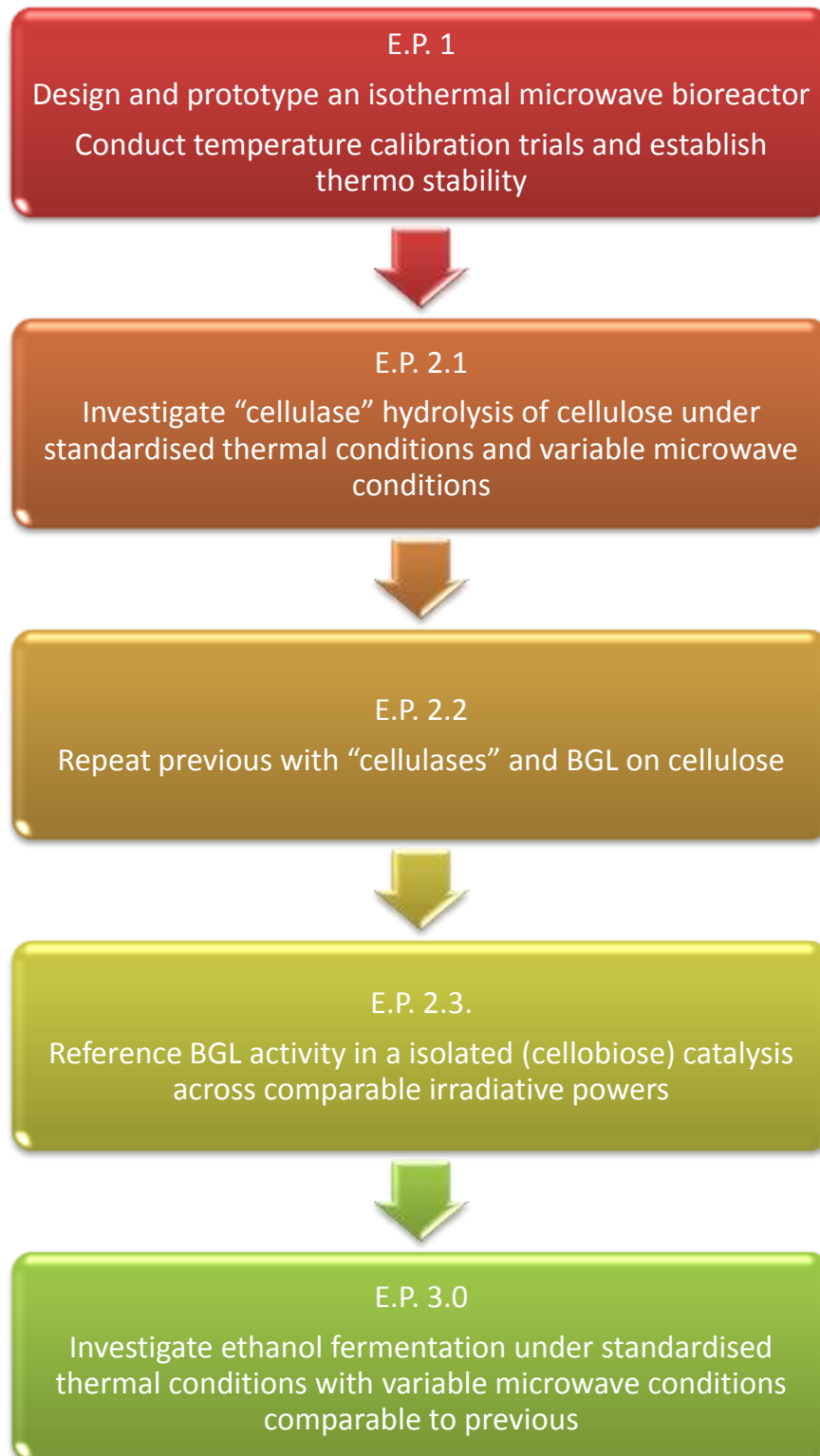


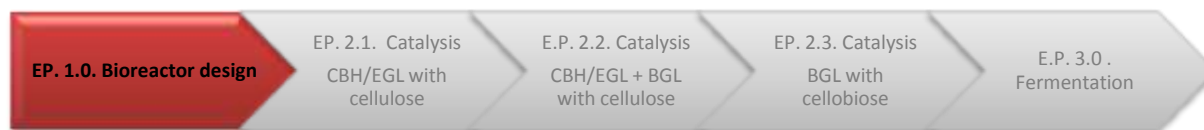
Figure 52. Experiment design by major unit tasks.

### ***3.1. Practical work***

**Material, methods and protocols.**

### 3.1. Practical work - Microwave

#### 3.1.1. Prototyping, design, operation and testing.



The development of a microwave bioreactor from an initial design concept was outside the scope of the study, thus the adaption of an existing design was more applicable. The design objective was for a reactor capable of continuous irradiation with a range of microwave powers and frequencies with isolated thermal and microwave experimental controls.

The basic design objectives, range, considerations and selected solutions are shown in Table 19. For a complete review of the equipment used in the development of the bioreactor system, the components are listed in the Appendix (page 32).

| Design objective                           | Range   | Consideration   | Solution selected  |
|--|---|---|--|
| <b>Reaction vessel for fluid exposure</b>  | Working volume of 1 – 2 litres. Practical range of 500ml – 16000ml  | Simplistic jar irradiation, chemical reaction vessel, biological STR  | Employment of a Applikon 2 litre fermentation STR.   |
| <b>Microwave exposure mode</b>             | Selectable continuous and/or pulse mode operation   | Bespoke microwave source from industrial/scientific supplier, adaption of domestic microwave oven apparatus.  | Specific scientific and industrial (Microtron and Sariem) units used.  |
| <b>Microwave power</b>                     | 0 – 200W (limited by launching system)  | Unknown range required. Greater energy density requires greater thermal compensation  | 0 – 150W initial power window. Re-evaluation depending on power response for optimal power seeking   |
| <b>Temperature stability</b>               | Total range 0 - >80°C with fine control over 20 - 60°C range. Ability to maintain a set temperature point with less than ±0.5°C error over exposure periods of up to 200 hours. | Heat compensation has to be matched to microwave power. Maximum initial microwave power exposures are up to 200W therefore heat exchanger must be able to compensate up to 200W thermal equivalence | Native submerged heat exchange loop within the STR coupled to an external heat exchange system in a close loop configuration. Heat exchanger rated greater than microwave irradiative power. |
| <b>Microwave cavity</b>                    | Size appropriate for the reaction vessel. Multimode cavity without excessive harmonics or reflection to prevent magnetron damage.   | Cavity dimensions to allow easy of operation, air flow around the vessel for hot spot heat dissipation. Cavity must be microwave sealed and capable of supporting STR mass.                         | Cavity based on vessel dimensions plus margin of free space for operational ease. Material thickness sufficient for STR mass support.  |
| <b>Biological containment and support.</b> | pH 2- 11, temperature stability, off gas analysis, aeration, agitation and control  | All facilities are within the design of the STR selected and bio-controller used.   | All facilities are within the design of the STR selected and bio-controller used.  |

Table 19. Microwave bioreactor design parameters

### 3.1.2 Isothermal microwave bioreactor overview

For this study, the primary variable of interest is the variability of microwave power on catalytic and metabolic profiles. All other variables are standardised to prevent experimental bias or artefacts. To conduct the irradiation of the catalytic and fermentation processes required the design, building and commissioning of a microwave cavity containing a stirred tank reaction vessel (STR) with temperature control to isolate the microwave field effect from any induced thermal effect. Figure 53 shows the three physical elements; STR; waveguide and cavity for irradiation; and the microwave generator.

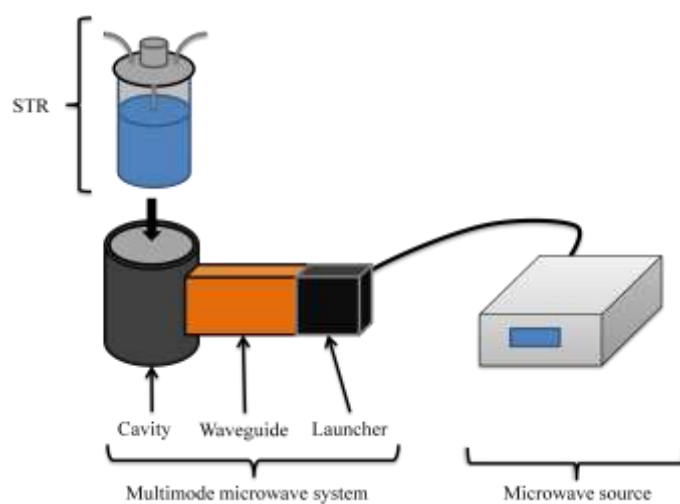


**Figure 53. Microwave reaction vessel design.**

Overview and simplistic exploded diagram to the three key system elements; the stirred tank reactor (STR), cavity and waveguide section, and microwave source. Waveguide detail shows the launcher in black while the waveguide/stub tuner is shown in orange (stubs not shown).

### 3.1.3. Stirred tank reactor

The reactor used was a 2 litre benchtop stirred tank fermentation bioreactor (STR, Metrohm Applikon, Figure 54)<sup>9</sup>. The vessel was a borosilicate glass vessel with stainless steel top plate, threaded for four 12mm probe ports (for incorporating dissolved oxygen (DO) probe, pH probe, triple port and condensing gas exhaust port), bottom draw sample tube, top draw sample tube (flush), top draw sample tube (protruding), submerged thermal regulation loop and bottom (central) sparger tube.

<sup>9</sup> See Appendix, page 32 for equipment details and pages 35 – 38 for additional images



**Figure 54. Benchtop research bioreactor**

Agitation was through a single central shaft with three Rushton turbines. Above the top plate the agitator shaft was coupled to a 24v DC geared motor (PI Systems) through the use of a modified union. To ensure agitation with the insoluble cellulose, rotation was set at 300 rpm for complete mixing without excessive aeration and foam formation. Work conducted by Zhang and Lynd has shown that agitation rate is not a limiting factor in hydrolysis [195], therefore the agitation speed was chosen based on previous work. For catalysis, 300rpm was shown to be the compromise position between over agitation causing influx of excessive amounts of dissolved gases and under agitation allowing suspension collapse and excessive time in the microwave window. For fermentation, the same system is used with agitation reduced to 150 rpm to ensure equal exposure to the microwave aperture with minimal aeration.

For temperature control, the reactor has the operational ability for forced cooling to prevent heat accumulation in the vessel due to the microwave source. This was carried out through the use of a circulating water bath pumping water through the heat exchanger coil within the reactor. In the event of the heating effect being less than the heat loss from the system, the heat exchanger automatically compensated using the same heating/cooling circuit (See Figure 55 and Figure 58 for diagrammatic representations, Figure 62 for a physical image, and Appendix pages 34 – 37 for additional details).

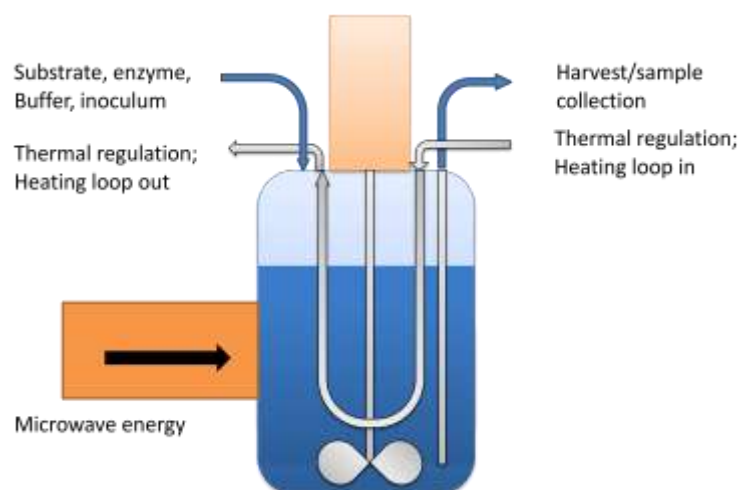


**Figure 55. Simplified schematic of microwave bioreactor**  
Simplistic illustration of the key microwave bioreactor design.

### 3.1.4. Microwave cavity, waveguide, tuning section and launcher

The prototype cavity used an aluminium cylinder with an internal diameter of 160 mm, and a wall thickness of 5mm. Wall thickness was selected for sufficient material depth for waveguide attachment and strength for suspending the STR and additional infrastructure. The top face of the cylinder was turned to provide a recess for the STR compression ring (165 mm diameter) to be seated and centralised. The cavity's cylindrical height was sufficient for clearance between the vessel and the bottom plate (ensuring no contact between the STR and cavity bottom; 190.5 mm base plate to top of cavity flange). As the microwave window was positioned at a height which targeted the liquid phase, the preferential energy absorption would be into the water phase, therefore the void space within the reactor would not be significant.

The microwave source used was connected using a co-axial cable (1m length, 50 Ohm, RG214 standard) to a 7 cm length, S band microwave launcher using an N-type connector. The transmission aerial protruded into the waveguide for wave propagation. The launching section and waveguide (incorporating stub tuning, both UK standardised copper WG 9A, rectangular section) were coupled to the circular cavity by a milled flat surface bisecting the circumference of the cylinder. The waveguide was attached with the waveguide orientated with the long aspect aligned vertically (see Figure 61 and appendix for additional images) and directed towards the centre of the STR along the cavities radius. The reactor vessel was placed within the cylindrical aluminium cavity where the bioreactor top plate is used as the microwave cavity top face.

Once the STR was placed within the cavity, tuning stubs were used to initially minimise reflected power. The reactor was then turned in its seating position and retuned to ensure minimal reflected power. The reactor orientation was noted on the side of the cavity to ensure repeated experiments

maintained the same orientation and physical parameters. The cavity was suboptimal as it had not been specifically designed for this purpose, had not had previous modelling data formed for the complex internal structures and had not been developed further at this point. The reflected power was typically less than 5% of input power and the reactor design was seen as a controlled variable in all subsequent experiments. Checks were conducted for microwave leakage using a HI-1501 Microwave Survey Meter from Holiday Industries. Negligible microwave leakage was observed. As such, the reactor was deemed safe for human operator control across all timed exposures. Neither the microwave cavity nor any additional infrastructure was thermally lagged in any of the experiments.

Through experimentation in the bioreactor prototyping phase, thermal stability was established and maintained in an unlagged system. As isothermal irradiation of the aqueous solution was the primary objective, the energy utilisation was not a core interest to the study (incidentally, quantification of energy consumption was problematic in determination due to the heat exchanger designs used). Thermal stability rather than control of heat loss was considered the parameter requiring control therefore once experiments were started in the unlagged system; all experiments were conducted in a similar manner.

### **3.1.5. The microwave source**

For continuous microwave exposure across the whole experiment time frame, two microwave generators were used over the course of the study. The original source used was a Microtron 200W unit at 2.45GHz that had been used in previous studies. The unit was used as it had controllable power from 0 to 200W through an analogue interface and a co-axial power output for coupling to any desired launcher and waveguide assembly. The unit had shown repeatable and dependable power output across the 40 -180W power band. The unit is based on a magnetron generator with a continuous wave output and monitored through analogue displays for output and reflected powers. The unit has a safety trip system for magnetron protection to prevent excessive reflected powers.

The control of the Microtron 200 series unit was limited and the power outputs at values below 40 Watts were inaccurate. Therefore, a Sairem 200W solid state unit was used specifically for this task especially given its proven reliability at low power outputs (0 – 40 Watts) over extended time periods. Like the Microtron unit, the Sairem unit provides a continuous output, although a pulsed mode is available. In this study, the unit was used exclusively at 2.45Ghz although frequency variation of 200Mhz was available. Validation of microwave source replacement was conducted to ensure no variation in results was observed due to the substitution of the microwave generator (see Figure 56 and Figure 57). Use of the Sairem unit assures validity of the claims at lower power levels.

Both microwave sources differentiate this study to many other previous works as throughout the experiment, the microwave source used was a non-pulsed, continuous source, allowing temperature control to be isolated from irradiation power. This allows the reaction to be conducted in a continuous microwave field for the entire study.

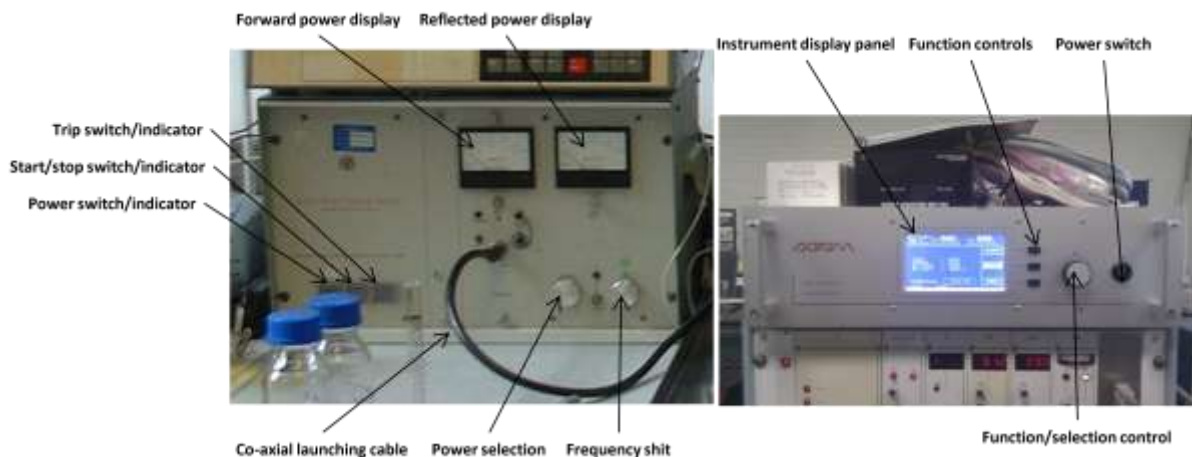


**Figure 56. Microwave generators**  
**Left;** Microtron 200 Series microwave generator. Rated at 0-200W power. Front panel coaxial launch cable. Analogue control U/I.  
**Right;** Sairem 200W air-cooled solid state microwave generator. Rated at 0-200W power. Rear panel coaxial launch cable. Digital control U/I with expansion to PC automation.

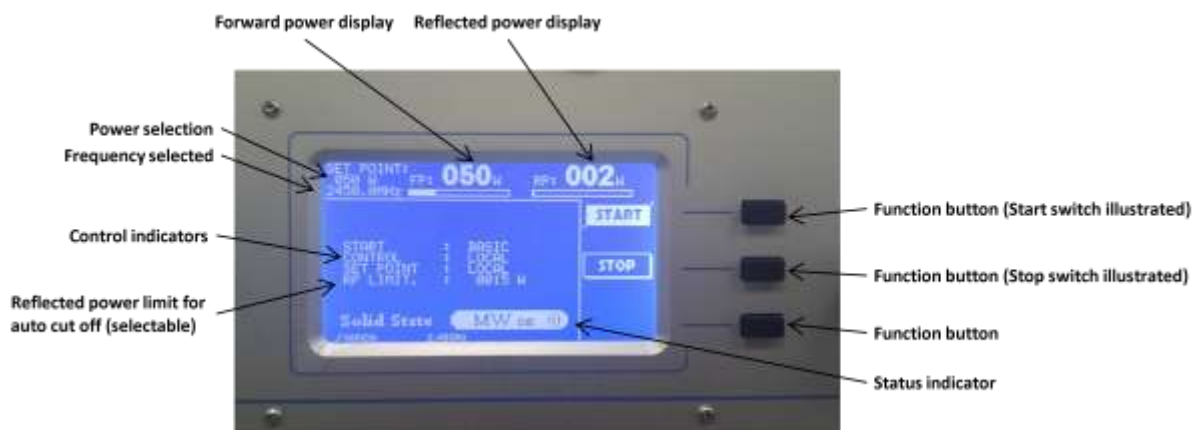


**Figure 57. Sairem microwave generator user interface**  
 Detail of Sairem unit user interface. Interface shows unit in operation at set point of 50W forward power, set from local control point.

### 3.1.6. Variation by microwave power (including thermal stability)

Variation of the microwave power was obtained through the use of the microwave generator control panel with a range of 0 – 200W. Microwave power levels were set through the use of the digital display on the microwave source (Sairem) or analogue input (Microtron). Tuning was done through the use of the stub tuning microwave waveguide section between the microwave aerial and the reaction chamber. For optimal tuning, microwave power was applied and the system tuned. The reactor chamber was then rotated within the cavity to give minimum reflected power and stubs retuned (typically <4% of input power). Once the equipment was tuned, the physical orientation was kept constant to prevent any major retuning being required. To ensure continual stable tuning, the

reflected power on the microwave source was monitored regularly. The unit was maintained at the required temperature through the use of an offline heat exchanger (Huber Polystat cc3). The temperature set point of the heat exchanger used was offset up to 10% below the desired operating temperature of the STR to compensate for microwave heating. Temperature stability was obtained over a period of several hours to allow for temperature equilibration across the whole system (STR, connection fittings, cavity, waveguides and associated heat sinks and radiators). Typical practice was to allow 16 hours (overnight) for this process.

### **3.1.7. Sampling**

For all experiments, sampling was conducted through the use of the bottom draw port. A syringe (20ml) attached to a sterile sampling device through a gas filter (2 $\mu$ m, PTFE) maintained sterility throughout the experiment. Withdrawing air from the sampling device (causing a negative pressure) caused material to be brought through the device and deposited in a 15ml universal vial. On completion of drawing, the syringe plunger was depressed to displace the air taken and clear the sample tube. Care was taken to assure displaced air returned did not exceed the sample volume to prevent gas bubbles aerating the solution/media. Once this had been done, the delivery tube was clamped closed, the universal vial removed. Sample processing was dependent on experimental protocol. Once cleaned, the universal vial was returned to the sampling device (mechanism seen in Figure 61, items 5-8).

### 3.1.8. Schematics and images of the prototype system

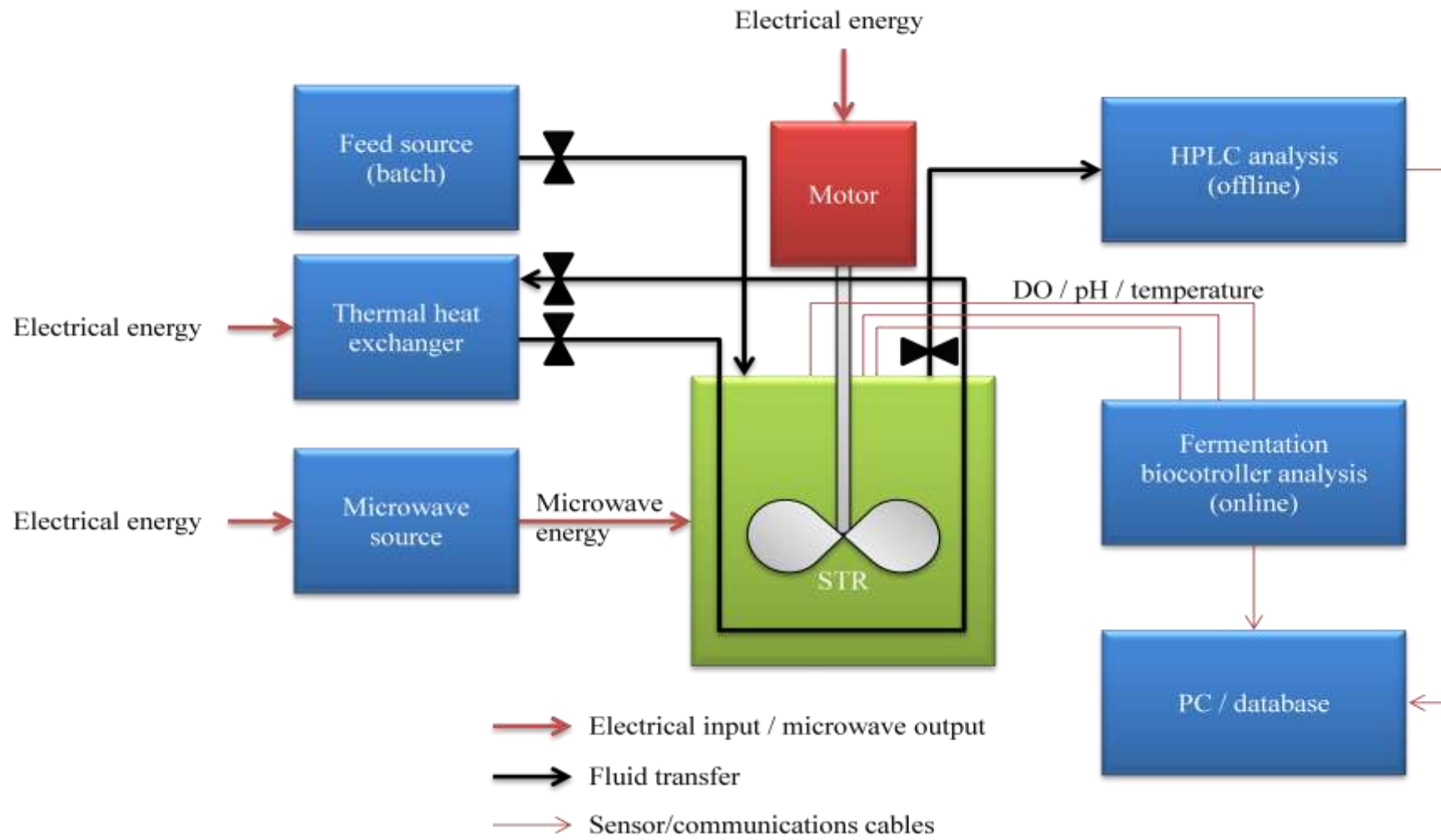
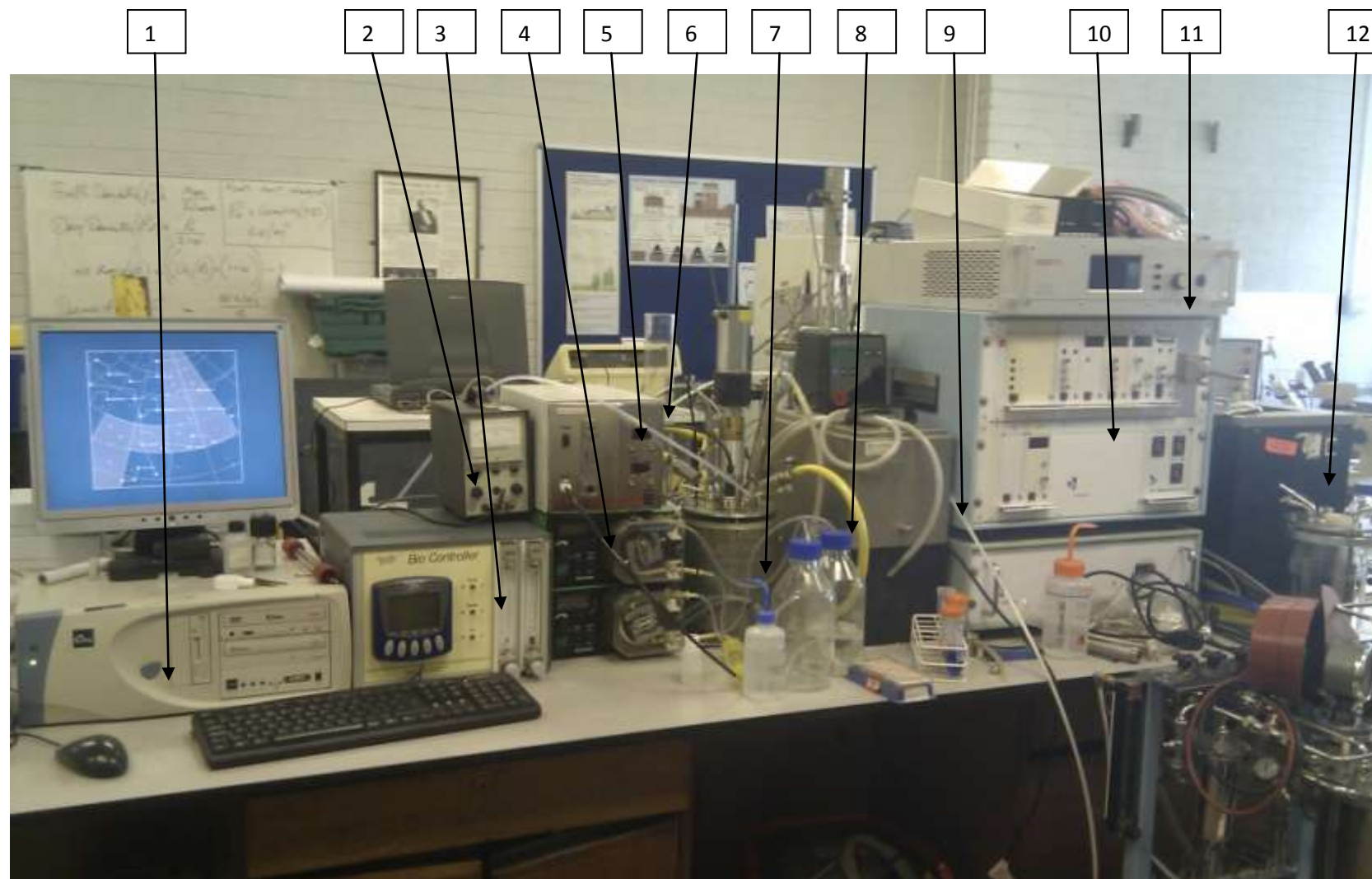


Figure 58. Schematic of prototype system



**Figure 59. Complete system overview**

Key; 1 – Control/monitoring PC; 2 – 24v DC power supply for agitation motor drive; 3 – Broadley Technologies Bio-Controller; 4 – Peristaltic pumps for Acid/Base addition; 5 – ElectroLabs exhaust gas analyser\*; 6 – Gas delivery pipe (Bio-Controller -> STR); 7 - Microwave bioreactor and microwave cavity (see subsequent images for detail); 8 – Acid/base reservoirs and overflow pot; 9 – Exhaust gas condenser heat exchanger\*; 10 – DCI-Biolaffite fermentation control unit; 11 – Sairem 0-200W solid state microwave generator and UI; 12 – Bioreactor heat exchanger

(Note - Image taken at point of wash down and rebuild. Those noted \* illustrated as part of complete system although not online at point of image being taken. BioLaffite fermentation controller unit used until Broadley Technologies acquisition. Compressed air compressor, regulator and accumulator not shown).

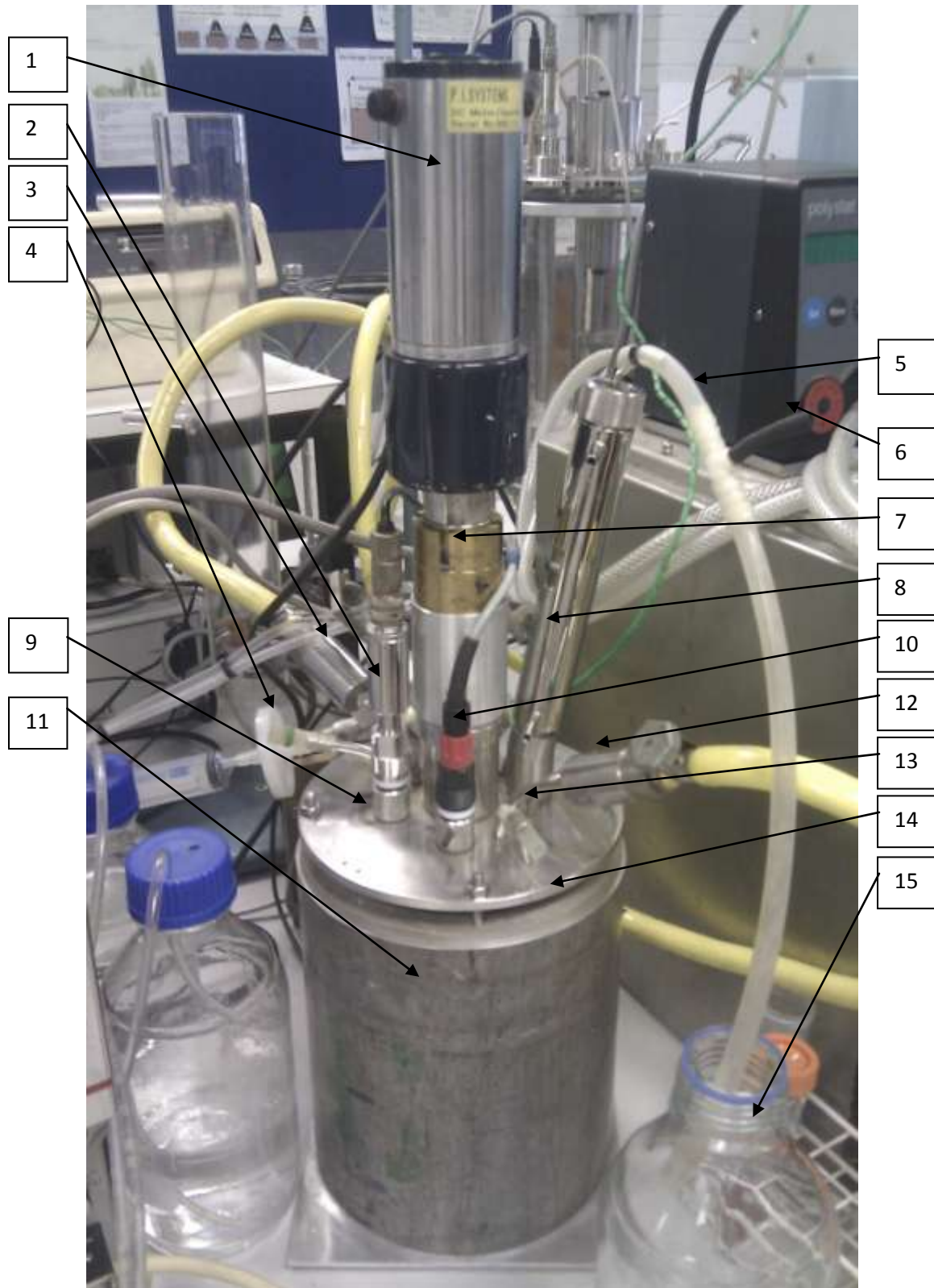


**Figure 60. Microwave bioreactor**

Key; 1 – 24V DC agitation motor; 2 – Dissolved oxygen probe; 3 – Heat exchanger feed; 4 – Sample port (hidden), filter and syringe; 5 – Exhaust gas flue; 6 – Exhaust gas analysis port; 7 – Shear coupling; 8 – Exhaust gas condenser (not in commission in this photo); 9 – Bioreactor top plate; 10 – pH probe; 11 – Steel microwave cavity; 12 – Heat exchanger return; 13 – Air input (not in commission in this photo) 14 – bioreactor compression seal ring; 15 – Expulsion/overflow dump vessel



**Figure 61. Microwave bioreactor (Profile view)**

Key; 1 – Sairem microwave generator; 2 – Co-axial cable; 3 – microwave antenna in S-band waveguide; 4 - S-band waveguide with tuning stubs (obscured); 5 – syringe (20ml); 6 – 0.45 µm filter; 7 – Glass universal vial for sample collection (50ml); 8 - Single direction sample port; 9 – Bioreactor cavity; 10 – Bioreactor cavity base plate and support

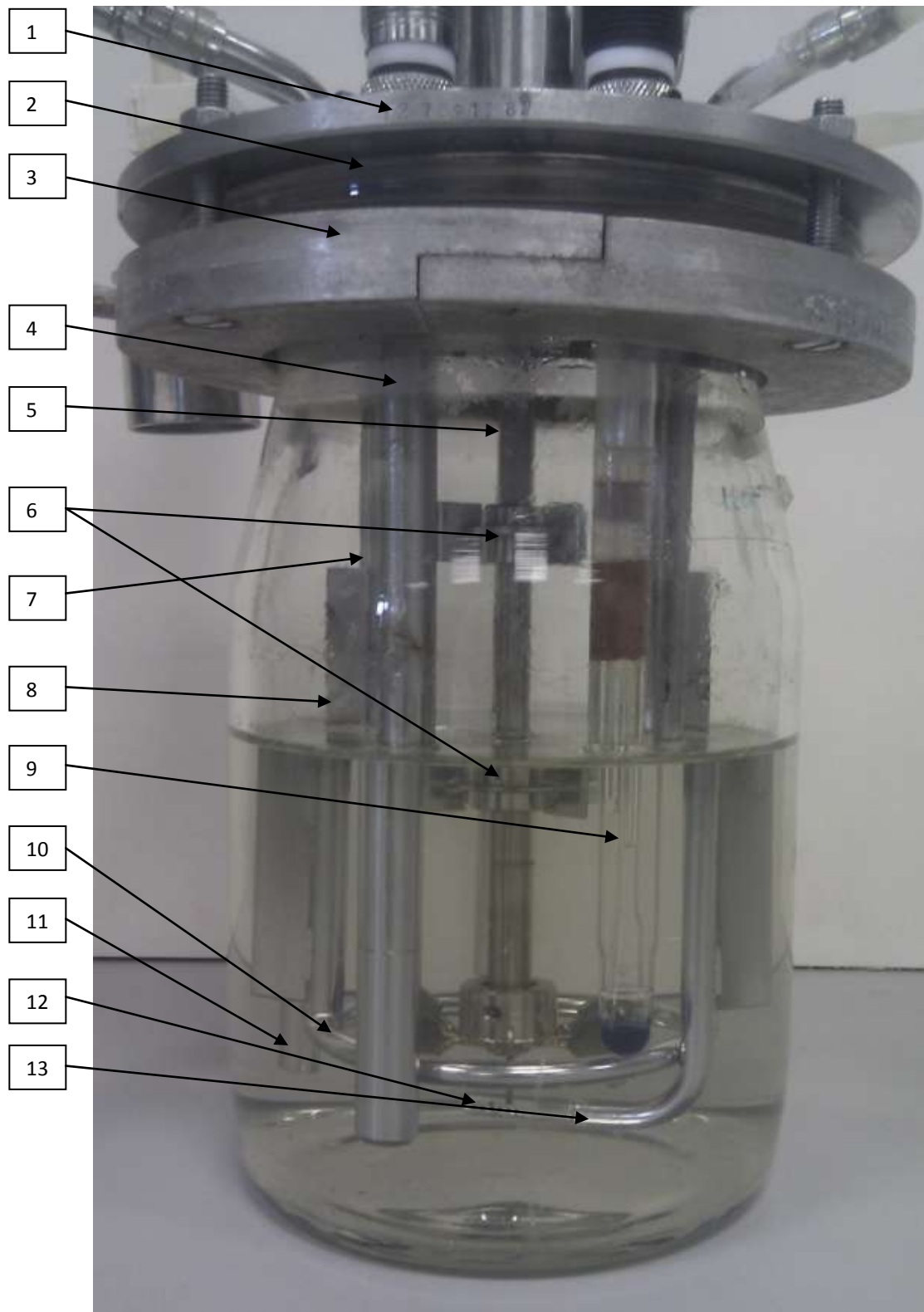


**Figure 62. Submerged elements of the STR**

View of the submerged elements in the STR. Volume of water shown is 1 litre. Key; 1 – STR top plate; 2 – STR vessel flange; 3 – STR compression ring; 4 - Dissolved oxygen probe; 5 - Agitator shaft; 6 - Ruston turbine; 7 - Heating/cooling loop; 8 - Baffle; 9 - pH probe; 10 – Heating/cooling loop; 11 - Bottom draw sample dip tube; 12 - Sparger; 13 - Air delivery pipe

### 3.1.9. Thermal profiling

The whole system design used various metals for its construction. The investigation is the isolation of the microwave field effect from the thermal effect; therefore an understanding of the behaviour of the bioreactor within the microwave cavity has to be determined. This was achieved through thermal profiling of the reactor system. K-type thermocouples and a Pt-100 were used at specific locations, and the temperature profile was determined at each of the following points:

Location:

1. Bioreactor thermal well
2. Ambient
3. Heat exchanger
4. Cavity wall

Data acquisition was achieved in three manners. Real-time data was recorded through the use of a PicoLog TC08 DAQ for all K-type thermocouples. An integrated eLogger DAQ in the Broadley Technologies Biocontroller was used for PT-100 placed within the thermowell while an alcohol thermometer was used in a minority of reference instances explained later in this section. With the use of DAQs over the time periods used, resolution was adjusted according to experiment lengths. In the initial thermal profiling, a recording interval of every second was used where the total time period was 60 minutes. In extended exposure times (up to and greater than 160 hours typical), recording resolution was dropped to greater than 5 second intervals to reduce file sizes. Where multiple files were produced, MS Excel functions were used to reduce the number of data entry points to below the thresholds required for interpretation in MS Excel.

For these experiments, the system remained unlagged and was not lagged in any subsequent experiment. In each instance, the STR was loaded with 1 litre of dH<sub>2</sub>O and agitated at 300 rpm to ensure complete thermal distribution throughout the system. Aeration of the fluid was through mixing at the interface between the head space and liquid as no additional air was added through the sparger system. Net gas flow through the reactor was zero. The reactor was left for a period of approximately 16 hours (overnight) for the whole system to equilibrate at ambient temperature. This was done to avoid the possibility of any section of the system acting as a heat sink which would affect a subsequent experiment if the system was reset in too short a time period. Once at equilibrium, the microwave source was applied at a predetermined power level for one hour with datalogging conducted throughout for ambient temperature, STR thermo-well and external cavity wall temperatures. For the initial profiling the minimum power level achievable from the Microtron unit was 20 Watts. From a 20 Watt base, 20 Watt increments were studied through to 120 Watts.

Prior to conducting any experiments, other studies had shown the difficulty of recording temperature of microwave irradiated reactions due to the temperature probe acting as an aerial for the microwave source and returning inaccurate results. To ensure that the temperature being recorded was representative of the fluid bulk temperature, microwave heated and conventionally heated solutions were recorded using alcohol and mercury thermometers, and K-type thermocouples. Due to the probes and thermometer being housed within the thermal well of the reactor top plate, no interference was observed either through the TC-08 interface or later Bio-Controller or the Sairem and Microtron microwave generators. There was negligible difference between each method of recording, qualifying the temperature recording as accurate measurements. Secondary checking was also conducted to make sure the fluid temperature was representative of the thermal well temperature. This was done through comparison of an immersed probe (K-type, PT-100 and alcohol probes used) compared to thermal well temperature (when required, the microwave source momentarily switched off for the time period of data gathering). Observed temperature difference was negligible ( $<0.02^{\circ}\text{C}$ ).

The use of the TC-08 datalogger and K-type thermocouple had been confirmed as accurate. When the Broadley James Bio-Controller was included into the systems, the temperature recorded through the TC-08 was used as a standard against which to test the Bio-Controller. Temperatures recorded through the Bio-Controller PT100 and DO probe were consistent with the TC-08, confirming justification of temperature detection (difference of  $<0.1^{\circ}\text{C}$ ).

## 3.2. Practical work - Catalysis

On the completion of isothermal bioreactor proofing and calibration, cellulolytic catalysis was conducted within the reactor. For a complete list of all materials and methods used in this section, a summary is provided in the Appendix, pages 31 - 33. In accordance with the objectives determined on page 95, the experimental design is shown in Figure 52 (page 96).

### 3.2.0.0. EP 2.0 – Microwave irradiation of cellulase systems



**Microwave enzymatic saccharification – validation, experiments conducted, reaction protocols, analytical methods.**

**Note;** For full protocol details, see Appendix page 40 for the list of protocols and pages 41 to 100 for the printed protocols.

For the scale of experimentation, the reactor vessel described in 3.1.3. Stirred tank reactor (page 99) was used with operating parameters set by either NREL LAPs or by peer papers.

Experimental design was through the isolation of individual unit operation seen in either the industrial setting or unit operations in cellulolytic fungal metabolism. As such, the experimental work is split into two distinct unit groups; enzymatic hydrolysis and microbial fermentation. In the investigation of microbial fermentation direct from either biomass or from purified cellulose, the enzymatic hydrolysis is conjoined with the fermentation.

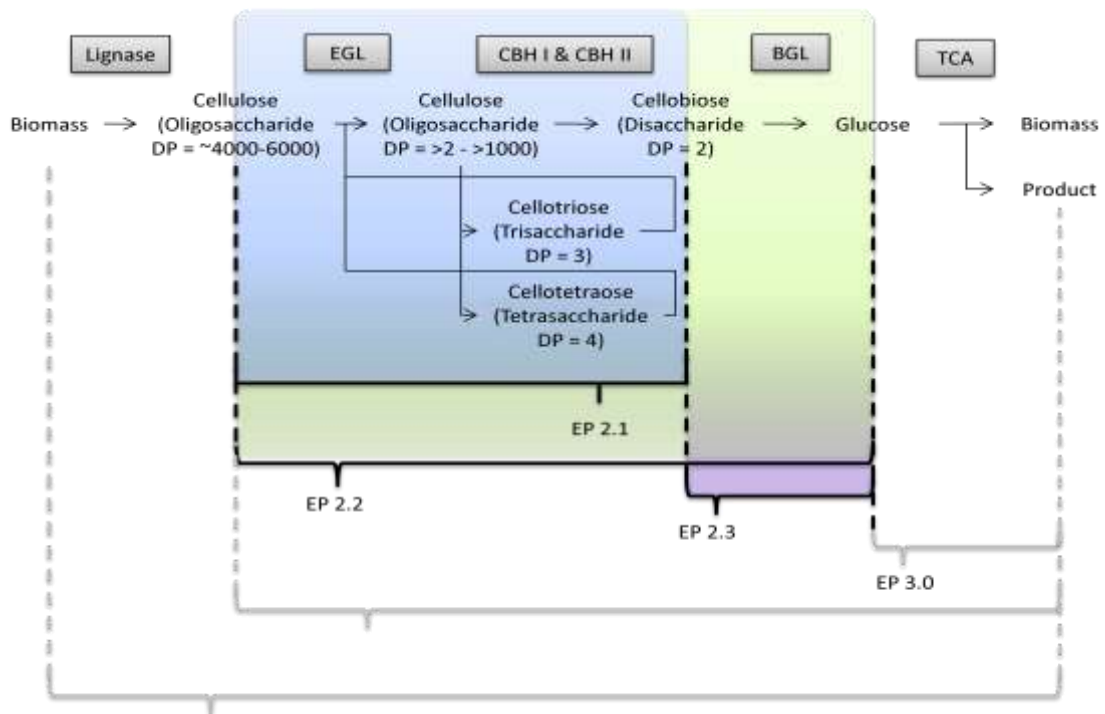


**Figure 63. Experimental Package 2. Enzymatic catalysis in a microwave field**

Overview for the development of experimental progression in studying the microwave influence on cellulytic enzymes. Blue area investigates the microwave influence only on the “cellulase” enzyme preparation (EGL and BGL with the possibility of BGL contamination). Green area illustrates investigation of complete hydrolysis with the use of CBH, EGL and BGL in excess. Purple area illustrates hydrolysis of a pure cellobiose source with BGL as the sole enzyme.

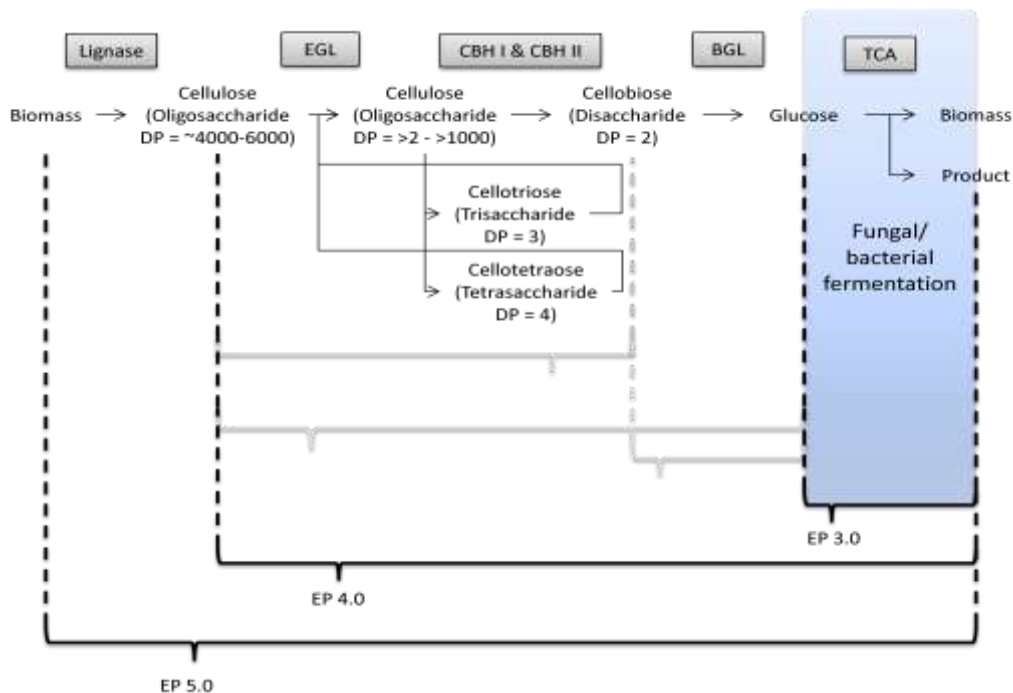


**Figure 64. Experimental Package 3. Fermentation**

**Experimental overview of fermentation in microwave field**

For the investigation of the microwave influence on a fermentation system. Light blue indicates standard fermentation conditions with either a prokaryote or eukaryote.

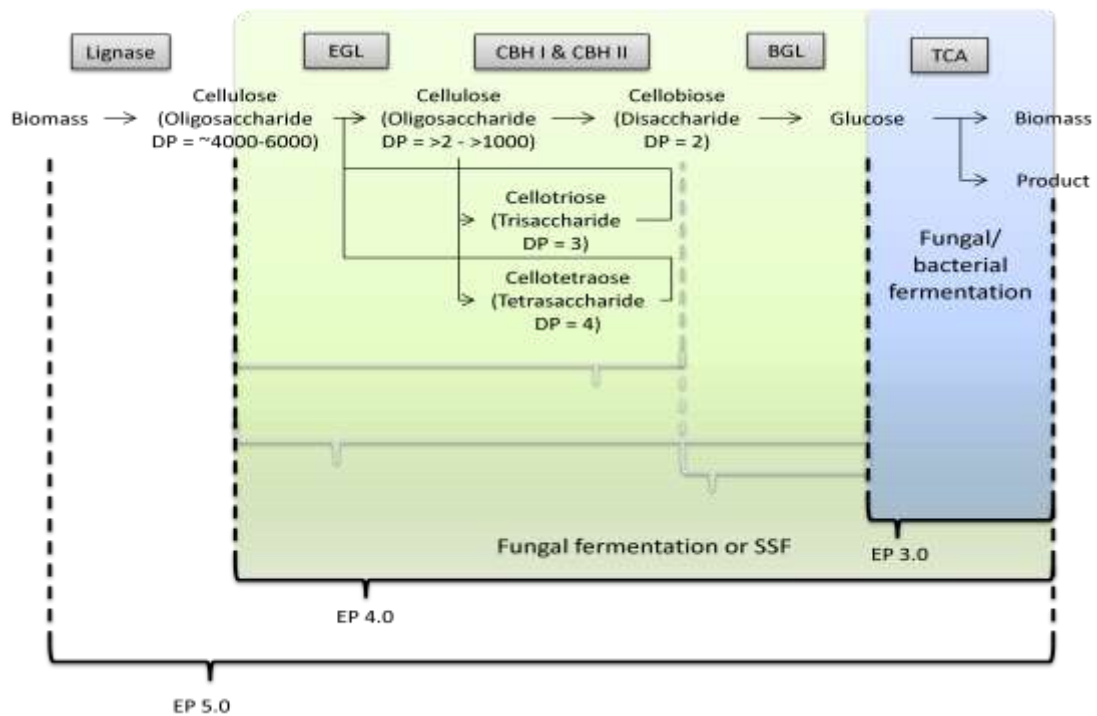


**Figure 65. Proposed Experimental packages 4 and 5. Cellulytic fermentation**

**Experimental overview of fermentation in microwave field**

For the investigation of the microwave influence on a fermentation system. Green area is for the investigation cellulose based fermentation in either direct conversion (cellulytic micro-organisms) or conjoined processing (simultaneous saccharification and fermentation) from a pre-treated biomass source. Purple area illustrates total fermentation from milled biomass by ligno-cellulytic micro-organisms from a direct lignocellulosic source.

For a summary of experiments completed in this project, Table 20 shows the order of experiments with the different parameters.

## Catalysis

| Exp. No.   | ID   | Substrate                      | Enzyme               | Microwave power | Additional comments/notes   |
|--|--|--------------------------------|----------------------|-----------------|---|
| -  | <b>Thermal profiles</b>                        | n/a                            | n/a                  | <b>000-120W</b> | Heat transfer studies   |
| <b>Reference and negative control experiments</b>            |  |                                |                      |                 |   |
| 1  | Microwave negative control                     | Cellulose                      | <i>CBH/EGL</i>       | n/a             | Thermal reference experiment  |
| 2  | Microwave negative control                     | Cellulose                      | <i>CBH/EGL + BGL</i> | n/a             | Thermal reference experiment  |
| 3  | Substrate negative control                     | Cellulose                      | <i>n/a</i>           | 150W            | <b>Investigation of possible autohydrolysis</b>   |
| 4  | Enzyme negative control                        | n/a<br>(Filter paper analysis) | <i>CBH/EGL</i>       | 100W            | 2 part experiment.<br>1) Enzyme/microwave exposure;<br>2) Substrate degradation testing |
| <b>Endoglucanase and Cellobiohydrolase</b>                   |  |                                |                      |                 |   |
| 5  | Cellulases under microwave irradiation         | Cellulose                      | CBH/EGL              | <b>050-200W</b> | Core experiment   |
| 6  | BGL inhibition                                 | Cellulose                      | CBH/EGL              | 050W            | <b>VAN inhibition on BGL for BGL contamination determination</b>                        |
| 7  | Biomass variation                              | Cellulose                      | CBH/EGL              | 050W            | <b>50g cellulose</b>  |
| <b>Endoglucanase, cellobiohydrolase and beta-glucosidase</b> |  |                                |                      |                 |   |
| 8  | Cellulases and BGL under microwave irradiation | Cellulose                      | <i>CBH/EGL /BGL</i>  | <b>012-075W</b> | Core experiment   |
| <b>Beta-glucosidase</b>                                      |  |                                |                      |                 |   |
| 9  | BGL under microwave irradiation                | Cellobiose                     | <i>BGL</i>           | <b>012-075W</b> | Core experiment   |
| <b>Fermentation</b>  |  |                                |                      |                 |   |
| Exp. No.   | ID   | Substrate                      | Enzyme               | Microwave power | Additional comments/notes   |
| 10   | Fermentation negative control                  | Glucose                        | n/a                  | n/a             | <i>Saccharomyces</i> fermentation reference experiment                                  |
| 11   | Fermentation under microwave irradiation       | Glucose                        | n/a                  | <b>012-075W</b> | <i>Saccharomyces</i> fermentations<br>Core experiment                                   |

**Table 20. List of experiments conducted**

List of experiments conducted over the course of the project.

### 3.2.0.1. Experiment validation

To ensure that any variation in the results observed is due to the microwave field being applied, and not an artefact of either a variable which has not been qualified or controlled, the experimental design employed both adherence to defined protocols and a set of negative controls to eliminate logical alternative hypotheses.

For standardisation against other data sets, NREL protocols were used (see “References to published protocols” and “Protocol Development” sections below). For investigation of microwave fields on the substrates and enzymes, negative control experiments were devised based on the NREL protocols. For consistency in analysis, the same analytical tools were used throughout the experiments, as detailed in the following subsections.

Through the use of these methods, it is understood each conclusion drawn in EP. 2.0 – EP. 3.0 can be validated against all known variables.

#### References to published protocols

For the development of the experimental design, published protocols by the National Energy Research Laboratory are used. As the nomenclature of the protocols has changed in revision processes, comparison to the published data can be confusing. For nomenclature comparison, Table 21 shows the previous published name with the revised code as published in June 2011. Each protocol is included in the appendix [pages 40 to 100 ].

| <b>Protocol name</b>  | <b>Previous identifier</b> | <b>Current published identifier June 2011</b> |
|---|----------------------------|---|
| <b>Determination of carbohydrates in biomass by HPLC</b>                                | LAP #002                   | NREL/TP-510-42618                             |
| <b>Measurement of cellulase activity</b>  | LAP #006                   | NREL/TP-510-42628                             |
| <b>Enzymatic saccharification of Lignocellulosic biomass</b>                            | LAP #009                   | NREL/TP-510-42629                             |
| <b>SSF Experimental protocols – Lignocellulosic biomass hydrolysis and fermentation</b> | n/a                        | NREL/TP-510-42630                             |

**Table 21. Nomenclature of published protocols**

Due to alteration of nomenclature of the NREL protocol database with compilation, the access codes to particular protocols have been modified. The current website published identification tags are shown with the previous iteration for use in referencing.

## **Protocol development**

For experiment development, the adoption of the NREL protocols was seen as an approved and verifiable standardised method. The limitation observed in the NREL/TP-510-42629 (Enzymatic Saccharification of Lignocellulosic Biomass) was the prescribed use of either a Yellow Spring Instruments Inc., Model 27 Glucose Analyser or Model 2700 Select Biochemistry Analyser. As the YSL analyser is limited to the identification of a single breakdown product (dependent on the sensor installed), automation and complete profiling of all products in a single sample is not available. By combining NREL/TP-510-42629 with NREL/TP-510-42618 (Determination of Carbohydrates in Biomass by High Performance Liquid Chromatography), deviation from NREL/TP-510-42629 at protocol point 10.5 (with the use of the microwave bioreactor over the LAP's sample size) then ceased at protocol point 10.9. Prior to transfer to the NREL/TP-510-42618 protocol, each sample required reaction quenching through boiling (10 minutes in a heating block set at 105°C. Once quenched, NREL/TP-510-42618 was used for the analysis of the saccharification profile.

Previous experimentation and experience using NREL/TP-510-42628 (Measurement of Cellulase Activity), for the determination of glucose content at low concentrations through the use of GOD-PAP (Glucose oxidase/Peroxidase) and DNS (3,5-dinitrosalicylic acid) were found to have insufficient accuracy and saccharide resolution. Therefore, a modification of the NREL/TP-510-42628 protocol was undertaken. In the development of the determination of enzyme activity, as seen in the enzyme negative control (NC-E), NREL/TP-510-42628 protocol was used with deviation observed at protocol point 8.2.6 through the reaction quenching through boiling as previously described. NREL/TP-510-42628 was then resumed through 8.3-8.4.4 with subsequent quenching also stopped through boiling. As protocol point 8.5 describes the subsequent colour development by addition of DNS, detection of saccharification products is conducted by HPLC using NREL/TP-510-4218.

### **HPLC analysis of breakdown products (NREL/TP-510-42628)**

For the determination of saccharification breakdown products, protocol NREL/TP-510-42628 was observed with initial experiments conducted using the named protocol. The NREL/TP-510-42628 protocol uses a HPX-87P HPLC column (Phenomenex) or equivalent for the identification of cellobiose, glucose, xylose, galactose, arabinose, mannose, xylitol, succinic acid, lactic acid, glycerol, acetic acid, ethanol, 5-hydroxy-2-furaldehyde and furfural with detection through refractive index (RI). In initial protocol trials, the HPX-87P was unavailable; however a comparable (but component reduced) HPX-87N column was available. In conducting trials with this column, results obtained were substandard compared to expected results due to the column's previous usage and age. Therefore a new REZEX ROA H+ column (Phenomenex) was chosen due to its ability to offer a broad spectrum profiling across both the saccharification and fermentation methods. Column comparisons are summarised in Table 22.

## HPLC column selection

| Column                                 | Bio-Rad Aminex HPX-87P  | Bio-Rad Aminex HPX-87N   | Phenomenex REZEX ROA – Organic Acid H+  |
|--|---|--|---|
| <b>Dimensions</b>                      | 300mm x 7.8mm   | 300mm x 7.8mm  | 300mm x 7.5mm   |
| <b>Separation method</b>               | Size-exclusion<br>Ligand exchange   | Size-exclusion<br>Ligand exchange  | Ion-exclusion   |
| <b>Stationary phase</b>                | Lead form,<br>9µm particle size,<br>8% cross linkage,<br>pH range 5-9   | Sodium form,<br>9µm particle size,<br>8% cross linkage,<br>pH range 5-9  | Hydrogen form<br>L22 packing<br>8% cross linked                                       |
| <b>Mobile phase</b>                    | HPLC grade water,<br>0.2µm filtered and<br>degassed   | HPLC grade H <sub>2</sub> SO <sub>4</sub> , 0.2µm<br>filtered and degassed   | HPLC grade H <sub>2</sub> SO <sub>4</sub> , 0.2µm<br>filtered and degassed            |
| <b>Mobile phase flow rate</b>          | 0.6ml min <sup>-1</sup>   | 0.6ml min <sup>-1</sup>  | 0.6ml min <sup>-1</sup>   |
| <b>Elution period (Run time)</b>       | 20 minutes data + 15<br>minutes post run  | 31 minutes   | 31 minutes, 5 minutes post<br>run   |
| <b>Injection volume</b>                | 10-50µl dependent on<br>concentration and<br>detector limit   | 10-50µl dependent on<br>concentration and detector<br>limit  | 10-50µl dependent on<br>concentration and detector<br>limit                           |
| <b>Column temperature</b>              | 80-85°C   | 65°C   | 65°C  |
| <b>Detector temperature</b>            | As close to column<br>temperature as possible   | 40°C   | 40°C (RI)<br>Ambient (UV/VIS)   |
| <b>Detector</b>                        | Refractive index  | Refractive index   | Refractive index<br>(UV/VIS at 210nm for<br>furfural)                                 |
| <b>Constituents detected/standards</b> | cellobiose, glucose,<br>xylose, galactose,<br>arabinose, mannose,<br>xylitol, succinic acid,<br>lactic acid, glycerol,<br>acetic acid, ethanol, 5-<br>hydroxy-2-furaldehyde<br>and furfural | cellobiose, glucose, xylose,<br>galactose, arabinose,<br>mannose, xylitol, succinic<br>acid, lactic acid, glycerol,<br>acetic acid, ethanol, 5-<br>hydroxy-2-furaldehyde and<br>furfural | DP4+, DP3, DP2, Glucose,<br>Xylose, Lactic acid,<br>Glycerol, Acetic acid,<br>Ethanol |

**Table 22. Comparison of HPLC columns for Saccharide detection**

For the determination of oligo-, di- and mono-saccharide constituents, HPLC was employed with the use of a REZEX ROA H<sup>+</sup> column on a Perkin Elmer 200 Series system<sup>10</sup>. All data was recorded on the proprietary Perkin Elmer TotalChrom software. Injection volumes were 10µl with 50µl being used where sample concentration was low to prevent diminished peak areas. Standards were prepared accordingly. Standard curves were used for peak identification and quantification was by calibration with the same standards but using the sodium citrate as the internal standard for sample standardisation.

<sup>10</sup> See Appendix page 33

### **Standardisation of reactor substrates**

To remove any bias due to variability of lignin content and feedstock, a standardised cellulosic feedstock was used.  $\alpha$ -cellulose (Sigma-Aldrich C8002) comprising of  $\beta$ 1-4 linked glucose chains of approximate fibre length of 4000-6000 units was used where the bulk substrate was mixed prior to experimentation to prevent substrate batch variability. As the material had come from a plant origin, the lignin and hemicellulosic material was stripped from the fibre with minimal residual contaminants remaining in the prepared material. By comparison of material degradation through enzymatic hydrolysis, bias derived from lignocelulosic pretreatment was avoided. In reactions investigating the enzymatic rate reaction of BGL, cellobiose (Sigma-Aldrich C7252) was used as the sole substrate.

### **Standardisation of enzyme preparations**

All of the reactions investigated made use of “cellulase” enzymes (Sigma-Aldrich C8546) from *Trichoderma reesei* strain ATCC26921, and  $\beta$ -glucosidase (Sigma-Aldrich C6105, synonym Novozyme 188) from *Aspergillus niger*. All materials were stored in accordance to the suppliers’ recommendations.

### **Standardisation of substrate and enzyme loading**

Substrate loading across all catalysis investigations was at 10g/l. The loading used is below commercial viability of 250g/l required for industrial adoption. Reduced substrate loading allows development of an aqueous system where rate limitations are observed and with a standardised method comparable across other studies. For experimental development, cellulose loading was justified through the data reported by Hari Krishna *et. al.* [196]. In reporting by Hari Krishna, work carried out by Plackett-Burman surface response methodology for temperature, pH, cellulose and cellulase loadings, where 10% biomass loading was considered appropriate. As a large selection of studies have also used 10% loading, cross comparison in methods become easier.

For enzyme loading (Cellulase mixture of EGL and CBHI and CBHII), the standardised loading of 40 filter paper units per gram cellulose (FPU/g cellulose) was derived from the NREL/TP-510-42628 where actual mass was scaled from the protocol descriptor. Qualification of loading was also supported by Hari Krishna [196] along with many other papers using TP-510-42628.

In experimentation with  $\beta$ -glucosidase, the loading of BGL was determined through a development of the NREL/TP-510-42629 protocol, where mass loading was based on the addition of liquid Novozyme 188 at 250 Cellobiase Units/g (CBU/g). NREL/TP-510-42628 descriptor uses p-Nitrophenyl- $\beta$ -D-glucoside (pNPGU) activity signifying an addition of “60FPU/g cellulose and the appropriate volume of  $\beta$ -glucosidase enzyme to equal 64 pNPGU/g cellulose.” Conversion of pNPGU to CBU/g was determined. Through the use of data compiled by the Louisiana State University (LSU) Agricultural Centre for submission to the US Department of Energy, whereby a 1

FPU: 2 CBU ratio was used through the employment of 15 FPU:42 CBU, therefore with preparations used in this study, 60 FPU: 168 CBU equates to 1 FPU:2 CBU, where BGL equals 250U/g and U = CBU. As such, the equivalent resultant loading was equal to the 64 *p*NPGU/g cellulose required and in excess in comparison to the EGL/CBH addition, preventing feedback inhibition in the system. For experiments conducted, 15 FPU equates to 42 CBU where the ratio employed is 2.8 FPU:CBU. Data taken from Days' report for the DOE looked variation of FPU:CBU ratios in the range of 2 to 3.3 FPU:CBU [197] supporting the case of using 2.8 ratio.

To summarise, this has led to the standardised methodology for catalysis where;

- 1) Substrate = 10g/l (cellulose or cellobiose)
- 2) "Cellulase" = 40FPU/g substrate, (5.54 FPU/mg dry mass)
- 3) BGI = 111.7CBU/g substrate (250CBU/g aqueous)

### Standard curves for determination of constituents

For analysis of the breakdown products, standard curves for HPLC analysis were constructed from analytical grade reagents. Standard curves for xylose (0.01g/l - 0.1g/l), glucose (0.1g/l - 10g/l), cellobiose (0.025g/l - 10g/l), cellotriose (0.01g/l - 2g/l) and cellotetraose (0.01g/l - 2g/l) were constructed for catalysis. Glucose (0.1mg/ml - 60mg/ml), ethanol (0.05% - 25%) were used for fermentation analysis in addition to peptone and yeast extract for peak identification and analysis. At least 5 separate data points were used per calibration. As all calibrations were linear over the range used, the LINEST function in Excel<sup>TM</sup> was used for determination of gradient and intercept for each reagent in conjunction with the correlation coefficient ( $R^2$ ) (see Figure 66). Standardisation was repeated for each exchange of mobile phase and within sample runs. Percentage error in repeat injections was typically less than 1.5% (Table 23 and Figure 66). For reagent product codes, see "Reagents used" list.

| <b>g/l</b> | <b>Glucose data</b> |          |          |          |          |          | <b>Average</b>  | <b>STDEV</b>     | <b>RSE</b> |
|------------|---------------------|----------|----------|----------|----------|----------|-----------------|------------------|------------|
| <b>120</b> | 28277924            | 27868955 | 28249735 |          |          |          | <b>28132205</b> | 228416           | 1%         |
| <b>100</b> | 24633589            | 24811089 |          |          |          |          | <b>24722339</b> | 125511           | 1%         |
| <b>80</b>  | 18983248            | 19027682 | 18993403 | 19186910 | 19624446 | 19053466 | <b>19144859</b> | 246135           | 1%         |
| <b>60</b>  | 14575078            | 14787238 |          |          |          |          | <b>14681158</b> | 150020           | 1%         |
| <b>40</b>  | 8949383             | 8918352  | 9204270  | 8985719  | 9234120  | 8974020  | <b>9044311</b>  | 137743           | 2%         |
| <b>20</b>  | 4902508             | 5343869  |          |          |          |          | <b>5123189</b>  | 312089           | 6%         |
|            |                     |          |          |          |          |          | <b>Gradient</b> | <b>Intercept</b> |            |
|            |                     |          |          |          |          |          | <b>237918</b>   | <b>153723</b>    |            |

Table 23. Calibration curve data analysis

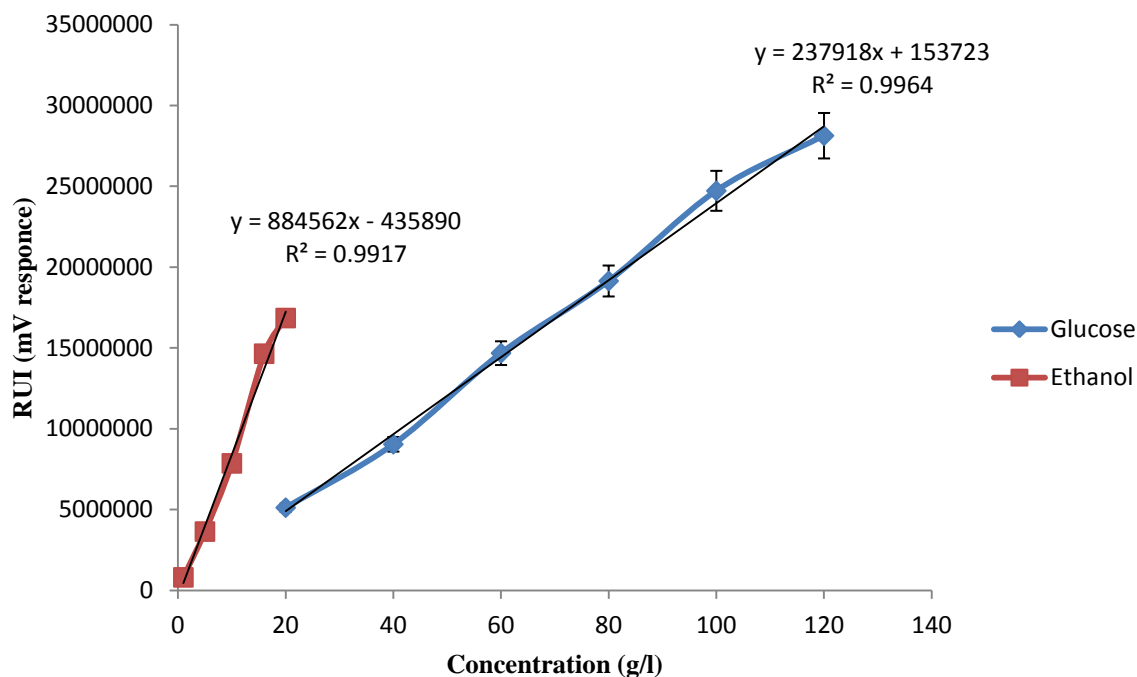


**Figure 66. Example standard curves**

Standard curves produced by multiple injections over the course of a fermentation experiment.

## Data processing

For data processing of saccharification events, the following mathematical processing steps are used.

From the raw data produced from the HPLC, several steps are required before the determination of analyte concentration can be inferred. With the initial start conditions known for any experimental procedure, commonality between experiments was the citrate buffer used, therefore the associated citrate peak was considered an internal standard across all catalysis experiments. Determination of peak identification was done by reference to known standards for elution time and peak area. Peak height/area is correlated to concentration through calibration with known standard curves for xylose, glucose, cellobiose, cellotriose and cellotetraose, with concentrations appropriate for the expected constituent parts. Standards were repeated for each new mobile phase.

### Standardisation by internal standard.

Following completion of the HPLC chromatogram and data acquisition, peak data is exported to Microsoft Excel. For the standardisation by internal standard, the mean citrate peak area is determined with all resultant peaks standardised using a calibration factor on the raw mV response peak area measurement.

### **Correction for water hydration.**

As each hydrolysis causes the addition of one molecule of water, hydration is considered.

#### **Equation 2. Correction for water hydration**

Calculation of percentage saccharification;

---

#### **Equation 3. Calculation of % saccharification**

### **Calibration by standard curve.**

From the transformed raw data, each value is referenced against their respective standard curves

---

#### **Equation 4. Calculation of concentration**

### **Curve fitting data**

For the determination of theoretical maximum product formation, curve fitting was conducted using Equation 5. By forward predicting the curve to a point of negligible rate increase, the theoretical yield can be calculated.

---

#### **Equation 5. Catalysis curve fitting**

Where  $y$  = predicted value;  $x$  = time;  $n_1$  and  $n_2$  = constants 1 and 2.

Curve fitting was conducted through the use of Equation 5 with the solver function in MS Excel used to find the values of  $n_1$  and  $n_2$  by the least sum method.

### **Exposure time periods**

Experiments on catalytic activity were conducted over a time course of 0-2 hours (BGL-cellobiose), 0-33 hours and/or 0-168 hours (CBH/EGL-cellulose) depending on the focus of the study. Samples were manually drawn hourly for the first 9 – 10 hours, followed by every two hours in the second 24 hour period and every four hours for subsequent 24 hour periods for experiments involving CBH/EGL and cellulose, and every 10 or 15 minutes in experiments involving cellobiose and BGL. With the exception of the first 24 hours, all subsequent days had samples taken between 0830 to 1800 hours. Fermentation experiments were conducted over a 53 hr time period. Inoculation occurred at T=0hrs

with hourly samples taken for the first 11 hours. Hourly samples were then taken at hourly time intervals for the time periods T=25 to 36hrs and T=49 to 57hrs. Gaps in the sampling regime were due to the experimenter being away from the laboratory (i.e. times outside the extended work day).

### Qualification by saccharification by-products.

In the absence of BGL, the process of hydrolysing polymeric cellulosic material to poly- and oligosaccharides of varying chain length, the initial polysaccharide chain (approximately 4,000 to 6,000 glucose units in length) was degraded synergistically by CBH and EGL to the disaccharide cellobiose with glucose. The theoretical end point for the reaction is the accumulation of cellobiose and glucose equivalent to the mass of cellulose. With the impurities in cellulase enzyme preparation, contamination (or residual) BGL maintained within the cellulase preparation will cause the excess production of glucose from the cellobiose. Results are determined by the accumulation of both cellobiose and glucose.

For the degradation of cellulose ( $DP_n$  where  $n$  is  $4 - \geq 4000$  glucose units), the multi step pathway of  $DP_n$  to  $DP_1$  uses a complex of four distinct enzymes in a (natively) simultaneous manner. As the system has a multiple pathway cascade, the recycling of oligosaccharides has to be considered. The system is illustrated in Figure 67.

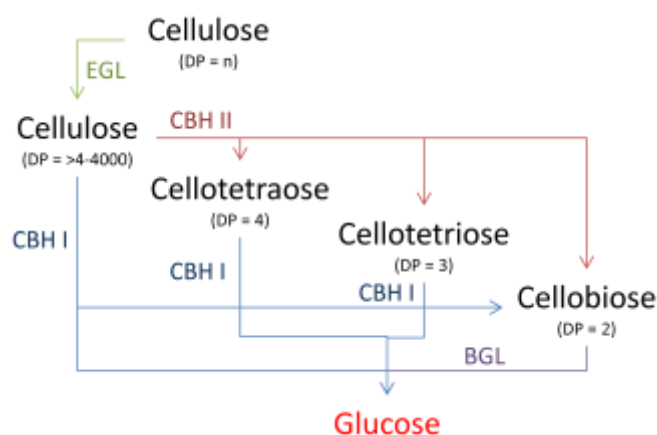


**Figure 67. EGL, CBHI, CBHII and BGL degradation of cellulosic material**

Illustration of enzymatic degradation. EGL is illustrated as initial enzyme although all enzymes can work in parallel at any time. For ease of reading, pathways are illustrated by colour whereby green = EGL, Red = CBHII, Blue = CBHI and Purple = BGL.

For the determination of microwave influence within the system, catalysis is segregated into three distinct units identified as Experimental Packages 2.1 to 2.3. The identification of each package is illustrated in the schematic (see Figure 68).

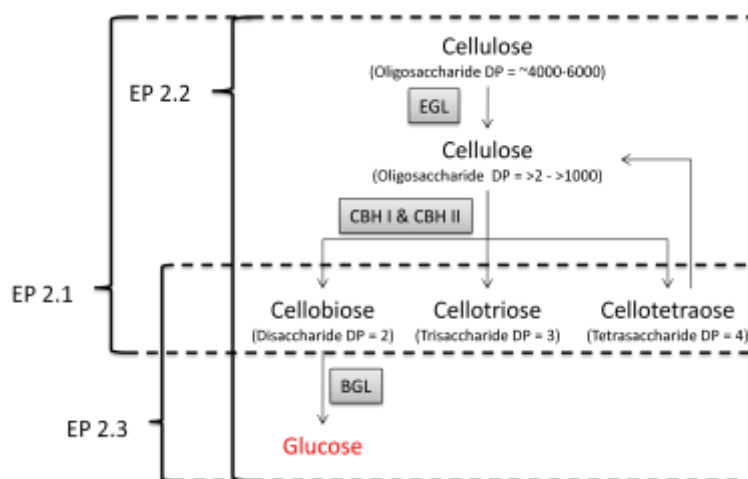


**Figure 68. Contextualised illustration of Experimental Package 2.1 -2.3**

Enzymatic progression of cellulose substrate through to glucose with intermediates cellotriose and cellotetraose noted. EP 2.1 donates to cellulose with CBH and EGL. EP 2.2 donates cellulose with CBH, EGL and BGL. EP 2.3 donates cellobiose with BGL.

Due to EGL lysis occurring midpoint in the cellulose chain, fraction sizes of varying length will be produced as intermediates prior to exo- and endo-cellobiohydrolase hydrolysis. The resolution limitation of the REZEX ROA column (only able to differentiate between DP4+, DP3, DP2 and specific monomeric sugars), means that the degree of depolymerisation where the chain length is greater than three cannot be determined accurately. As such, degradation rate is quoted as the production of glucose, cellobiose or fermentable sugar (glucose) equivalents (See Figure 69). In contrast to the mono- and disaccharides where solubility reflects decreased chain length, the HPLC method used with the REZEX ROA column causes the elution of the DP4+ peak very close to the solvent front, making quantification problematic. As DP4+ is a transitional material from the polymeric saccharide to the dimeric cellobiose, DP4 is not seen in this methodology as a sufficient indicator of hydrolysis. With the use of an oligo-saccharide column, this information can be obtained to support this assumption.

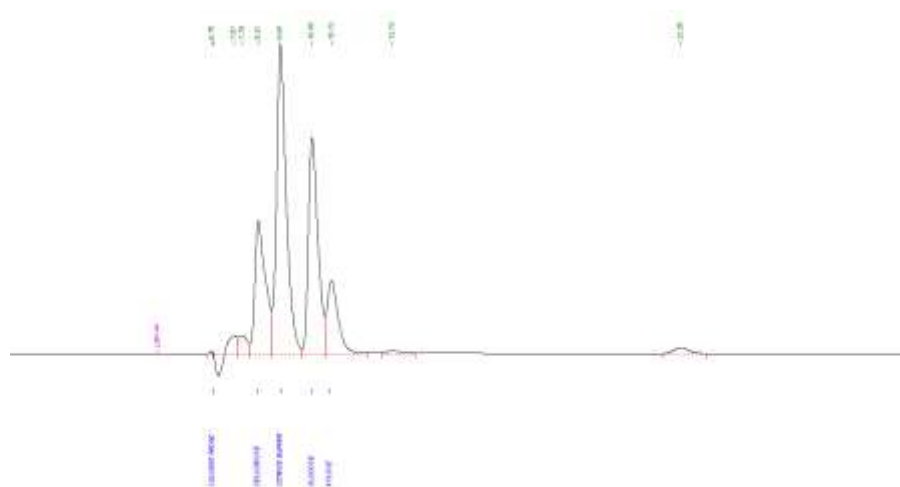


**Figure 69. Example of a REZEX ROA HPLC Chromatogram**

Edited example of a chromatogram produced using the REZEX ROA column, 0.6ml/min H<sub>2</sub>SO<sub>4</sub> where the column heater is at 65°C, RI detection at 40°C, 10 - 50µl sample injection has been 0.2µm filtered reaction product, where the experimental conditions have been 50W microwave power from the Sairem microwave generator, 50°C reaction temperature, 50g/l biomass after a time period of 81 hours post enzyme addition. Baseline time period illustrates 31 min elution period where solvent front elutes at 6.7 minutes, DP4+ to xylose from 6.7 – 10.7 minutes, trace background elements at 12 minutes and ethanol due to antibiotic suspension appears at 22.25 minutes.

### **3.2.0.2. Negative controls**

#### **Hydrolysis under standard thermal condition (Microwave negative control (NC-MW))**

For the determination of saccharification in the reactor system, the NREL/TP-510-42628 was used with protocol modifications for the reactor. In execution of NREL/TP-510-42628, the expectation is for a test tube scale reaction for analytical processing. In contrast, the desired procedure was for a continuous microwave exposure experiment with frequent sample extractions over extended time periods. To modify the equipment and apparatus, scaling was increased from a sample volume of 10ml to 1 litre for all reagents. Temperature control was through the use of the heat exchanger to maintain the reactor temperature setting which required approximately 12- 16 hours for the system to equilibrate. Standard biomass loading of 10g/l substrate was used with enzyme selection according to study with sampling taken at set time points. Without any microwave field being applied and the sole heating mechanism being through the submerged thermal exchange loop, three experiments operating in this mode (cellulose with EGL/CBH minus BGL, cellulose with EGL/CBH and BGL, and cellobiose with BGL) are considered to be microwave negative controls.

#### **Influence of microwave power on substrate (Substrate negative control (NC-S))**

To determine any possible effect of the microwave field on the substrate, alpha cellulose (10g/l) was loaded into the microwave reactor in accordance to the standard NREL/TP-510-42629. The microwave source was then activated with the microwave power output of 150W (4 – 5W reflected power, 50°C) and subjected to 9 hours exposure. Samples were withdrawn at hourly intervals with preparation for HPLC analysis.

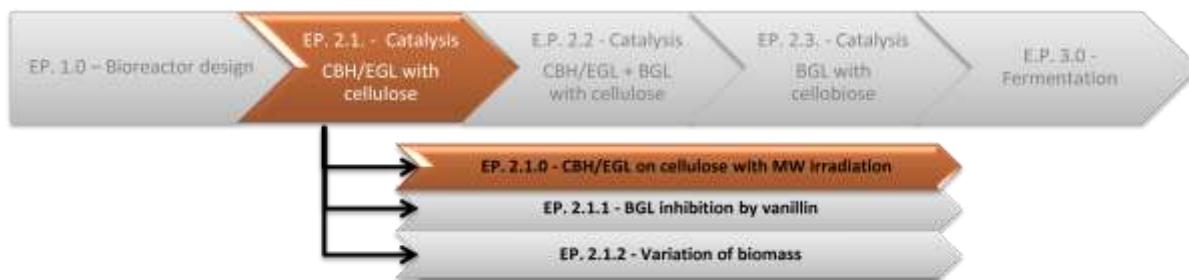
#### **Influence of microwave on enzyme degradation (Enzyme negative control (NC-E))**

It was suspected that the microwave energy would have the ability to alter the kinetic rate of the enzyme and excessive microwave power was hypothesised to degrade the enzyme. To determine the rate of enzyme degradation as a function of exposure time for any known microwave power, the enzyme was subjected to microwave energy for set time periods in the absence of a cellulosic source and then used in NREL/TP-510-42629 for the determination of cellulase FPU activity. To determine the influence of the microwave field on the enzyme and possibility of enzyme degradation through interaction with the microwave field, the enzymes were subjected to the microwave field in the absence of substrate. To test for enzyme degradation, an adaption of the NREL/TP-510-42628 was used where HPLC analysis was used over the colourimetric method described. In modification of the protocol, enzyme loading equivalent to 60FPU/g cellulose assuming a standard loading of 10g cellulose per litre was suspended in citrate buffer (1 litre) exposed to microwave energy at 100W for a maximum of 10 hours. Samples (5-15ml) were taken at hourly intervals, filtered and stored on ice before 0.5ml was transferred to the filter paper as per protocol. On completion of the incubation (1

hour at 50°C), instead of DNS being added, the samples were pipetted from the sample tube into a 1.5ml Eppendorf before being heat de-natured (105°C for 5 minutes). Total sample preparation was then filtered through a 0.2µm HPLC grade filter before storage on ice for HPCL analysis.

Following results obtained at lower powers, the negative control was later repeated at a power setting of 24W for examination at the re-established optimal power.

### 3.2.1.0. EP. 2.1.0. – Cellulose hydrolysis by CBH/EGL – BGL with varying microwave irradiation



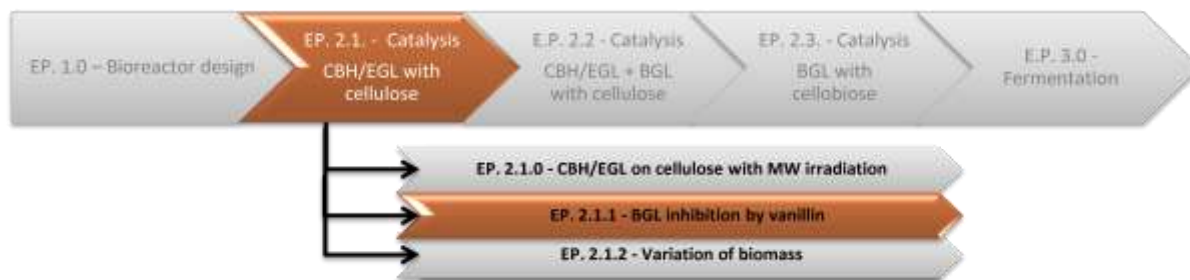
| Microwave power | Substrate           | Enzyme                    | Protocols         | Additional standards/comment |
|-----------------|---------------------|---------------------------|-------------------|------------------------------|
| 000W            |                     |                           |                   | Negative control             |
| 050W            | $\alpha$ -cellulose | "Cellulase"<br>(CBH, EGL) | NREL/TP-510-42618 |                              |
| 100W            |                     |                           |                   |                              |
| 150W            |                     |                           |                   |                              |
| 200W            |                     |                           |                   |                              |

**Table 24. EP 2.1.0. Variable focus; Microwave power (000W-200W)**

The cellulase preparation used was known to contain CBH derived from a submerged *T. reesei* fermentation and purified for the expression of CBH. In the application of CBH complex to the  $\alpha$ -cellulose, the reaction endpoint should be cellobiose and glucose with feedback inhibition of the cellobiose on the CBH limiting cellobiose yield.

All conditions are independent of microwave power. No pH control was used except for solution buffering at set up. Microwave power levels used are shown in Table 24.

### 3.2.1.1. EP. 2.1.1. - Investigation for inhibition of residual BGL through the addition of vanillin



| Microwave power | Substrate           | Enzyme                    | Protocols                              | Additional standards/comment   |
|-----------------|---------------------|---------------------------|--|--|
|                 |                     |                           |  | Negative control (Enzyme)<br>Negative control (vanillin)<br>Negative control (Substrate)   |
| <b>050W</b>     | $\alpha$ -cellulose | “Cellulase”<br>(CBH, EGL) | NREL/TP-510-42618<br>NREL/TP-510-42628 | <b>0.05mg vanillin</b><br><b>0.2mg vanillin</b><br><b>0.4mg vanillin</b><br><b>0.8mg vanillin</b><br><b>1.2mg vanillin</b><br><b>1.6mg vanillin</b><br><b>2mg vanillin</b> |

**Table 25. EP 2.1.1. Variable focus; BGL inhibition**

Vanillin (VAN) is known to down regulate BGL activity [34] where a vanillin : cellulase ratio of 4:1 by mass (or 4mg:0.5FPU) is shown to retard BGL activity by 50%. In the assumption that the majority of mass in the “cellulase” preparation is EGL and CBH (due to the product showing clear signs of EGL and CBH activity), it can be assumed that any BGL contamination will be of low mass in the total solid protein. In the instance of a pure CBH preparation, the addition of varying VAN concentrations should have no significant effect on rate or yield. With the presence of BGL contamination in none irradiated enhanced investigation, VAN inhibition would be indicated by the reduction of the glucose accumulation with increasing VAN concentration. As a total cellulase mass of used is 0.12g/l where substrate loading is 10g/l, a vanillin loading of 0.05mg/ml – 2mg/ml equates to a vanillin : cellulase ratio of 0.41:1 to 16:1 by g (vanillin):g (cellulase).

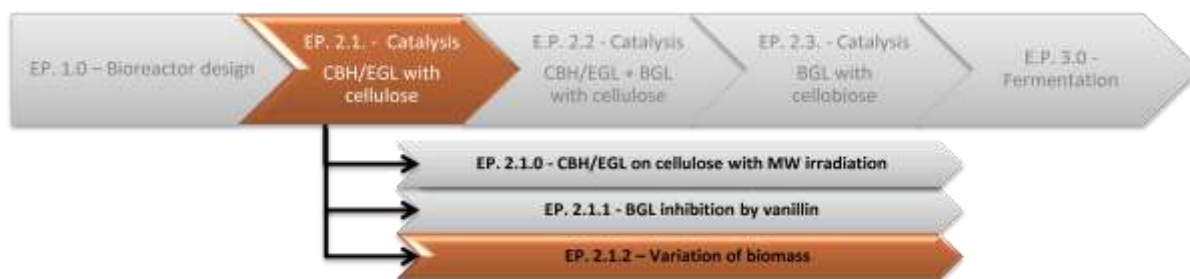
As a derivation of the NREL/TP-510-42628,  $\alpha$ -cellulose (10g/l) was used as the substrate with cellulase enzyme used as the catalyst (60FPU/g substrate). VAN concentrations varying from 5mg/l to 0.2g/l were explored. The experiment constituents are shown in Table 26.

| <b>Condition/Test number</b>      | <b>Antibiotic (total)</b> | <b>H<sub>2</sub>O</b> | <b>Enzyme addition</b> | <b>Vanillin addition</b> | <b>Vanillin concentration</b> |
|-----------------------------------|---------------------------|-----------------------|------------------------|--------------------------|-------------------------------|
| <b>1</b>                          | 200µl                     | 2975 µl               | 2000µl                 | 25 µl                    | 0.05mg/ml                     |
| <b>2</b>                          | 200µl                     | 2900 µl               | 2000µl                 | 100 µl                   | 0.2mg/ml                      |
| <b>3</b>                          | 200µl                     | 2800 µl               | 2000µl                 | 200 µl                   | 0.4mg/ml                      |
| <b>4</b>                          | 200µl                     | 2600 µl               | 2000µl                 | 400 µl                   | 0.8mg/ml                      |
| <b>5</b>                          | 200µl                     | 2400 µl               | 2000µl                 | 600 µl                   | 1.2mg/ml                      |
| <b>6</b>                          | 200µl                     | 2200 µl               | 2000µl                 | 800 µl                   | 1.6mg/ml                      |
| <b>7</b>                          | 200µl                     | 2000 µl               | 2000µl                 | 1000 µl                  | 2mg/ml                        |
| <b>Vanillin negative control</b>  | 200µl                     | 2000 µl               | 2000µl                 | 0                        | 0mg/ml                        |
| <b>Enzyme negative control</b>    | 200µl                     | 4000 µl               | 0                      | 1000 µl                  | 2mg/ml                        |
| <b>Substrate negative control</b> | 200µl                     | 2000 µl               | 2000µl                 | 1000 µl                  | 2mg/ml                        |

**Table 26. EP 2.1.1. Experimental design for BGL inhibition**

Each experiment was conducted in a 20ml glass universal bottle with 300 rpm agitation in a 50°C shake flask incubator for standardised conditions. All experiments were conducted in parallel.

### 3.2.1.2. EP. 2.1.2. - Variation of cellulose loading with hydrolysis by CBH/EGL –BGL with varying microwave irradiation



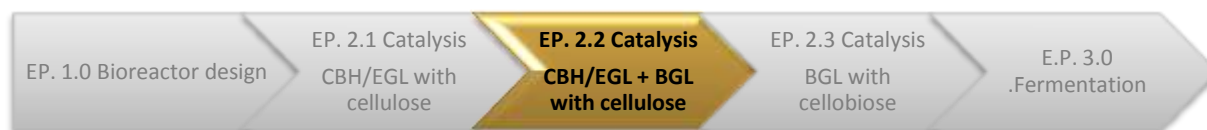
| Microwave power | Substrate           | Enzyme                 | Protocols                              | Additional standards/comment       |
|-----------------|---------------------|------------------------|--|------------------------------------|
| 050W            | $\alpha$ -cellulose | “Cellulase” (CBH, EGL) | NREL/TP-510-42618<br>NREL/TP-510-42628 | Negative control<br>10g/l<br>50g/l |

**Table 27. EP 2.1.2. Variable focus; Biomass loading**

For variation of biomass, the desired end product formation (ethanol) has an economic feasibility bottom line of 105g/l glucose fermentation media. Assuming a classical ethanol fermentation using *S. uvarum* with a yield of 0.44g/g glucose, to obtain the minimal ethanol concentration, initial glucose concentration would be 250g/l. Assuming complete conversion of substrate ( $\alpha$ -cellulose) to glucose, 250g/l cellulose would be required. The viscosity of 250g/l cellulose loading causes the mixture to adopt the characteristic form a non-Newtonian fluid, where agitation causes cavitations around the turbines used. As such, the loading parameter of the bioreactor design is considered as the  $[S]_{\max}$  limitation.

To investigate enzyme saturation, the increase in cellulose loading can elucidate if the lower 10g/l loading as at saturation as suggested. Thus, initial  $[S]$  for pilot scale investigations is in accordance with the LAP loading of 10g/l. For increase in  $[S]$ , this was increased to 50g/l representing one-fifth of substrate loading. Comparison of 10g/l at 50W irradiation to 50g/l irradiation shows the comparison of enzymatic rate assuming substrate saturation where  $[S] \gg [E]$ .

### 3.2.2.0. EP. 2.2.0. – Cellulose hydrolysis by CBH/EGL +BGL with varying microwave irradiation.



| Microwave power | Substrate   | Enzyme              | Protocols         | Additional standards/comment |
|-----------------|-------------|---------------------|-------------------|------------------------------|
| 000W            |             |                     |                   | Negative control             |
| 012W            | α-cellulose | “Cellulase”         | NREL/TP-510-42618 |                              |
| 024W            |             | (CBH, EGL)          |                   |                              |
| 050W            |             | β-glucosidase (BGL) | NREL/TP-510-42628 |                              |
| 075W            |             |                     |                   |                              |

**Table 28. EP 2.2.0. Variable focus; Enzyme addition (EGL and BGL)**

EP 2.2.0 investigated total hydrolysis with the use of the CBH, EGL and BGL with BGL in excess. The parameters used were the same as seen in the previous experiment (E.P. 2.1.0), however with the addition of BGL. With the optimal irradiation parameter in the previous experiments seen at the 50W power point, values less than 100W were selected (Table 28). For understanding of the influence, 50W was seen as nominal, with values above and below this starting point considered. With the apparent non-linear relationship between increase the in saccharification and microwave power 75 Watts and 25 Watts were taken as the initial variable values with further values being decided upon following initial result analysis. BGL loading was at 250 CBU/g.

### 3.2.3.0. EP 2.3.0. – Cellobiose hydrolysis by BGL with microwave irradiation



| Microwave power | Substrate  | Enzyme                     | Protocols         | Additional standards/comment |
|-----------------|------------|----------------------------|-------------------|------------------------------|
| <b>000W</b>     |            |                            |                   | Negative control             |
| <b>012W</b>     | Cellobiose | $\beta$ -glucosidase (BGL) | NREL/TP-510-42618 |                              |
| <b>050W</b>     |            |                            | NREL/TP-510-42628 |                              |
| <b>075W</b>     |            |                            |                   |                              |

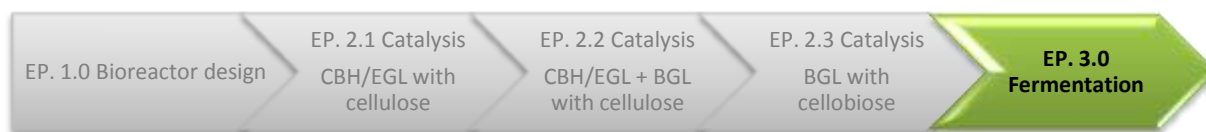
**Table 29. EP 2.3.0. Variable focus; Carbohydrate with BGL**

The experimentation of BGL complementary to CBH was investigated through the use of NREL/TP-510-42629. The BGL used was Novozyme 188 supplied by Sigma-Aldrich (product code; C6105) under the pseudonym of BGL from *A. niger*.

Due to the power correlations observed in E.P. 2.1.0, microwave power was reduced in range from 0 – 150W to 0 – 75W. For separation of BGL activity from the overall process, cellobiose as a pure substrate was used to prevent prior treatment influence (Table 29 and Standardisation of reactor substrates (page 119)).

The experiments were conducted under the same conditions and parameters as E.P. 2.1.0 and E.P.2.2.0 with only substrate and enzyme variation.

### 3.3.0.0. EP. 3.0 - Fermentation



To demonstrate the microwave reactor being used in a simple unicellular system for chemostat cultivation, brewer's yeast (*Saccharomyces cerevisiae*) was cultured for the production of ethanol as end product using standardised conditions. The conditions for the stirred tank reactor were determined through literature searching, where agitation and operation were controlled as salient parameters. The generalised fermentation conditions used are based on the NREL Protocol NREL/TP-510-42630.

#### ***Stain culture, frozen stock culture and inoculum preparation.***

Strains used are commercially available brewers' yeast supplied through Alcotec Ltd. YPD plates (19/1 yeast extract, 20g/l peptone, 20g/l dextrose, 20g/l agar) were inoculated from reconstituted freeze dried samples as described below and incubated (30°C).

Media (40% glycerol in DI water) was autoclaved and returned to room temperature. The initial plate inoculum was transferred into 100ml YDP media in a sterile 250ml shake flask and incubated (38°C, 24hrs). A sample of cell free media was tested by HPLC for pH, glucose and ethanol and checked for media properties (desired ranges of pH 4.5-5, 0-5g/l glucose and 8-10g/l ethanol). The cell culture was observed microscopically for contamination and culture purity.

The glycerol solution was then mixed with the inoculum aseptically and dispensed in aliquots into 1ml sterile cryovials and stored at -80°C.

Inoculum flasks (250ml flasks, 50ml YPD and 5% w/v glucose) were prepared with 1:5 working volume in baffled flask, and incubated (rotary incubator, 130rpm, 30°C) for a period of 10 - 14 hours. Transfer to the bioreactor was completed once the inoculum's glucose concentration had dropped below 2 g/L. Optical density (O.D.) at 600nm was used as an indication of biomass with OD value at 600nm <0.800 being acceptable. Values greater than 0.8 were diluted to bring within range.

At the point of transfer, inoculum determination was done through the use of Equation 6 .

---

#### **Equation 6. Calculation of fermentation inoculum**

In addition to active inocula described previously, freeze dried additions were also prepared in a manner analogous to industrial practice where known masses of inoculum are added direct.

### ***Relating optical density to cell density***

Total cell mass was conducted using standard haemocytometer methods. The haemocytometer (Improved Neubauer design, see Figure 70) was cleaned with the use of dH<sub>2</sub>O and de-greased by ethanol washing. The haemocytometer was moistened through the use of warm breath to affix the coverslip to the haemocytometer. Adhesion was checked through the observation of “Newton’s rings.” A small (>1ml) sample of media was shaken to ensure suspension of cell material before 5µl of fermentation media was pipetted towards the edge of the cover slip and left to run under the slip and onto the counting cells.

Cells were counted on the middle squares. Random sampling of 7 – 10 small squares (0.005mm x 0.005mm) was used to formulate the average cell density across the 16 cell central square (total area 0.2mm x 0.2mm) giving cell density per 0.004mm<sup>2</sup>. Where personal preference was for counting via the use of small squares with random sampling across the whole small square matrix, a calibration was applied (see Equation 7 and Equation 8).

#### **Equation 7. Conversion for cell counting (Small to large squares)**

For calculation of cell concentration per ml, Equation 8 was used.

#### **Equation 8. Calculation of cell number**

Where a = average number of cells per large square (see ); b = dilution factor; 10<sup>4</sup> = conversion factor to 1ml.

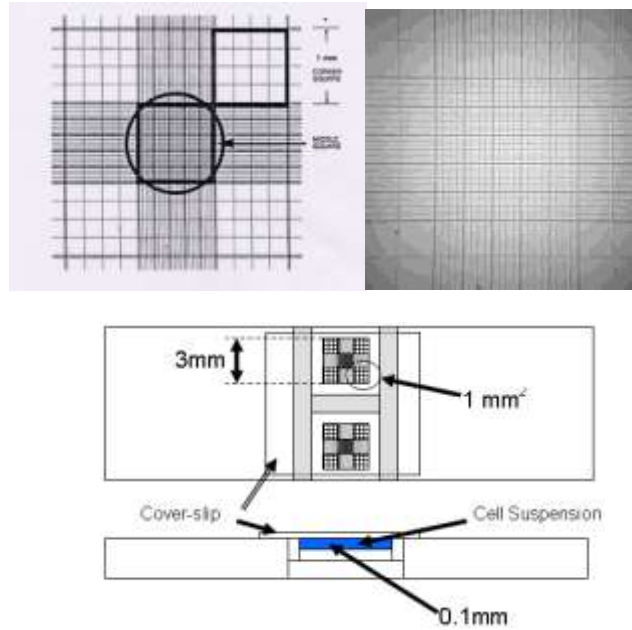


**Figure 70. Calculation of cell density through the use of a haemocytometer**

Top left; diagrammatic representation of the haemocytometer reading grid with annotation of square sizing. Top right; actual light microscope observation of haemocytometer (grey scaled for contrast). Below; arrangement of counting grids on the haemocytometer.

### ***Fermentation***

The fermentation STR was filled with 1 litre of defined media, sterilised and brought to equilibrium at a set temperature of 30°C. Media composition is defined by NREL/TP-510-42630 where 5% dextrose YPD media is used.

The fermentation media was prepared under clean standard conditions with the omission of dextrose, with the reactor heated to 30°C by combined thermal and microwave heating with stability established over an approximate 16 hour resting period. Agitation was through the use of the three Rushton turbine system with agitation rate of 150 rpm to ensure mixing without excessive agitation to cause aeration of the media.

Prior to time zero, the system was primed with dextrose (50g/l). At time zero, the fermentation was started with the inoculum added. In the case of thawed frozen inoculums, this was added through a syringe in the triple port system. For freeze dried inoculum, this is done through the addition of the dried mass directly into the media.

### ***Fermentation profiling***

The fermentation profile was maintained through the use of the Broadley James Ltd fermentation controller system for determination and/or control of pH, temperature, dissolved oxygen. An ElectroLab FerMac 368 Gas analyser was used for exhaust CO<sub>2</sub> and O<sub>2</sub>. Data was compiled by ElectroLab eLogger and eGrapher software for export to Microsoft Excel for data analysis.

In addition, temperature profiling was carried out in parallel with a PicoLog TC08 data logger for ambient, cavity wall, reactor thermowell and heat exchanger water sump temperature profiles.

For determination of biomass, a sample was removed and the optical density read at a wavelength of 600nm for each time point. A calibration was conducted to correlate OD to cell count by curve fitting. Dry weight and viable cell count was not determined.

### ***HPLC analysis of fermentation products***

Fermentation profiling by HPLC (Perkin Elmer 200 Series with RI detection) was carried out with the use of a REZEX ROA column (Phenomenex). A sample frequency of one hour was conducted through the first 16 hours of the experiment.

For full details of the HPLC analysis, see Chapter 3, subsection “HPLC analysis of breakdown products (NREL/TP-510-42628)” on page 117.

### ***Standard curves for determination of fermentation products***

HPLC product formation is determined through the use of glucose and ethanol standard curves where concentration ranges are comparable with the maximum and minimum concentration expected (0 – 60g/l glucose, 0 – 25% ethanol). For full details of calibration curve construction, see Chapter 3 subsections “Standard curves for determination of constituents” (page 120) and “Calibration by standard curve.” (page 122)

### ***Data processing***

For determination of fermentation progress, analysis of optical density, glucose metabolism and ethanol evolution will be undertaken. For ethanol evolution, the trend expressed will be an exponential curve. For analysis, curve fitting was undertaken using the equation shown in Equation 9

---

#### **Equation 9. Exponential curve fit**

Terms; a – range; b – midpoint; c – CURVE FACTOR; d – off set; e – exponential constant

### **Negative controls**

#### ***Sampling frequency and structure***

On observing and analysis of the data produced, repetition of the NC-MW was deemed necessary. On examination of the data, the exponential phase where the transition from the lag phase to the linear growth phase was omitted due to leaving the lab. This is shown the blue sections of Figure 71. Therefore, re-evaluation of the time frame was conducted. Due to the observed exponential phase in the time period 17 – 36 hours, initial data recording windows only collected data between 0 - 16 hours

and 24 - 41 hours. In repeating the NC-MW, the opportunity was taken to move the physical sampling time. This allowed sampling between 0 – 4hours, and 17 – 32 hours. Sampling time frames are shown in Figure 71, allowing the exponential phase to fall into the time frame of 9am through to 1am the following morning (shown by the green sections).

***Fermentation under thermal conditions (Microwave negative control (NC-MW))***

A negative control for the yeast fermentation was conducted over a time period of approximately 50 hours. Thermal control was used to maintain the culture conditions of 30°C throughout.

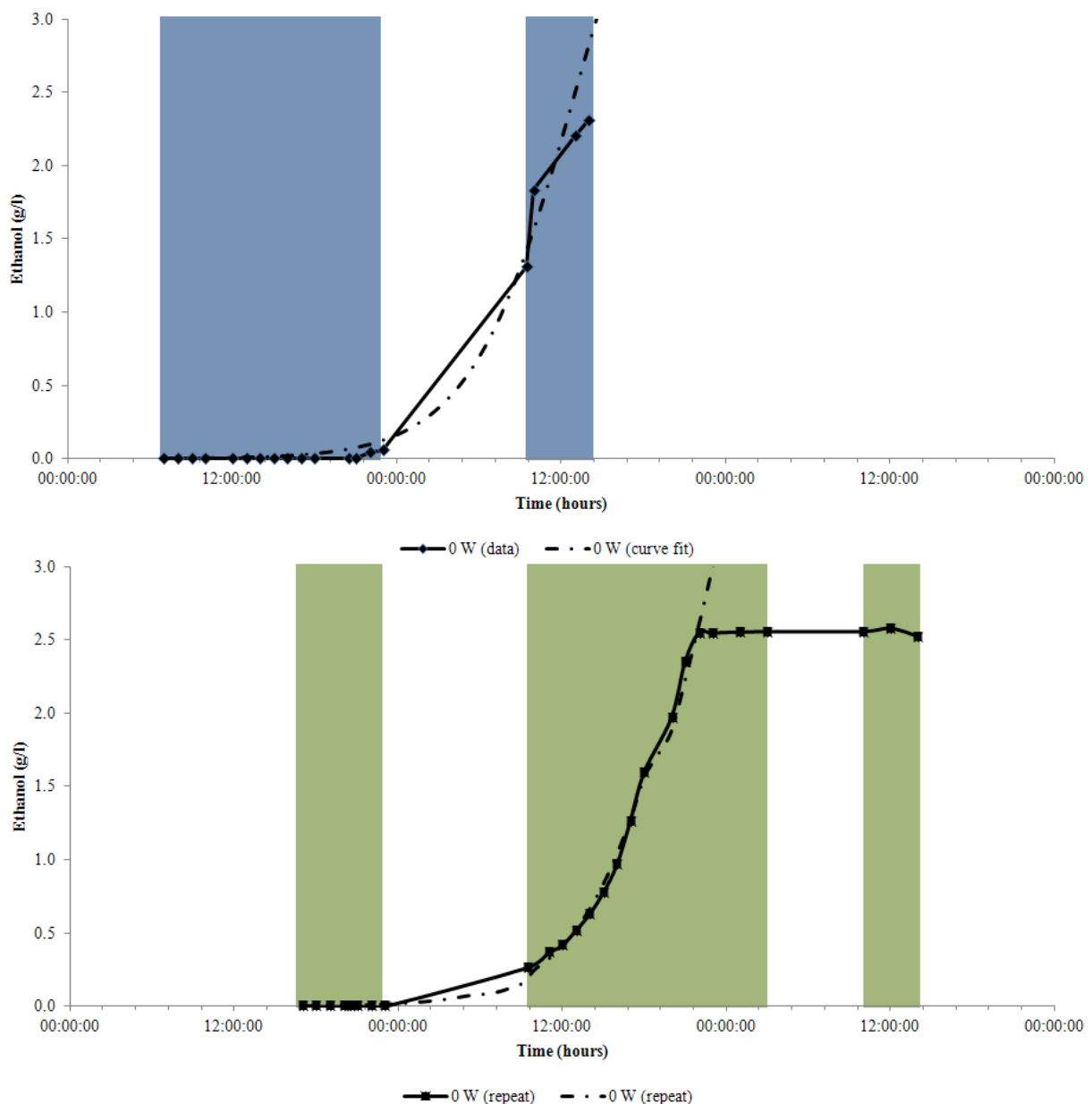


**Figure 71. Sampling time frames for the microwave negative control**  
 Blue overlay highlights initial sampling time frames. Green overlay highlights modified time frame on repeat sampling.

### 3.3.3.1. EP 3.1.0. – Anaerobic glucose fermentation with varying microwave irradiation

| Microwave power | Substrate | Conditions   | Protocols                              | Additional standards/comment |
|-----------------|-----------|--|--|------------------------------|
| 000W            |           |  |  | Negative control             |
| 012W            | Dextrose  | Alcotec 24hr yeast.<br>5% YDP media at<br>30°C net temperature | NREL/TP-510-42618<br>NREL/TP-510-42630 |                              |
| 024w            |           |  |  |                              |
| 050W            |           |  |  |                              |
| 075W            |           |  |  |                              |

**Table 30. EP 3.1.0. Variable focus; Microwave power on yeast growth**

Area highlighted in green shows the variable of interest.

The protocol used is a development of NREL/TP-510-42630 (SSF Experimentation protocols – Lignocellulosic biomass hydrolysis and fermentation) where the saccharification is omitted for a pure glucose substrate.

Variation from NREL/TP-510-42630 occurs where each experiment is conducted under isothermal conditions within the microwave bioreactor under a steady state temperature of 30°C. Fermentation time is dependent on lag phase and exponential phase time periods that were determined by experimental means, plus sufficient time extension to ensure n of the fermentation.

For a real time indication of fermentation progress, both OD and CO<sub>2</sub> concentration were used. As OD will give indication of biomass accumulation, OD measurements are recorded at each sample draw point giving a progress resolution of every one to two hours through the sampling periods. CO<sub>2</sub> in the configuration used cannot be used for mass balance due to the lack of a standardised gas flow rate from the fermentation vessel; however the CO<sub>2</sub> concentration can be used to show the production period as the CO<sub>2</sub> produced will displace the air contained within the head space. This was recorded with the use of the Broadley Technologies Biocontroller and ElectroLabs gas analyser with a resolution of every 5 seconds throughout the start up and fermentation time. On the fermentation finishing, the diffusion of air back into the head space lowered the CO<sub>2</sub> concentration indicating that the fermentation had ended.

This gave a standard lag period in the order of 17 hours and an exponential period of 15 hours. As the fermentation finish point (approximately 30 – 32 hours) often coincided with the end of the work period, the fermentation was left to carry on into the next day with samples taken to ensure that the fermentation had concluded, given a total experiment time of around 50 hours (±5hrs for safety margin).

## Conclusion

Chapter 3 has detailed the research methods used in the design and development of the research project. Information gained in Chapter 2 has been used to aid the design of the reactor described in Chapter 3 and subsequent catalysis and fermentation experiments. The Chapter has looked at three key research areas;

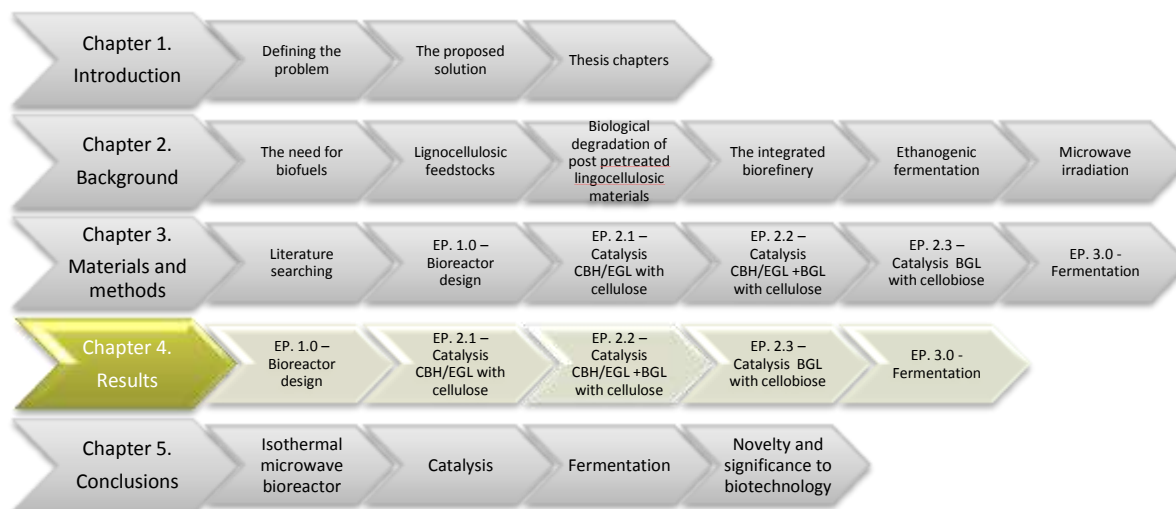
- 1) The tools and methods required for literature searching
- 2) The development of the isothermal microwave reactor and precautions taken to ensure validity of results and claims
- 3) The development and adaption of the NREL protocols to allow the investigation of cellulase catalysis and *Saccharomyces* fermentation in varying microwave irradiation.

Where possible, previous work has been built upon to prevent excessive process development and to allow comparison between the research conducted here to previous studies. This is explained in detail in Chapter Two and influenced the choice of methods and equipment in Chapter Three. Where previous work has been built upon, this has entailed the use of a pre-constructed STR and the use of the NREL protocols.

Due to the variation caused by conducting the NREL protocols in the microwave bioreactor, the development and justification for protocol modification is explained. With modifications causing potential variation in results to previous studies, internal references were established through the use of negative controls for comparison. This has allowed for the development of a reporting system that will support the claims cited in the results section.

*Chapter 4. Results and critical  
analysis*

## Chapter 4. Results and critical analysis



### Note!

The majority of Figures/Graphs used in the results sections are edited sections of complete experiment analysis graphs. For reading clarity, many of the graphs have been reduced in timescale to illustrate the initial changes in conditions which would otherwise be less-discernable to the reader. For completeness, and to aid the understanding of each complete process, each extended graph (showing the whole experiment time course) is included in the Appendix pages 101 - 123.

The results presented are split into the three subject strands of bioreactor development, isothermal cellulase catalysis and isothermal fermentation, each under varying powers of microwave irradiation. Included within each strand are additional reactions which aid and support the conclusions drawn.

For development of the microwave bioreactor system, EP. 1.0 shows that the controlled microwave irradiation of an aqueous solution can be achieved through the system designed, tested and prototyped. The limitations of irradiative power and resolution of temperature control are defined. Irradiation at increasing powers was proven to cause microwave heating of the water contained within the reactor in a linear fashion. As such, it was concluded that the transfer of energy could be accounted for in a predictable manner and the reactor could be run without damage to the equipment being used or the operator, and that the system was appropriate to the experiments to be conducted within it.

The results presented in EP 2.1 - 2.3 show an observable and significant alteration in catalysis due to the use of microwave irradiation of the enzyme-substrate complex in an aqueous solution. Endoglucanase, cellobiohydrolase and beta-glucosidase have each shown significant increase in initial rates (summarised in Table 31, Table 32 and in detail in each subsequent section). For the understanding of the complete system, there are many feedback loops, alternative hydrolysis routes and multi-oligosaccharide intermediates within the system. To understand the exact mechanism of each individual subsystem empirically is nearly impossible within the experimental design carried out.

Equally, the end product evolution can be evaluated, however the molecular reasoning behind the amplification can only be suggested.

Finally, in section 4.3.1.0 EP 3.1. – Investigation of variable microwave power on the growth of *Saccharomyces cerevisiae* (page 194) has shown the effect of irradiation in a way which has retarded microbial growth, although the exact mechanism is not understood.

The data presented show the following;

---

**Results summary**

---

- 1 Microwave energy can be launched into the reactor independent of the thermal profile, maintaining steady state conditions for the total reaction time.  
(EP. 1., page 146)
  - 2 Microwave exposure of the cellulose does not alter the cellulosic material  
(EP. 2. – NC-S, page 158)
  - 3 Microwave exposure of the enzyme independently does not alter the enzyme's catalytic progress  
(E.P 2 – NC-E, page 159)
  - 4 50W irradiation of EGL/CBH with cellulose increases the initial glucose formation rate by 206% over the microwave negative control at the same temperature.  
(EP. 2.1.0., page 161)
  - 5 The result seen in 4 (above) is not due to BGL contamination  
(EP. 2.1.1., page 169)
  - 6 25W irradiation of EGL/CBH with BGL on cellulose increases the initial glucose formation rate by 65% and glucose yield by 25%  
(EP. 2.2.0., page 177)
  - 8 Microwave irradiation of BGL on cellobiose showed a peak enhancement of 70% increase and net increase of 50% in the initial glucose formation rate across the 0-75W power band  
(EP. 2.3.0., page 185)
  - 9 All catalytic results show a non-linear response (increase in rate is not proportional to increase in microwave power)  
(E.P. 2.1. - 2.3., pages 161, 177 and 185 and E.P. 3.1., page 189)
  - 10 The results observed are not due to thermal effects
  - 11 Microwave enhancement for catalysis is only observed when the enzyme and substrate are jointly irradiated in complex.
- 

**Table 31. Results summary**

## Bioreactor prototyping

| Experiment number | ID               | Substrate | Enzyme | Microwave power | Additional comments/notes | Result   |
|-------------------|------------------|-----------|--------|-----------------|---------------------------|--|
| 1.0               | Thermal profiles | n/a       | n/a    | 000-120W        | Heat transfer studies     | Consistent and proportional energy transfer seen between the microwave power and media temperature |

## Catalysis

### Reference and negative control experiments

| Experiment number | ID                         | Substrate                      | Enzyme               | Microwave power | Additional comments/notes   | Result  |
|-------------------|----------------------------|--------------------------------|----------------------|-----------------|---|---|
| NC-MW             | Microwave negative control | Cellulose                      | <i>CBH/EGL</i>       | n/a             | Thermal reference experiment  | Establishment of baseline data  |
| NC-MW             | Microwave negative control | Cellulose                      | <i>CBH/EGL + BGL</i> | n/a             | Thermal reference experiment  | Establishment of baseline data  |
| NC-S              | Substrate negative control | Cellulose                      | <i>n/a</i>           | 150W            | <i>Investigation of possible autohydrolysis</i>   | No autohydrolysis observed. Concluding that cellulose breakdown is not through autohydrolysis induced by a microwave field. |
| NC-E              | Enzyme negative control    | n/a<br>(Filter paper analysis) | <i>CBH/EGL</i>       | 100W            | 2 part experiment.<br>3) Enzyme/microwave exposure;<br>4) Substrate degradation testing | Microwave field on CBH/EGL does not modify the enzyme structure in a permanent manner which can be used post exposure       |

**Endoglucanase and Cellobiohydrolase**

| <b>Experiment number</b> | <b>ID</b>                              | <b>Substrate</b> | <b>Enzyme</b> | <b>Microwave power</b> | <b>Additional comments/notes</b>                                 | <b>Result</b>   |
|--------------------------|--|------------------|---------------|------------------------|--|---|
| 2.1.0                    | Cellulases under microwave irradiation | Cellulose        | CBH/EGL       | 050-200W               | Core experiment  | Microwave exposure at 50W shows the greatest alteration of enzymatic rate (3.01 times greater than the reference). Rate is not proportional to the microwave power as 100W has little increase and 150W reduces the initial rate to below the non-microwave reference experiment. |
| 2.1.1                    | BGL inhibition                         | Cellulose        | CBH/EGL       | 050W                   | <i>VAN inhibition on BGL for BGL contamination determination</i> | Addition of vanillin does not reduce the enzymatic rate indicating negligible BGL contamination. Elevated glucose evolution seen in the previous experiments is not due to enhancement of a BGL contaminant.  |
| 2.1.2                    | Biomass variation                      | Cellulose        | CBH/EGL       | 050W                   | <i>50g loading, 160 hours Enzyme endpoint activity</i>           | Secondary feed seen to hydrolyse. Indication that enzyme endpoint is not due to enzyme exhaustion.  |

**Endoglucanase, cellobiohydrolase and beta-glucosidase**

| <b>Experiment number</b> | <b>ID</b>                                      | <b>Substrate</b> | <b>Enzyme</b>       | <b>Microwave power</b> | <b>Additional comments/notes</b> | <b>Result</b>   |
|--------------------------|--|------------------|---------------------|------------------------|----------------------------------|---|
| 2.2.0                    | Cellulases and BGL under microwave irradiation | Cellulose        | <i>CBH/EGL +BGL</i> | 012-075W               | Core experiment                  | 25W power seen as the greatest initial rate, with % saccharification reaching 100%, contrasting to 70% saccharification seen in the reference experiment. |
| <b>Beta-glucosidase</b>  |  |                  |                     |                        |                                  |   |
| 2.3.0                    | BGL under microwave irradiation                | Cellobiose       | <i>BGL</i>          | 012-075W               | Core experiment                  | All microwave irradiation showed an increase in initial rates (peak initial rate; 12W with 70% increase, net increase of 50% over negative control)       |

## Fermentation

| Experiment number | ID                                       | Substrate | Enzyme | Microwave power | Additional comments/notes                              | Results   |
|-------------------|--|-----------|--------|-----------------|--|---|
| 3.0               | Fermentation negative control            | Glucose   | n/a    | n/a             | <i>Saccharomyces</i> fermentation reference experiment | Establishment of baseline data  |
| 3.0               | Fermentation under microwave irradiation | Glucose   | n/a    | <i>012-075W</i> | <i>Saccharomyces</i> fermentations Core experiment     | Fermentation maintains cell viability at irradiation powers of up to 50W. Subtle alteration of fermentation kinetics which require further experiment development |

**Table 32. Overview and summary of experiments conducted.**

Overview of the experiments concluded. This table is comparable to Table 2 in Chapter 3 – Experimental Design.

#### 4.1. EP 1.0. – Bioreactor thermal profiling



- Energy input to the reaction vessel equates to  $0.0056 T \text{ min}^{-1} \text{ W}^{-1}$

**Summary;** Heating by microwave irradiation can be accomplished with a power range from 0 to approximately 150W forward power. From this study of energy transfer, the heating attributed to the microwave source can be described using the equation  $y=0.0056x$  where  $y$  is the microwave power and  $x$  is the increase in temperature per minute (system loaded with 1 litre of media). From the investigation conducted, the system limitation was observed to be greater than 150W with power between 150W and 200W seen to be restricted by Ohmic resistance in the transmission cable.

Thermal profiling was carried out in accordance to the methodology described in EP. 1.0. (see page 110). From the data produced, heating profiles are produced to show the rate of heating with each power level and show in Table 33 and Figure 72.

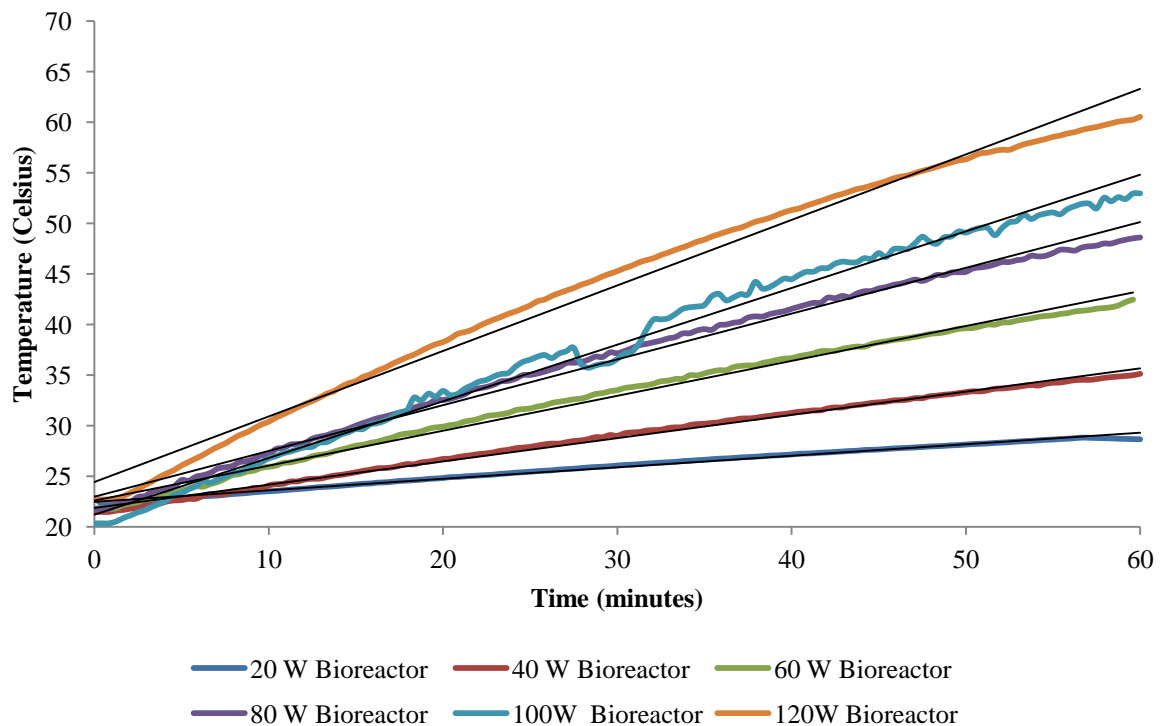


**Figure 72. Heating profiles of the microwave bioreactor under different microwave powers**

Graphical data from the heating of the bioreactor system with the sole energy source being the microwave. Gradient determined by Excel trend line function (Linear). Deviation seen in 100W power is due to sensor feedback when coupling additional probes onto the same interface. 100W deviation not seen as significant. All gradients are reported in Table 33.

| Power output | Temperature at T = 0 minutes | Temperature at T = 60 minutes | $\Delta T$ ( $^{\circ}C$ ) | Fit coefficient | Gradient $\Delta T/min$ |
|--------------|------------------------------|-------------------------------|----------------------------|-----------------|-------------------------|
| 020W         | 22.87                        | 28.65                         | 6.34                       | 0.9928          | 0.1142                  |
| 040W         | 21.47                        | 35.12                         | 13.61                      | 0.9952          | 0.2304                  |
| 060W         | 21.83                        | 42.46                         | 19.67                      | 0.9925          | 0.3451                  |
| 080W         | 21.72                        | 48.59                         | 26.86                      | 0.9920          | 0.4524                  |
| 100W         | 20.32                        | 52.95                         | 31.83                      | 0.9911          | 0.5600                  |
| 120W         | 22.73                        | 60.54                         | 40.53                      | 0.9875          | 0.6477                  |

**Table 33. Heating profiles with different microwave powers**

Tabulated data from the heating of the bioreactor system with the sole energy source being the microwave generator.

From Figure 72, the relationship between microwave power and the rate of temperature increase is determined by the gradient of the line. As each experiment has focused on the standard time frame of one hour, the gradient is determined over the whole time period. For the trend line fitting, a linear trend line has been used. At lower power settings, the trend line fit coefficient of 0.9928 shows very close linearity. As the level of power exposure increases, the fit coefficient decreases as the trend expresses greater curvature. For the analysis of the power transmission in this experiment, and with  $R^2$  values ranging from 0.9928 to 0.9875, the assumption of linear fit can be held as valid. At increasing powers and as the temperature increases towards phase transition, the dipole properties of the media would affect power absorption. When considered as temperature increase per unit energy per minute per litre in this instance, the whole system has a value of 0.0056 dT/min/W supplied with a fit coefficient of 0.9968 showing a linear relationship between microwave powers and heating rate through the power band investigated. This is shown in Figure 73.

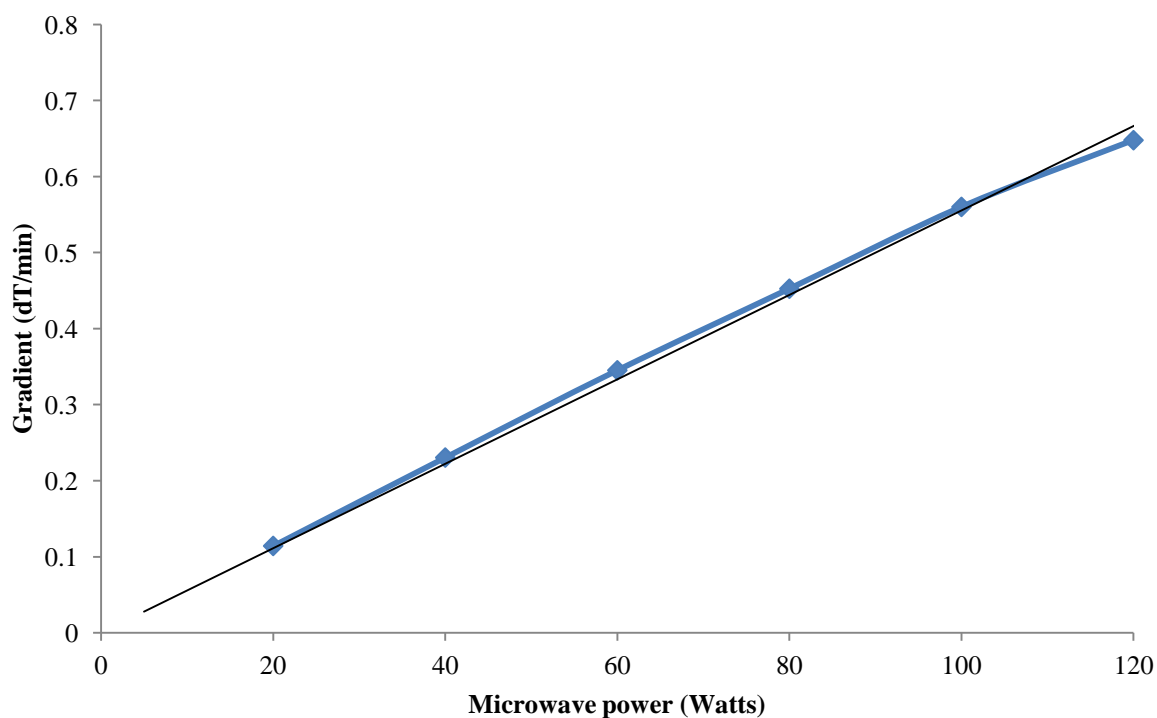


**Figure 73. Microwave power in relation to heating rate.**

Gradient  $y = 0.0056x$ ,  $R^2 = 0.9968$

From the system used, the method of irradiation was through a microwave generator with coaxial cable transferring the electrical signal to the launching section and transmission waveguide attached to the STR cavity (for details see “3.1.4. Microwave cavity, waveguide, tuning section and launcher” (page 101) for whole system descriptions and methodologies, and the Appendix pages 34 - 37). As the microwave cavity has complex internal furniture, the limitation of the apparatus is dependent on the absorption of energy within the fluid, penetration depth of the microwave energy and energy returned by reflection back towards the microwave source.

Although not quantified by any analytical approaches (for example, the data logging of the cable temperature profile or reflected power on the Microtron unit), the observation of temperature increase in the coaxial cable indicated energy inefficiency. The two scenarios hypothesised to account for the observed temperature increase are;

- 1) Power saturation of the cavity, accounted for by the inability of the fluid to absorb any additional energy from the microwave source. Excess energy exits the cavity by returning along the waveguide and towards the microwave source via the co-axial cable. As cable can be considered as an extension of the waveguide, standing waves within the cable account for increase in cable temperature without showing increased reflected power.
- 2) Ohmic losses within the cable can cause losses in transmission to the STR through the heating of the cable. As the cable (and therefore resistance) increases, the loss is self reinforcing. As the resistance is proportional to the power transmitted, length of the cable and the internal resistance, increasing the power increases the potential loss and therefore heating of the coaxial cable.

With the Microtron used in the EP 2.1.0, system limitations with the recording of forward and reflected verse powers obscures the observation of energy loss through the heating effect of the coaxial cable. With the set up used 150W power transmission showed marginal heating within the cable (cable heating that was not apparent at 100W transmission). Using 200W, the cable quickly showed heating in the start up period (the cable becoming hot to the touch) and was deemed as inappropriate to use due to the potential damage that could be done to the cable through the degradation and melting of the PTFE insulators, and uncertainty of the real power transmission along the waveguide following energy loss in cable heating. Following results from the catalysis of cellulose by CBH and EGL at microwave powers between 0 and 150W, product evolution was observed to increase in the 0 – 100W range with peak at 50W. 150W showed little or no improvement over the negative control. Consequently, exploration of catalysis at 200W was not seen as justifiable.

Following this trial, 150W was assumed as the upper power limit in the equipment used and no other experiments exceeded this limit. All subsequent irradiative experiments (negative control or side process investigation for example the substrate and enzyme negative controls), were conducted at 100W or below.

For isothermal stability, Figure 74 shows a section of a typical thermal profile for the hydrolysis experiments (Cellulose-EGL/CBH -BGL, 50W). The step in temperature seen at 12 hours corresponds to thermal correction at the beginning of the hydrolysis time frame (T=0, point of enzyme addition). Time prior to the step in temperature accounts for the overnight system equilibration. Subsequent files (not shown) account for whole experiment time frame (up to 160 hours).

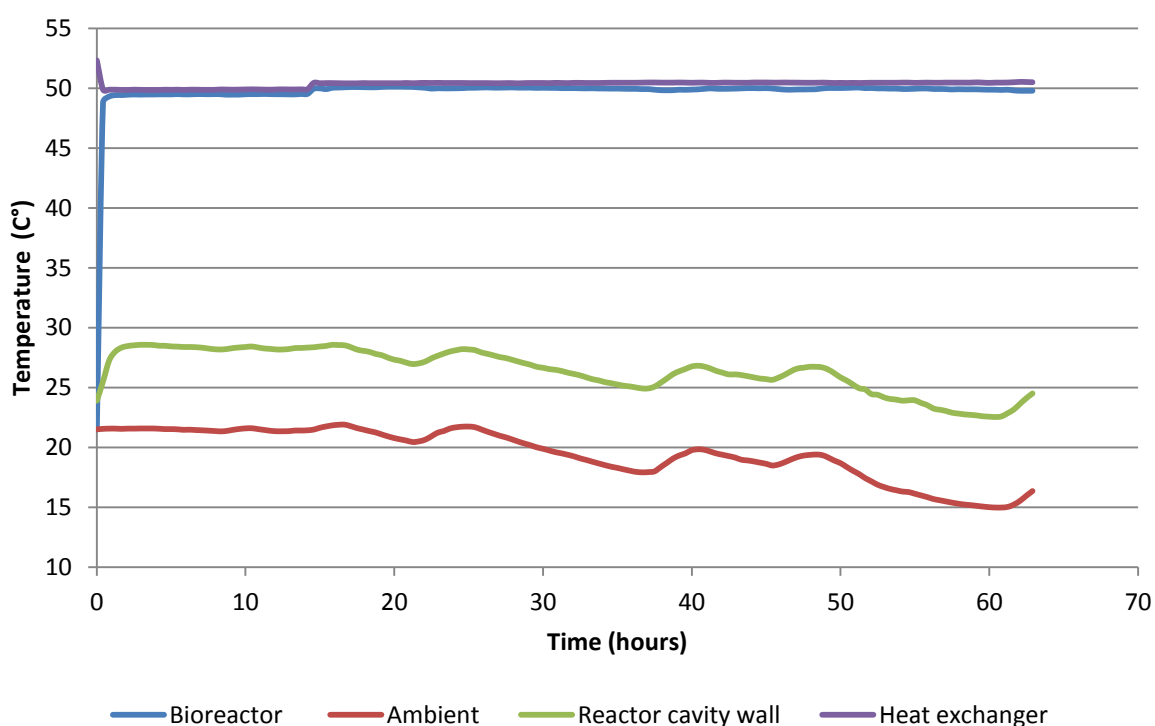


**Figure 74. Section of thermal profile from experimental data.**

Sample data taken from the thermal trace for the experiment conducted with cellulose hydrolysis by EGL/CBH -BGL, 50W microwave power. Data record shown over the first >5000 data points

The data produced demonstrated that the steady state system developed shows repeatable and verifiable results where thermal variation is excluded. Using the data from the 12<sup>th</sup> hour onwards, the average bulk media temperature is 49.9°C with a standard deviation of 0.096 where n = 118 data points. For comparison to the thermal heat exchanger (Average = 49.97°C, STDEV = 0.077, n = 118), cavity wall (mean = 25.98°C, STDEV = 1.71, n = 118) and ambient (mean = 18.937, STDEV = 2.071, n=118), the conclusion being that the implementation of reactor temperature control has isolated the thermal effects from the microwave effects being studied.

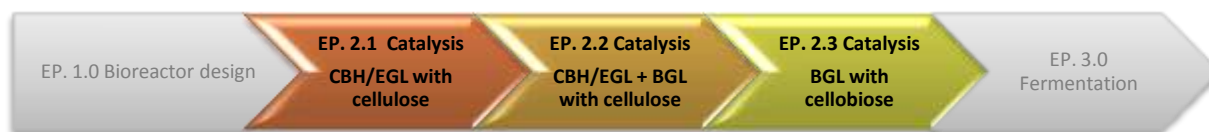
The use of the K-type thermocouples were seen as reliable sensor for temperature detection, with verification against both mercury and alcohol thermometers, and against the integrated temperature probes in the DO probe and biocontroller. As a diagnostic tool, thermal images were taken with the whole system in operation through the use of an infrared thermal imaging camera (Figure 75). Although images shown show relative temperature difference between system areas, the observed temperatures are not comparable to the temperature compiled by direct contact, and as such are included to show the system thermal profile and not for critical analysis.



**Figure 75. Thermal image of reactor in operation**

Image shows the thermal reflection of the whole system under operating conditions. Approximate temperature are; 1 - microwave launcher (26.5 – 27.2°C); 2 – waveguide (23.7 – 28.1°C); 3 - external cavity wall (26.4 to 28.5°C); 4 - STR flange (29.9 – 34.2°C); 5 - STR thermal input feed (39.6 - 41.6°C); 6 - STR thermal return feed (40.2 – 38.2°C); 7 – condenser; 8 – agitator motor and gear box; 9 - The large area with a high thermal return behind the system is the head section for the Huber heat exchanger.

#### 4.2.0. EP 2 – Saccharification of cellulosic materials



#### **Negative Controls**

##### ***Hydrolysis under standard thermal condition (Microwave negative control (NC-MW))***

**Summary;** *The NC-MW has shown the reference reaction progression to which controlled variables will be applied. The reaction was repeated with BGL action on cellulose; without BGL action on cellulose; and for BGL action with cellobiose. This gives three datasets which will be the basis for other comparisons.*

To determine the normal enzymatic rate for the modified NREL/TP-510-42629 protocol, the reaction was conducted without microwave irradiation and thermally compensated. In each negative control (-BGL and +BGL on cellulose, and BGL on cellobiose), a long exposure and short exposure experiment was conducted to identify total hydrolysis profile. For EGL/CBH-cellulose based experiments, up to 160 hours were recorded or until microbial contamination was observed. The first 30 hours were noted for significance. For BGL-cellobiose experiments, 4 hour total reaction times were used with the first 2 hours noted for rate determination. All NC-MWs were conducted in accordance to the methodology described in Chapter 3, 3.2.0.2. Negative controls (page 125). For the NC-MW with respect to each subsection (E.P. 2.1, 2.2 and 2.3), three NC-MW plots are produced.

#### 4.2.0.1. NC-MW – EGL/CBH without BGL

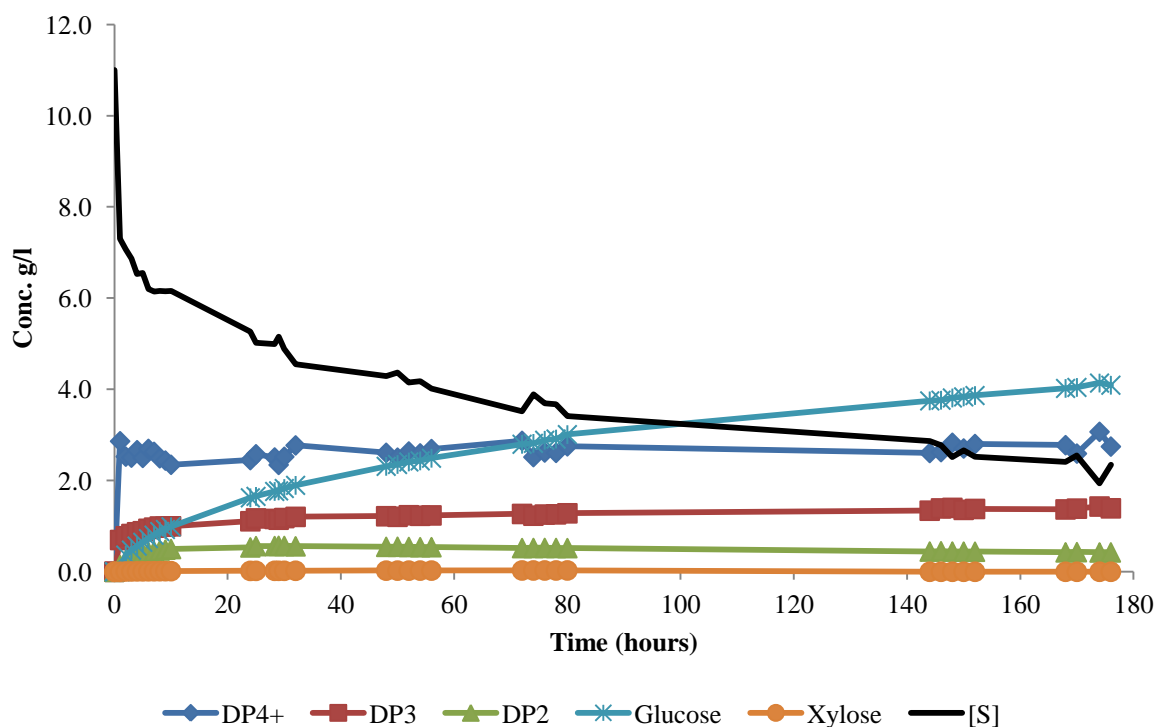


**Figure 76. Enzymatic hydrolysis (CBH/EGL on cellulose) in the absence of microwave irradiation (NC-MW)**

Experimental conditions of 10g/l biomass ( $\alpha$ -cellulose), 50°C, 300rpm agitation, CBH loading of 60FPU/g cellulose, absence of BGL. Analysis through RI-HPLC with REZEX ROA as described previously. Data presented as grams per litre by breakdown constituent. Substrate concentration is plotted as the reciprocal of the total accounted mass.

For the complete profile of cellulose in the presence of EGL and CBH but without BGL the following process curves were constructed. Figure 76 shows the progression of saccharification without the application of any microwave power over a time period in excess of 160 hours, where microbial contamination became problematic at  $T = >170$  hrs. From the curves shown, the major saccharification product was glucose.

From this initial (complete) overview, individual constituents can be compared and initial rates calculated. The significance of the evolution and maintenance of the DP4+ peak show is that it showed the reduction in DP of the long chain polysaccharides where DP4+ relate to all saccharides ranging from cellotetraose through to the longest soluble oligosaccharide. With the DP4+ at a steady state, it may be assumed that the evolution of DP4+ was equal to the destruction of DP4+. As the DP4+ trend appeared static over the time period investigated, there was a clear indication that saccharification is incomplete at the end of the experiment.

As cellulose as substrate can only be determined at any given time point through solid dry mass, [S] is inferred by mass balance. The known initial substrate concentration was 10g/l cellulose. Including hydration when hydrolysed, the glucose equivalent [S] can be calculated by Equation 10.

**Equation 10. Empirical determination of [S]**

Both [S] and [P] show rate reduction. Extrapolating both trend lines forwards suggest that with  $T = \infty$  [P] will plateau at around 6g/l suggesting a maximum yield of around 60%. As theoretical conversion suggests that 100% conversion should be achieved in a simplistic system, observation of a limiting system suggest either feedback inhibition related to [P] or inactivation of the enzyme to a point where  $[E] = 0$ .

#### 4.2.0.2. NC-MW – EGL/CBH with BGL

In same manner as the previous negative control, the hydrolysis reaction was conducted however this time with the addition of BGL, simultaneously with EGL and CBH. Figure 77 shows the results.

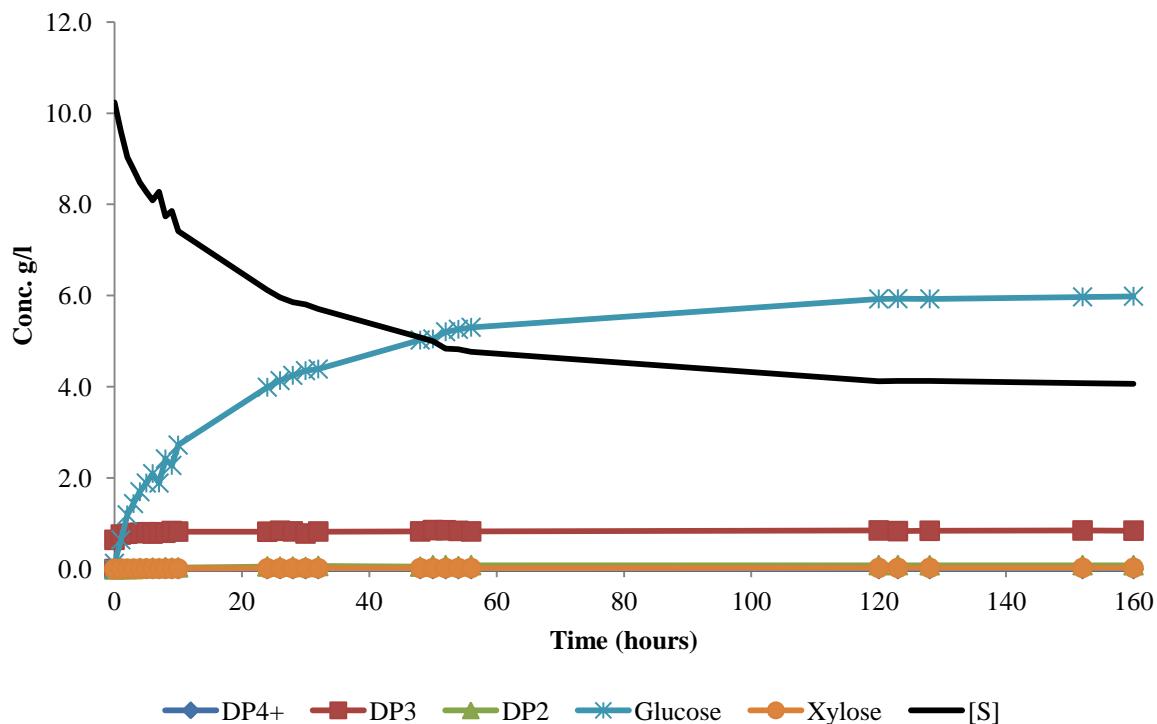


**Figure 77. Enzymatic hydrolysis (CBH/EGL +BGL on cellulose) in the absence of microwave irradiation (NC-MW)**  
Experimental condition of 10g/l biomass ( $\alpha$ -cellulose), 50°C, 300rpm agitation, CBH loading of 60FPU/g cellulose, absence of BGL. Analysis through RI-HPLC with REZEX ROA as described previously. Data presented as grams per litre by breakdown constituent. Substrate concentration is plotted as the reciprocal of the total accounted for mass.

Comparison of Figure 76 and Figure 77 shows that adding BGL causes an increase in the rate of glucose formation. The total glucose yield at around 120 hours was just above 50% of the theoretical maximum with minimal cellobiose concentration. The absence of cellobiose is consistent with excess BGL as cellobiose to glucose conversion is greater than that of cellobiose evolution. From the progress curve shown, it is concluded that the saccharification has reached an endpoint in the time frame of 150 to 160 hours due to the observed reduction of rate to zero. [S] is calculated by mass balance as described by Equation 10.

To focus on the initial rate conditions, the first two hours of the progress curves were examined to estimate initial rates. The two hour time frame was the minimum that could be used as reduction to a single hour would only contain two data points. Increasing the time frame to two hours was deemed acceptable for the reduction of error however the lessening of the rate due to increasing the time frame is noted. As such, all other comparisons are conducted on the same time scale (with the exception of BGL/cellobiose) to allow direct comparison.

### 4.2.0.3. Comparison of NC-MW – EGL/CBH with and without BGL

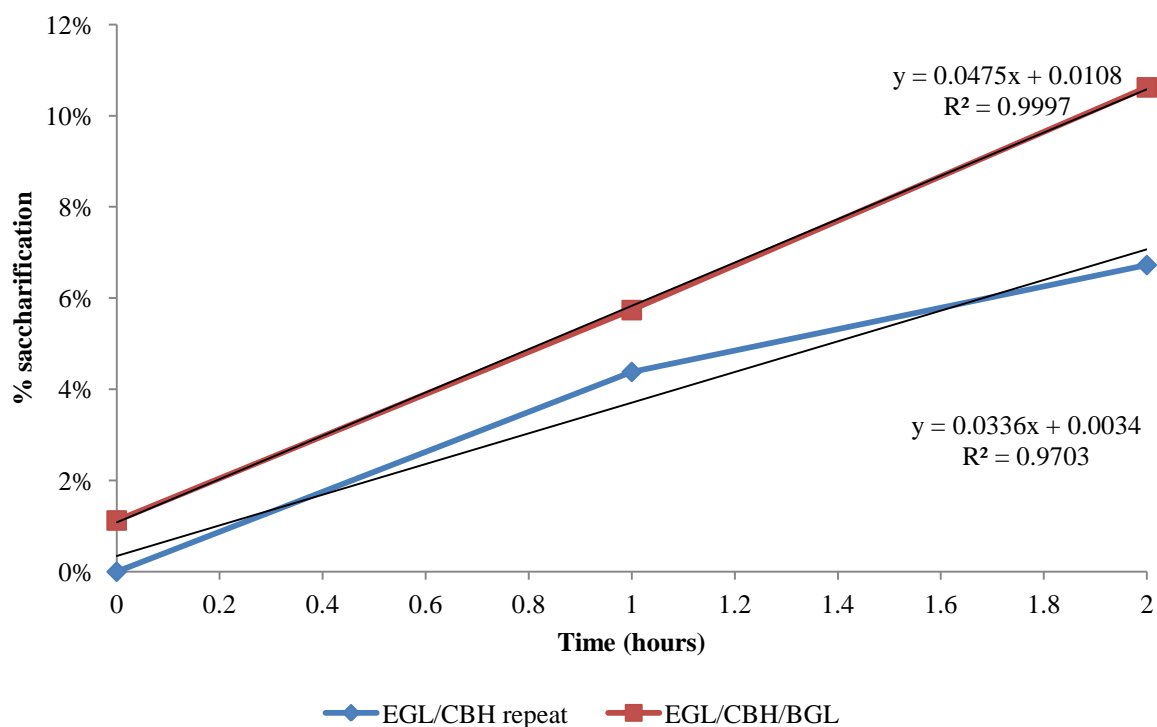


**Figure 78. Comparison of percentage saccharification with EGL/CBH and EGL/CBH/BGL**

Graph illustrating the saccharification rate of the two microwave negative controls with the presence of EGL/CBH with and without the presence of BGL. Initial rate (first 6 hours) shown. Rates determined through trend line gradient; EGL/CBH = 0.023x; EGL/CBH/BGL = 0.0358x.

From the chromatograms and results produced for CBH/EGL with and without BGL, the trends are consistent with the expected. With xylose a constituent of hemicellulose, the residual xylose observed (<0.007g/l) is consistent with processing contamination and is not regarded as a significant factor and therefore has not been included in yield calculations.

Cellotriose (DP3) is a minor constituent with a low capacity to be resolved to mono and disaccharide species without the use of BGL. As such, accumulation is noted, although not used in process definition as trisaccharides are not seen as suitable feedstock for fermentation in industrial strains. With DP3 concentration typical of 0.5g/l (0.5% w/w), it has little significance in application.

The accumulation of cellobiose and glucose is a clear indicators of enzymatic saccharification. Of particular interest is the accumulation of glucose in significant concentrations, significantly higher than the expected values due to omission of BGL.

#### 4.2.0.4. NC-MW – BGL with cellobiose

The negative control looked at the normal progression of cellobiose degradation by BGL. For this experiment, the first negative control conducted expressed a very rapid progress curve with a low sample rate (to mirror EP. 2.1. and EP. 2.2.). Consequently the negative control was repeated with a higher frequency of sampling.

As cellobiose was the sole substrate in the reaction, only glucose was produced. This results in the reduction of cellobiose being the substrate degradation curve and glucose evolution being the product formation curve.

BGL loading was comparable to E.P. 2.1. NC. Following development of the previous experiments, the initial cellobiose/BGL catalysis reaction was undertaken with an hourly sampling regime over a time period of 600minutes with batch HPLC processing being undertaken post experiment. Initial results recorded from the hydrolysis of cellobiose with BGL were far quicker than the expected. From obtaining the HPLC profile, the very obvious conclusion was that the speed of the reaction under the enzyme load used caused nearly 100% conversion within the 60 minutes, with the reaction concluding within 120 minutes. Following the initial trial, all subsequent sampling frequencies were reduced to 10 minutes and total reaction time reduced to 120 minutes. In repetition of the negative control, Figure 79 was produced.

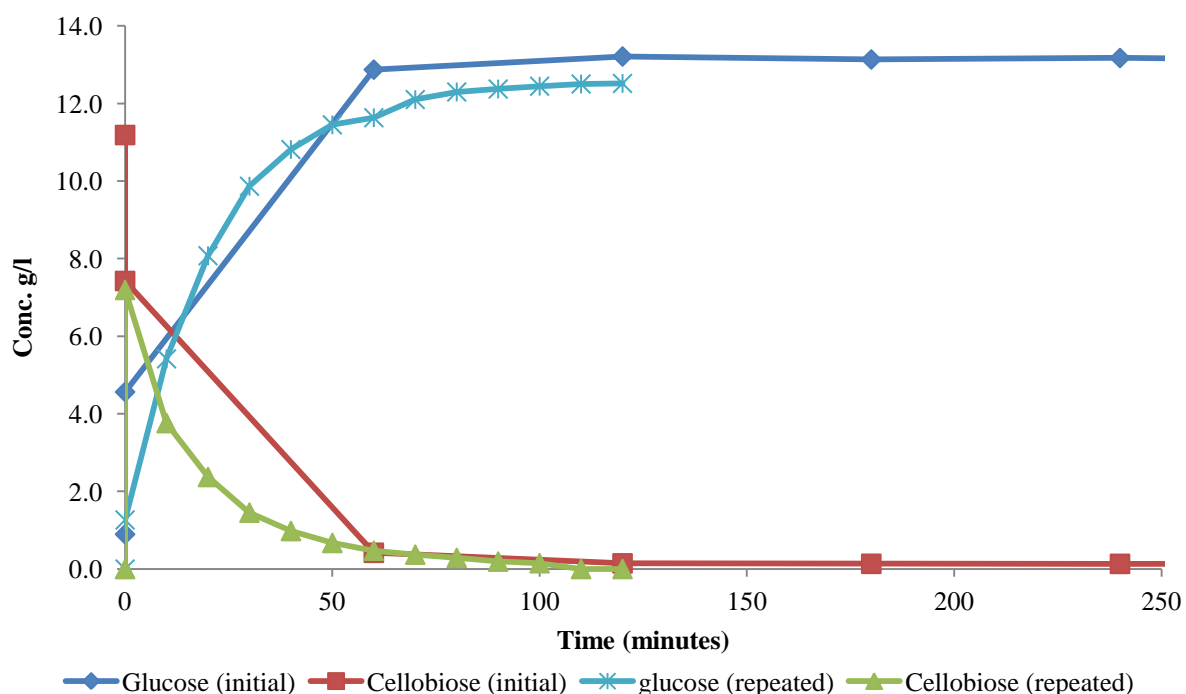


**Figure 79. Cellobiose catalysis with BGL - Initial and repeated values for glucose and cellobiose**

Edited graph to show the overlay of the initial experiment of cellobiose with BGL to the developed cellobiose-BGL protocol. Particular note is the progression in cellobiose conversion in the initial experiment where the sampling was at a 60 minute interval over the 600 minute time frame. Where the catalytic rate is at its greatest, only 2 data points cover the reaction. Development of the protocol by increasing sampling rate (10 minute interval) and reducing total experiment time (120 minutes) shows greater detail in the initial rate of reaction.

The enzymatic rate was determined by the cellobiose and glucose gradients. Assuming Michaelis-Menton kinetics where a single substrate goes to a single product, the glucose productions should be the inversely proportional of cellobiose destruction and described by Equation 11. Where cellobiose is plotted against a logarithmic scale, and the trend line plotted as a natural log of the cellobiose concentration, a gradient of  $y = 5.1871e^{-0.037x}$  is obtained with a  $R^2$  value of 0.98 over the 100 minute initial time interval. Extending the sample set beyond the 100 minute mark and away from the logarithmic stage reduces the  $R^2$  value, as the rate reduces with substrate exhaustion. For completeness, the rate is also calculated for the initial experiment where the sample size used is two. A comparative gradient ( $y = 7.4253e^{-0.048x}$ ) is obtained, with an artificially high  $R^2$  value due to being a two point plot. Through showing the value of the initial experiment to the developed frequent sampling experiment, the difference in data interpretation is observed.

— —

**Equation 11. Cellobiose : Glucose correlation**

Where t = time; C = cellobiose; G = glucose

#### 4.2.0.5. Influence of microwave energy on substrate (substrate negative control (NC-S))

- *100W/l aqueous solution of 10g/l does not undergo microwave induced hydrolysis*

*Summary; To establish the possibility of irradiation inducing a mechanism of autohydrolysis, the microwave field was applied in the absence of enzyme addition. From the results compiled, the microwave field does not cause spontaneous cellulose fibre cleavage.*

Determination of microwave field effect directly on the substrate for evidence (any microwave hydrolysis or polysaccharide degradation) was by reactor loading in accordance to a modified NREL/TP-510-42629, with the omission of enzymes (see Chapter 3 – Experimental Design). The reaction was carried out under irradiation at 100W forward power (<5% reflected power), over a time course of 33 hours. 100W was selected with the expectation that increasing irradiation should induce greater stress on the protein without using 150W that would have been at the limitation of the microwave system being used (the Microtron sources and results are described on pages 102 and 146). The results concluded that in the absence of enzymes, no substrate degradation is observed. Figure 80 shows the resultant HPLC chromatogram overlays where the solvent front (peak A) is observed at approximately 7 minutes, citrate buffer (peak B) at 9.5 minutes. No peaks were seen in the time period 7 to 12 minutes with the exception of the citrate peak, demonstrating the lack of action by microwave power as a direct breakdown mechanism. In comparison of the citrate peak as an internal standard, the average peak area value is equal to 1462225 RIU, standard deviation is 19285,  $n = 12$ , equating to a Relative Standard Error (RSE) of 1.32%. Repeatability shows that the negative control shows high repeatability and supports the conclusions drawn.

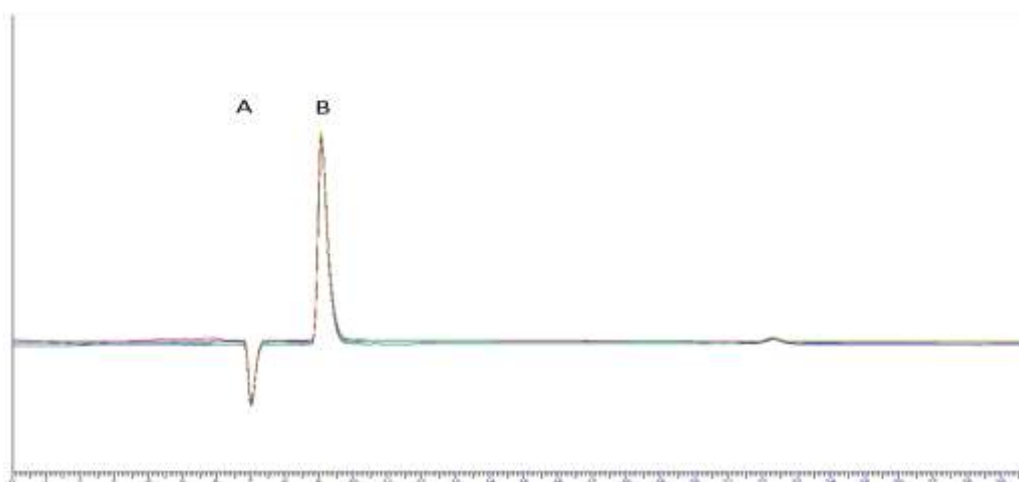


**Figure 80. Overlay of HPLC traces for 33 hour exposure of alpha-cellulose in 100W microwave field**

RI-HPLC chromatogram overlay of 33 hour microwave exposure, 10g/l  $\alpha$ -cellulose, 100W microwave power. HPLC conditions used were REZEX ROA column with 4mM  $H_2SO_4$  mobile phase at 0.6ml/min in a column oven at 65°C. A; solvent front. B; Citrate buffer. Horizontal axis is indicative of elution time with total elution phase of 30 minutes, vertical axis is in mV response ( $\Delta$  RIU).

With the exposure of the substrate to the microwave field, it can be concluded that any hydrolysis observed in the standard enzymatic reaction is due to an enzymatic effect rather than autohydrolysis of the substrate in the microwave field.

#### 4.2.0.6. Influence of microwave on enzyme degradation (Enzyme negative control (NC-E))

- *100W/l aqueous solution containing 40FPU/g cellulose “cellulase” (EGL & CBH) does not exhibit modification post irradiation*

*Summary; Applying a microwave field to CBH and EGL in aqueous solution does not modify the enzyme structure in a permanent manner which can be used post exposure. The effects seen in later experiments, (expressly the increase in rate while in solution with cellulose), can be concluded to only occur when the enzyme is in complex with the substrate within the microwave field.*

To determine the effect of the microwave field on the enzyme in free solution, a modified protocol of the NREL/TP-510-42629 (Measurement of Cellulase Activities) was used (see Chapter 3 – Experimental Design) whereby the selected enzymes were exposed to the microwave field and then reacted with a known mass of cellulose material (filter paper, 10mm x 60mm) under standard conditions. The liberation of the glucose and cellobiose from the filter paper will correlate to the enzyme activity using NREL/TP-510-42628.

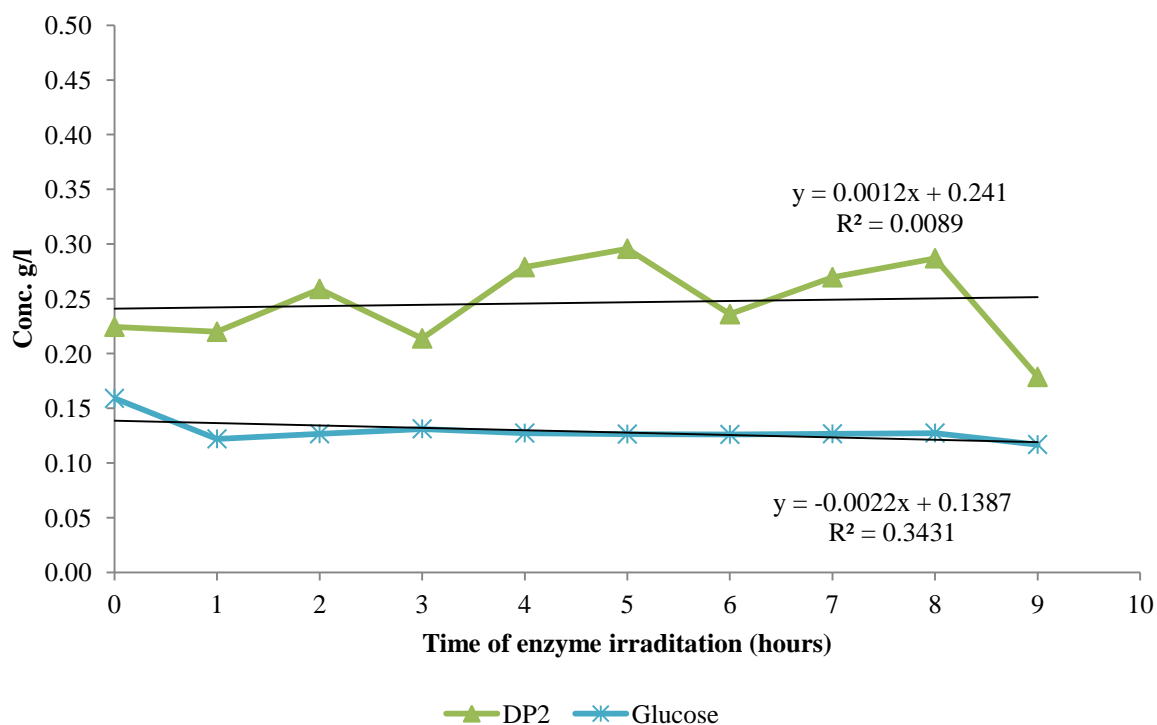


**Figure 81. Determination of enzyme activity after microwave exposure determined by a modified NREL/TP-510-42628**

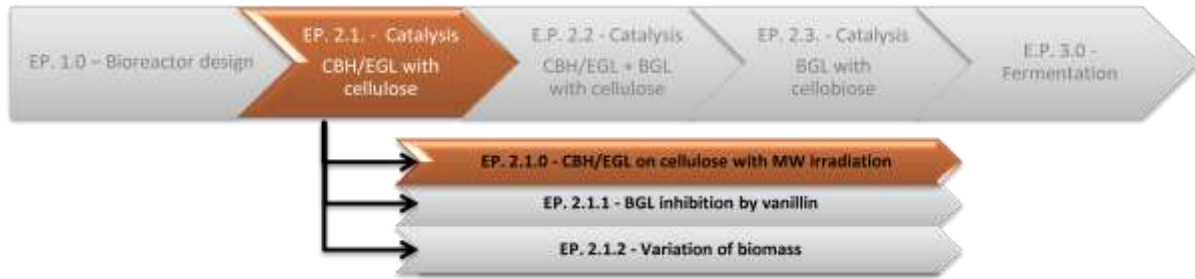
Yield of DP2 and glucose. Gradients; glucose =  $-0.002 \text{ g.l}^{-1}\text{hr}^{-1}$  exposure; cellobiose =  $0.0012 \text{ g.l}^{-1}\text{hr}^{-1}$  exposure.

From the data produced, irradiation of the “cellulase” (CBH and EGL at 100W) for up to 33 hours does not appear to significantly alter the enzyme activity. The data presented in Figure 81 highlights the initial exposure period (0-10 hours), while the complete profile is shown in the Appendix. With increased exposure times from 0 to 10 hours, the concentration of cellobiose was seen to mean average 0.226g/l, with a standard deviation of 0.004 (where n=10) and a confidence limit of 0.128. With respect to glucose, the mean is 0.0124g/l, with a standard deviation of 0.004 (where n=10) and a

confidence limit of 0.07. With consistent values for glucose, the mechanism of action is seen to be unaltered over the time period. By looking at the percentage saccharification for each individual sample time point, the average conversion is 1.121% of input biomass, with a standard deviation of 0.0003 (n=10) when considering a time frame of 0 to 10 hours. From this experiment, it can be concluded that the effects seen in subsequent experiments are specific to the enzyme being in complex with the substrate. This concludes that there is no correlation between microwave exposure in the absence of substrate with irradiation time.

As the procedure is based on the NREL/TP-510-42628 protocol, the incubation period used was limited to 1 hour and the enzyme loading is identical to the enzyme loading used in the reactor to mimic experimental condition (enzyme per unit volume of aqueous media and microwave field density). As such, a number of observations have to be assumed. In NREL/TP-510-42628, the assumption is that the assay is used for the determination of FPU from a fungal strain. In extracellular cellulase expressions, the complement of enzymes is undefined, therefore it will be a mixture of EGL, CBH and BGL of varying ratios. As the FPU method does not differentiate between individual enzyme classes, the FPU value is determined as “cellulase” FPU. Experiments carried out in this iteration of the negative control are through the omission of BGL, thus reducing the glucose observed to the limit of the current HPLC method of detection. For greater insight into the FPU in relation to known enzyme loading, redevelopment of this protocol is required.

#### 4.2.1.0. EP 2.1.0. – Cellulase hydrolysis by CBH/EGL – BGL with microwave irradiation



- 50W/l aqueous solution containing 10g/l cellulose and 40FPU/g “cellulase” (EGL & CBH) showed the greatest (205%) increase in initial rate over the negative control
- The relationship between irradiation power and alteration of initial rate is non-linear

**Summary;** 50W microwave power in this instance of this experiment increase the initial rate by 3.06 times that of the reference negative control as measured by initial rate of saccharification (%). Glucose evolution has the greatest enhancement, suggesting an alteration in glucose/cellobiose liberation. Increasing the microwave power does not result in increased saccharification, with 150W showing only marginal benefit over the reference control experiment.

For the investigation of the influence of microwave energy on the enzymatic rate of cellulase enzymes, microwave power settings of 50, 100 and 150W were implemented in comparison to the negative control of no microwave power. Conditions were standardised and temperatures were constant at 50°C to avoid thermal bias. From the experiments conducted, the system showed a constraint on the maximum power that reactor could be subjected to. The planned upper limit of 200W was not used due to the observations described in EP 1.0 (page 146).

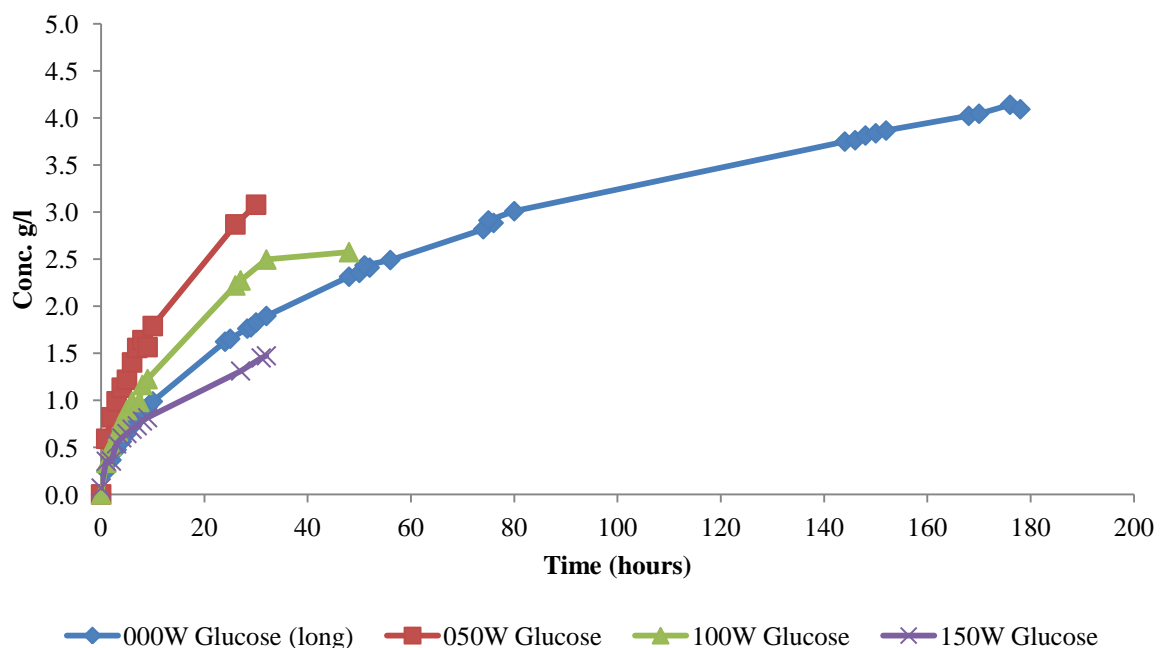


**Figure 82. Glucose production in varying microwave power (full plot)**  
Full plot of glucose evolution by microwave power.

For subsequent fermentations, the product with the greatest significance will be glucose. From the glucose evolution profile, the greatest rate production was seen in the 50W reaction with reducing catalysis seen in 100W (see Figure 82). Increasing the microwave power to 150W was seen to decrease the rate to below the rate observed for catalysis without any microwave irradiation. It can be seen that glucose evolution rate is not simply proportional to the applied microwave power. As the glucose evolution will be dependent on the rate of depolymerisation and as cellobiose will be the intermediate on the pathway to glucose, the cellobiose profiles are shown in Figure 83.

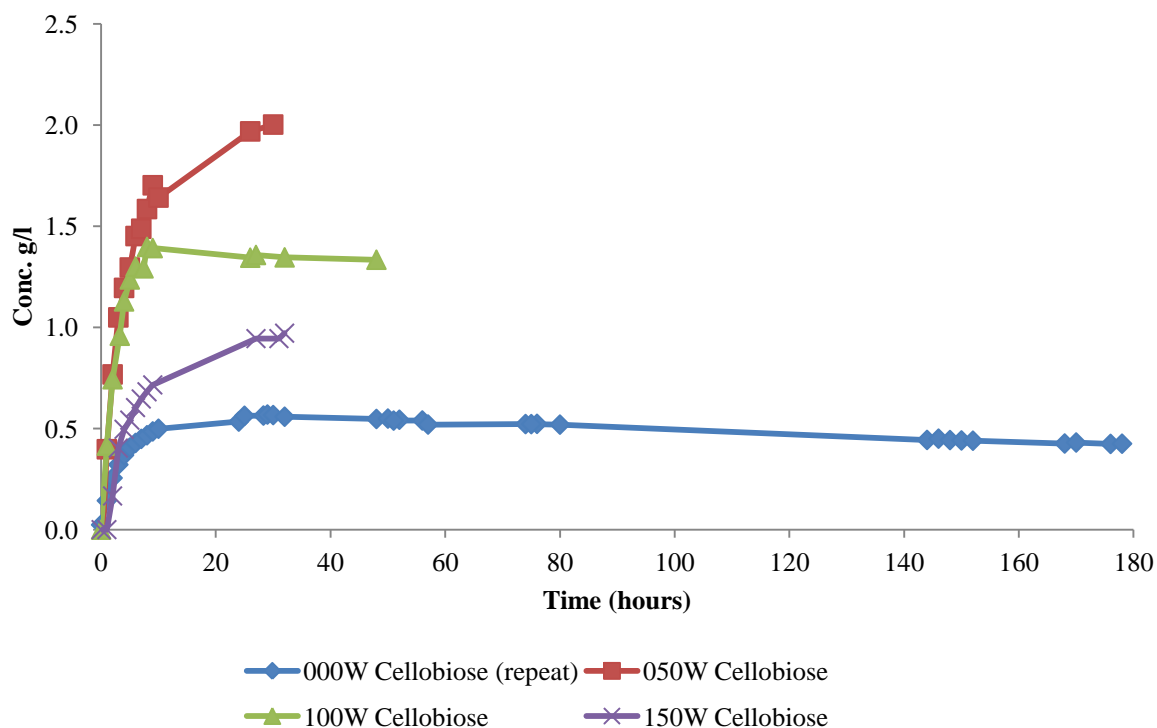


**Figure 83. Cellobiose production in varying microwave power (full plot)**

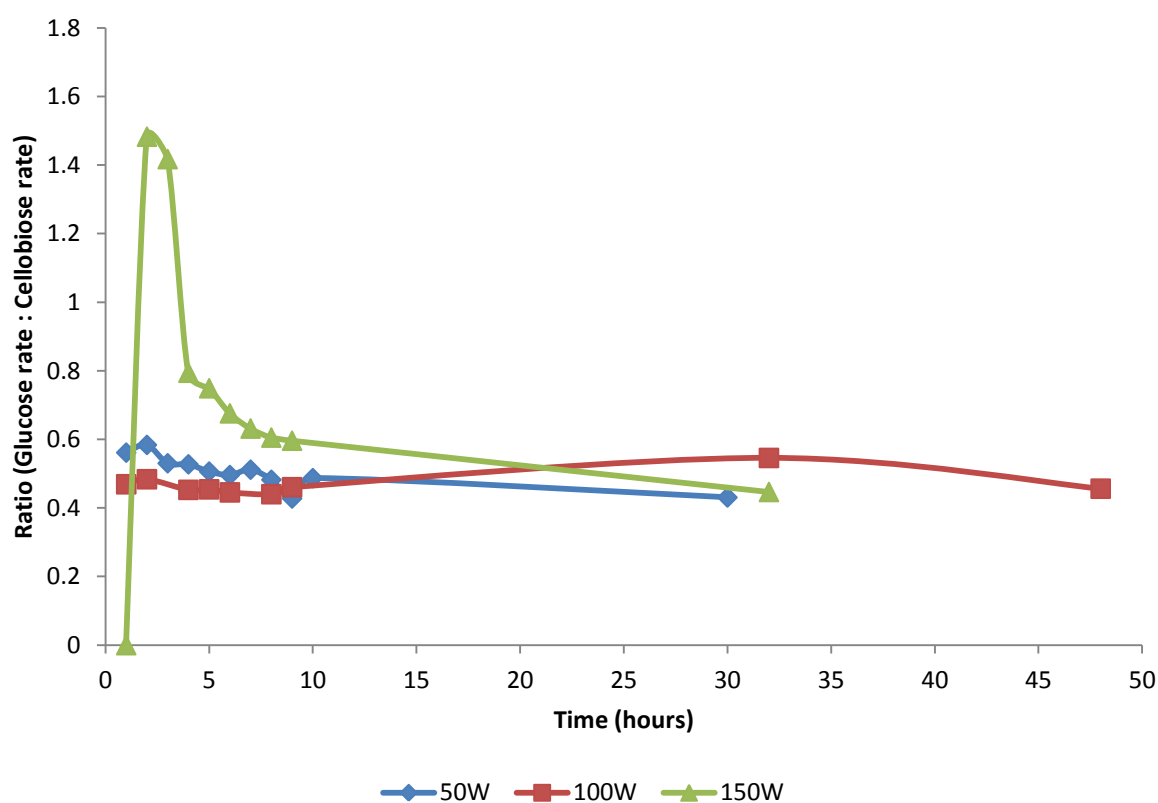
Full plot of cellobiose evolution by microwave power.

Figure 83 shows the microwave irradiation to have a clear rate altering effect across the 50 – 150W power band with the greatest rate alteration seen in the concentration of cellobiose under 50W microwave power. By looking at the time point of 32 hours in both the glucose and cellobiose evolution plots, the difference between concentrations of product obtained at different microwave power settings can be quoted (see Table 34). The table shows that through the irradiation of the reaction, the concentration of products is enhanced.

| CBH/EGL - BGL   |               | T = 32hrs        |                  | Increase upon 000W value |  |
|-----------------|---------------|------------------|------------------|--------------------------|--|
| Microwave power | Glucose (g/l) | Cellobiose (g/l) | Glucose (factor) | Cellobiose (factor)      |  |
| 0               | 1.895         | 0.558            | 1                | 1                        |  |
| 50              | 3.550         | 2.100            | 1.873            | 3.763                    |  |
| 100             | 2.495         | 1.345            | 1.136            | 2.410                    |  |
| 150             | 1.473         | 0.971            | 0.777            | 1.740                    |  |

**Table 34. Table of microwave influence on product formation and rate alteration**

In Table 34 it is noticeable that the increase in concentrations between glucose and cellobiose are proportional by a factor of two, where the cellobiose increase factor is twice that of the glucose increase. Using the same data interpretation through the other comparable time periods, this is not seen as a consistent trend (see Figure 84).



**Figure 84. Comparison of microwave power rates to MW-NC**

Data normalised against 000W MW-NC.

Basing further analysis on the initial rates of hydrolysis, the time frame considered was reduced to two hours. Plotting glucose as the major constituent of interest, and cellobiose as the major intermediate of interest, the graph presented in Figure 85 was produced along with the % saccharification graph Figure 86.

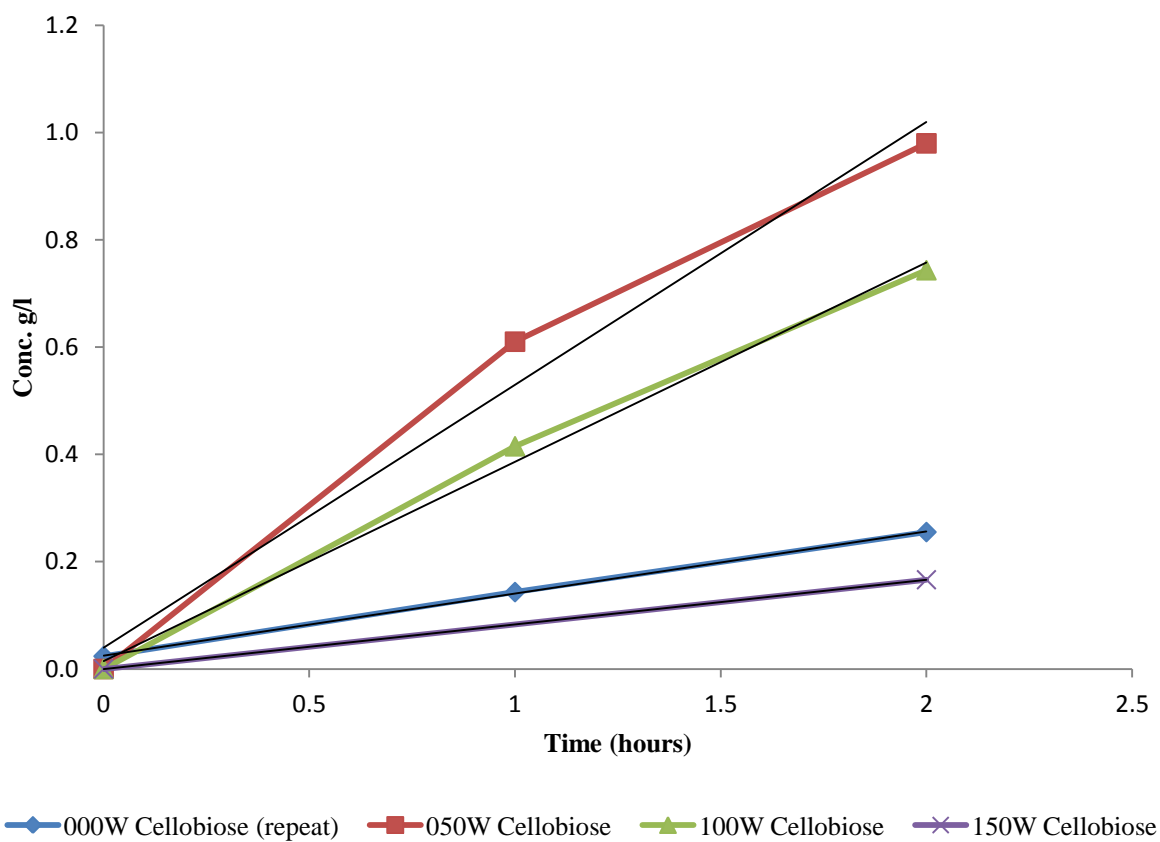
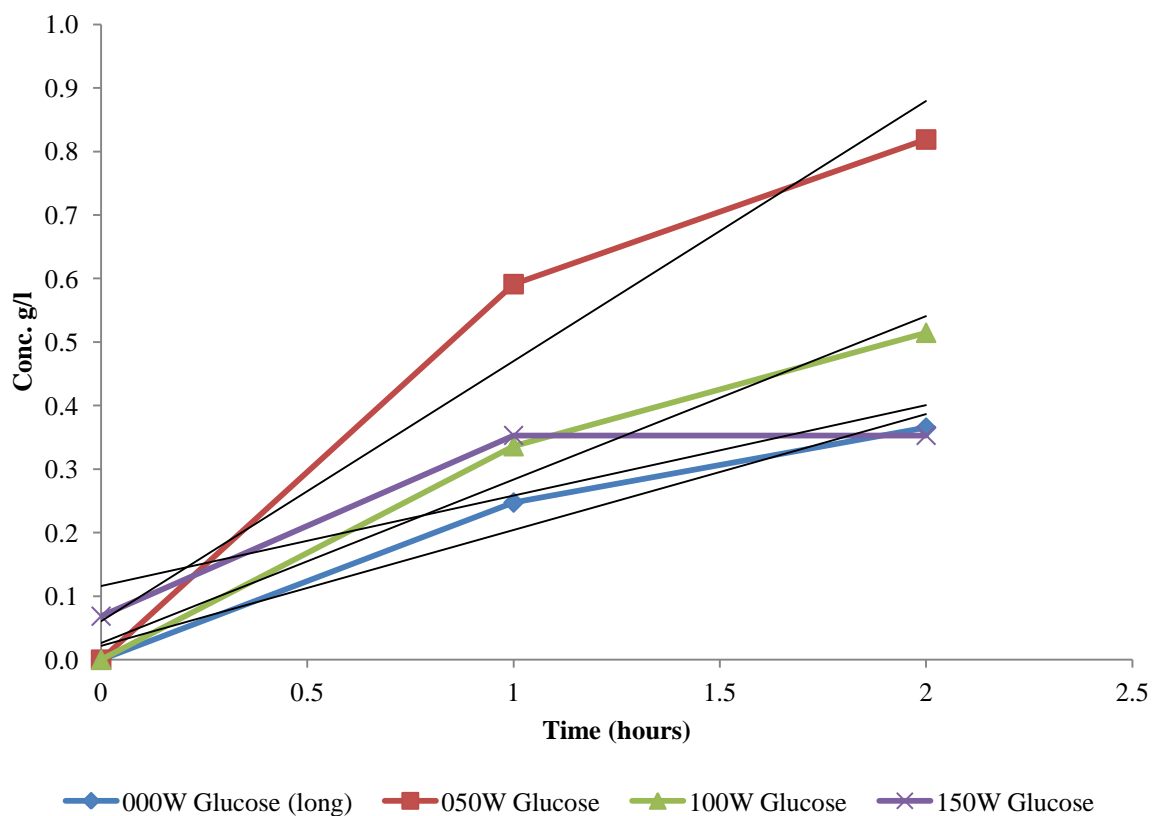


**Figure 85. Initial rates for glucose and cellobiose production in varying microwave power**  
 Conditions; 10g/l biomass ( $\alpha$ -cellulose), 50°C, 300rpm agitation, CBH loading of 60FPU/g cellulose, absence of BGL. Analysis through RI-HPLC with REZEX ROA as described previously. Data presented as grams per litre by breakdown constituent (glucose).

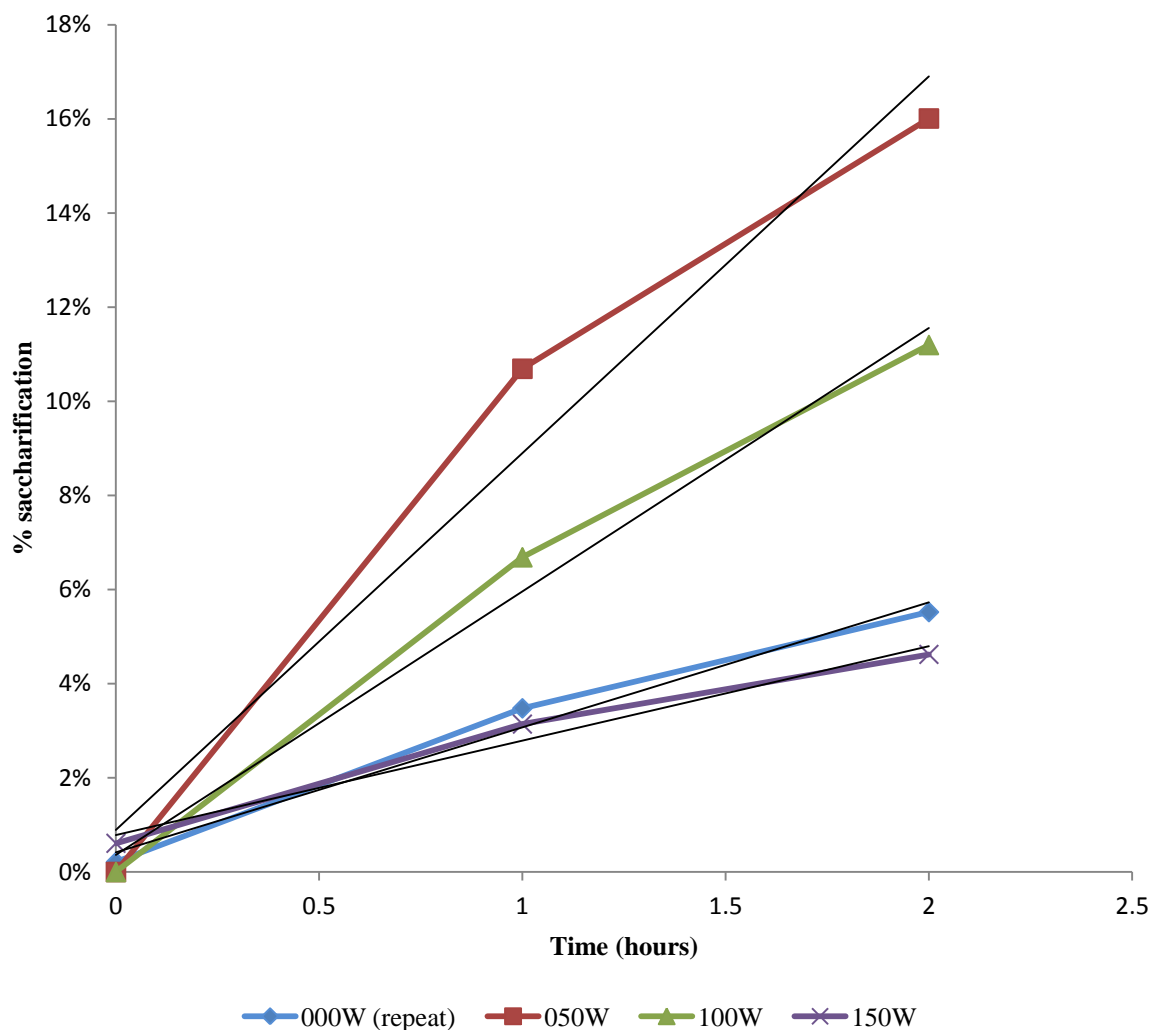


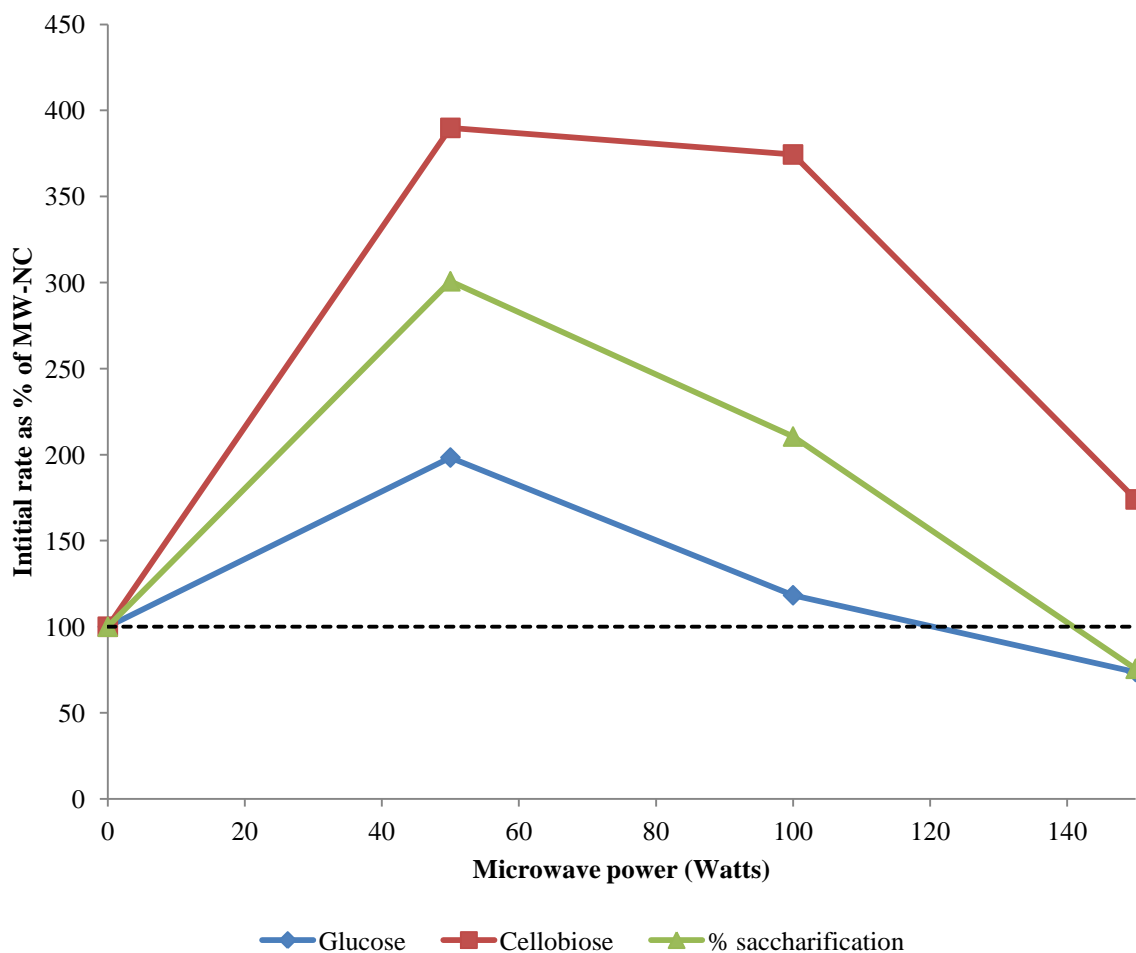
**Figure 86. Summary of results – Percentage saccharification by microwave irradiation (+EGL/CBH -BGL)**  
 Conditions; 10g/l biomass ( $\alpha$ -cellulose), 50°C, 300rpm agitation, CBH loading of 60FPU/g cellulose, absence of BGL. Analysis through RI-HPLC with REZEX ROA as described previously. Data presented as percentage of material hydrolysed per unit of time against power of microwave irradiation.

| Microwave power<br>Watts | Glucose               |                    |                |                   | Cellobiose            |                    |                |                   |
|--------------------------|-----------------------|--------------------|----------------|-------------------|-----------------------|--------------------|----------------|-------------------|
|                          | Gradient<br>(dP/d[T]) | Intercept<br>(g/l) | R <sup>2</sup> | Difference<br>(%) | Gradient<br>(dP/d[T]) | Intercept<br>(g/l) | R <sup>2</sup> | Difference<br>(%) |
| 0                        | 0.131                 | 0.00               | 0.924          | 100               | 0.066                 | 0.08               | 0.926          | 100               |
| 50                       | 0.206                 | 0.66               | 0.899          | 198.3             | 0.258                 | 0.08               | 0.903          | 389.9             |
| 100                      | 0.155                 | 0.12               | 0.953          | 118.3             | 0.248                 | 0.60               | 0.874          | 374.4             |
| 150                      | 0.096                 | 0.17               | 0.901          | 73.7              | 0.115                 | -0.03              | 0.938          | 174.0             |

| Microwave power<br>Watts | % saccharification    |                    |                |                   |
|--------------------------|-----------------------|--------------------|----------------|-------------------|
|                          | Gradient<br>(dP/d[T]) | Intercept<br>(g/l) | R <sup>2</sup> | Difference<br>(%) |
| 0                        | 0.026                 | 0.00               | 0.893          | 100               |
| 50                       | 0.080                 | 0.03               | 0.964          | 300.8             |
| 100                      | 0.056                 | 0.00               | 0.988          | 210.5             |
| 150                      | 0.020                 | 0.01               | 0.978          | 75.6              |

**Table 35. Summary of initial rates for CBH/EGL on cellulose with varying microwave irradiation**



**Figure 87. Percentage difference in initial rates to MW-NC**

Difference in [P] (glucose and cellobiose) and % saccharification by microwave power when normalised against the microwave negative control. Data used from Table 35. Black dotted line used to show 100% reference.

From the comparison of results, the microwave field was shown to produce a measurable difference when compared to the negative control. The greatest increase in initial enzymatic rate in comparison to the negative control was observed in the 50W reaction (increase of 289% in cellobiose, 198% in glucose and 200% in saccharification).

Using the rate of saccharification, 50W irradiation is shown to show the greatest initial rate increase in comparison to the negative control. Decreasing conversion is seen with increasing field strength in comparison to the control (100W = x3 increase). At powers greater than 100W, the enzymatic rate is retarded in comparison to the negative control (150W = x1.29 decrease).

The two part mechanism of cellulose to glucose conversion is observed first in the cellobiose profile; and secondly in the oligosaccharide (cellobiose, DP3, DP4, DP4+) to glucose.

The diminishing product formation seen in the 100W cellobiose trend line is countered by an increase in glucose concentration. When observed as total fermentable sugars or as % of saccharification, the continual evolution of yield reflects a proportionate decrease in substrate.

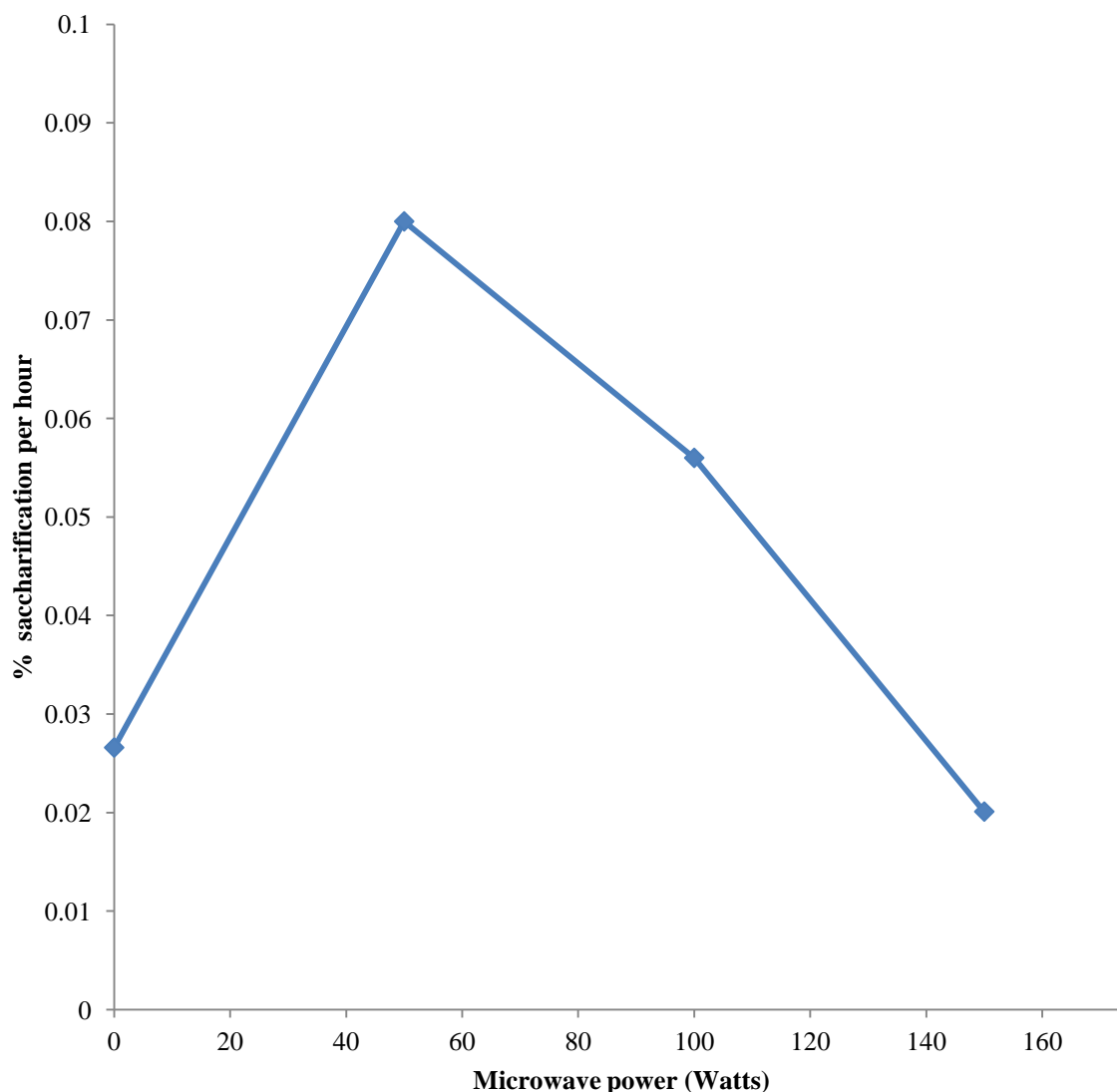


**Figure 88. Percentage saccharification against microwave power based on initial rates**  
 Figure shows the power curve in cellulose conversion.

Figure 88 clearly shows the non-linear relationship between the rate of saccharification and microwave power. The conclusions that can be drawn from this section of experiments show that where the increase in power applied is non-linear to the resultant saccharification, the greatest beneficial effects are apparently seen at 50W forward power. Further increase to 100W or 150W gave no further enhancement but instead decreased. Based on the data produced from the initial rates of each experiment, subjecting the enzyme catalysed reaction to 50W microwave power increases the initial rate by 4 times.

Detailing the rate alteration in the constituents of glucose and cellobiose gives comparable results (see Figure 89) each showing the increased rate at 50 Watts. From the data produced, the optimal power appears to be in the region of 50W power per litre solution containing 10g/l cellulose.

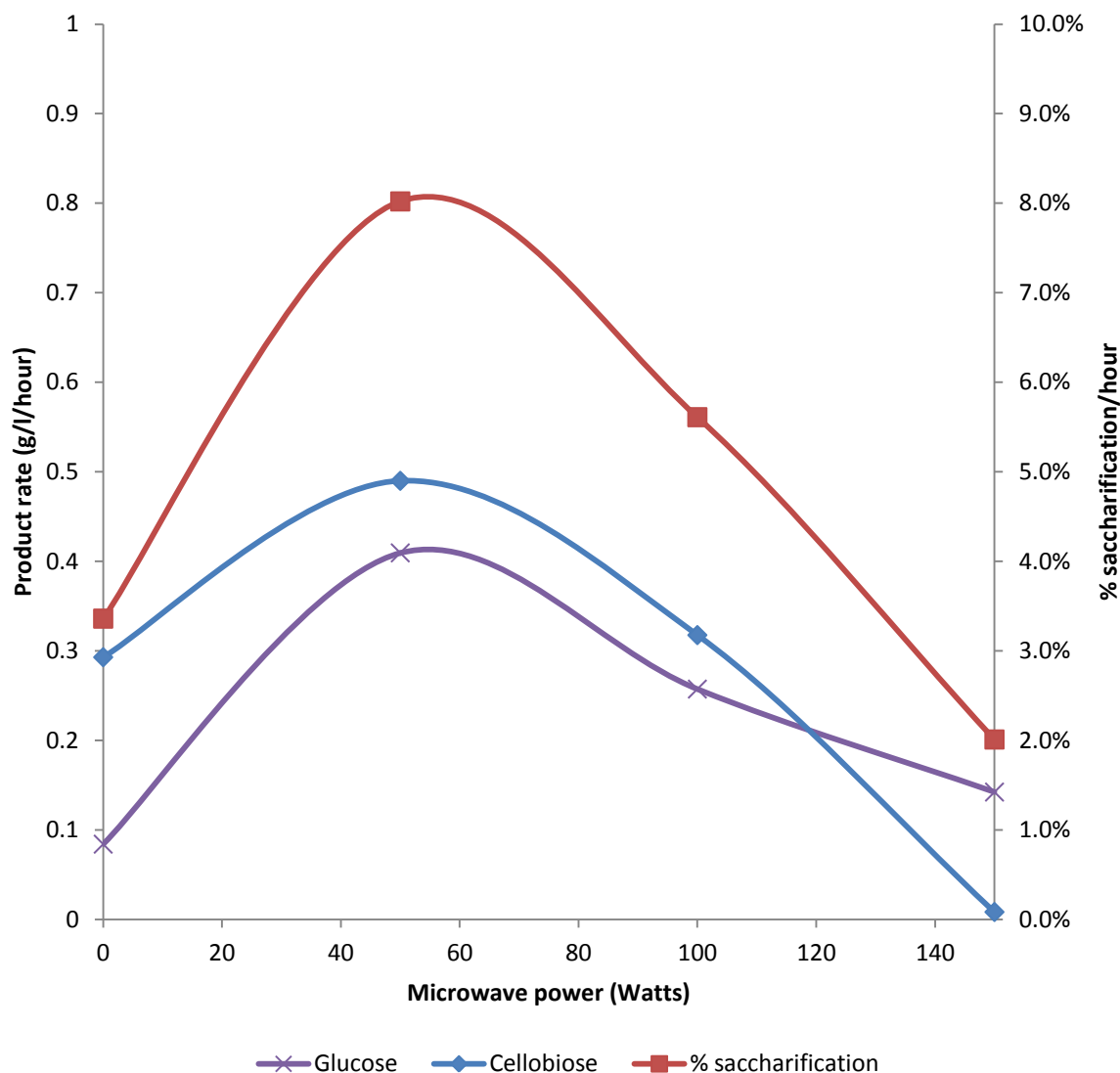
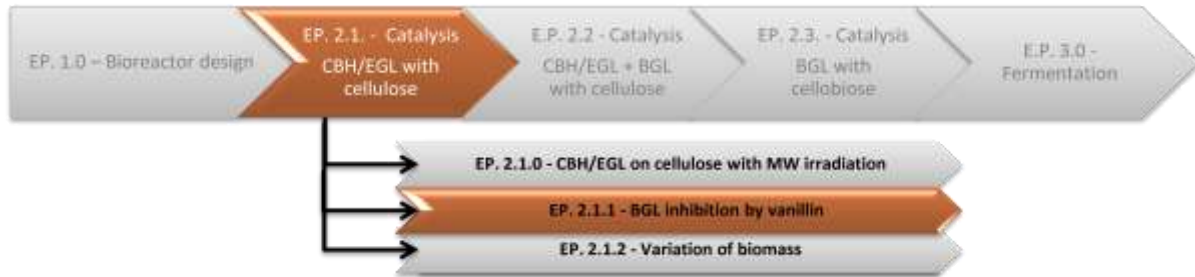


**Figure 89. Initial rates for EGL/CBH -BGL on cellulose with variable microwave irradiation (Constituents and percentage saccharification)**

As the analysis is based on a four value plot (negative control and three variables), the true optimal value is unknown but hypothesised to lie between 0 and 100W with 50W shown to closest to optimal in this experiment. Sweeping the power band for dose response (Bayesian inference) was not pursued due to time pressures.

#### 4.2.1.1. EP 2.1.1. –Investigation for inhibition of residual BGL through the addition of vanillin



- *The alteration of rate observed in EP 2.1.0. is not due to BGL contamination in the commercial “cellulase” preparation*

*Summary; With the addition of vanillin to the CBH/EGL enzyme preparation at varying vanillin concentrations, no effect is seen on enzymatic rate, indicating that increased glucose evolution seen in the previous experiment is not due to enhancement of a BGL contaminant.*

BGL catalysis is known to be inhibited by vanillin addition [59]. By looking for alteration in glucose evolution in the presence of vanillin, the determination of BGL contamination in the EGL/CBH preparation can be determined as a meaningful alternative to protein separation and SDS-PAGE analysis. Experiments were conducted using the previously described methods where the aim is to see if the increased evolution of glucose is due to alteration of EGL/CBH activity or through the amplification of contaminant BGL. Vanillin has a greater inhibitory effect on BGL over CBH and EGL, therefore BGL inhibition will be observed if the glucose:cellobiose ratio shifts in favour of cellobiose accumulation. From the data produced, no shift in ratio is observed (see Figure 90). Vanillin to cellulase ratios of 0.41:1 through to 16:1 were explored where the expected 50% reduction in BGL would be expected at a ratio of 4:1 assuming a pure BGL enzyme preparation. The results compiled show no deviation in hydrolysis across the ratio range, indicating that BGL contamination was not present.

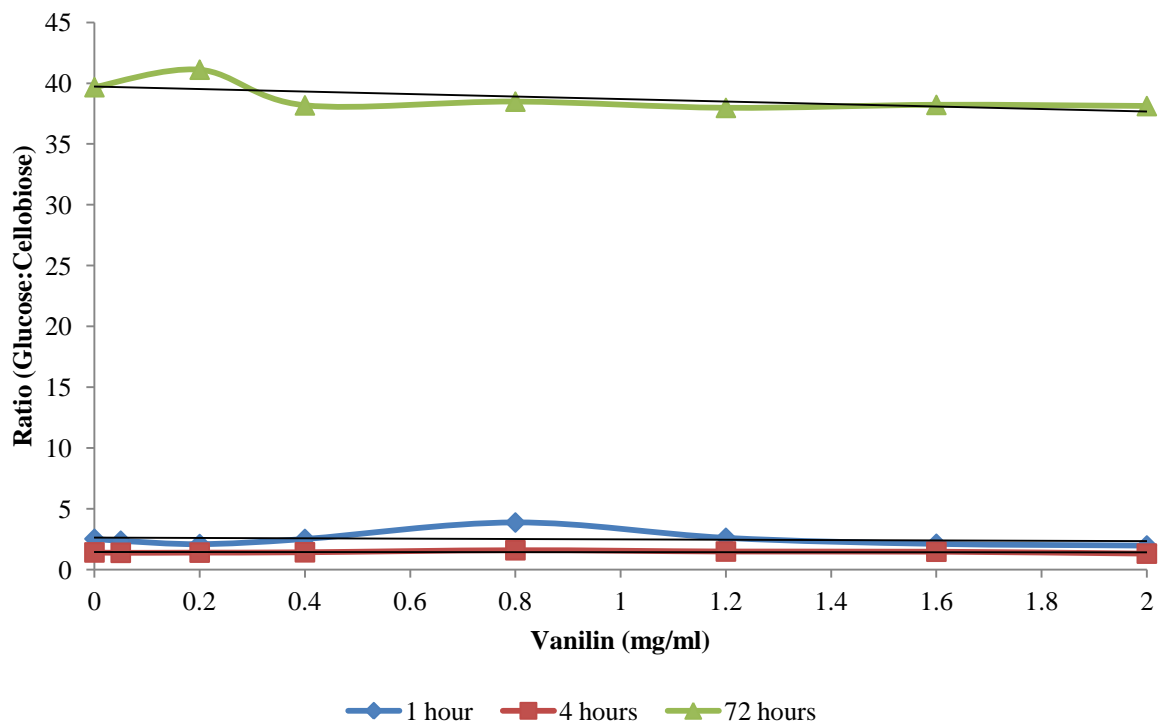


**Figure 90. Glucose:Cellulose ratio in comparison to Vanillin concentration**

Tend lines; 1 hour =  $-0.002x + 1.4331$ ; 4 hours =  $-0.1455x + 2.6247$ ; 72 hours =  $-1.0346 + 39.737$ .

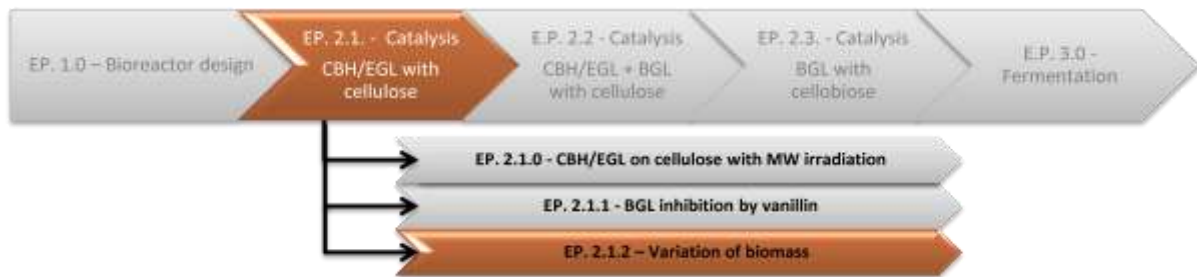
From the data produced, no apparent alteration in catalysis profile was observed with vanillin addition indicating that BGL contamination is not a significant factor and the results observed in E.P. 2.1.0. cannot be attributed to preferential enhancement of BGL content.

In development of the process, samples were taken at the 1 hour time point as described in the initial method, with more detailed examination by the addition of further time extensions. In extending the time profile to 4 hours, the resolution of the reaction was increased with respect to glucose (error margin reduced from 6.18% at 1 hour to 0.02% after 4 hours taking into account experimental error) whereas extension of the experiment to 72 hours showed an increase in error to 10% due to the opportunity for contamination. The alteration of incubation time was seen as beneficial for the removal of potential variability that can be observed in the initial rate conditions, especially in low catalytic rate reactions where product concentrations may be low. By extension to the 72 hour point (analogous to the 60 hour reaction previously undertaken) sufficient product could be formed, however under the constraint of potential microbial contamination. To counter product degradation due to contamination, all experiments were conducted with microbial repression by the inclusion of antibiotics at the start of incubation. Repeated dosing was not conducted to prevent alteration of ethanol concentration for the antibody dilution factors in each reaction.

By regression of the obtained sample results by time variable and vanillin concentration, analysis of saccharification rate and glucose/cellobiose evolution can be determined. Examination of variation of vanillin concentration shows the increase in vanillin from 0 mg/ml through to 2 mg/ml does not show

measurable alteration of rate in comparison to the negative control of 0 mg/ml vanillin. As such, increased glucose evolution due to the microwave stimulation of BGL over CBH/EGL can be concluded as not being the mechanism of action in E.P. 2.1.0.

#### 4.2.1.2. EP 2.1.2. - Variation by biomass



**Summary;** By the study of glucose formation, variation of biomass in the microwave field of 50W is shown to maintain the same hydrolytic rate. As such, it can be assumed that [E] is at saturation by cellulose. In overall product formation, 50g/l and 10g/l loading show comparable rate. Viewed as cellobiose formation, 50g/l is shown to have a greater evolution due to the increase of binding sites with hydrolytic affinity (free ends). By percentage saccharification, 50g/l shows a scaler factor of 4.3 compared to 5 that would be expected.

For the determination of enzyme saturation due to the low loading of cellulase enzymes, biomass variation was conducted through the increase of cellulose from 10g/l to 50g/l in an irradiated microwave field of 50W. 50W power was selected following analysis of the previous experiments concluded in EP. 2.1.

For analysis, the results are compared to previously obtained values for 50W catalysis with 10g/l substrate loading.

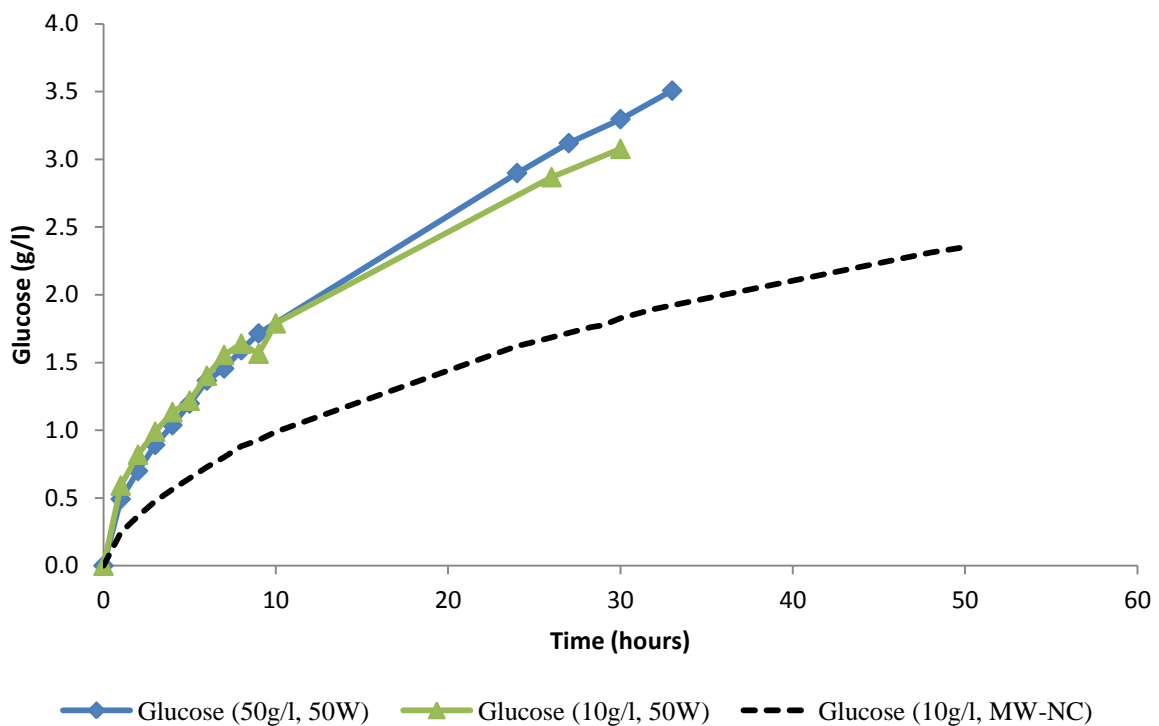
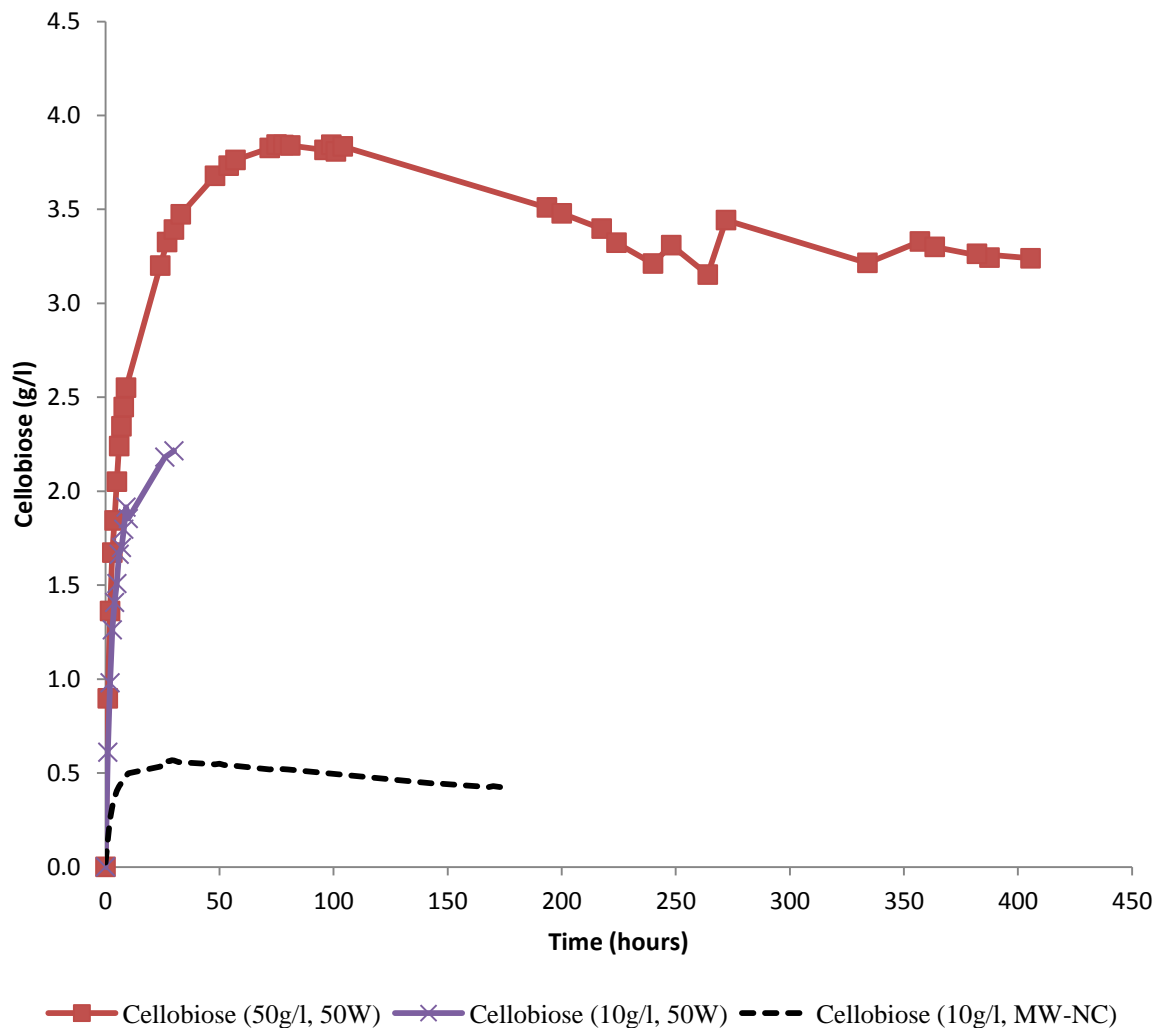


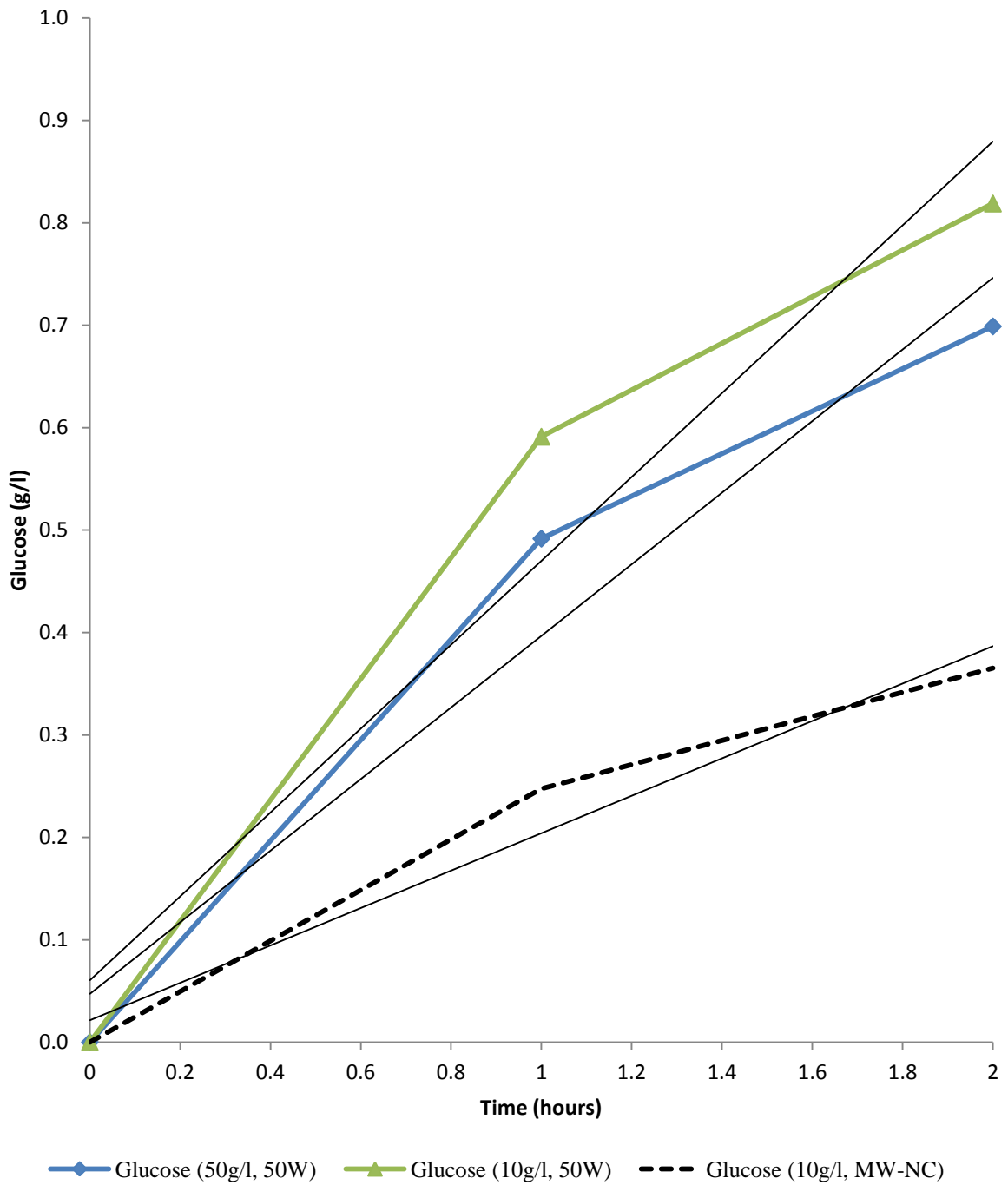
Figure 91. Glucose production at substrate loadings of 10g/l and 50g/l cellobiose at 50W and NC-MW at 10g/l

Figure 91 shows the evolution of glucose by biomass variation with the MW-NC for E.P. 2.x included. From the traces produced, there is little discernable variation in total rate with variation of loading, indicating that the system is most likely to be in substrate saturation. As the curve created at 10g/l is comparable to 50g/l at 50W, amplification in rate is observed in both systems in comparison to the MW-NC. Of note in this reaction is the omission of BGL, therefore the glucose end product is derived from CBH action.



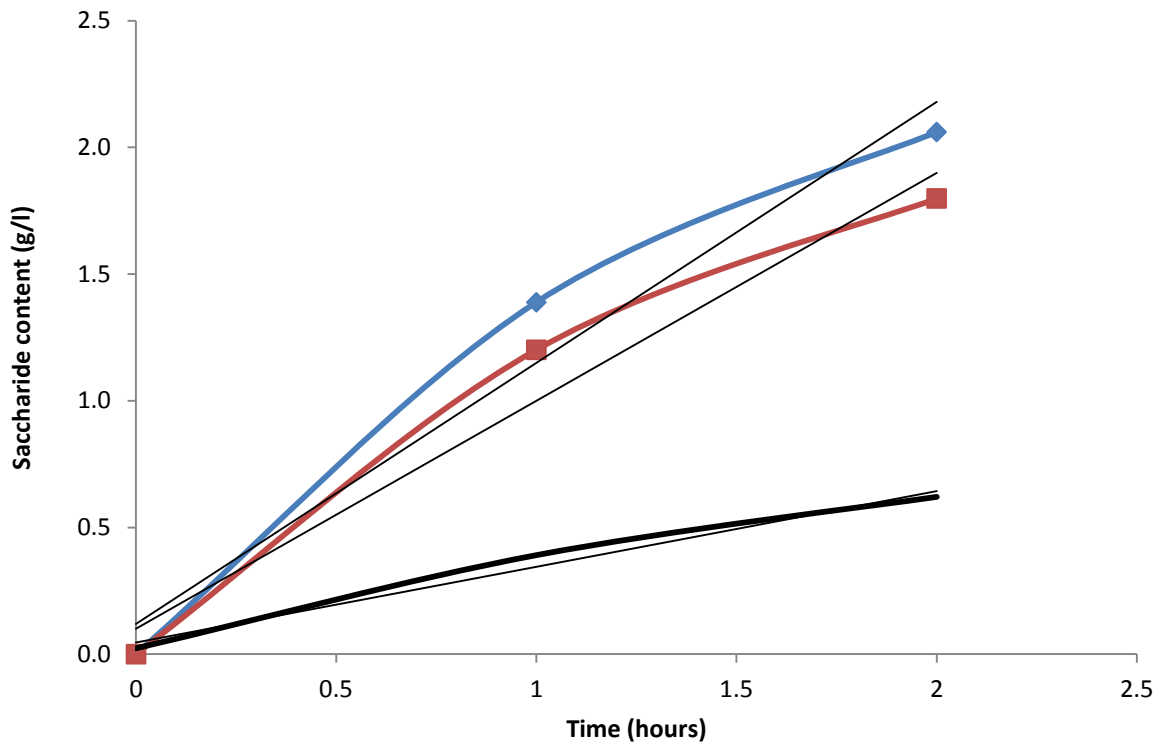
**Figure 92. Cellobiose production at substrate loadings of 10g/l and 50g/l cellobiose at 50W and MW-NC at 10g/l**  
For full plot, refer to appendix.

In the experiment conducted, the omission of BGL should equate to a variation in the evolution of cellobiose which is observed in Figure 92. In confirmation to Figure 91, variation to the MW-NC was observed. Of note is the variability for cellobiose yield between 50g/l and 10g/l. the increase in cellobiose concentration is hypothesised to be in relation to the number of free ends due to EGL hydrolysis and the increase probability of CBH/substrate complex.

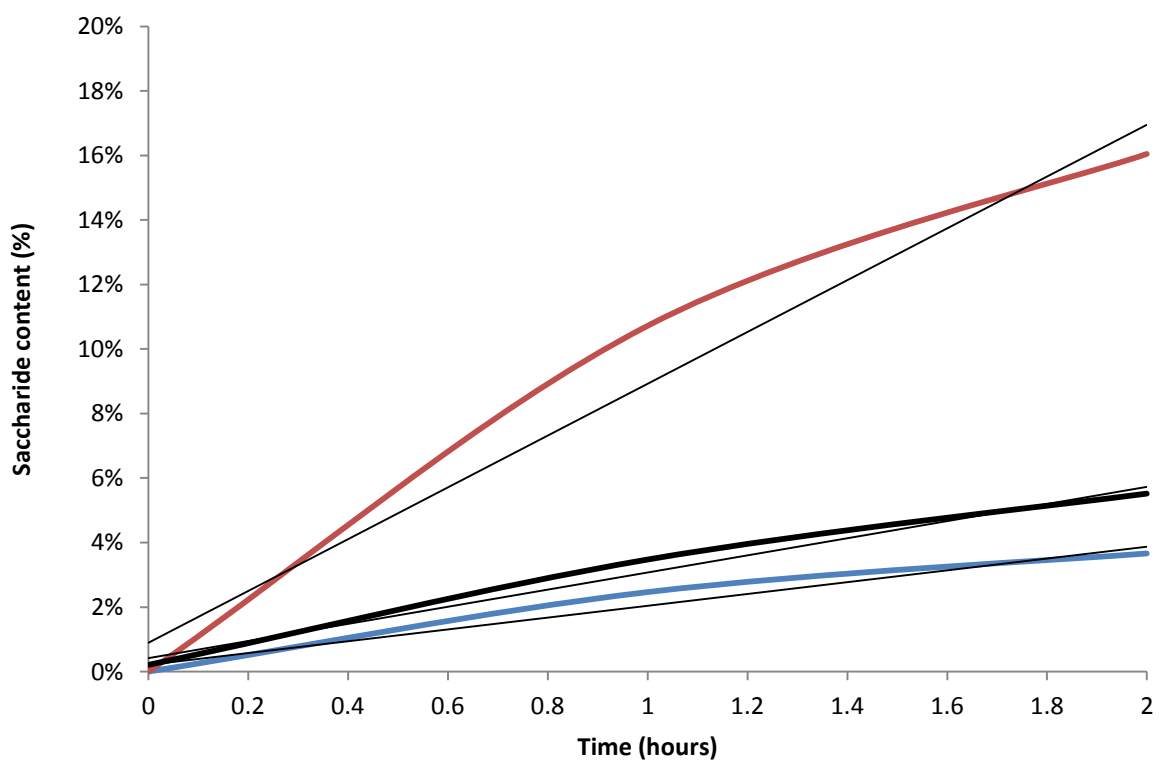


**Figure 93. Initial rates for glucose production at substrate loadings of 10g/l and 50g/l cellobiose with 50W and NC-MW at 10g/l**

Initial rates for both glucose and cellobiose were determined by comparison of the first two hours. The rates observed show clear deviation to the negative control with glucose rates approximately 3 times greater than the thermal and cellobiose approximately 5 times greater.



◆ Total (50g/l, 50W)    ■ Total (10g/l, 50W)    — 10g/l, MW-NC



— % saccharification (50g/l, 50W)    — % saccharification (10g/l, 50W)  
 — % saccharification (10g/l, MW-NC)

Figure 94. Comparison of 10g/l and 50g/l substrate loading with 50W irradiation by initial rates of percentage saccharification.

Observation of total saccharide release by initial rates shows similarity between 50g/l and 10g/l at 50W irradiation. In comparison, % saccharification belies the conversion factor by total mass. Where the rate of % saccharification appears below the rate observed in the MW-NC, this is expected due to the increase in substrate. By interpretation of rate based where the initial rate at 50g/l is compared to 10g/l, a rate factor of 4.27 is observed, typifying the 5x increase in biomass.

| Microwave power | Biomass loading | Glucose |     |                    |                 | Cellobiose     |                |                    |                 |                |                |
|-----------------|-----------------|---------|-----|--------------------|-----------------|----------------|----------------|--------------------|-----------------|----------------|----------------|
|                 |                 | Watts   | g/L | Gradient (dP/d[T]) | Intercept (g/l) | R <sup>2</sup> | Difference (%) | Gradient (dP/d[T]) | Intercept (g/l) | R <sup>2</sup> | Difference (%) |
| 10              | 10              |         |     | 0.182              | 0.02            | 0.959          | 100            | 0.116              | 0.06            | 0.999          | 100            |
| 50              | 10              |         |     | 0.409              | 0.06            | 0.938          | 224.2          | 0.490              | 0.04            | 0.980          | 423.4          |
| 50              | 50              |         |     | 0.349              | 0.05            | 0.947          | 191.3          | 0.681              | 0.07            | 0.968          | 588.5          |

| Microwave power | Biomass loading | % saccharification |     |                    |                 |                |                |
|-----------------|-----------------|--------------------|-----|--------------------|-----------------|----------------|----------------|
|                 |                 | Watts              | g/L | Gradient (dP/d[T]) | Intercept (g/l) | R <sup>2</sup> | Difference (%) |
| 10              | 10              |                    |     | 0.298              | 0.05            | 0.983          | 100            |
| 50              | 10              |                    |     | 0.899              | 0.10            | 0.964          | 301.4          |
| 50              | 50              |                    |     | 1.030              | 0.12            | 0.963          | 345.3          |

Table 36. Summary of initial rates for biomass variation (10 and 50g/l at 50W irradiation) against MW-NC (10g/l)

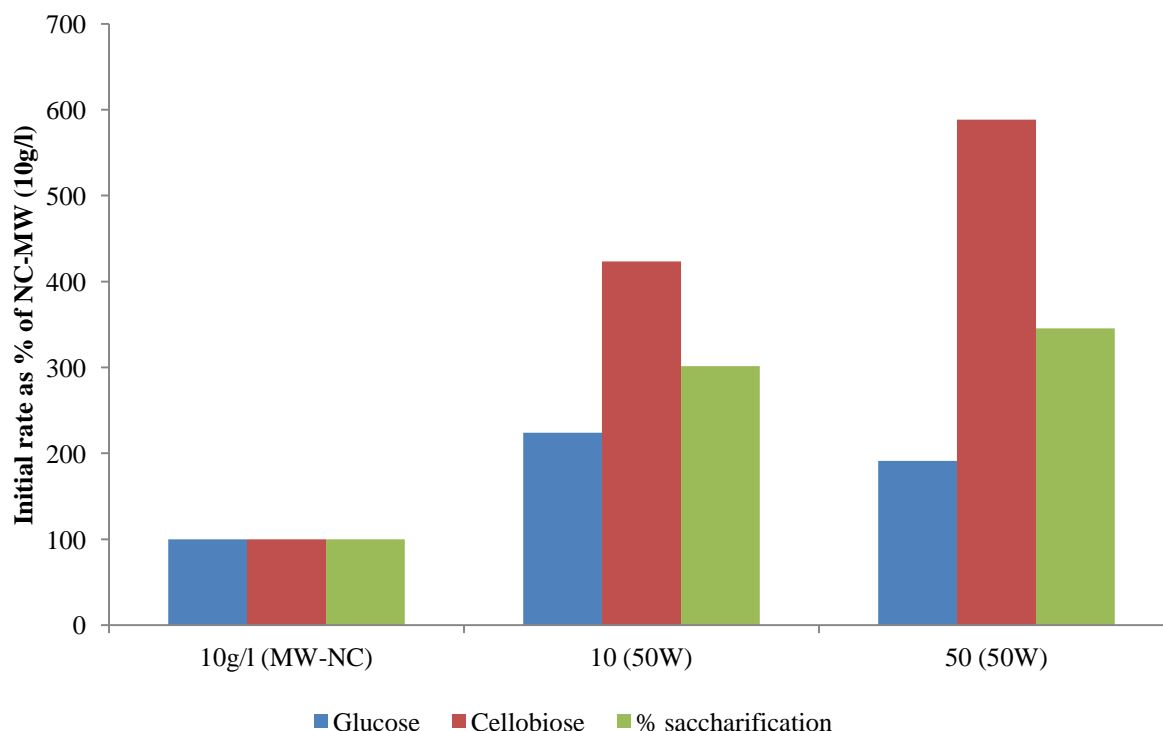
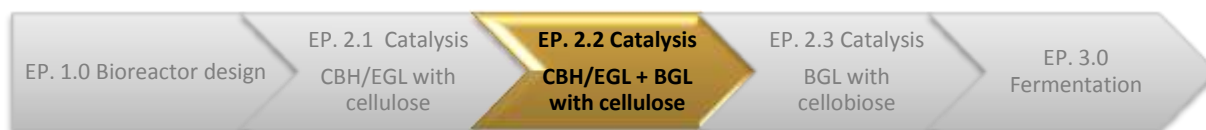


Figure 95. Percentage difference in initial rates of 10g/l and 50g/l at 50W to 10g/l MW-NC

#### 4.2.2.0. EP 2.2.0. – Cellulose hydrolysis by CBH/EGL +BGL with varying microwave irradiation



- 25W/l aqueous solution containing 10g/l cellulose and 40 FPU/g substrate “cellulase” (EGL & CBH) and 111.7CBU/g BGL showed the greatest (65%) increase in initial glucose rate and greatest glucose yield ( $\approx 30\%$ ) over the negative control
- The relationship between irradiation power and alteration of initial rate is non-linear

**Summary;** The most significant conclusion from this experimental package is that microwave irradiation has increased both the initial hydrolytic rate and the total reaction yield. With a non-linear relationship between rate and microwave power, 25W irradiation was shown to increase total yield by 25%, initial glucose rate by 65% and initial % saccharification rate by 65%

For the determination of EGL/CBH hydrolysis with excess BGL, the previous experiments were repeated with the addition of excess BGL as previously described. The power of the microwave irradiation was reduced in accordance to the 50W optimum seen in EP. 2.1 (Variable microwave power on EGL/CBH with cellulose). Re-establishment of the optimum around the 50W threshold was executed with powers ranging from 12W through to 75W.

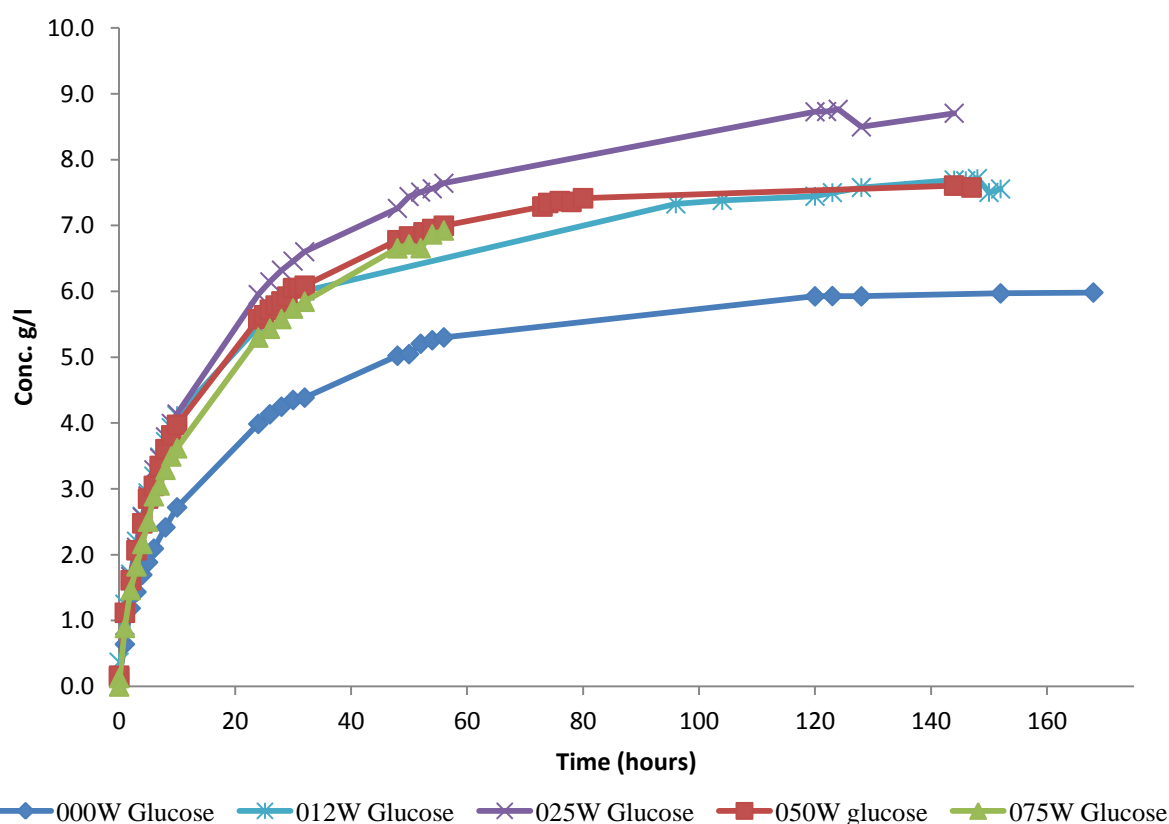


**Figure 96. Glucose production in varying microwave power (full plot)**  
Full plot of glucose evolution by microwave power.

As previously discussed, the product of greatest interest was glucose. With the presence of BGL in the solution for the hydrolysis of cellobiose, the completed end reaction product should have been solely glucose, assuming no inhibition in an ideal system. From the full time scale plot for glucose seen in Figure 96. 25W microwave power saw the greatest product formation over the total time period. Powers of 12W, 50W and 75W are all above the negative control values. Of considerable note is the lack of further product formation in the MW-NC beyond 120 hours with a final glucose concentration of approximately 6g/l. Compared to the microwave irradiated results, each microwave power shows greater total product formation (between 7 and 8.7g/l) to the MW-NC.

The expectation of BGL in excess should show minimal trace amounts of cellobiose. This is seen and confirmed as expected in Figure 97.

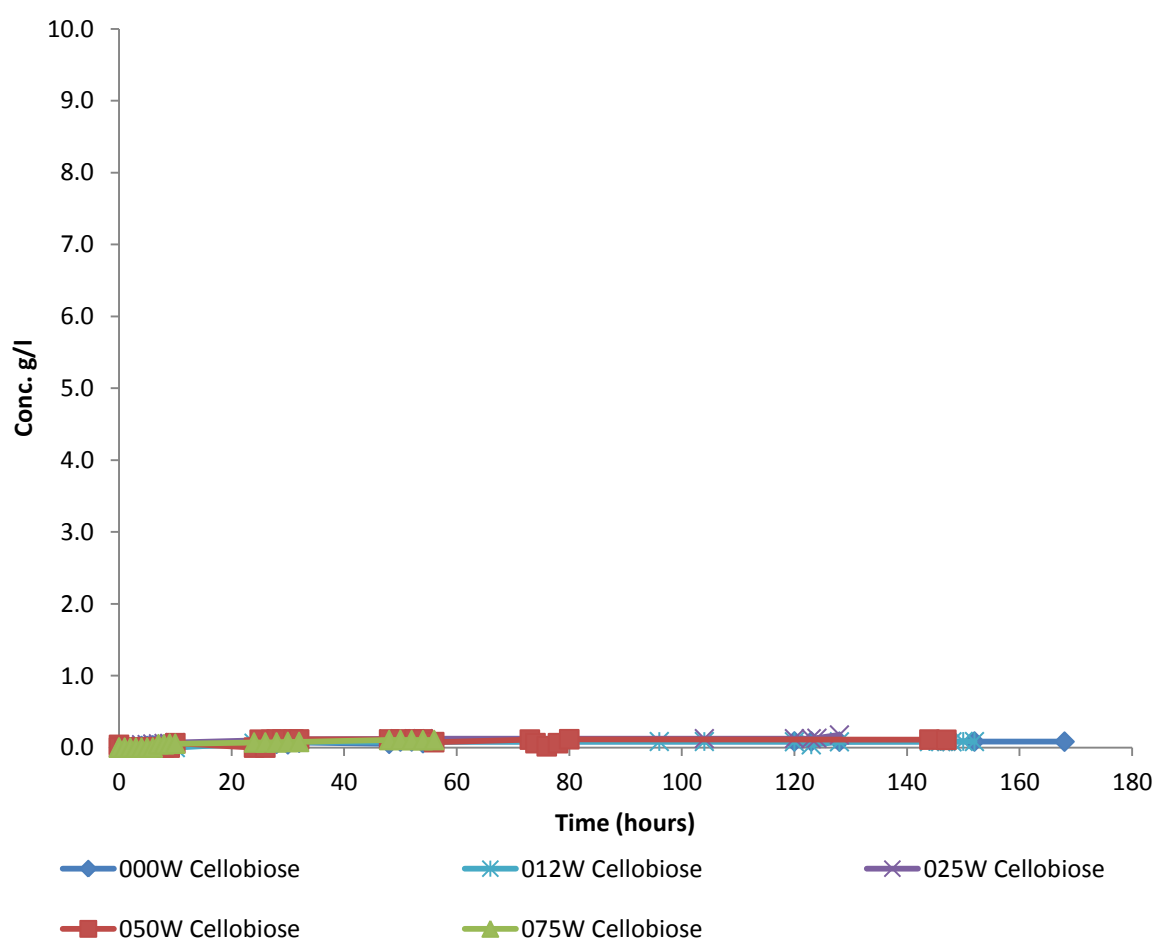


**Figure 97. Cellobiose production in varying microwave power (full plot)**  
Full plot of cellobiose evolution by microwave power.

Further analysis of the initial rates for glucose and cellobiose are presented in Figure 98 for constituent accumulation and Figure 99 for percentage saccharification. Noticable is the inverted relationship of initial rates compared to trend in the 12W and 24W initial rates. This is expected to be an artefact in data collection due to sample resolution

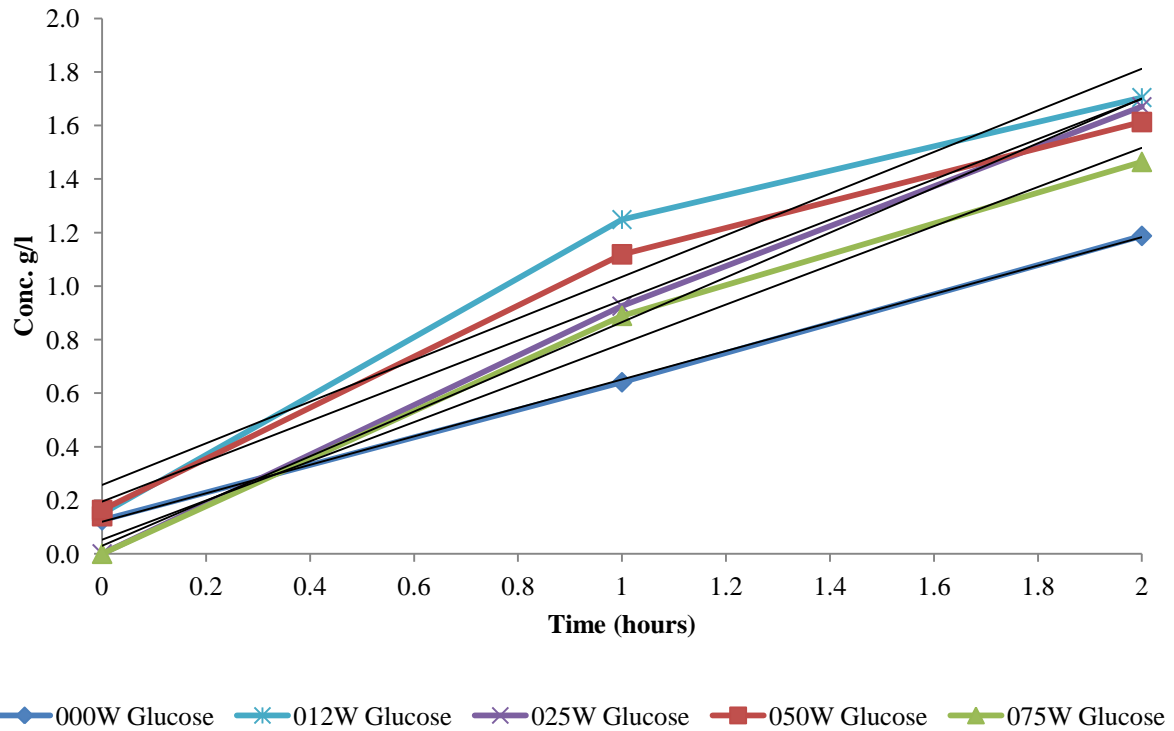


**Figure 98. Initial rates for Glucose production in varying microwave power**  
 Conditions; 10g/l biomass ( $\alpha$ -cellulose), 50°C, 300rpm agitation, CBH loading of 60FPU/g cellulose, BGL loading of 168GBU/g cellulose. Analysis through RI-HPLC with REZEX ROA as described previously. Data presented as grams per litre by breakdown constituent (cellobiose).

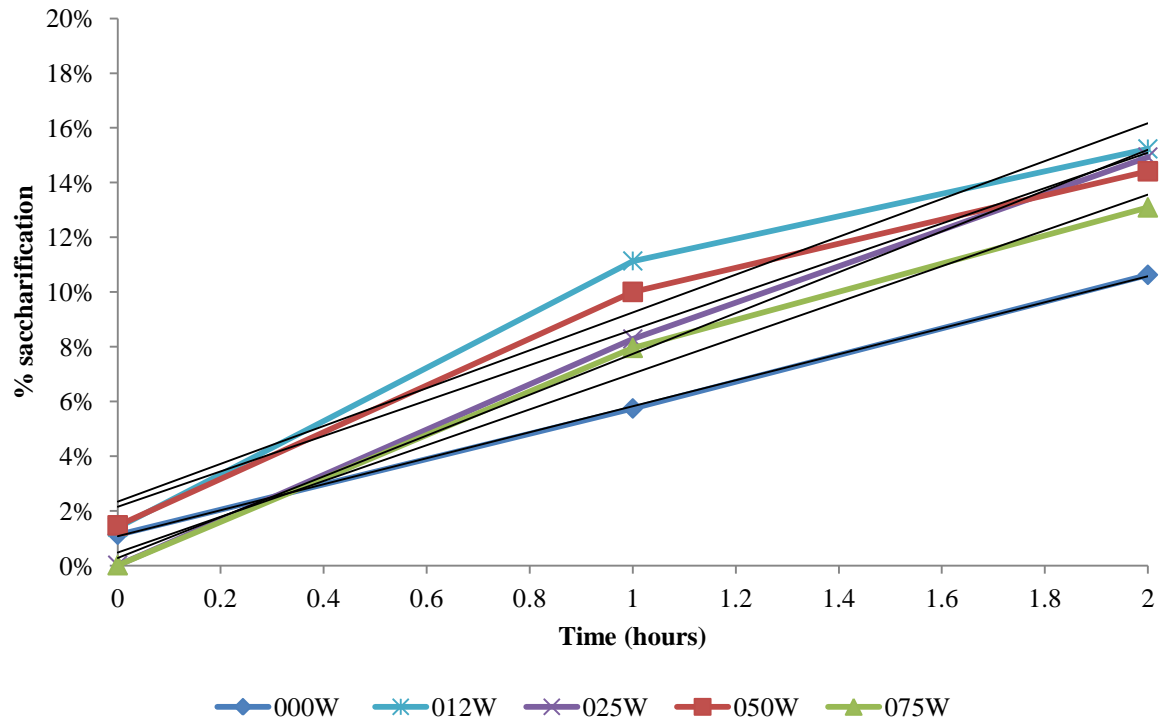


**Figure 99. Percentage saccharification of cellulose with EGL, CBH and BGL with variable microwave irradiation (EGL/CBH/BGL)**  
 Conditions; 10g/l biomass ( $\alpha$ -cellulose), 50°C, 300rpm agitation, CBH loading of 60FPU/g cellulose, BGL loading of 168GBU/g cellulose. Analysis through RI-HPLC with REZEX ROA as described previously. Data presented as percentage of material hydrolysed per unit time against power of microwave irradiation.

For the determination of the theoretical maximum yield, curve fitting of the raw data was undertaken using the method explained in “Curve fitting data” on page 122. The resulting plot with combined raw data and curve fit data is shown in Figure 100. For clarity, the raw data is shown as black lines and is a replication of the data displayed in Figure 96.

Of significance for further investigation is the increase in yield observed, particularly at 25W where the yield is 44% higher than the negative control. Whereas yield limitation is expected (as outlined in “2.3.6. Cellulase enzyme quantification/qualification” on page 44), the increase in yield as opposed to rate suggests a modification to a mechanism within the enzyme-complex relationship – possible alteration of either a feedback inhibition loop or increase mobility to carry out further catalysis.. Further investigation of this phenomenon would be of significance to the processing industry as it would allow greater product yield per unit cellulase added.

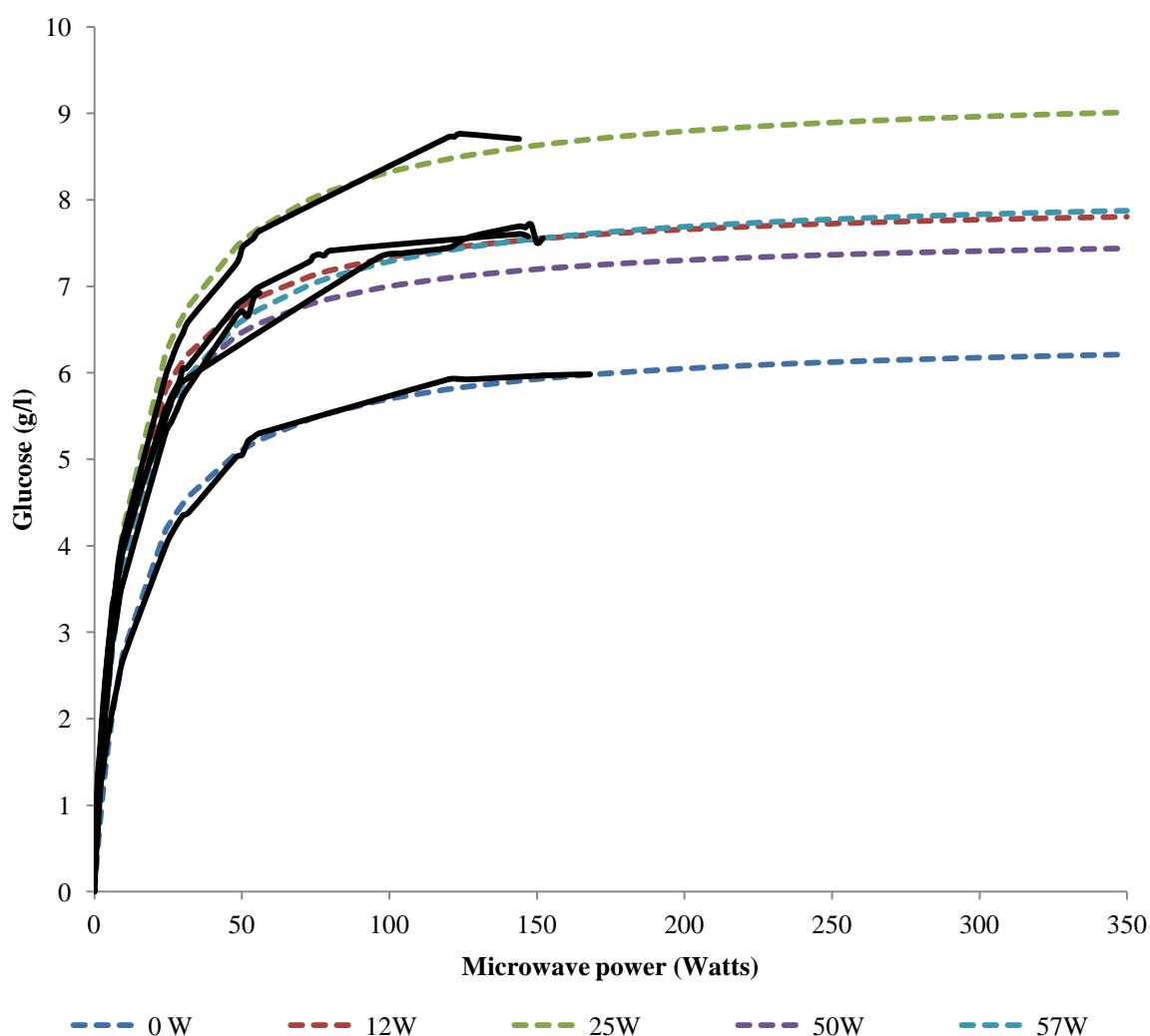


**Figure 100. Curve fit data for CBH/EGL/BGL catalysis of cellulose with microwave irradiation**  
Dashed lines show the curve fit data. Black lines the raw data, replication of data as seen in Figure 99. Colours in the raw data have been omitted to show clarity in the curve fit plots.

| Microwave power<br>Watts | Glucose               |           |                |                   |                 | Percentage saccharification |                    |           |                |                   |
|--------------------------|-----------------------|-----------|----------------|-------------------|-----------------|-----------------------------|--------------------|-----------|----------------|-------------------|
|                          | Gradient<br>(d[P]/dT) | Intercept | R <sup>2</sup> | Difference<br>(%) | Yield*<br>(g/l) | Difference<br>(%)           | Gradient<br>(%/hr) | Intercept | R <sup>2</sup> | Difference<br>(%) |
| 0                        | 0.318                 | 0.34      | 0.95           | 100               | 6.2             | 100                         | 0.0289             | 0.03      | 0.955          | 100               |
| 12                       | 0.454                 | 0.67      | 0.96           | 143               | 7.7             | 124.2                       | 0.0375             | 0.08      | 0.985          | 129.7             |
| 25                       | 0.525                 | 0.34      | 0.96           | 165.2             | 8.9             | 143.5                       | 0.0477             | 0.03      | 0.965          | 165               |
| 50                       | 0.491                 | 0.39      | 0.95           | 154.4             | 7.4             | 119.6                       | 0.0414             | 0.05      | 0.956          | 143.2             |
| 75                       | 0.464                 | 0.26      | 0.96           | 146               | 7.8             | 125.8                       | 0.0402             | 0.03      | 0.962          | 139.1             |

**Table 37. Summary of initial rates for CBH/EGL + BGL on cellulose with varying microwave irradiation**  
\*yield determined by extrapolation of data from curve fitting to a suitable point of negligible rate change.

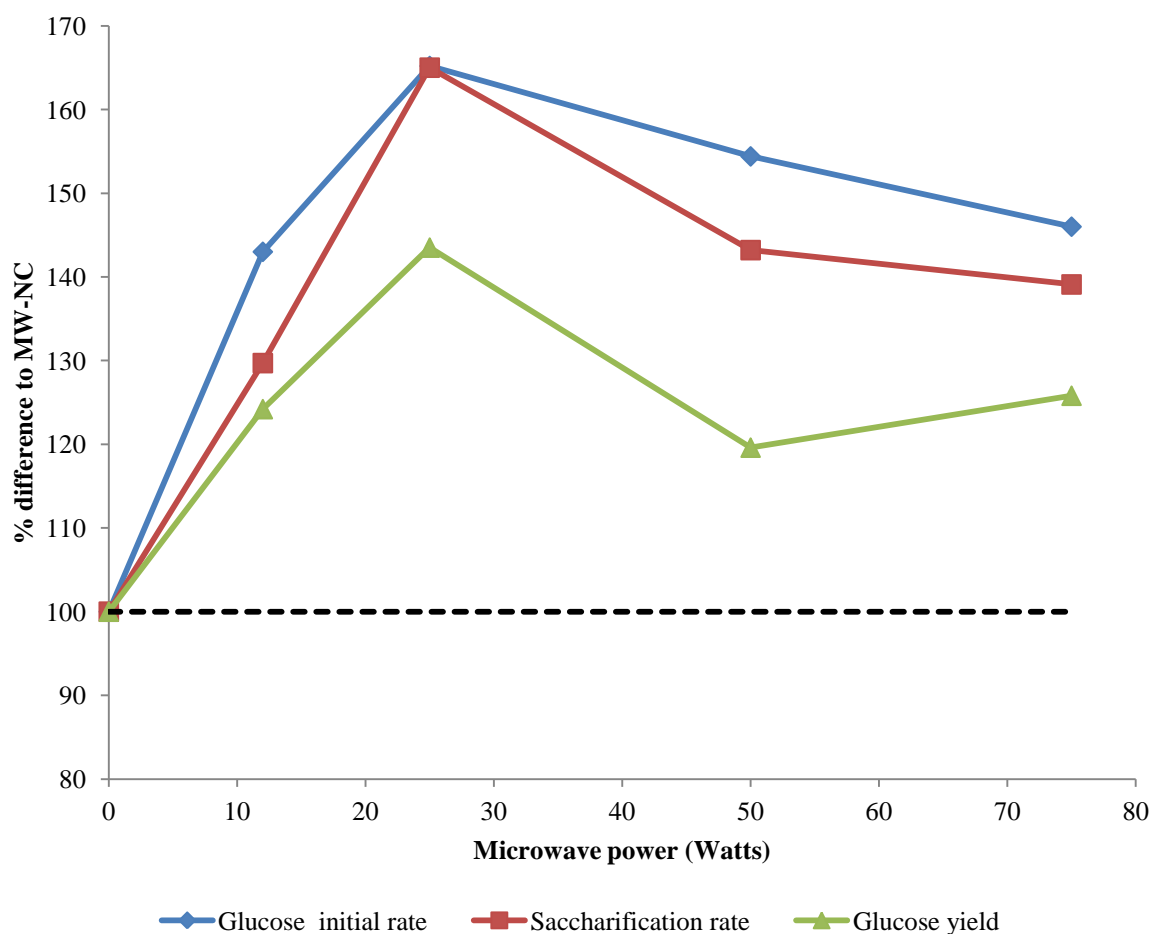


**Figure 101. Percentage difference in initial rates**

From the graphs presented, the percentage saccharification near matches glucose evolution as the majority of intermediates were converted either directly or indirectly to glucose. Both initial rates plots showed the greatest enhancement at 25W over the MW-NC. As the powers used in this study were a refined band of the previous study, variation between powers was much less. Even so, a noticeable increase was still observed above the MW-NC. The percentage saccharification rate in E.P. 2.2. was much lower than E.P. 2.1. due to increased action through the whole process.

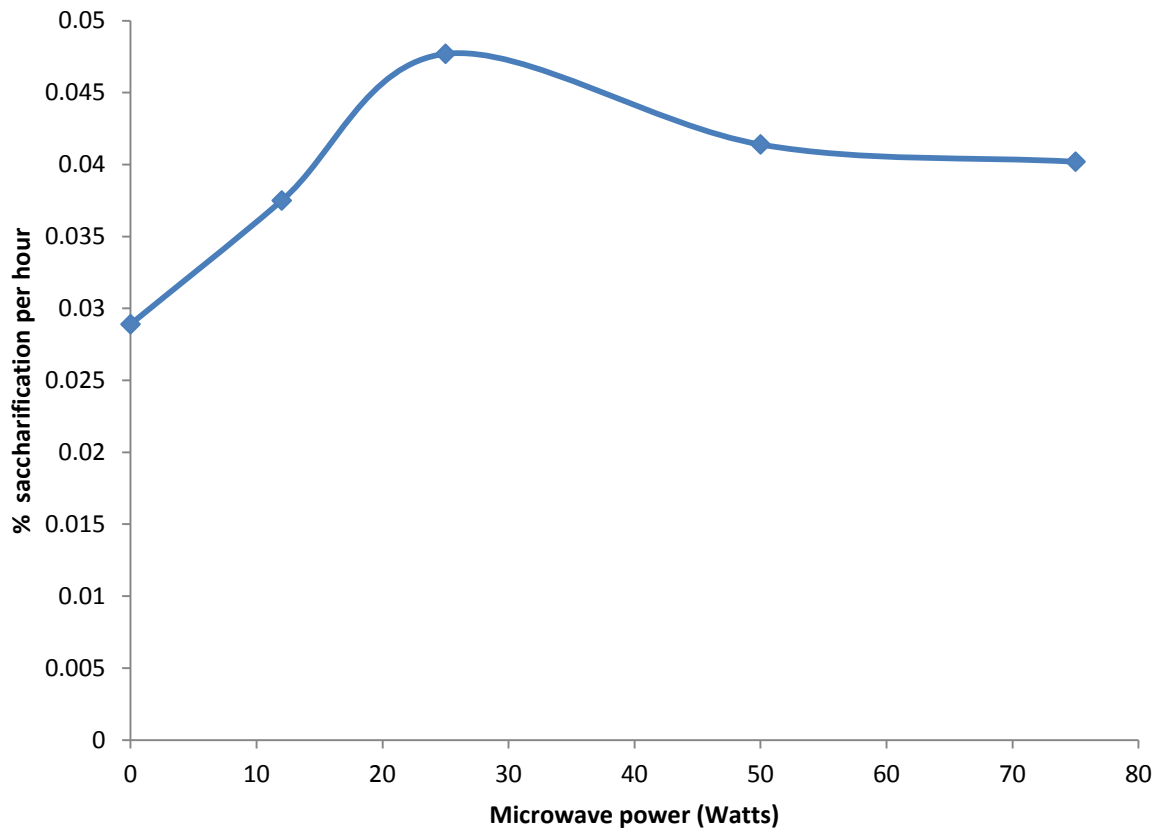


Figure 102. Percentage saccharification rate against microwave power

#### 4.2.2.1. Comparison of reference reactions (+BGL and –BGL) to 50W microwave irradiated (+BGL and –BGL)

**Summary;** Comparison of the reference reactions (+BGL and –BGL) were examined in the NC-MW section. Development into the microwave enhanced experiments looks at each +BGL and –BGL variant as separate entities. In this section, cross referencing the effect of BGL in the EGL/CBH +BGL system against EGL/CBH –BGL system at a common microwave irradiance point is examined. From the results obtained, 50W of microwave power increases the –BGL initial rate by 3.5 times compared to +BGL initial rate increase of 2.29 times.

From the data seen in the previous negative controls, the inclusion of BGL in the hydrolysis process increases the initial rate from 0.0336 to 0.0475 % saccharification per minute (1.4 times increase in rate). As the 50W power range was used in both +BGL and –BGL reactions, cross referencing initial rates from the experiments involving cellulose breakdown due to hydrolysis with EGL and CBH with BGL against analogous experiments without BGL at the same microwave exposure allows the examination of rates at comparable points.

From the graphs shown in Figure 103 for 50W microwave irradiation, the figures quoted for initial rate do not represent to whole catalysis profile. Whereas the hydrolysis in the absence of BGL shows a higher initial rate (1.848% saccharification/min) in comparison to with the presence of BGL (0.065% saccharification/min), by extending the time period (as seen in the left image of Figure 103), the % saccharification at times greater than approximately 6 hours favours the hydrolysis in the presence of BGL. As feedback cellobiose inhibition can cause limitation in hydrolysis, it is hypothesised that this is what is observed as the EGL/CBH –BGL catalysis reaches approximately 40% saccharification. With extrapolation of the curve seen in the +BGL reaction, it is suggested that total saccharification in this instance is likely to be greater than 60%. This is within the expected system’s feedback inhibition removal through the clearing of cellobiose to glucose. By cross referencing Figure 103, Table 19 can be drawn.

|               | Glucose ([P]/min) |       |               | Cellobiose ([P]/min) |      |               | Percentage saccharification (%/min) |       |               |
|---------------|-------------------|-------|---------------|----------------------|------|---------------|-------------------------------------|-------|---------------|
|               | -BGL              | +BGL  | As % of NC-MW | -BGL                 | +BGL | As % of NC-MW | -BGL                                | +BGL  | As % of NC-MW |
| NC-MW         | 0.131             | 0.318 | 142.7         | 0.066                | n/a  |               | 0.026                               | 0.027 | 93.1          |
| 50W           | 0.206             | 0.491 | 138.6         | 0.258                | n/a  |               | 0.080                               | 0.065 | 81.25         |
| As % of NC-MW | 157.3             | 154.0 |               | 390.9                | n/a  |               | 275.86                              | 240.7 |               |

**Table 38. Comparison of addition of BGL with and without microwave irradiation**

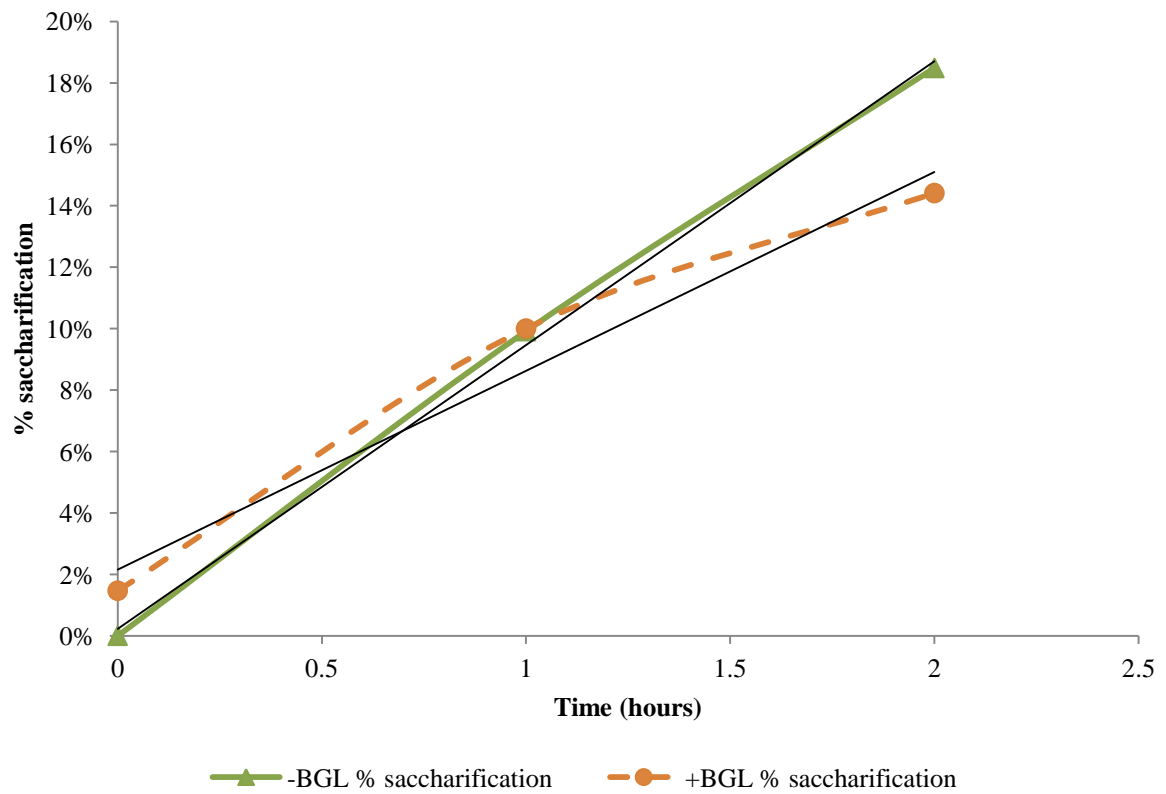
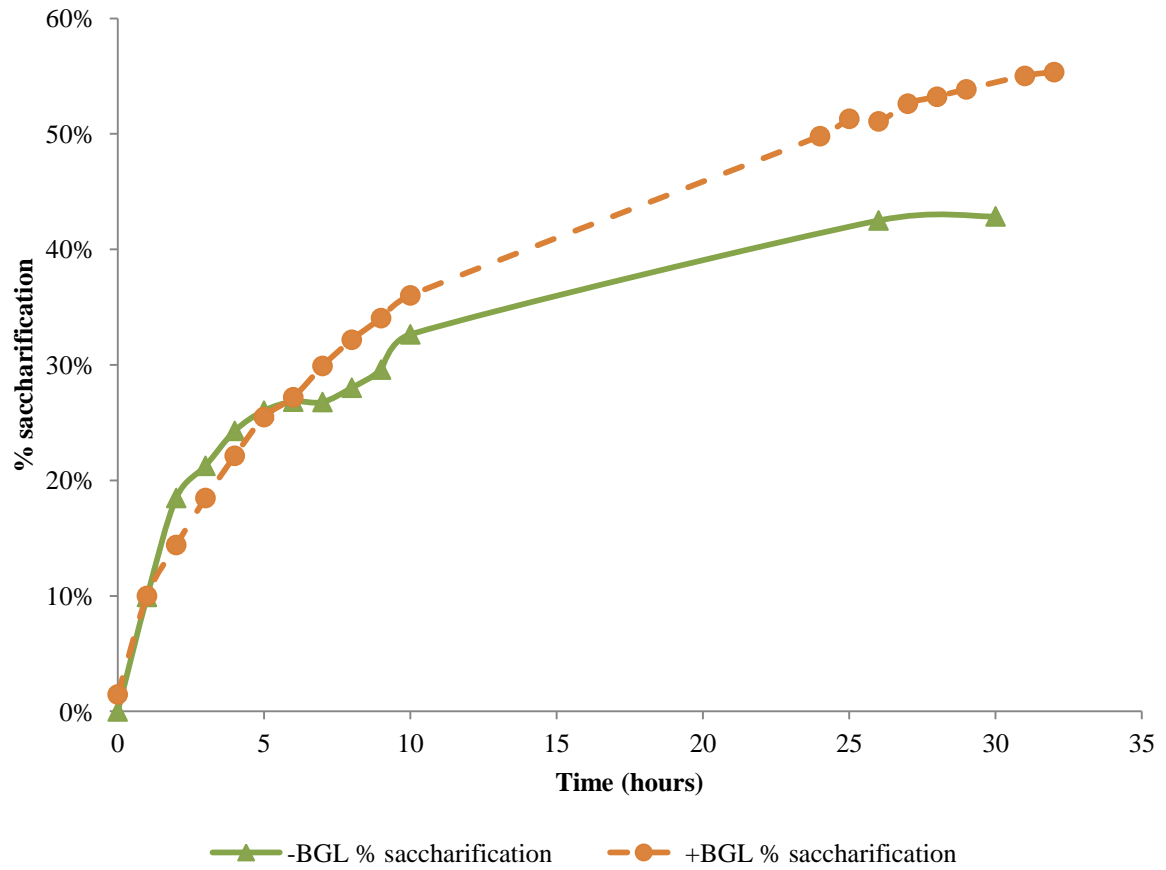


**Figure 103. 50W comparison of EGL/CBH -BGL and EGL/CBH +BGL**  
 Total hydrolysis and initial hydrolysis plots. Top: % saccharification evolution of the time course of >30hrs. Bottom; Initial rates determined by first 2 hours of hydrolysis.

### 4.2.3.0. EP. 2.3.0. – Cellobiose hydrolysis by BGL with varying microwave irradiation



- ***Irradiating 1 litre solution containing 10g/l cellobiose and 117CBU/g substrate BGL shows a non-linear increase in initial reaction rate at cross the 12-75W power band investigated.***

**Summary;** In the investigation of microwave influence on BGL, rate amplification is observed across the microwave power range of 12 – 75 Watts. The peak observed enhancement is 1.7 times greater than the reference negative control, with a mean enhancement of 1.5 times above the reference rate across the 12 – 75W power band.

For the comparison of microwave energy on BGL catalysis, the experiment was conducted according to the methods described in Chapter 3 (3.2.3.0. EP 2.3.0. – Cellobiose hydrolysis by BGL with microwave irradiation, page 132), with the sampling frequency increased due to the results seen in the negative control as described previously (4.2.0.4. NC-MW – BGL with cellobiose, page 156). The conversions observed where microwave power is the only variable are shown in Figure 79 and Figure 104

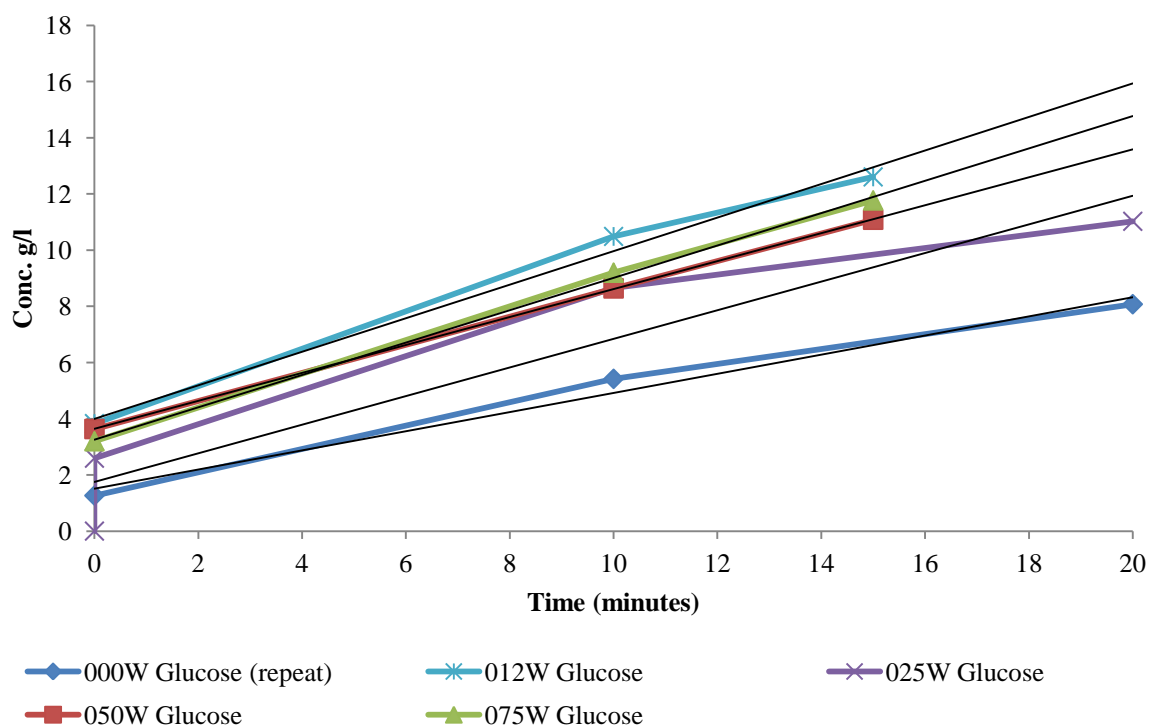


**Figure 104. Glucose evolution through the hydrolysis of cellobiose by BGL with variable microwave irradiation**  
 Conditions; 10g/l biomass (cellobiose), 50°C, 300rpm agitation, BGL loading of 168GBU/g cellobiose. Analysis through RI-HPLC with REZEX ROA as described previously. Data presented as grams per litre by breakdown constituent (glucose).

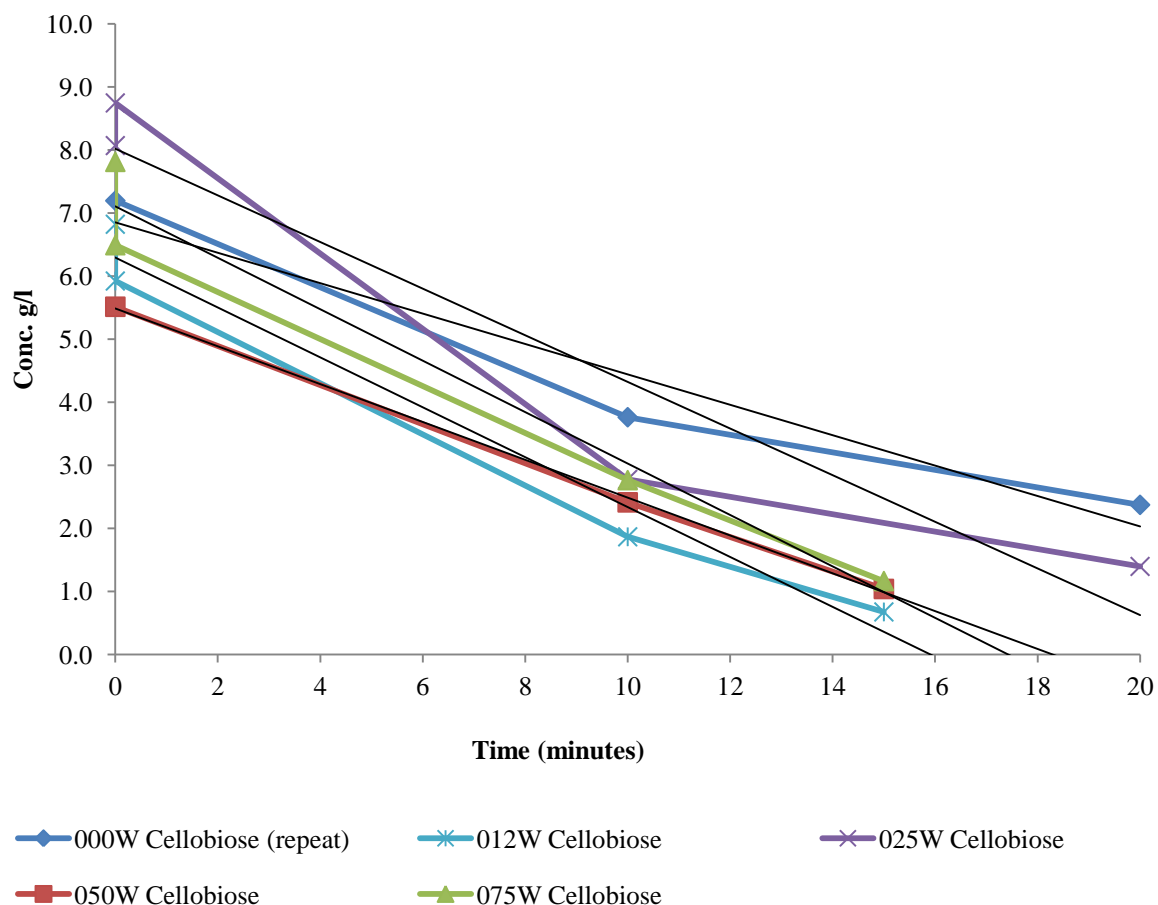


**Figure 105. Cellobiose degradation through the hydrolysis of cellobiose by BGL with variable microwave irradiation**  
 Conditions; 10g/l biomass (cellobiose), 50°C, 300rpm agitation, BGL loading of 168GBU/g cellobiose. Analysis through RI-HPLC with REZEX ROA as described previously. Data presented as grams per litre by breakdown constituent (cellobiose).

| Microwave power<br>Watts | Glucose               |                    |                |                   | Cellobiose            |                    |                |                   |
|--------------------------|-----------------------|--------------------|----------------|-------------------|-----------------------|--------------------|----------------|-------------------|
|                          | Gradient<br>(dP/d[T]) | Intercept<br>(g/l) | R <sup>2</sup> | Difference<br>(%) | Gradient<br>(dP/d[T]) | Intercept<br>(g/l) | R <sup>2</sup> | Difference<br>(%) |
| 0                        | 0.341                 | 1.51               | 0.984          | 100               | -0.241                | 6.85               | 0.944          |                   |
| 12                       | 0.597                 | 4.00               | 0.990          | 173.1             | -0.396                | 6.29               | 0.973          | 164.3             |
| 25                       | 0.509                 | 1.75               | 0.900          | 149.3             | -0.342                | 6.53               | 0.481          | 141.9             |
| 50                       | 0.497                 | 3.64               | 1.000          | 145.8             | -0.300                | 5.48               | 0.999          | 124.5             |
| 75                       | 0.576                 | 3.26               | 0.999          | 168.9             | -0.408                | 7.11               | 0.966          | 169.3             |

**Table 39. Summary of initial rates for BGL on cellobiose with varying microwave irradiation**

The data produced has shown the excessive rate of catalysis seen in the reaction of BGL and cellobiose. Where the rate has been determined, the data can only be used as a representative of the reaction system, rather than a refined study of irradiative influence. Slowing the reaction through the reduction of BGL addition to allow greater sample resolution and accuracy would greatly improve the quality of the data presented. However, by looking at loading variation, the correlation between the isolated BGL-cellobiose system and the total CBH/EGL/BGL-cellulose system would be lost.

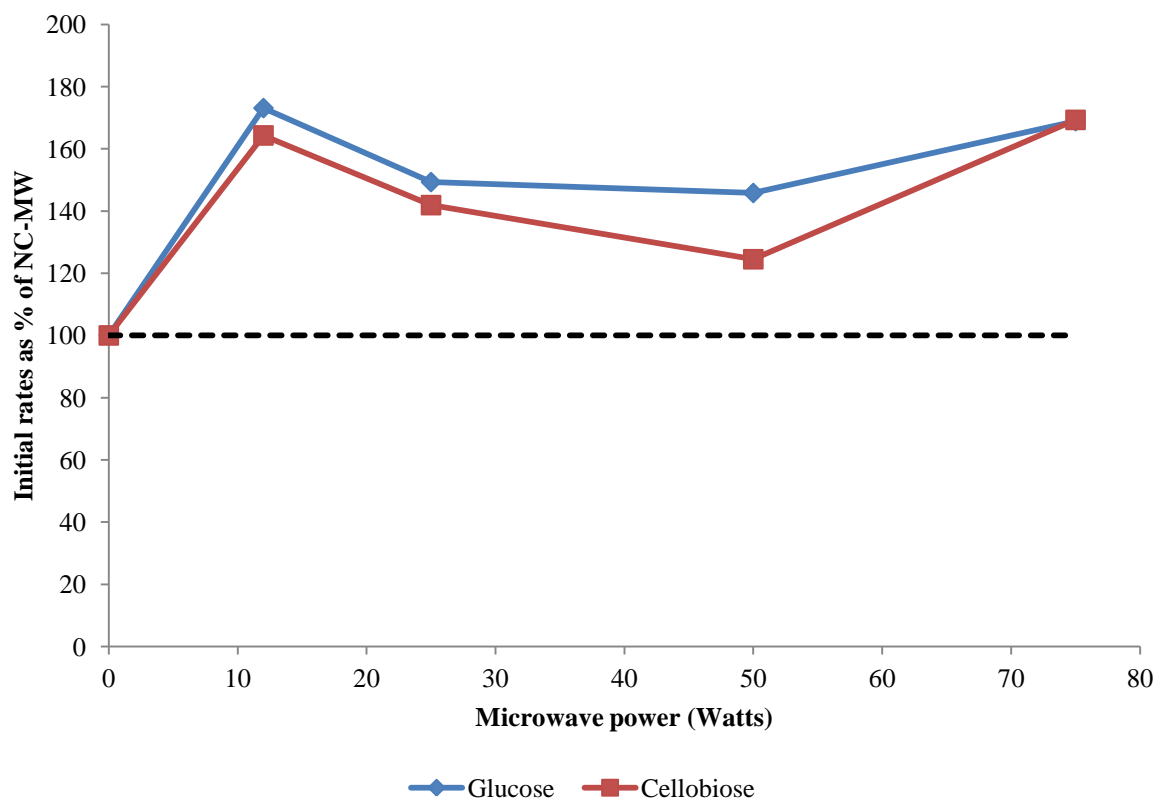


Figure 106. Percentage difference in initial rates

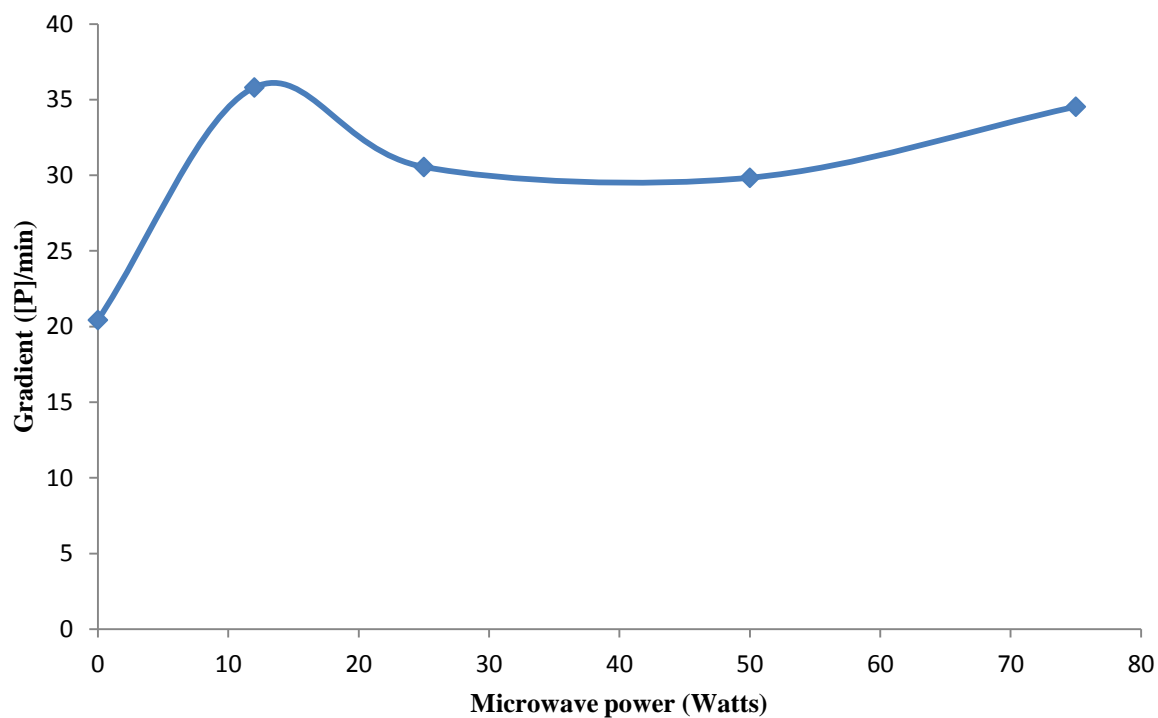


Figure 107. Glucose evolution rate against microwave power

Figure shows the power curve in cellobiose to glucose conversion based on initial reaction rates. Error bars defined using standard error function.

From the graph produced in Figure 107 it is apparent that the influence of the microwave irradiation on the enzyme is non-proportional and non-linear in nature, therefore a term of  $[P].\text{min}^{-1}.\text{W}^{-1}$  cannot be defined. As such, it can be noted that under microwave influence, the rate of product formation per minute ( $[P].\text{min}^{-1}$ ) is elevated across the power band of 12-75W (mean average of 1.5 times above reference data) with the greatest increase seen at 12W (1.7 times greater than the reference).

In the initial experiment, the reference initial rate of catalysis is  $20\text{g}.\text{min}^{-1}.\text{Watt}^{-1}$  compared to  $32\text{g}.\text{min}^{-1}.\text{Watt}^{-1}$  for the mean average of the power range 12-75W. With a standard deviation of  $2.9\text{g}.\text{min}^{-1}.\text{Watt}^{-1}$  with irradiated rates, the degree of confidence limit is defined as  $2.8\text{g}.\text{min}^{-1}.\text{Watt}^{-1}$  indicating that the likelihood of this pattern occurring through random sampling being less than 0.5% chance. This confirms that the increase in initial rate observed is from microwave irradiation and not from chance.

From the shape of the graph in Figure 107 there is the suggestion that the microwave effect maybe in an “all or nothing” action in the powers studied. With the 12W value being significantly greater than that for the reference reaction, it is highly likely that there will be a response curve between 0 and 12W.

#### 4.3.0.0. EP 3 – Fermentation of *Saccharomyces cerevisiae* as a model eukaryotic system



*Saccharomyces cerevisiae* (brewer's yeast) fermentations were undertaken using the methods previously described in "3.3.0.0. EP. 3.0 - Fermentation," pages 133. Each fermentation was data logged according to the described method and regular samples were taken for HPLC analysis.

##### *Negative control (thermal conditions) and data analysis*

##### *Relating optical density to cell density*

Optical density was recorded at each fermentation sampling point, with recordings made at 600nm. Following the first few hours of fermentation, the analysis was further enhanced by the recording of a 50% and 75% dilution as well as the 0% dilution to ensure OD readings were maintained within the range of the spectrophotometer.

For calibration, a standard fermentation without microwave influence was conducted, with cell counting being recorded simultaneously to optical density. Cell counts were taken with the 0% dilution and 50% dilution to ensure recording within a suitable reading frame. The results for the relating of OD to cell density are shown in Figure 109 while an example microscope image is shown in Figure 108.

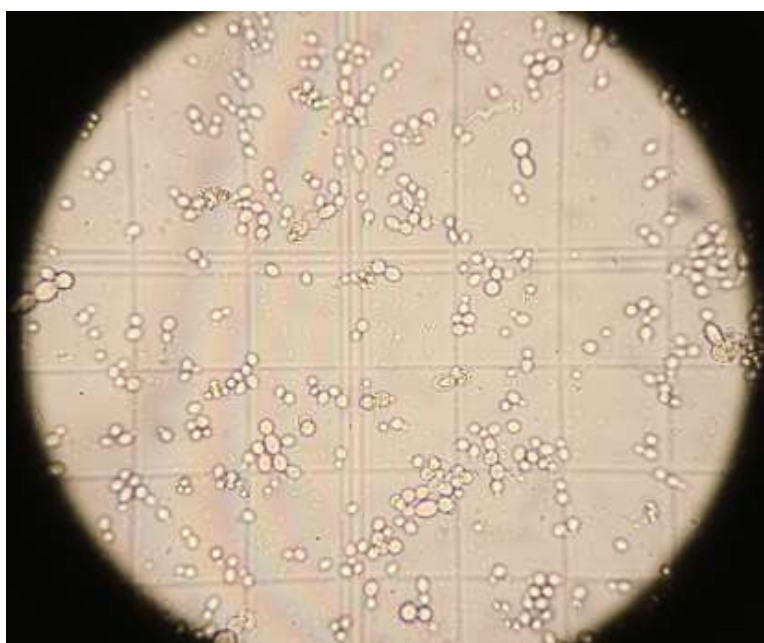


Figure 108. Light microscope determination of cell density

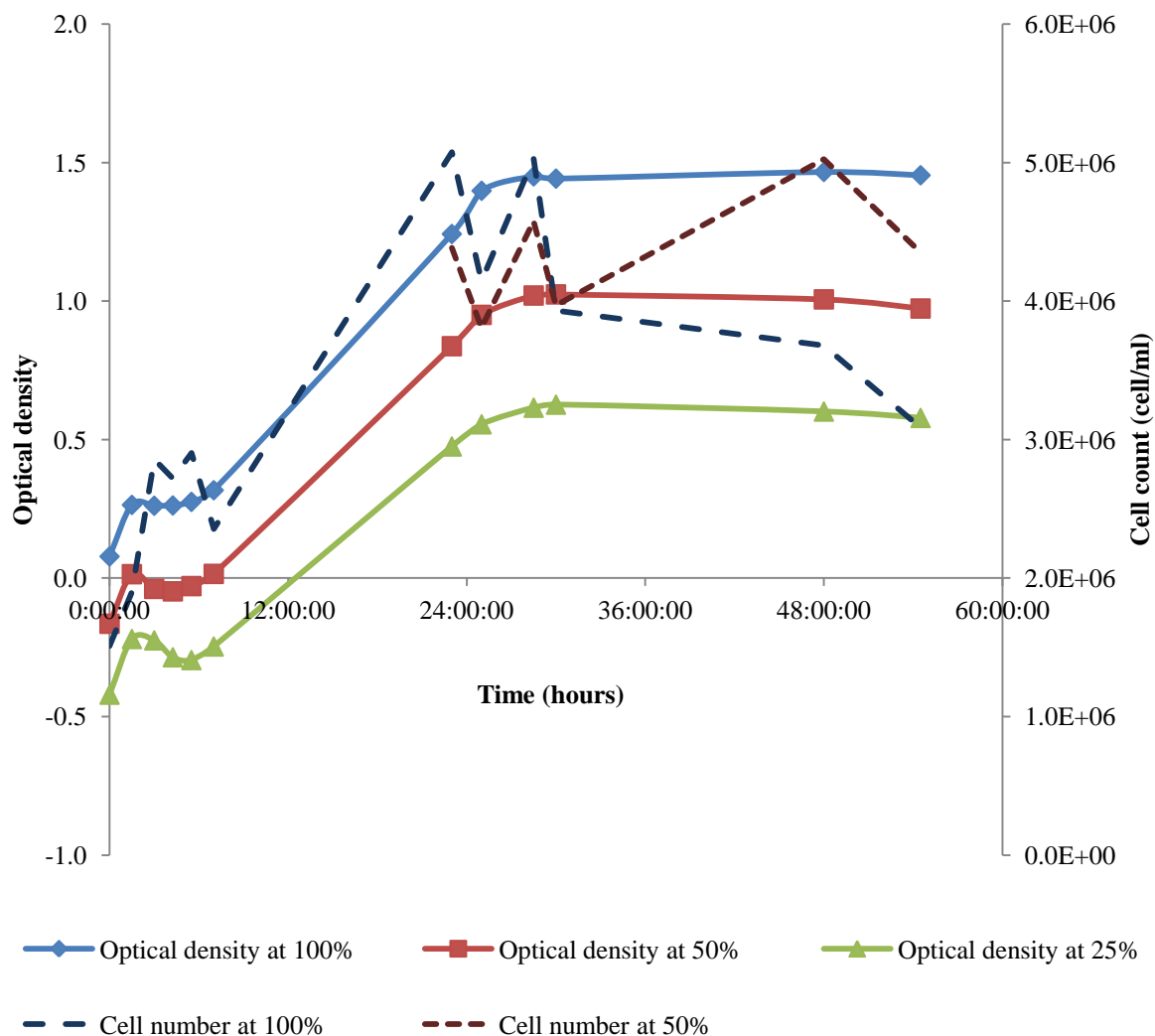


Figure 109. Relating optical density to cell density

### *Fermentation profiling*

Fermentation profiling was done through the use of the Broadley James Technologies Ltd biocontroller interfaced through the eLogger software (complete methods are described in Chapter 3 - Fermentation profiling, page 135). Figure 110 illustrates a difficulty observed in determining fermentation progress. In comparison to aerobic fermentation where continuous gas flow through the system allows for empirical determination of oxygen uptake and carbon dioxide evolution, anaerobic fermentation has an inherent limitation in mass flow. With the equipment used, the determination of mass flow with known concentration was not feasible. For development, a theoretical system has been devised although not deployed due to the time constraint for development and verification.

With the limitation noted, fermentation profiling by OD/cell density correlated to glucose uptake and EtOH evolution has greater empirical justification.

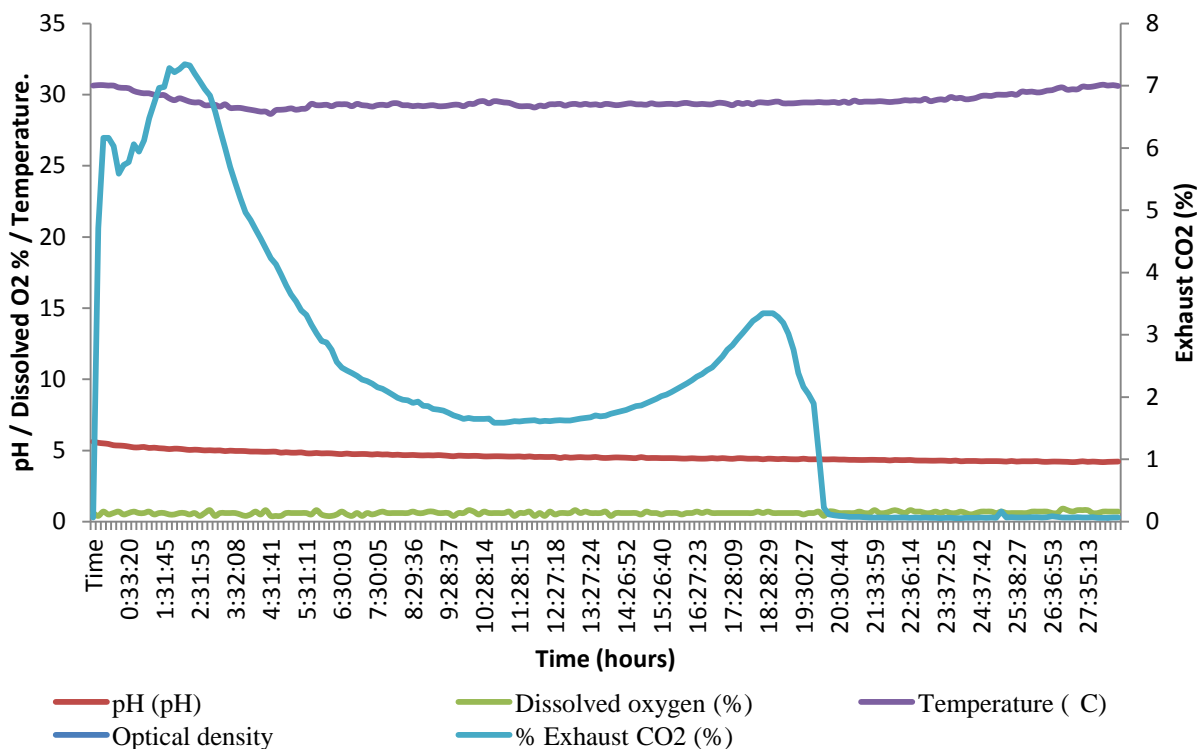


Figure 110. Fermentation profiling by pH, gas exchange and temperature

### HPLC analysis of fermentation products

For the determination of glucose uptake and ethanol evolution, methods described previously were used (see pages “HPLC analysis of fermentation products” (page 136); “Standard curves for determination of fermentation products,”(page 136); “Data processing,”( page 136)).

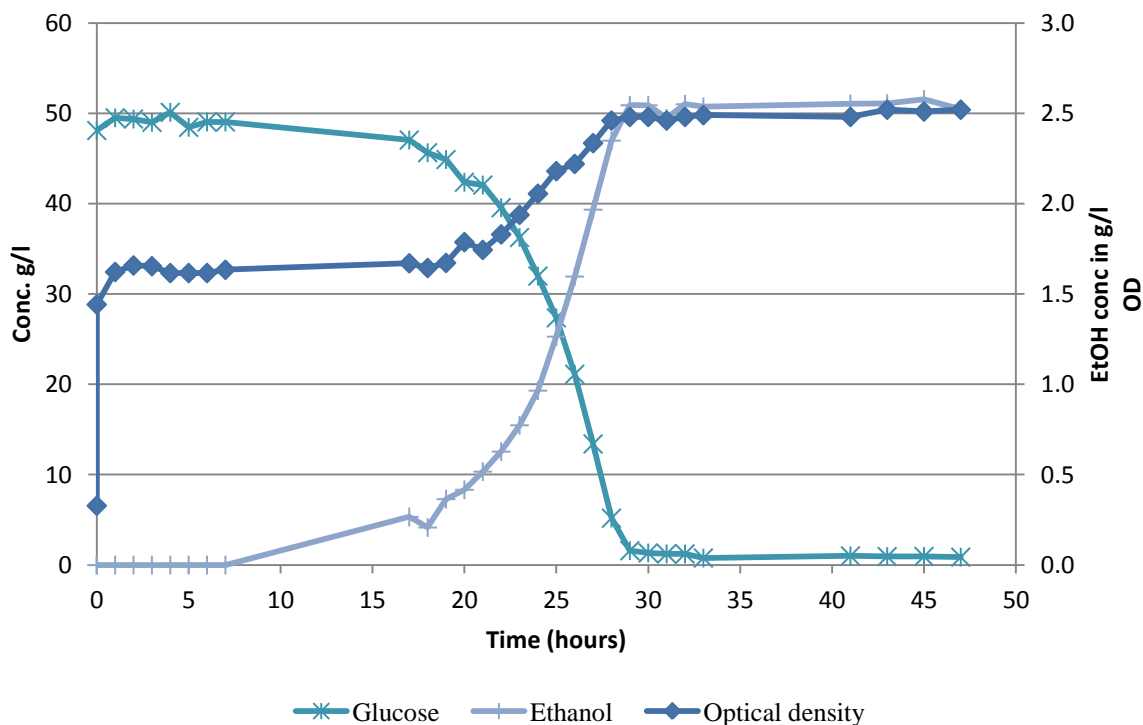
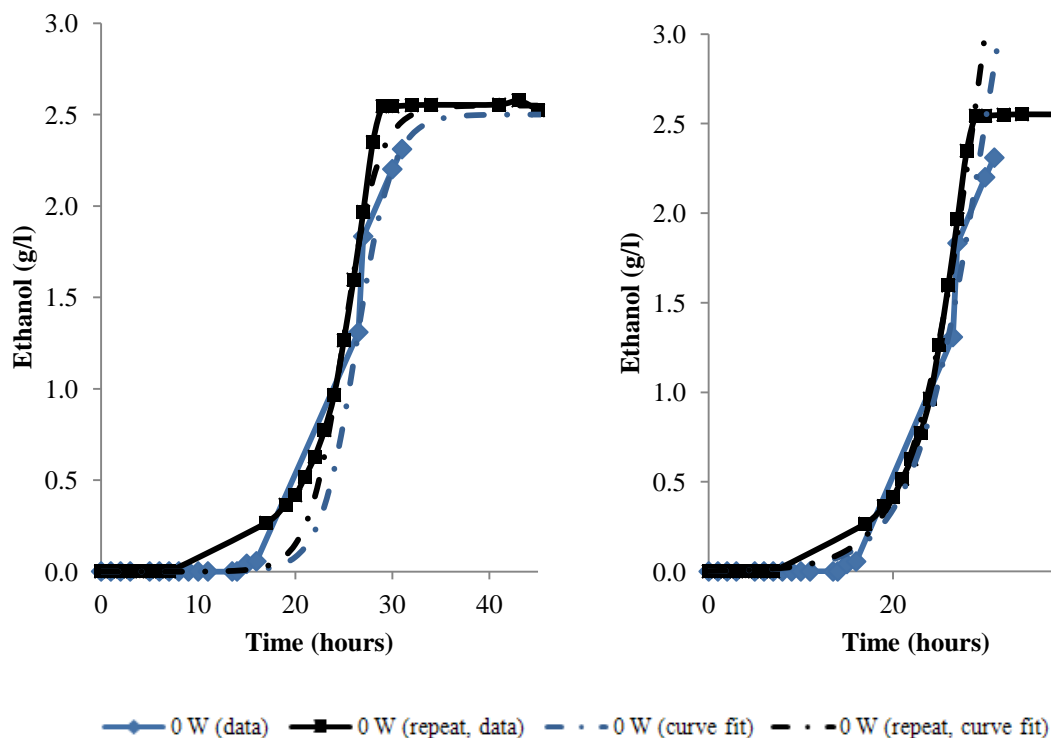


Figure 111. Fermentation negative control. Profile by glucose, ethanol and optical density

The profile produced through thermal control of the media temperature was used as the base line by which varying microwave irradiative powers could be compared. Figure 111 shows the raw data plot produced prior to curve fit analysis. Key fermentation features are the lag phase (0 - ~9hrs); exponential growth phase (~9 - 30hrs); and carbon exhaustion (~29-30 hrs).

As the carbon source is seen to be completely consumed and the corresponding stop in product and biomass production, the fermentations conducted are defined by carbon limitation. In further investigation with varying irradiation, each parameter of glucose uptake, ethanol evolution and biomass increase are considered individually.

For evaluation of repeatability, the comparison of the negative control by ethanol production is compared (see Figure 112). Of note is the result frequency, particularly in the 15 to 30 hour time frame. In the original data set, the 15 - 30 hour time frame coincided with the time period away from the laboratory. Modification of the inoculation time to a later start point, allows the 16<sup>th</sup> hour to be delayed to a suitable time point at the start of the working day. This has allowed greater result resolution through the exponential phase for curve fitting.



**Figure 112. Comparison on ethanol production with no irradiation in repeat data sets and fit modelling**  
Fit modelling using two curve fit models. Left; Assumed sigmoid curve. Right; Growth limited curve.

In Figure 112 two data analysis methods are used for curve fitting. In the upper plot, the curve fit is assuming that the data fits a sigmoid trend, where ethanol production is exponential in the first phase, linear in the middle phase and inverse exponential as the rate retards. In reality, the data shows a sudden stop in ethanol production due to carbon exhaustion. As such, the slowing of the rate is not

observed. To cater for this discrepancy, the lower plot in Figure 112 is produced where the curve fitting is based on curve matching of the fit line to the actual data, regardless of upper limit.

For comparison, the gradient of the exponential phase is used for determination of production rate. In comparing the two curve fit models, Table 40 is produced.

|                    | <b>Curve fit model 1</b> | <b>Curve fit model 2.</b> |
|--------------------|--------------------------|---------------------------|
| <b>0W</b>          | 0.32                     | 0.32                      |
| <b>0W (repeat)</b> | 0.24                     | 0.24                      |

**Table 40. Comparison of gradients in two curve fit models**

With no observed difference in gradient by fit model, the established model previously described (“3.3.0.0. EP. 3.0 - Fermentation - Data processing,” page 136) was used in the processing of all subsequent data set – including glucose uptake.

#### **4.3.1.0 EP 3.1. – Investigation of variable microwave power on the growth of *Saccharomyces cerevisiae***

- **Irradiation of *S. cerevisiae* in the power range has little observable effect in the power range of 0 to 50 Watts**
- **Alteration in rate observed are subtle and not conclusive of enhancement, but show that cells maintain viability**

Experimental data shows that through the irradiation of the *Saccharomyces* fermentation in microwave field strengths of 0 – 50 Watts has little effect on either growth rate or metabolic turnover as values of show little appreciable difference to the negative control.

##### ***Biomass by optical density.***

From the biomass determination, variability in the record results is shown in Figure 113. For analysis, curve fitting was undertaken to provided data points for rate determination.

With the initial negative control deemed unsatisfactory due to too short an exposure period, it was repeated. In the processes, the original spectrophotometer used became unavailable due to mechanical malfunction. As such, a second spectrophotometer was used but incapable of being calibrated to the original. As such, the data appears with a different response curve. Based on relative OD shift, the use of a second spectrophotometer is not observed as a variable or constraint (see Figure 113).

From the raw data produced, determination of rate is difficult due to sample resolution. To determine an empirical value for growth rate comparison, curve fitting was employed, as seen in Figure 113 (for methods, see “Data processing,” page 136). For highlighting the pseudo-linear phase of the exponential growth phase, curve fit data was limited and Figure 114 produced. Using this limited data range, the data was interoperated through the use of Excel LINEST function for gradient, intercept and fit coefficient determination. This is summarised in Table 41.

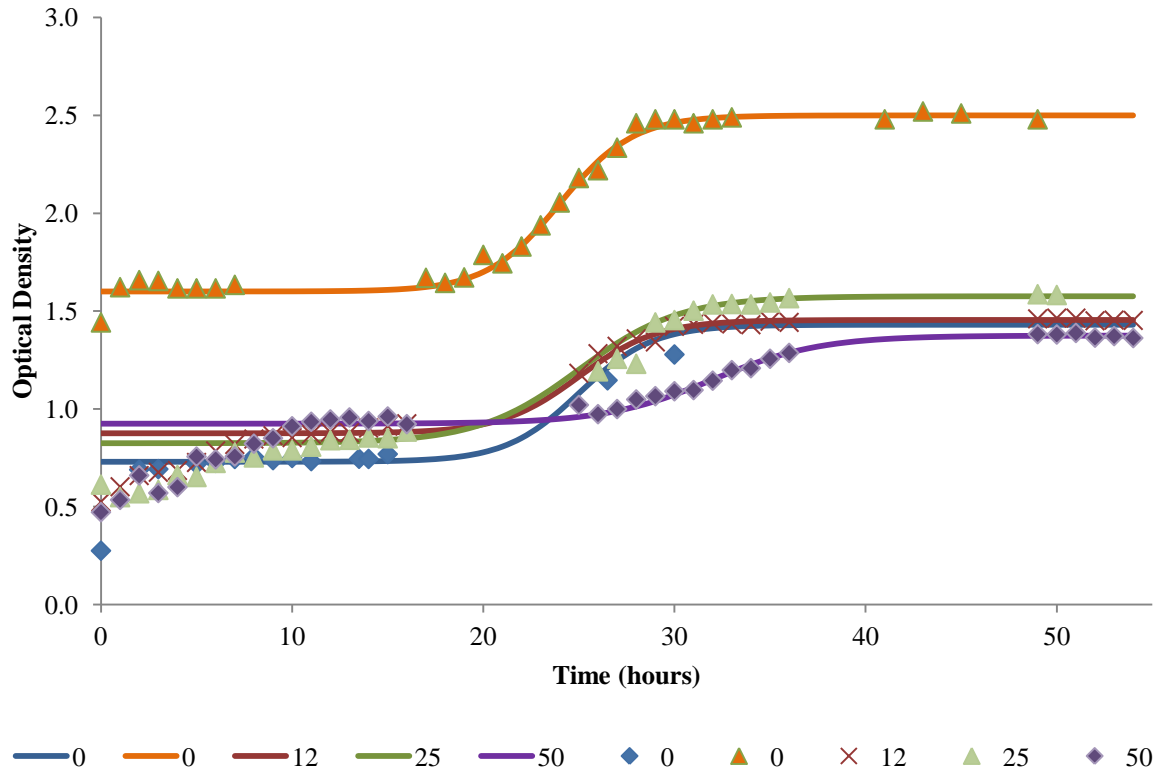


**Figure 113. Optical density under varying microwave power against time**  
 Time plot of optical density (biomass) against time. Coloured markers represent data entries. Continuous lines drawn through curve fitting to show trends. Curve equation used; equation  $y = (a/(1+e^{-(x-c)/b})) + d$  where a = data range; b = midpoint; c = curve factor; d = off set; e = curve form x = experiment time; and y = cell density.

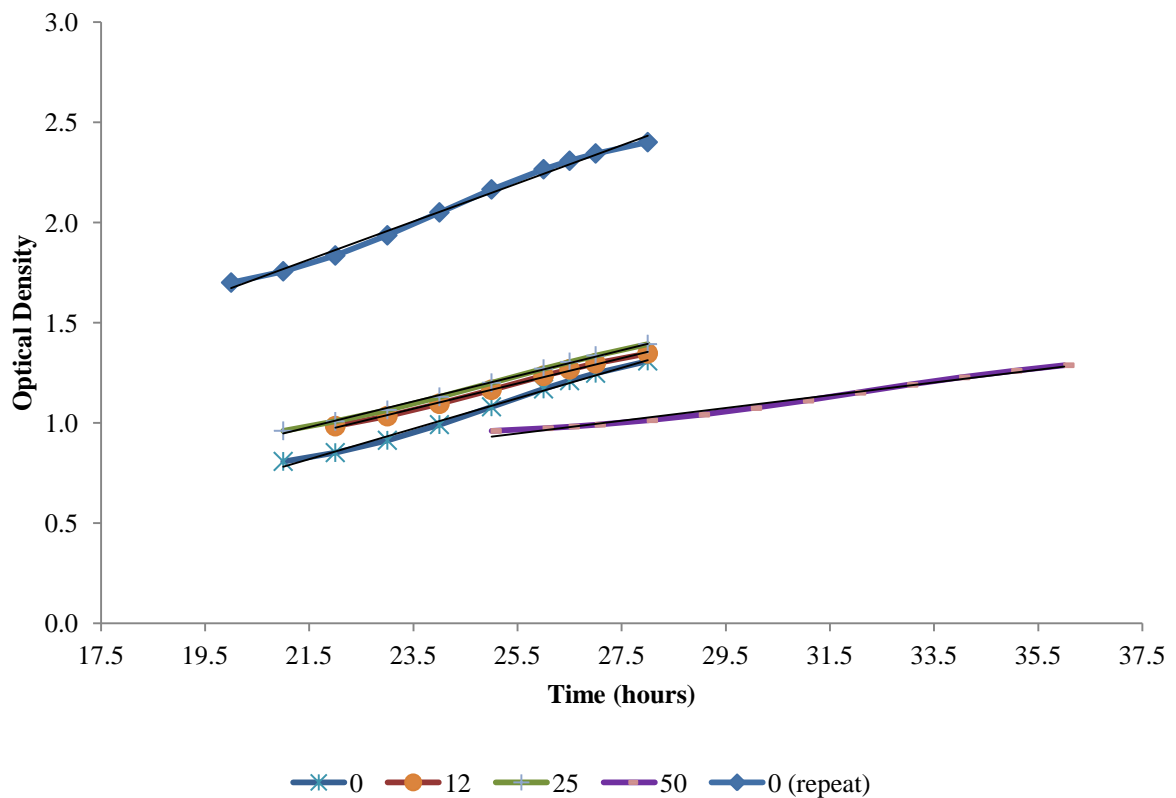


**Figure 114. Change in optical density during exponential growth.**  
 Data points plotted are derived points from curve fitting experimental data.

| Microwave power |  | Optical density (exponential phase) |           |                |                |
|-----------------|--|-------------------------------------|-----------|----------------|----------------|
| Watts           |  | Gradient (OD/hr)                    | Intercept | R <sup>2</sup> | Difference (%) |
| 0               |  | 0.095                               | -0.228    | 0.993          |                |
| 0 (repeat)      |  | 0.076                               | -0.816    | 0.998          | 100            |
| 12              |  | 0.063                               | -0.410    | 0.997          | 82.89          |
| 25              |  | 0.064                               | -0.397    | 0.998          | 84.21          |
| 50              |  | 0.032                               | 0.1389    | 0.987          | 42.11          |

**Table 41. Summary of exponential growth phase by optical density**  
Empirical determination of microbial growth rate.

Using the data summarised in Table 41, Figure 115 is used to visualise the effect of microwave power on optical density.

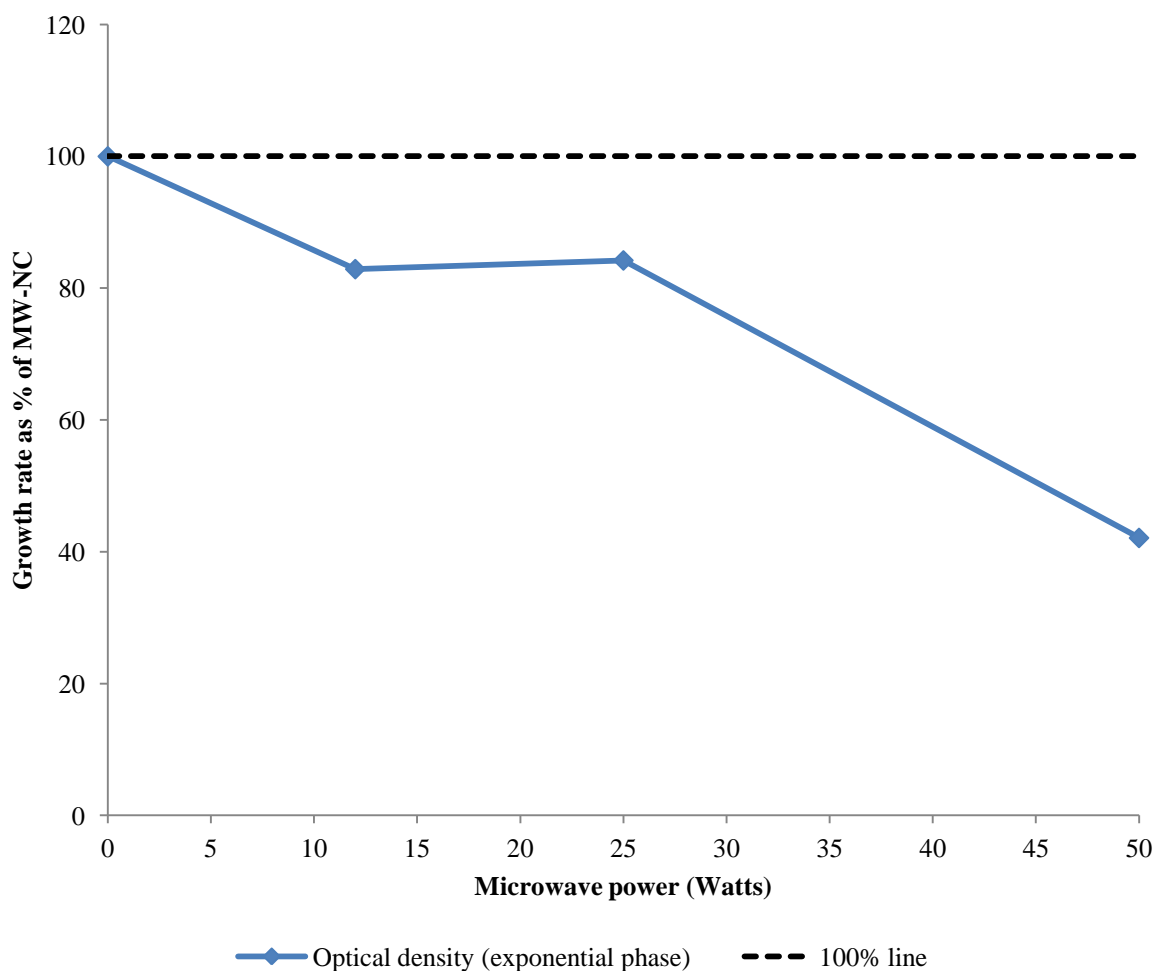


**Figure 115. Percentage difference to thermal negative control**

The conclusion drawn from the study of optical density is that the application of microwave power has an effect of retarding the rate at 12W (82% of MW-NC) and 24W (84% of MW-NC) microwave power.

## Substrate utilisation

Substrate uptake can be used to determine fermentation processing. As the limitation highlighted in “Fermentation profiling” (page 190) prevents the accounting of carbon balancing by product formation, glucose uptake can only be used for determination of metabolism. Initial raw data is shown in Figure 116. Glucose rate determination by curve fitting was conducted as described in “Data processing” on page 136 and shown in Figure 117. Variation in initial glucose concentrations is an artefact of the autoclave process with variation attributed to caramelisation.

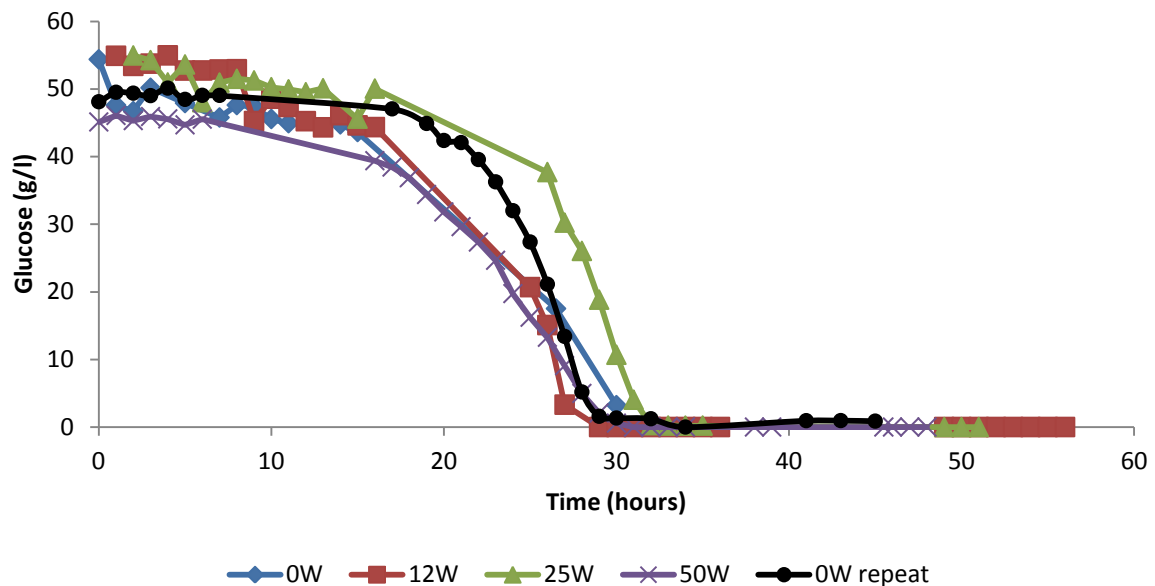


**Figure 116. Data plot of glucose uptake with varying microwave irradiation**

Top; Raw data plotting by HPLC analysis of glucose metabolism

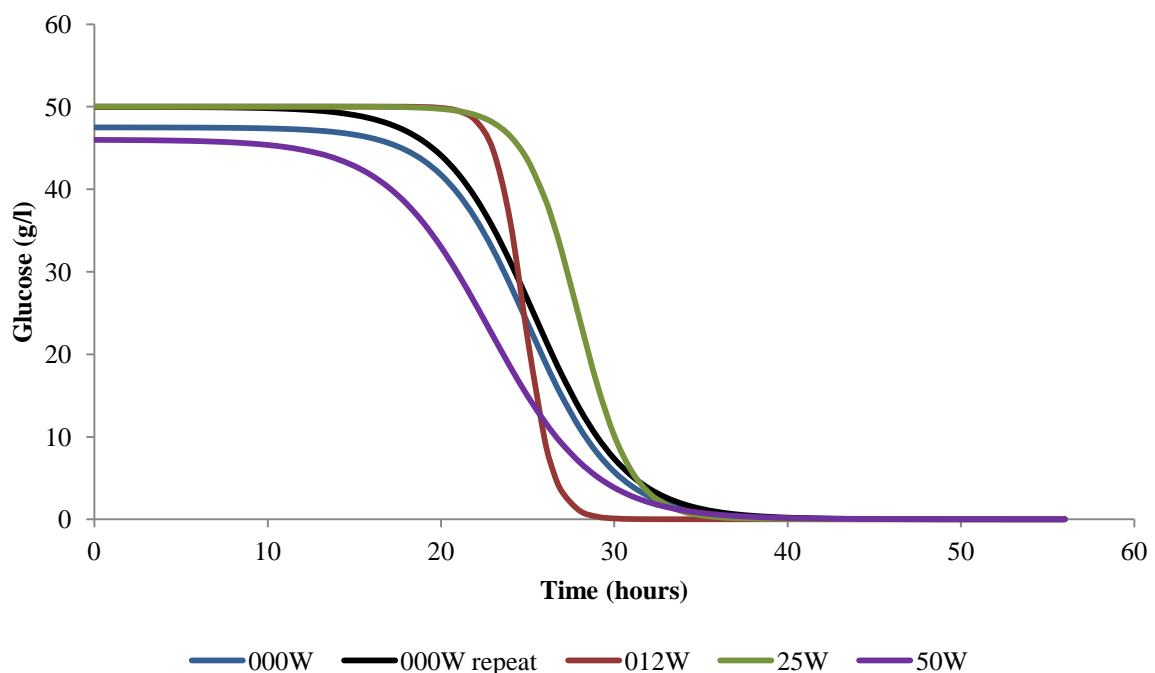


**Figure 117. Glucose uptake - curve fit**

Data interpolation using the equation  $y = \frac{a}{1+e^{-(x-c)/b}} + d$  where a = data range; b = midpoint; c = curve factor; d = off set; e = curve form x = experiment time; and y = glucose concentration.

For highlighting the pseudo-linear phase of the glucose uptake curve that corresponds to the exponential growth phase, curve fit data was limited and shown in Figure 118. Using this limited data range, the data was interpreted through the use of Excel LINEST function for gradient, intercept and fit coefficient determination. This is summarised in Table 42 and shown in Figure 118.

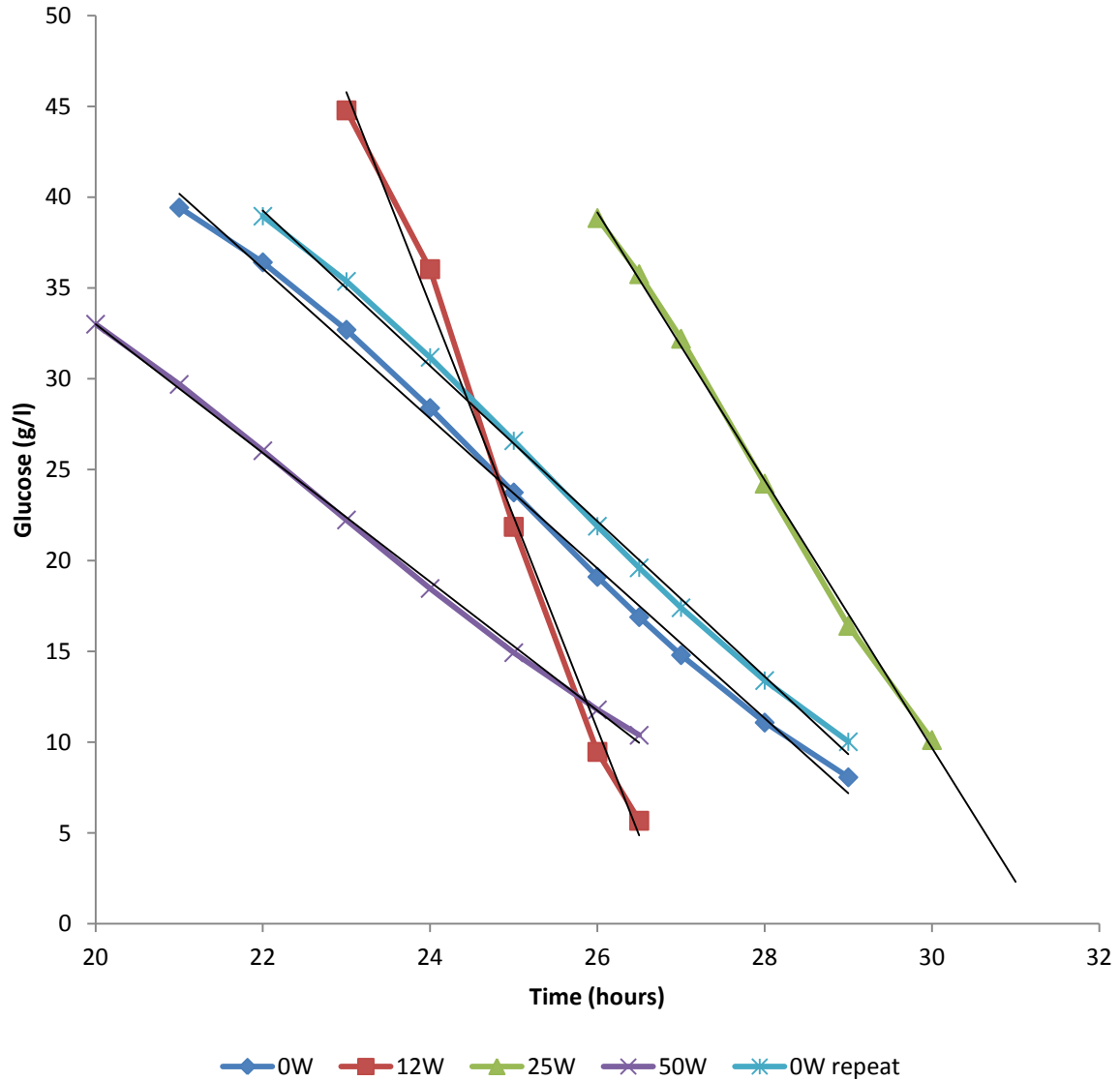
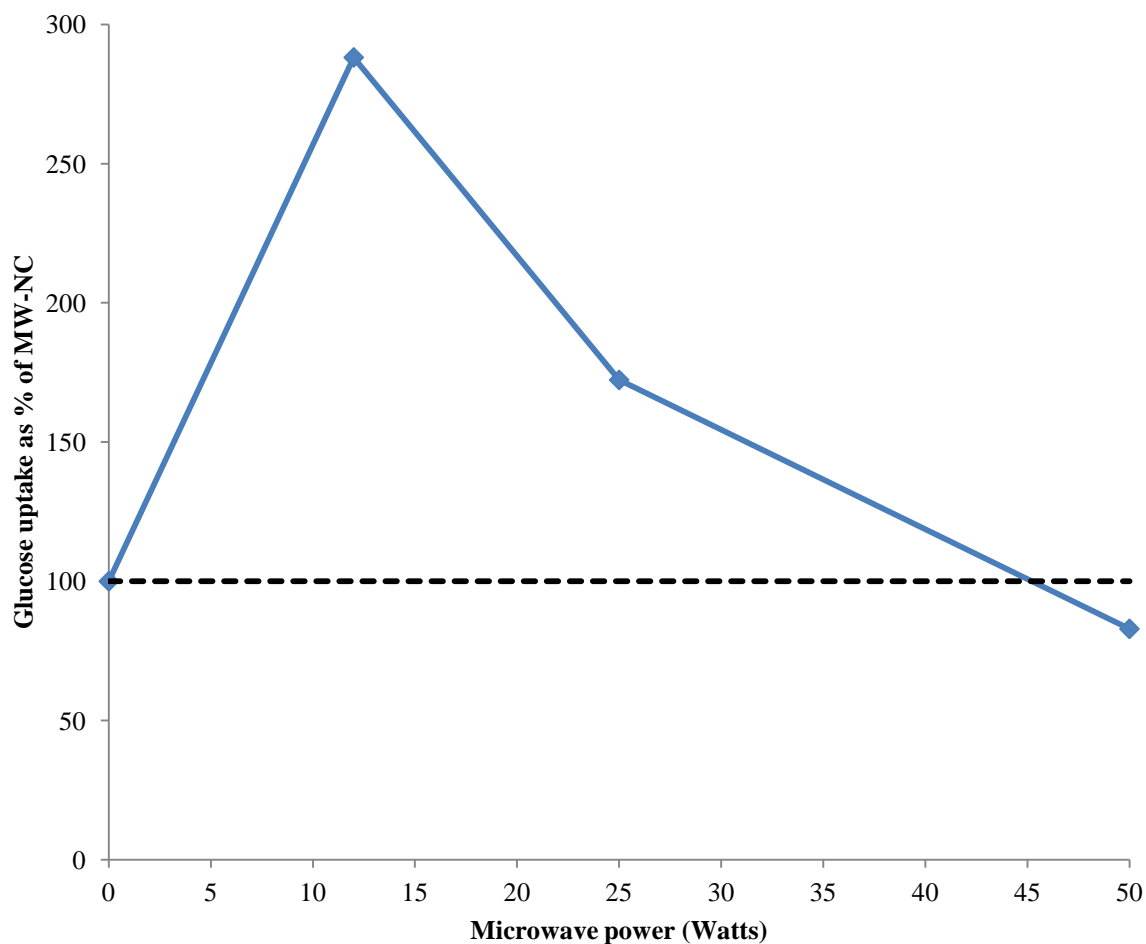


Figure 118. Glucose uptake rate - gradient determination

| Microwave power |                   | Glucose uptake rate (exponential phase) |            |  |
|-----------------|-------------------|---|------------|--|
| Watts           | Gradient (g/l/hr) | R <sup>2</sup>                          | Difference |  |
| 0               | -4.12             | 0.998                                   |            |  |
| 0               | -4.28             | 0.998                                   | 100.00     |  |
| 12              | -12.33            | 0.992                                   | 288.14     |  |
| 25              | -7.37             | 0.999                                   | 172.30     |  |
| 50              | -3.55             | 0.999                                   | 82.92      |  |

Table 42. Summary of glucose uptake rates where biomass growth is exponential



**Figure 119. Percentage difference to thermal negative control**

The analysis constructed in Table 42 is used for plotting Figure 119 to illustrate the relationship between microwave power and glucose uptake. The microwave negative control (0W) is used as the base line against which the irradiative effect can be observed.

From the data produced, it is observed that the glucose uptake at 12W is 2.8 times the uptake rate of the negative control. With increased power, the trend diminishes with an uptake rate below the negative control (82% at 50W).

## Ethanol formation

Ethanol is the endpoint product in the research study, therefore product formation is of greatest importance. In parallel to the previous results presented, ethanol formation is analysed by HPLC and plotted in Figure 120. Of note is the end point in each plot. Each fermentation is carbon limited therefore the fermentation ends according to glucose exhaustion with product threshold at around 2.5g/l ethanol with the exception of 50W irradiation. The production of 11g/l ethanol at 50W irradiation can either be described as a erroneous result or an actual shift in metabolism only seen at powers greater than 25W. Due to time restriction, the opportunity to investigate further has not been available. As such, the conclusion drawn is that with microwave irradiation up to 50W power, the growth of a viable culture is observed.

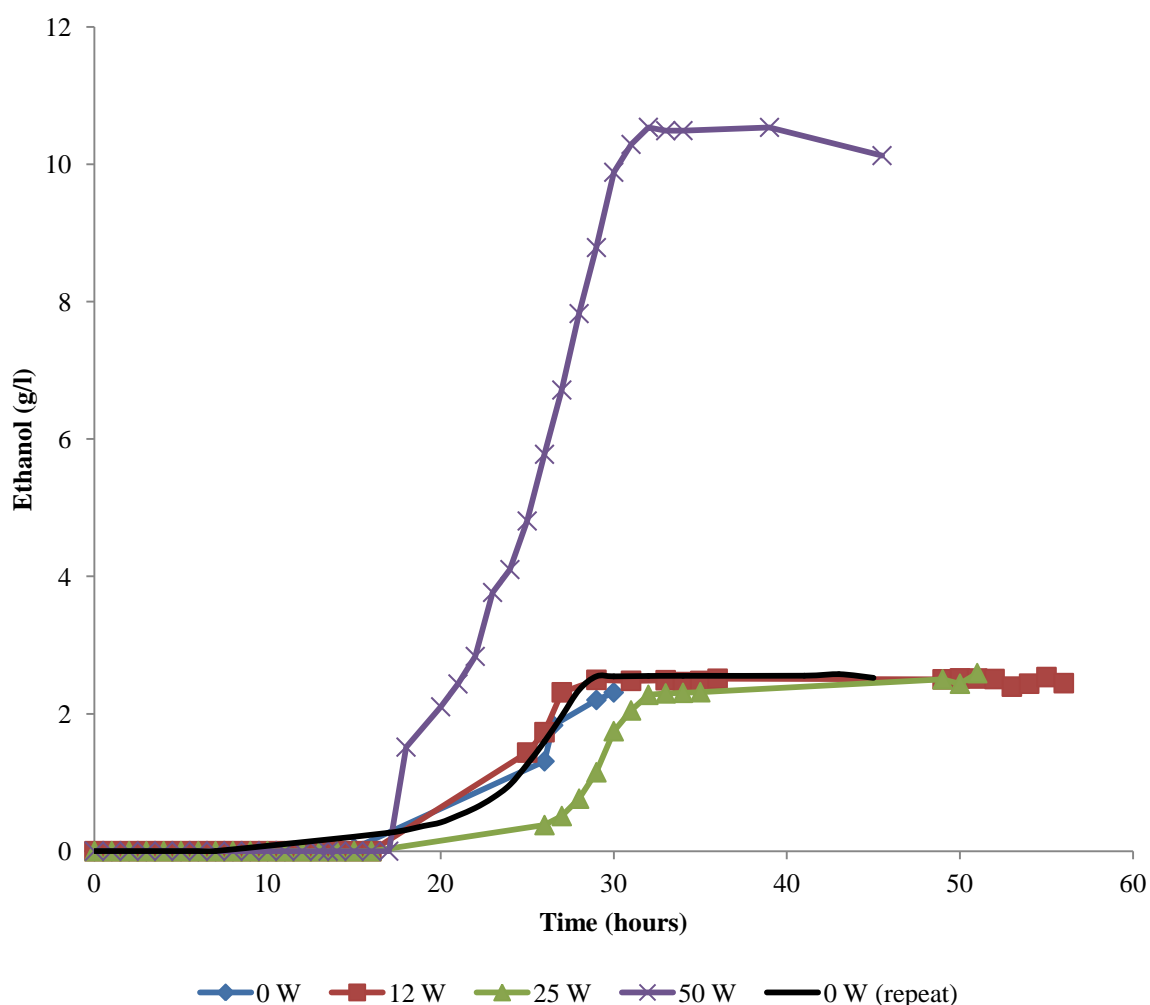


Figure 120. Ethanol formation under varying microwave powers (raw data)

From the data compiled and the graph produced in Figure 120, curve fitting is conducted to produce Figure 121. As previously described, the linear gradient of the ethanol evolution curve is used for determination of rate comparison by microwave powers. This is shown in Figure 122.

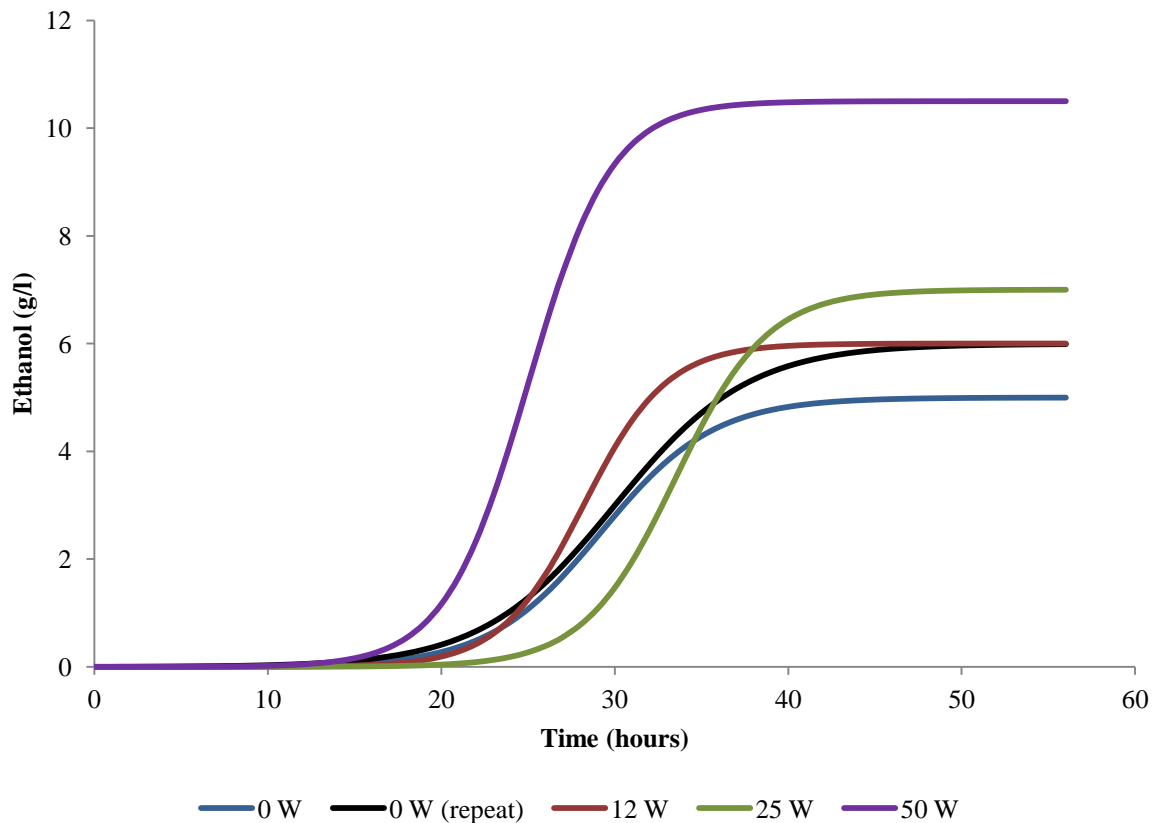


Figure 121. Ethanol formation under varying microwave powers (curve fitting)

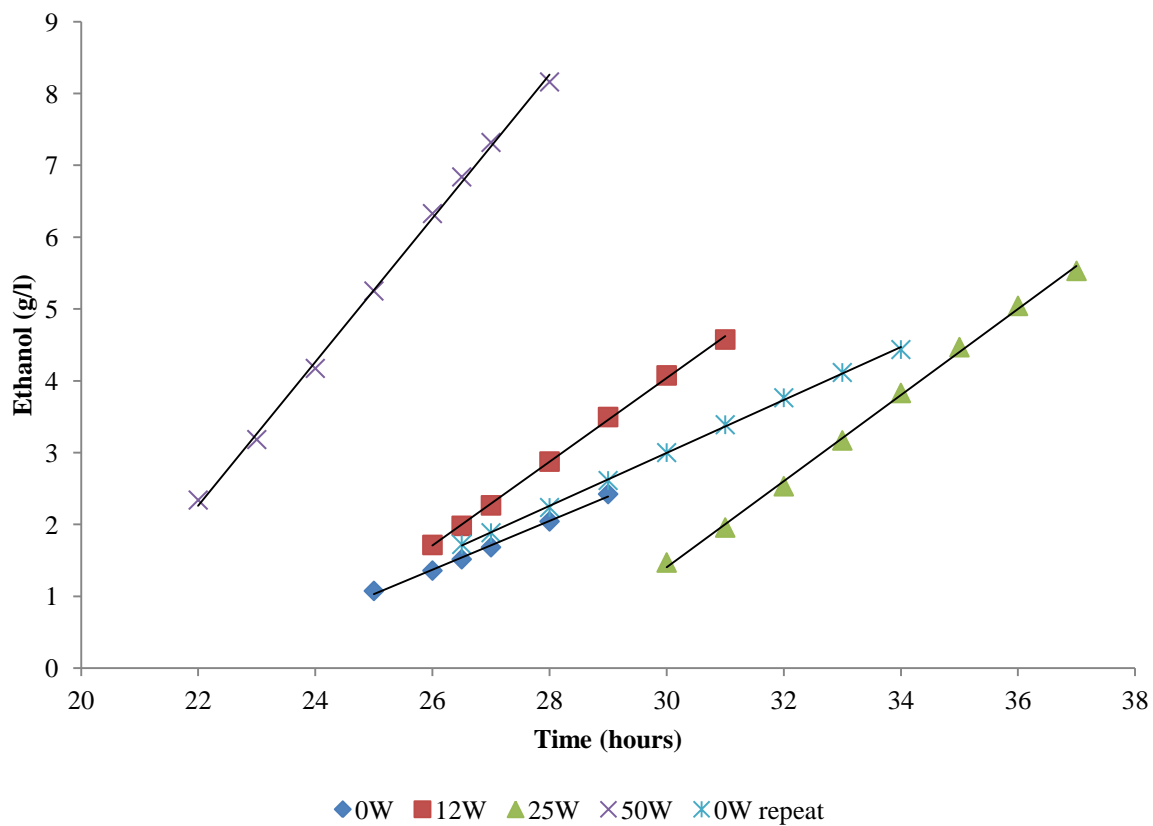


Figure 122. Ethanol formation rate.

| Microwave power | Ethanol production (exponential phase) |                |                |
|-----------------|--|----------------|----------------|
| Watts           | Gradient (g/l/hr)                      | R <sup>2</sup> | Difference (%) |
| 0               | 0.34                                   | 0.999          | 100            |
| 0 (repeat)      | 0.37                                   | 0.994          | 100            |
| 12              | 0.58                                   | 0.998          | 158.2          |
| 25              | 0.60                                   | 0.9969         | 162.5          |
| 50              | 1.00                                   | 0.9981         | 271.3          |

Table 43. Summary of ethanol formation rate by HPLC analysis and curve fitting

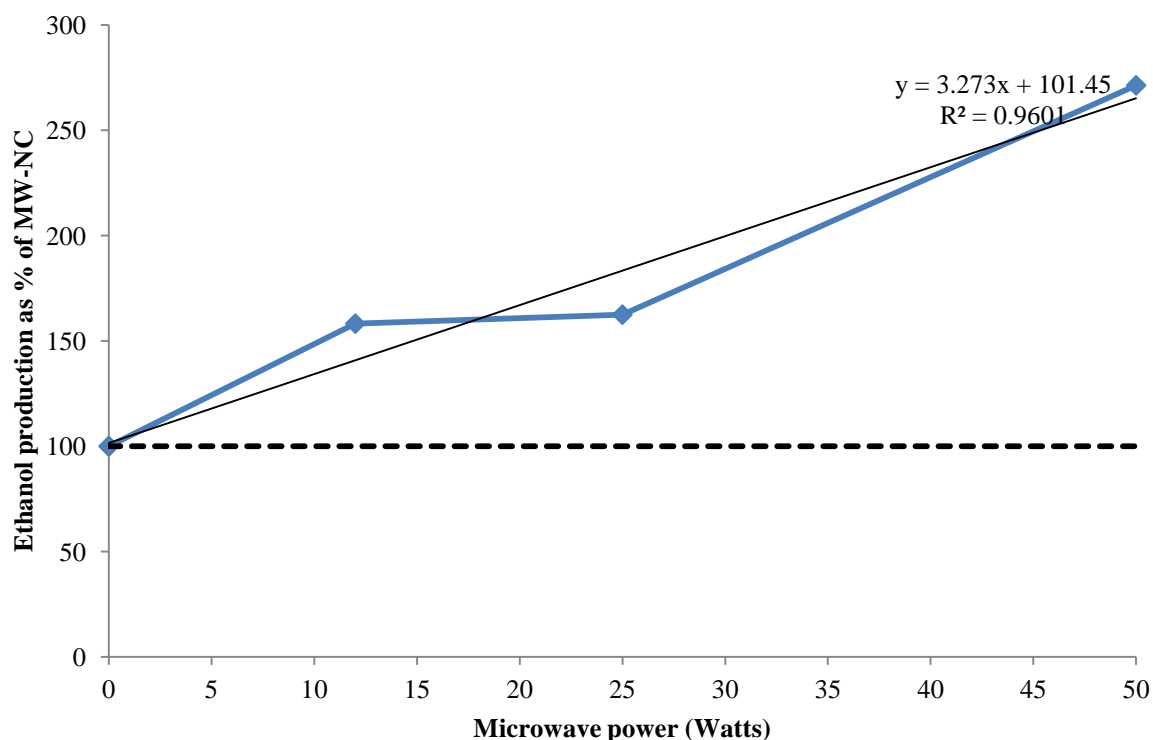


Figure 123. Ethanol production rate as percentage of MW-NC against microwave power  
Trendline equation;  $y = 3.273x + 101.45$ ,  $R^2 = 0.9601$

Using the previously described methods, the gradient is determined from the curve fitted data (for method, see page 136), the linear plot of ethanol evolution was plotted (Figure 122) and used in the compilation of Table 43. Conversion of the data into a graphical form is shown in Figure 123 for comparison against the negative control.

From the data produced, it is shown that the irradiation of the fermentation has increased the ethanol production rate by 94% at 12 Watts and 56% at 25 Watts. As previously described, the values obtained for 50W were compromised by contamination, therefore a reduced ethanol formation rate is quoted. However, by yield, all microwave powers (0-50W) each yielded the same total volume for 25.g/l due to glucose exhaustion.

For the direct comparison of growth rate, ethanol production and glucose uptake in comparison to the negative control, Figure 124 is shown, indicating that there is a clear but subtle alteration in fermentation under irradiative exposure with the greatest deviation observed at 12W power.

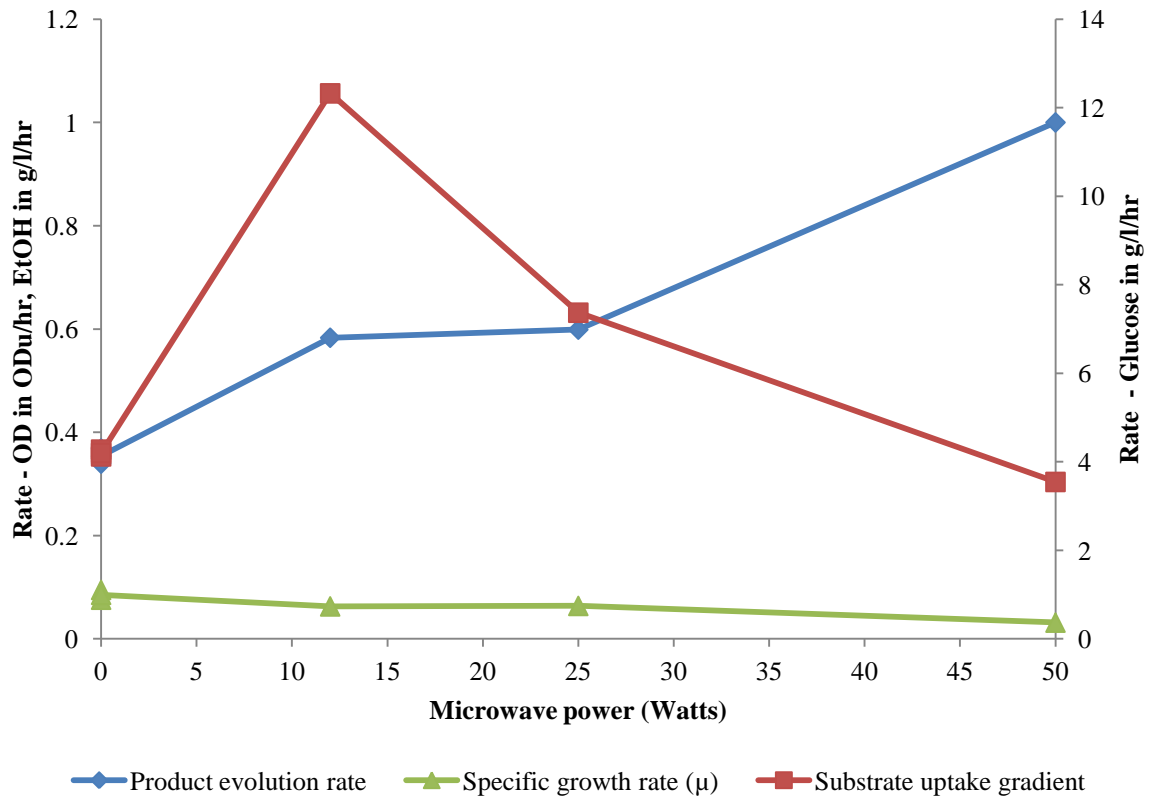


Figure 124. Comparison of fermentation indicators by rate

## Conclusion

### BIOREACTOR PERFORMANCE

The performance of the bioreactor is within the parameters set out in “Chapter 1.2. The proposed solution” (page 3), and as designed in “Chapter 3.1. Practical work - Microwave” (page 98) and the results are presented in “Chapter 4.1. EP 1.0. – Bioreactor thermal profiling” (page 146). Over the time period of each experiment, the temperature deviation of 0.07°C with an average temperature of 49.98°C over the time period of >40hrs was deemed acceptable to conclude that the reaction vessel could be termed “isothermal.”

### CATALYSIS;

**CBH/EGL** - Substrate utilisation was limited as expected and the data produced showed that microwave irradiation of the “cellulase” preparation can be enhanced. Comparing the result with the greatest effect to the negative control, 50W was observed to be the most effective with irradiation showing a non-linear response curve. 50W power is shown to increase the initial saccharification rate from 0.03%.hr<sup>-1</sup> to 0.08%.hr<sup>-1</sup>.

**CBH/EGL + BGL** - By combining the cellulase enzymes of EGL and CBH with BGL, the complete conversion from cellulose through to glucose was shown through the minimal production of cellobiose. The result of the experiments conducted has shown the by initial rates, 25W increases the initial saccharification rate from 0.029%.hr<sup>-1</sup> to 0.048%.hr<sup>-1</sup>. More importantly, was the increase in liberated glucose, with yield lifting from 5.9g/l to 8.7g/l.

**BGL** - From the work conducted for this part of the project, it can be concluded that the irradiation of BGL with between 12 and 75W microwave power significantly increases the catalytic rate above the reference negative control rate. In comparison to the enhancement seen in the previous experiments (see work by Zhu *et. al.* [189]), the power curve observed is not of the same nature, suggesting an “all or nothing” response in the studied powers. BGL experiments show enzyme enhancement on a simplistic, single enzyme, single substrate and single product model. Whereas previous experiments have had complex multi-step processes, the use of cellobiose and BGL has ruled out the possibility of a purely SWO induced effect. As SWO will not be present in this experiment, amplification of rate can only be attributed to BGL.

The additional experiments conducted within each group of experiments have all been used to support the catalysis conclusions.

## **FERMENTATION;**

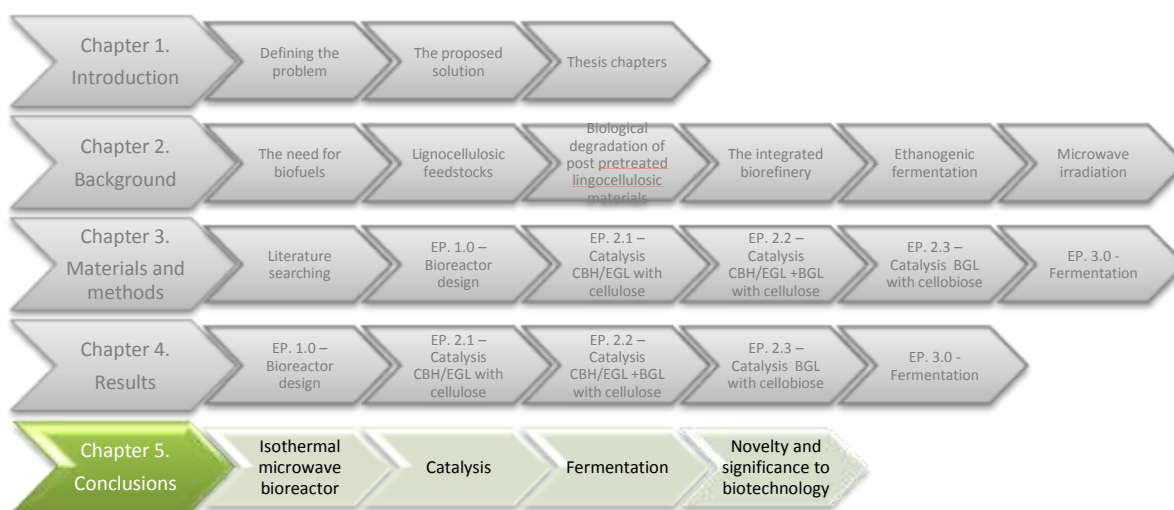
In conclusion of the experiments done to investigate the irradiation of a fermentation system, Figure 124 is produced as a method of cross referencing the parameters of specific growth rate ( $\mu$ ), glucose uptake and ethanol production. From the data plotted, it can be concluded that the irradiation of an isothermal fermentation does show variance in each parameter, with non-linear responses observed in glucose uptake. With the reduction of growth rate, increase in ethanol production, concluding an exact correlation is difficult with the low number of experiments conducted.

Although the data is insufficient to support a detailed investigation into the exact mechanics where the microwave irradiation alters a specific biochemical pathway, the study shows that the microwave powers required for the increase of catalytic rate are not detrimental to microbial growth and product formation. This is of significance due to the potential to combine the saccharification process and fermentation into a single unit operation.

Of particular notice is the anomalous data produced in the 50W fermentation. Whereas fermentations at 0W, 12W and 25W ceased ethanol production at approximately 2.5g/l due to carbon exhaustion, the 50W fermentation accumulated approximately 11g/l in the same time period. Thorough investigation is required for repetition of the experiment to illicit the cause of the erroneous result.

## ***Chapter 5. Conclusions***

## Chapter 5. Conclusions



Due the multiple aspects of the project seen in previous chapters, the discussion and conclusions are split into the three research themes. Relating to the original project description (page 3) and the experiment design (page 95), the objectives of the project have been met. These are summarised as;

- 1) The production of a prototype microwave bioreactor with independent thermal and microwave controls.
- 2) The catalysis of cellulose substrate by “cellulase” enzymes resulting in a non-linear relationship between microwave power and rate/yield increase at steady state thermal conditions
- 3) The irradiation of a eukaryotic fermentation under isothermal conditions and a power range results in small changes in fermentative rate. Of critical importance is that irradiation at the powers used in catalysis does not reduce or prevent microbial growth.

The three objectives are evaluated by the criteria of;

- 1) Critical evaluation - attaining the research object; novelty or inventive step.
- 2) “Blue skies” research - relationship to scientific significance
- 3) Real World research - industrial relevance

The fourth criterion of evaluation is the potential development, or lead on work from this research. This is discussed within the evaluation points 1 to 3.

As a brief summary, Table 44 is produced using the above themes and criteria.

| Assessment criteria        | Research theme  |  |  |
|----------------------------|---|--|--|
|                            | Microwave bioreactor  | Catalysis  | Fermentation   |
| <b>Critical Evaluation</b> | <ol style="list-style-type: none"> <li>1) Accomplished objective of independent control of thermal stability and microwave irradiation.</li> <li>2) Qualification and verification of accurate bulk temperature recording and stability over extended time periods.</li> <li>3) Shown feasibility microwave and temperature independence across 0- &gt;200 Watts microwave power range, and &lt;0 – 150°C temperature range.</li> </ol> | <ol style="list-style-type: none"> <li>1) Determination of enzymatic rate in a microwave variable and thermo static reaction chamber.</li> <li>2) Correlation of rate to power in a non-linear relationship.</li> </ol>  | <ol style="list-style-type: none"> <li>1) Determination of fermentative rate has been accomplished within a thermally isolated, microwave irradiated chamber at non-lethal powers for the study of microbial response</li> <li>2) Irradiation at powers that are comparable to the powers required for enzyme enhancement do not provide lethal dosage to an ethanogen (<i>Saccharomyces spp.</i>)</li> <li>3) Alteration in rate is subtle, and indicative of scope for further research</li> </ol> |
| <b>Blue Skies</b>          | <ol style="list-style-type: none"> <li>1) Reactor can be deployed directly into research for repetition or validation of previous peer experiments and results.</li> <li>2) Unit can be used for research in independent variables; frequency range, pH, agitation, rheology, DO, solution composition, microbial content, immobilised bead systems, batch/fed batch/continuous mode, pulsed/continuous irradiation.</li> </ol>         | <ol style="list-style-type: none"> <li>1) Evidence of nonthermal microwave effect on an enzyme catalysed system.</li> <li>2) Direct influence on the choke point in cellulytic microbial growth, therefore does microwave irradiation influence growth rate?</li> <li>3) What variable correlates to protein excitation</li> </ol> | <ol style="list-style-type: none"> <li>1) The reaction chamber can be used for both aerobic and anaerobic fermentations for investigation of EM irradiation on fluid fermentations</li> <li>2) Evidence of variation in metabolic pathways in irradiated fermentation</li> <li>3) In the assumption of biochemical or physical alteration to the microbe, can this be exploited (transfection, pathway selection, continual random mutagenesis etc)</li> </ol>                                       |
| <b>Real World</b>          | <ol style="list-style-type: none"> <li>1) 1 litre – fine chemical or high value preparations with optimisation based on above parameters.</li> <li>2) &gt;1 litre – requires development through scalability (scale up or scale out)</li> </ol>   | <ol style="list-style-type: none"> <li>1) More saccharide produced per unit cellulase.</li> <li>2) Reduction of processing cost in cellulosic biomass conversion to fermentable sugars.</li> </ol>   | <ol style="list-style-type: none"> <li>1) Potential of increased product formation rate if developed further</li> <li>2) 1 litre scale – development of high value fermentation products</li> </ol>  |

**Table 44. Summary of project contribution to knowledge**

## ***The microwave bioreactor***

***Achievement of study objective;*** The research project accomplished the research aim of prototyping a microwave reactor capable of operating in both thermal and isothermal microwave operations. Comparing varying isothermal microwave irradiation to an isothermal negative control shows separation between the microwave influence and thermal temperature. The reactor prototyped is credited with being able to carry out repeat experiments under isolated thermal conditions regardless of microwave power and ambient temperature.

The limitations of the system configuration observed in this study have been the maximum power that can be transmitted using a coaxial launching systems and/or microwave reflection from the bioreactor internal structures, and the efficiency at which excess heat can be compensated for. This is detailed in 4.1. EP 1.0. – Bioreactor thermal profiling on page 146.

To increase the energy supplied to the reaction chamber, the launch system used may be substituted with a direct launch system, dispensing of the coaxial cable launching limitation. Within the research unit, microwave sources are available in the kW and MW ranges and knowledge on power matching and application. An example of this system used is shown in Figure 125, where direct launching and a circulator are used.

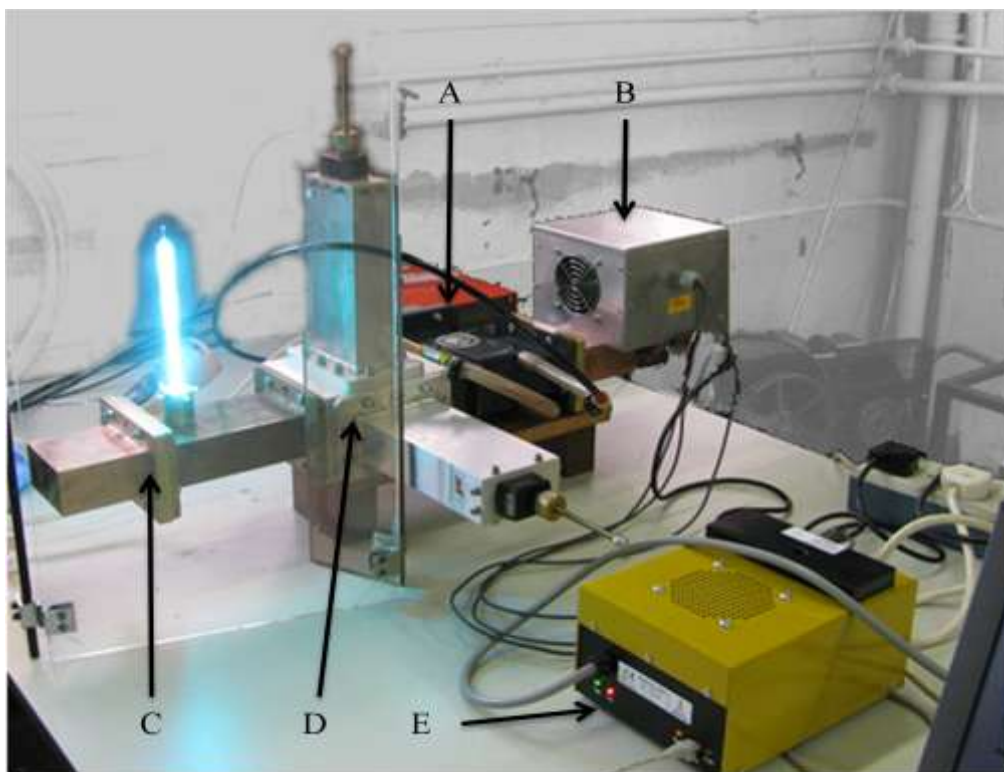


**Figure 125. Alternative method of direct microwave launching**

A = circulator; B = magnetron (contained within housing); S-band waveguide (end flange shown used to contain EM field while allowing observation); D = E-H tuner; E = magnetron power supply unit

The increase in microwave power has not been deemed necessary in this study due the results presented in the previous chapter showing effects seen in the sub-100W range. This has the implication of a significant enhancement with a low or negligible energy addition (energy supplied through microwave irradiation would be supplementary or offset set energy provided through thermal means). Theoretical exploration of the using a higher powered source would conclude that penetrative depth would increase, as would field density. The STR used has internal furniture designed for biological work and not microwave studies. It would be suggest that possible arcing would occur across the furniture with unknown consequence to both the sample being irradiated and the equipment being used. As such, the microwave powers used were suitable for the task.

The thermal limitation of the bioreactor system is dependent on the weakest element. In this prototype system, the heat exchanger system used in the immersed heat exchange loop is assumed to be the limitation. Assuming that energy is lost through thermal radiation from the cavity and metallic materials of the reactor, the maximum required heat removal would be equal to the irradiating power in a perfect thermally isolated system. For increasing microwave power, the ability for heat compensation via the heat exchanger would have to be specified in excess to the intended microwave source. The maximum thermal limitation of the STR structure is in the order  $\geq 134^{\circ}\text{C}$  as the STR design and instrumentation originates from fermentation biology, therefore the STR, DO and pH probes and ancillary reactor components are capable of autoclave conditions. Therefore the feasible temperature range is  $\approx 0^{\circ}\text{C}$  through to  $100^{\circ}\text{C}$  when oil is used as the exchange fluid in the immersed loop. Maintaining temperatures above  $100^{\circ}\text{C}$  though the sealing of the vessel would not be advisable as the reactor is not designed as a pressure vessel. Temperatures below  $0^{\circ}\text{C}$  may be achievable with this system by the use of polyethylene glycol (PEG) in the heat exchange system. Practical system limitations are areas of malleable materials, particularly in the insulating fabrics of sensor cables and the drive motor.

For the irradiation of samples, the length of exposure is far greater than exposure rates seen in comparable experiments, particularly at the isothermal set point. With the reactor being used for cellulose hydrolysis by cellulases, the only comparable paper by Zhu *et.al.*, where the former irradiate for a exposure period of 0.07% of reaction time compared to 100% of the time in this experimental report [189]. Based on evidence available, total irradiative energy comparison over a 160 hour reaction would be 35 W.hrs for Zhu compared to between 1,920 W.hrs to 24,000 W.hrs for this research study based on a power range of 12 to 150W<sup>11</sup>.

---

<sup>11</sup> Data adapted from Zhu *et. al.* 189. Zhu, S., et al., *The effect of microwave irradiation on enzymatic hydrolysis of rice straw*. Bioresource Technology, 2006. **97**(15): p. 1964-1968. where 0.07% determined according to the explanation given on page 85

| Study             |              | Power range (Watts) | Exposure interval (hrs) | Consumption range (total) (Watt.hr) <sup>[1]</sup> | Rate (W/hr) <sup>[2]</sup> |
|-------------------|--------------|---------------------|-------------------------|--|----------------------------|
| <b>Zhu</b>        | Catalysis    | 300 (static)        | 0.004                   | 35   | 1.23                       |
|                   | Catalysis    | 50 – 150            | 30 - 160                | 150 – 24,000                                       | 50 - 150                   |
| <b>This study</b> | Catalysis    | 12 – 75             | 30 - 160                | 360 – 12,000                                       | 12 – 75                    |
|                   | Catalysis    | 12 – 75             | 30 – 160                | 360 – 12,000                                       | 12 – 75                    |
|                   | Fermentation | 12 – 50             | 50 - 60                 | 600 – 3,000  | 15 – 50                    |

**Table 45. Comparison of energy exposure between this study and Zhu *et. al.***

Data generated from this study in comparison to inferred figures from [189]. <sup>1</sup>Ranges quoted are based on the variability of microwave irradiation and time of exposure with lowest and highest figures shown. <sup>2</sup>Ranges quoted by variable irradiation.

As previously highlighted, microwave power is dependent on the launching system with multi-kW units available. For research and optimisation, greater interest is the flexibility of microwave frequency range and operational mode. In the experiments conducted, 2.45GHz was used due to the original prototyping being conducted with the Microtron system. Following the initial observation of rate change at 2.45GHz, further investigations were developed on this frequency. With the S band waveguide, a frequency range between 2 and 4GHz can be investigated without any physical modification to the system. For frequencies outside the S band range, adapter plates have been suggested for reduction of aperture size and orientation to allow the coupling of smaller waveguides - standard sizes from WR248 through to WR28 for example covering bands S through to D. This adaptability easily facilitates the use of microwave sources from 2GHz through to 170GHz

In addition to frequency range is the variation of signal form. In this study, the irradiation has come from a continuous signal generator. The Sairem unit has the capability of producing a pulsed source (although not used in this report). By alteration of the duty cycle, the peak power and average power can be modulated to investigate both response in correlation to duty cycle and response in correlation to pulsed peak energy. This would enable further investigation of the work conducted by Laurence *et. al.* [166].

**Scientific significance:** The implication of a versatile reactor system allows the study of thermal and isothermal reactions with a range of controllable variables. These include;

- Frequency range – ISM frequencies, S – D bands plus others with minor modification
- Operation modes (microwave) - pulsed/continuous
- Operation modes (processing) - batch, fed-batch and continuous
- Fluid systems - aqueous, none aqueous and immobilised fluidised bed systems
- Sterility conditions
- Microwave energy densities
- Thermal profiles and isothermal temperature range

Development of the system would look at further automation and integration of the system with PID feedback control. As system has been operated as isothermal, the dielectric properties of the water were constant throughout all the experiments conducted. In reaction which may have significant alteration of the dielectric point, real-time online tuning maybe appropriate if the effect is significant. Co-launching of other frequencies into the system for either compound irradiation in a two step system with differing frequency optima or for frequency sweeping for progress analysis is also being considered. This versatility will enable the reactions highlighted in the Background Research chapter to be replicated under standardised condition and re-investigated.

From the research undertaken in this study, and by the examination of previous peer work, the observation of the non-linear response to irradiation is apparent. The conclusion that irradiation has no effect on any given reaction now shows the distinct possibility that the reactions conducted may have been either irradiated at an energy level or frequency that is an order of magnitude removed from the reaction's optimal conditions, therefore either irradiating at too low a response point or well above the lethal dose threshold. This would infer a "Goldilocks" point in some biochemical systems. By using this system, surface response methodology applied to each reaction could challenge some of the current conclusions (or at least improve the conclusions formed in this study).

**Industrial acceptance:** The bioreactor adoption in industry will be dependent on scalability. The current reactor may either be considered as a proof of concept for scale up or a prototype for scale out. With relation to the original description of a bioreactor for the enhancement of catalysis and fermentation in biofuel production, the obvious exploitation will be the increase in reaction volume, therefore the work completed would be considered as a proof of concept. If the system is used as an isothermal irradiative system for the study of electromagnetic irradiation on biological systems, then the equipment used would be considered as a prototype, with little development required for laboratory use immediately.

From the results produced in this thesis, the conclusion drawn is that the application of microwaves to the catalysis of cellulose in an isolated system can cause significant increase in the initial catalytic rate and the increase in yield when using the commercially available “cellulase” preparations. The summary of the results compiled is presented in Table 46, a repetition of the table shown at the start of the results chapter.

The significance of the results builds upon the work conducted by Zhu *et. al.* [189] with the major deviation of qualification of microwave field exposure. Where the previous study possibly exposed the reaction to 0.21% of the total reaction time, the work presented here maintained the reaction within the known microwave field for the total reaction time.

The significance of the catalysis experiments is the conclusion that irradiation of the enzymes used can enhance the activity. In comparison to other studies where either thermal control has not been critically evaluated or irradiative power has been subjective to arbitrary values, this experiment has made a significant step into identifying a specific microwave power to either an increase or decrease in catalytic rate.

As the system has been applied to potentially five proteins (CBHI, CBHII, EGL, BGL and SWO), the data produced suggests that at least CBHI or CBHII has been induced to activate at a higher rate.

| Results summary   | Contribution to knowledge  |
|---|--|
| 1 <b>EP. 1.</b> Microwave energy can be launched into the reactor independent to the thermal profile, maintaining steady state conditions for the total reaction time.                | Microwave irradiation of aqueous and non-aqueous systems can be accomplished with microwave power levels ranging from 1-200W. Power of irradiation at set temperature points is dependent of microwave launching system and heat exchanger ability to compensate for thermal heating.  |
| 2 <b>EP. 2. – NC-S</b> Microwave exposure of the cellulose does not alter the cellulose material.   | The spontaneous hydrolysis of cellulose by microwave energy is not achievable in the 1-150W power band in the aqueous system.  |
| 3 <b>E.P 2 – NC-E</b> Microwave exposure of the enzyme independently does not alter the enzymes enzymatic rate.   | Proof that any modification to the cellulase enzyme is momentary, preventing the opportunity to pre-irradiate and apply. This concludes that microwave irradiation, enzyme and substrate are all required simultaneously.  |
| 4 <b>EP. 2.1.0.</b> 50W irradiation of EGL/CBH with cellulose increases the initial glucose rate by 206% over the thermal negative control.   | The microwave field effect where EM irradiation has a distinct interaction above the expected from the thermal increase, as suggested by Giombini <i>et. al.</i> [176], Porcelli <i>et al.</i> [190], Bradoo <i>et. al.</i> [193], Ward <i>et. al.</i> [179], and Zhu <i>et. al.</i> [189] is isolated. This is proven in this system although the mechanism can only be suggested |
| 5 <b>EP. 2.1.1.</b> The result seen in 4 (above) is not due to BGL contamination.   | Isolation of the enzyme systems has shown the rate increase in CBH/EGL. Inhibition of BGL by vanillin has shown there is no BGL contamination of the CBH/EGL enzyme stock.   |
| 6 <b>EP. 2.2.0.</b> 25W irradiation of EGL/CBH with BGL on cellulose increases the initial rate by 64.95% and glucose yield by 25%.   | Evidence of an increase in reaction rate with the application of microwave power, with a non-linear relationship between rate and power.   |
| 8 <b>EP. 2.3.0.</b> Microwave irradiation of BGL on cellobiose showed a peak enhancement of 70% increase and net increase of 50% in glucose initial rate across the 0-75W power band. | Evidence of an increase in reaction rate in an isolated enzyme pathway.  |
| 9 The results observed are not due to thermal effects.  | All experiments conducted with an isothermal bulk temperature, with the only variable being irradiation.   |
| 10 Microwave enhancement for catalysis is only observed when the enzyme and substrate are irradiated in complex.  | Irradiation of the reaction constituents does not elevate the reaction rate, concluding that the increase in rate has to be a combination of enzyme-substrate complex in the presence of a microwave field.  |

**Table 46. Summary of results (Catalysis)**

## **Cellulose catalysis industrial significance**

In industrial significance and adoption, two progression pathways are modelled; low value bulk commodity products (i.e. enzymatic hydrolysis and fermentation for biofuels); and low volume, high value products and/or research exploitations. The differentiation between the two models is in terms of scalability. Bulk processing requires volumes in the order of thousands to millions of litres throughput per annum compared to high value products and research applications where annual throughput will be in the order of tens to hundreds of litres per annum.

In the bulk low value product application, the technologies developed in this PhD project apply to the cellulosic ethanol market. The study has shown that through the use of microwave energy, the efficiency of enzymatic hydrolysis can be increased without temperature/pH/media alteration, protein modification or increased enzyme loading. Of importance to the cellulosic ethanol industry will be the increased hydrolysis yield per unit of cellulase purchased, offering a cost reduction in hydrolysis, and an increased hydrolytic rate which reduces the required residence time within the hydrolysis reaction vessel. On the plant scale consideration, this can lead to either reducing infrastructure volume or increasing cycle turnover rate for the same gross product yield.

In discussing the industrial adoption, a number of factors should be considered and kept in mind as possible limitations. The experiments conducted were on a 1 litre basis and with a single reactor design tested. The system is considered non-optimised, as no attempt was made in modifying the prototype's physical form for better microwave, thermal or flow dynamic characteristics once constructed and proof of energy transfer had been ascertained. Enzyme, substrate and inoculum loadings were all kept within defined limits throughout each experimental system and should not be extrapolated for load variations, as the study does not present information to determine relationships. As such, the conclusions drawn can only be based on this reaction vessel with the reactions quoted.

A simplistic development of the system is the thermal isolation of the reactor system. From the temperature profiles presented in Chapter 4, EP. 1 (page 146), it is clear that there is thermal loss through the cavity walls to the surrounding environment. Lagging was not used during this study due to the development of the reactor moving from the prototyping phase into experimentation phase as an unlagged system. Therefore, the introduction of lagging during the study could have caused a variable between data sets. Under the assumption that the effect observed is correlated to the energy density delivered by the microwave source rather than the rate of temperature flow, lagging would not reduce the microwave energy applied to the reactor. Lagging would affect temperature compensation (heat removal) via the heat exchanger. Further development will address this through the use of insulating materials being applied around the external cavity walls, at the interface between the cavity bottom and any supporting structures, and at the waveguide-cavity interface (Davidovitz paper in

1996 illustrates the design of a waveguide coupling for thermally isolated wave transmission in cryogenic systems [198]). A short synopsis of thermal improvements is shown in Table 47.

| Mechanism of thermal loss  | Consideration for improvement   |
|--|---|
| <b>Conduction</b> Thermal flow seen across the compression ring into the cavity wall due to surface contact area. Thermal flow from the head plate via retaining bolts into the compression collar. Some prevention due to non-conductive gaskets but no active prevention used. | Consideration of an insulating gasket between the compression ring and the cavity wall.   |
| <b>Convection</b> Air within the void space between the glass vessel and the cavity wall has freedom of movement but is isolated from the external environment. Heat accumulation in this body of air will allow convection transfer between the materials.                      | Removal of air from the void space (impractical). Constant air flow through to prevent heat accumulation. Filling void space with insulating material providing that the material is microwave transparent. |
| <b>Irradiation</b> Heat irradiated through the void space between the glass vessel exterior and the interior cavity wall.  | Microwave transparent, thermally reflective coating on the internal cavity wall surface. Removal of void space by vessel/cavity consolidation.  |

**Table 47. Thermal heat flow through the microwave bioreactor system**

In terms of scalability, theoretical scaling is a function of microwave design, not thermal flow dynamics. The optimal microwave power used for the irradiation of 1 litre of fluid in these cellulase catalysed experiments was 24 Watts from a 200 Watt Microtron source. For this reaction, scaling out would be the most simplistic method of scaling. 8 identical vessels could be irradiated off the same launching system with duplication of instrumentation and a scaled heat exchange system be employed across a reactor array. As hydrolysis scale in bioethanol production is in the order of tonnes of cellulose per month, out scaling is impractical (1 tonne per month using the process described would equal 25,000 1 litre reactors on a 1 reaction per week recycle programme), therefore scale up is inevitable.

For scale up, the three parameter of microwave, fluid and thermal dynamics each require consideration. Scalability of thermal and fluid dynamics are well understood and common practice across industry. Microwave scalability is much more difficult. As penetrative depth and power are nonlinear, the doubling of the reaction vessel volume does not equate to the doubling of microwave power. As such, modelling through HFSS (or other software packages) is required.

## Scientific significance

To compare a nonthermal and thermal effect may be dependent of the definition “thermal” and “nonthermal.” In each instance, dielectric heating could be considered the sole mechanism, but observed at the macroscopic scale in comparison to the microscopic scale, the energy progression and temperature dissipation could be indistinct.

In thermal heating, a temperature gradient occurs between the heating element and the immediate surroundings. In an agitated system, the gradient is maintained with fresh (cooler) material displacing the fluid that has just been heated through contact with the element. Once away from the element, heat energy will be dissipated through random contacts between molecules of different heat energies until energy equilibrium is achieved across the whole system, equal to the temperature of the heat source assuming perfect insulation and no losses; or where increase in thermal energy is equal to loss of thermal energy.

In contrast, dielectric heating at 2.45GHz preferentially heats the water molecules according to energy density per unit volume across the whole resonant cavity (assuming perfect conditions and the applied frequency). Energy losses will only occur where a temperature gradient can occur i.e. at the fluid interface with the containing vessel. In the agitated system, the accumulation of hot spots is prevented through complete free motion in the multimode cavity.

For the determination of temperature, only the bulk fluid temperature was measured and maintained as the isothermal parameter. This was due to the constraints of the system and means of measurement (the description of temperature measurement is described in detail in 3.1.9. *Thermal profiling* on page 110). In contrast, the localised temperature at specific points within the reaction complexes may have had temperatures exceeding the bulk temperature depending on the rate of heat diffusion. Without the ability to measure or qualify localised temperatures (requirement of either x-ray or neutron scattering), the theoretical localised heating effect due to either physically confined polar water molecules or hydroxyl groups in the vicinity of an enzyme system. As such, the limitation is the ability to record temperature with molecular resolution. This can lead to the assertion that an isothermal effect may well be considered a specific localised thermal effect. To illustrate, Figure 126 shows a theoretical temperature gradient from a cellulase enzyme where localised heating effects causes the molecular temperature of the enzyme to be 5°C greater than the recorded bulk temperature. Diffusion of heat from the molecule would induce a localised temperature gradient. In the figure shown, 30 arbitrary units is shown as the minimum physical distance by which temperature can be determined, showing the principle of difficulty measuring localised point temperatures. Therefore the determination of temperature through physical means would be unfeasible. Additionally, due to motion of the water in the agitated system where the predominant mass (water) has greater contact

with the thermal well; and physical obstruction of the cellulosic mass preventing direct enzyme-thermometer contact, there will be a limit in ability to detect the exact enzyme temperature.

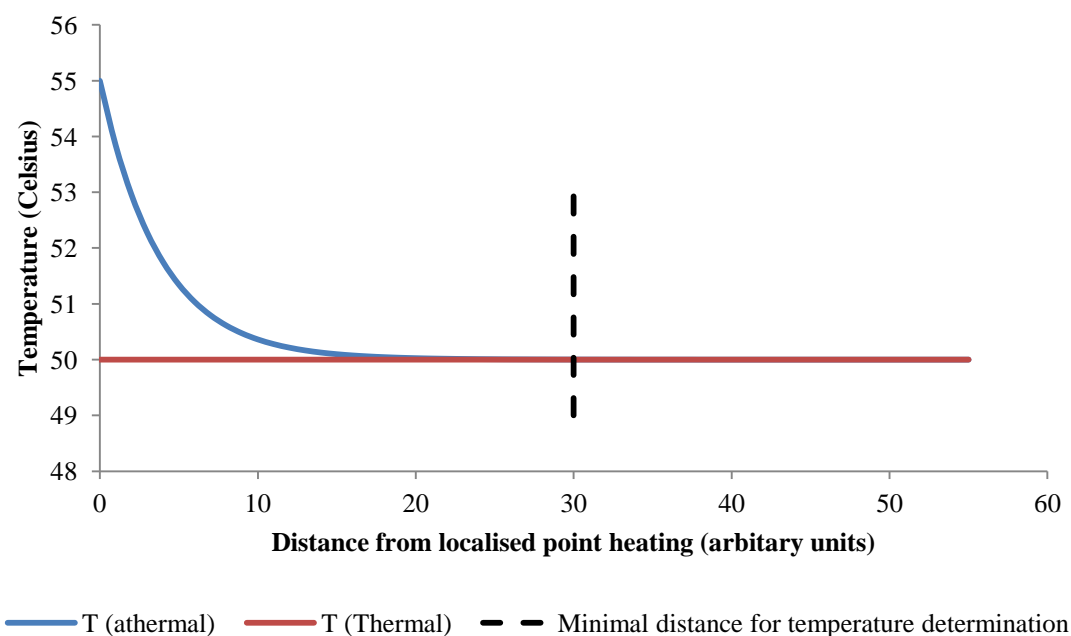


**Figure 126. Illustration of localised heat distribution versus thermal bulk recording**

In relationship to the study undertaken, the dielectric heating through microwave irradiation was counteracted by the heat removal through the thermal sink. Thermal energy was also lost through the cavity walls, and through the submerged heating loop (with fluid exchange for the heat exchanger). This has led to the experiment being classified as isothermal as the bulk fluid temperature was 50°C where  $\Delta T=0^\circ\text{C}$  for catalysis; and 30°C where  $\Delta T=0^\circ\text{C}$  for fermentation.

From the work presented and the results concluded, a number of questions have risen to the mechanism observed. In the catalysis of cellulose by “cellulase” enzymes, it is highly suggestive that the mechanism seen is a nonthermal system, where rate amplification is through the influence of a microwave field. The significance of the results and accountability of thermal stability in each experiment, the likelihood that it is a thermal effect is remote.

An additional complication is the position of the CBH and EGL on the substrate. Where the substrate has maintained some of the porous form of the plant structure, localised heating may occur where the rate of fluid exchange is reduced comparable to the bulk.

In the study conducted, a continuous microwave source was used for microwave irradiation, therefore the exposure has been assumed to be continuous throughout. However, the system infrastructure has the possibility of causing a quasi pulsed system due to the liquid rheology. With the material in constant motion, it would only spend a proportion of its time in front of the microwave window.

Within the STR, the furniture used for agitation and temperature control may have caused microwave shading in areas of the cavity furthest away from the microwave window. As the microwave beam was shone along the waveguide, any metallic or microwave impermeable material would prevent the progression of the microwave beam. This would cause material in front of the furniture to be irradiated at a higher incidence at that time instance in relationship to the material behind the infrastructure. To investigate the effect and understand if this possibly occurred, HFSS was used to model the cavity. The limitation of modelling is that the model only represents an ideal system, where surfaces are simple and have no abrasions or defects to alter the reflective surfaces (such as baffles, heating/cooling loops, sample/sparger pipes and agitation structures). With the intricate structure of the internal furniture, modelling of the complete system was beyond the capabilities of both the University computer facilities available at the time and research resources. This aspect would be an area for further investigation in future experimentation or collaboration. The significance of the quasi-pulsed system is explained in 2.6.6. Microwave and biofuel/cellulase research on page 81.

From the background research shown and the results compiled, the possible mechanisms of enhancement appears to be in the increased rate of the CBH and EGL activity as BGL has been used in excess. As such, the suggested mechanisms are representative to possible relationships between the cellulose, CBH/EGL and microwave field, with particular focus on CBH.

In the context of an isothermal microwave effect, a number of hypothesis can be raised as to the mechanism of enhancement. Through discussions with peers, selections of these mechanisms are suggested along with reasonable critical response to each.

**1) Hydrogel coating on the linker sequence has altered flexibility.**

2.45GHz which has a resonance frequency corresponding to that of water. Any field effect may be correlated to the dipole action of the water or hydroxyl residues that are capable of limited free motion, giving the possibility of localised heating. With the evidence of increased hydrolytic rate, the mechanism of movement along the fibre has the possibility of effecting rate. As described in Chapter 2 – Background Research, the movement of the CBH protein is governed by the flexibility of the linker system with a critical energy barrier to extension. As the linker is a highly o-linked glycosolated sequence creating a “gel-like” zone between the CBH and the catalytic core [101] (see page 42), the semi-immobilised water molecules in the region of the linker may show increased energy through dipole rotation causing a localised heating effect..

**2) Dipole of water around the CBD anhydrous affinity pad alters cellulose fibre adhesion**

Nimlos *et. al.* highlighted the hydrophobic nature of the residues around the CBD [99]. By alteration of water molecule orientation at the localisation around the CBM, the area in immediate vicinity of

the CBM has the opportunity for alteration of affinity or modification of progress. As the mechanism of CBM is not fully understood (hypothesis of CBM “leading” compared to CBM “pushing” does not allow sufficient evidence of modification).

### **3) Increased vibration of the whole molecule prevents fractal jamming on the cellulose fibre.**

Originally suggested as a potential mechanism, although subsequently discouraged. With the size of the protein involved and the frequency of the microwave sources, for the vibration of the whole protein is very unlikely due to mass. The theory of fractal jamming was originally raised has been discredited due to two areas of evidence. 1) the enzyme loading is below the typical threshold required for fractal jamming to be suggested and 2) addition of a secondary load of cellobiose was seen to show continued saccharification. Where fractal jamming has occurred in high enzyme to substrate ratios, jamming prevent free enzyme in solution to saccharify a second biomass load. This was not seen.

A modification of the hypothesis is that the quasi-pulsed situation suggested could have lead to a pulse related protein modification in enzyme folding. As stated in Chapter 2, work carried out by Laurence *et. al.* suggested that conformation of proteins in pulsed fields can have short period alteration. In addition to this, Daniells *et. al.* go on to explain the nonlinear response observed within a pulsed field. In light of these papers, and the results obtained, the non-linear nature of the catalysis response suggests this correlation [166, 194].

To support this hypothesis, there has to be the suggestion or proof of which element has undergone conformational alteration. Due to the facilities available, and the technical difficulties that would be incurred in modelling an enzyme conformation alteration while in complex with the substrate, this has not been considered in this study. A theoretical approach maybe through computer modelling of the whole EGL or CBH enzyme, and running simulations based on stimulations of the protein in an oscillating electromagnetic field to determine the most likely location of free movement. Following the determination of likely base locations, conducting amino acid substitution through the production of recombinant proteins for repeat testing, looking for alteration in rate according to structure alteration.

### **4) Water molecules or water molecule ingress tunnel on the CBH catalytic head has alteration of conformation/action allowing increase water availability for hydrolysis**

Analogous of the conclusions drawn by Laurence *et. al.* [166] (see page 88) where protein ring is observed allowing the alteration of protein confirmation, a similar system maybe occurring within the CBH catalytic domain. Where protein fold is altered, the two key physical pathways of water movement on cellulose fibre progression maybe altered. This is discussed in detail on pages 88.

**5) Water molecules move into the cellulose fibre cleft once the CBH catalytic head lifts the fibre to feed the active site.**

As the frequency used is the predominant frequency used in the excitation of water molecules through dipole rotation, the investigation of semi-immobilised water molecules is of significance. In addition to water molecules within the catalytic domain, there is evidence of water molecule action in the cleft produced in the planning of the cellulose fibre from the cellulose bundle. This is described on page 43 and highlighted in the work conducted by Zhong *et. al.* [101].

**6) Localised temperatures are not represented in the bulk temperature.**

All experiments conducted have been isothermal (i.e. thermally static). As the reaction occurred in an aqueous solution, the microwave irradiation will have caused dielectric heating of the water molecules. Due to agitation of the solution, complete mixing of the solution should have ensured even thermal transfer throughout the thermal mass. This is what has been recorded as the thermal bulk temperature. The assumed action is that the water molecules are all in free movement and by complete mixing will all have equal time in free solution, with contact to the thermal well, within the microwave window and in contact with thermal sinks (vessel walls, internal furniture and specifically the thermal coil in the external heat exchanger system). In the case of water molecules that are involved in the enzyme interaction, temporary involvement may cause partial immobilisation with close proximity to the cellulase enzyme, substrate or both. This leads to the possibility that the localised temperature may be greater than the bulk temperature at specific locations.

**7) Swollenin action**

Due to the possible presence of swollenin and expansins in either the cellulase enzyme preparation or the cellulose substrate, the possible action of microwave stimulation of either protein has to be considered. As the structure of the SWO protein has high similarity to CBH, it can be suggested that any enhancement of CBH could also be inferred onto the SWO protein. Where SWO and expansins lack the ability to cleave but have the ability to loosen cellulose fibre bundles, the loosening may allow increase access to the fibres.

Although this action may occur to some extent, there is no evidence of this action. Counter to this hypothesis, the increase in rate observed in the hydrolysis of cellobiose with BGL can only be accounted for through the microwave interaction with the BGL-cellobiose complex due to the lack of SWO or expansins.

The fermentation investigation cannot be concluded through the suggestion of a modified mechanism as there is insufficient data to support a hypothesis. Of greater importance is the observation of maintained cell viability of microwave power that are seen to enhance catalysis. As described in section 2.4. The ethanol biorefinery (page 49), the integration of catalysis and fermentation is a developing trend in bioethanol production. Had the fermentation shown detrimental effects on cell viability, the possibility of integration would prevent process consolidation. This work has pointed towards the opportunity to lift the cellulase rate limiting factor in combined catalysis and fermentation with increasing cellulase mass.

This thesis has investigated the effect of microwave irradiation on both the catalysis and fermentation. In its completion, the work has shown the prototyping of a novel microwave reactor capable of separating the thermal and microwave effects. The experimentation on the biological systems of cellulose enzyme catalysis and *Saccharomyces* spp. fermentation concludes that irradiation with sufficient energy to increase catalytic rate does not compromise ethanol function.

## ***Bibliography***

1. Fairley, P., *Introduction: Next generation biofuels*. Nature, 2011. **474**(7352): p. S2-S5.
2. Balat, M., H. Balat, and C. Oz, *Progress in bioethanol processing*. Progress in Energy and Combustion Science, 2008. **34**.
3. Hammond, G.P., S. Kallu, and M.C. McManus, *Development of Biofuels for the UK automotive market*. Applied Energy, 2008(85): p. 506-515.
4. Liao, W., R. Heijungs, and G. Huppes, *Natural resource demand of global biofuels in the Anthropocene: A review*. Renewable and Sustainable Energy Reviews, 2012. **16**(1): p. 996-1003.
5. Alvira, P., et al., *Pretreatment technologies for an efficient bioethanol production process based on enzymatic hydrolysis: A review*. Bioresour Technol, 2010. **101**(13): p. 4851-61.
6. Godfrey, N., *Lignin variability in plant cell walls: Contribution of new models*. Plant Science, 2011. **181**(4): p. 379-386.
7. Uusitalo, J.M., et al., *Enzyme production by recombinant Trichoderma reesei strains*. Journal of Biotechnology, 1991. **17**(1): p. 35-49.
8. Vlasenko, E.Y., et al., *Enzymatic hydrolysis of pretreated rice straw*. Bioresource Technology, 1997. **59**(2-3): p. 109-119.
9. Frei, P., et al., *Use of mobile phones and risk of brain tumours: update of Danish cohort study*. BMJ, 2011. **343**.
10. Maina, J.Y., et al., *Complex radio frequency (RF) communications with virtual pulses*. Computers & Electrical Engineering, 2008. **34**(5): p. 423-437.
11. Kim, D., et al., *Accelerated esterification of free fatty acid using pulsed microwaves*. Bioresource Technology, 2011. **102**(14): p. 7229-7231.
12. Safaei Mohamadabadi, H., G. Tichkowsky, and A. Kumar, *Development of a multi-criteria assessment model for ranking of renewable and non-renewable transportation fuel vehicles*. Energy, 2009. **34**(1): p. 112-125.
13. Himadri Roy, G., *Biorefineries from the perspective of sustainability: Feedstocks, products, and processes*. Renewable and Sustainable Energy Reviews, 2011. **15**(8): p. 4042-4052.
14. *Biofuels for Transport - An International Perspective*. 2004, International Energy Agency: Paris. p. 1-216.
15. Walter, A., et al., *Perspectives on fuel ethanol consumption and trade*. Biomass and Bioenergy, 2008. **32**(8): p. 730-748.
16. *Energy and Independence and Security Act*. 2007, The Library of Congress: United States of America. p. 311.
17. EPA, *EPA ViewPoint - Renewable Energy*, E.P. Agency, Editor. 2006, Environmental Protection Agency: Johnstown Castle, Co Wexford, Ireland. p. 1-5.
18. DfT, *Carbon and Sustainability Reporting Within the Renewable Transport Fuel Obligation; Requirements and Guidance, Government Recommendation to the Office of the Renewable Fuels Agency*, D.f. Transport, Editor. 2008, Crown: London. p. 242.
19. Tao, L. and A. Aden, *The economics of current and future biofuels*. In Vitro Cellular & Developmental Biology - Plant, 2009. **45**(3): p. 199-217.
20. Mojovic, L., et al., *Production of bioethanol from corn meal hydrolyzates*. Fuel, 2006. **85**(12-13): p. 1750-1755.
21. Nielsen, D.R., et al., *Engineering alternative butanol production platforms in heterologous bacteria*. Met Eng, 2009.
22. Balat, M., H. Balat, and C. Öz, *Progress in bioethanol processing*. Progress in Energy and Combustion Science, 2008. **34**(5): p. 551-573.
23. Sukumaran, R.K., et al., *Cellulase production using biomass feed stock and its application in lignocellulose saccharification for bio-ethanol production*. Renewable Energy, 2009. **34**(2): p. 421-424.

24. RFA, *Changing the Climate - Ethanol Industry Outlook 2008*, in *Ethano Industry Outlook*. 2008, Renewable Fuels Association: Washington D.C., USA. p. 28.
25. Ingram, L.O.N. and T. Buttke, M., *Effects of Alcohols on Micro-Organisms*. Advances in Microbial Physiology, 1985. **25**: p. 253-300.
26. Sánchez, Ó.J. and C.A. Cardona, *Trends in biotechnological production of fuel ethanol from different feedstocks*. Bioresource Technology, 2008. **99**(13): p. 5270-5295.
27. Talebnia, F., D. Karakashev, and I. Angelidaki, *Production of bioethanol from wheat straw: An overview on pretreatment, hydrolysis and fermentation*. Bioresour Technol, 2010. **101**(13): p. 4744-53.
28. *Bloom Energy Server SOFC to power buildings*. Fuel Cells Bulletin, 2010. **2010**(3): p. 1.
29. Hershlag, N., I. Hurley, and J. Woodward, *A simple method to demonstrate the enzymatic production of hydrogen from sugar*. Journal of Chemical Education, 1998. **75**(10): p. 1270-1274.
30. Xu, Q., A. Singh, and M.E. Himmel, *Perspectives and new directions for the production of bioethanol using consolidated bioprocessing of lignocellulose*. Current Opinion in Biotechnology, 2009. **20**(3): p. 364-371.
31. Mathiesen, B.V., H. Lund, and P. Nogaard, *Integrated transport and renewable energy systems*. *Utilities Policy*, 2008(doi:10.1016/j.jup.2007.11.007): p. 1-10.
32. Kim, S. and B.E. Dale, *Global potential bioethanol production from wasted crops and crop residues*. *Biomass and Bioenergy*, 2004. **26**: p. 361-375.
33. Pearce, F., *Chernobyl wastelands to be 'greened' by biofuels*. The New Scientist, 2009. **202**(2714): p. 14-14.
34. Ximenes, E., et al., *Enzyme production by industrially relevant fungi cultured on coproduct from corn dry grind ethanol plants*. Applied Biochemistry and Biotechnology, 2007. **137-140**(1): p. 171-183.
35. Akin, D., *Grass lignocellulose*. Applied Biochemistry and Biotechnology, 2007. **137-140**(1): p. 3-15.
36. Pearce, F., *Biofuels could clean up Chernobyl 'badlands'*, in *New Scientist Magazine*. 2009, Reed Business Information: London.
37. Wee, S.-L., C.-T. Tye, and S. Bhatia, *Membrane separation process--Pervaporation through zeolite membrane*. Separation and Purification Technology, 2008. **63**(3): p. 500-516.
38. Sun, Y. and J. Cheng, *Hydrolysis of lignocellulosic materials for ethanol production: a review*. Bioresource Technology, 2002. **83**(1): p. 1-11.
39. Vásquez, M., et al., *Enzymatic hydrolysis optimization to ethanol production by simultaneous saccharification and fermentation*. Applied Biochemistry and Biotechnology, 2007. **137-140**(1): p. 141-153.
40. Keshwani, D.R., *Microwave pretreatment of switchgrass for bioethanol production in Biological and Agricultural Engineering*. 2009, North Carolina State University: Raleigh. p. 238.
41. Rubin, E.M., *Genomics of cellulosic biofuels*. Nature, 2008. **454**(14): p. 841-845.
42. *Bio battery generates electricity from sugar*. Focus on Catalysts, 2007. **2007**(11): p. 7.
43. Stanbury, P.F., A. Whitaker, and S.J. Hall, *Principles of Fermentation Technology*. 2 ed. 1984, Oxford: Butterworth-Heinmann. 357.
44. Lerouxel, O., et al., *Biosynthesis of plant cell wall polysaccharides - a complex process*. *Current Opinion in Plant Biology*, 2006. **9**: p. 621-630.
45. Sigma-Aldrich. *Enzymes for alternative energy research*. [JPG] 2010 2010 [cited 2010 2010/03/15]; 3D representation of cell wall constituents]. Available from: <http://www.sigmaaldrich.com/life-science/metabolomics/enzyme-explorer/analytical-enzymes/enzymes-for-aer.html>

<http://www.sigmaaldrich.com/etc/medialib/life-science/metabolomics/enzyme-explorer/enzymes-for-alternative/plant-cell-wall.Par.0001.Image.550.gif>

46. LadyofHats, *A section of plant wall in a plant cell*. 2008, en/Wikipedia.org.
47. Toussaint, B., G. Excoffier, and M.R. Vignon, *Effect of steam explosion treatment on the physico-chemical characteristics and enzymic hydrolysis of poplar cell wall components*. *Animal Feed Science and Technology*, 1991. **32**(1-3): p. 235-242.
48. *Cotton Nonwoven technical guide*. 2010 [cited 2010 8thDecember 2010]; Image of crystalline and amorphous cellulose]. Available from: <http://www.cottoninc.com/Cotton-Nonwoven-Technical-Guide/images/ChemicalStructureOfCellulose.gif>.
49. Goyal, A., B. Ghosh, and D. Eveleigh, *Characteristics of fungal cellulases*. *Bioresource Technology*, 1991. **36**(1): p. 37-50.
50. Ramos, L.P., *The chemistry involved in the steam treatment of lignocellulosic materials*. *Química Nova*, 2003. **26**: p. 863-871.
51. El-Mansi, E.M.T. and F.B. Ward, *Microbiology of Industrial Fermentation*, in *Fermentation Microbiology and Biotechnology*, E.M.T. El-Mansi, et al., Editors. 2007, Taylor & Francis Group: Boca Raton, FL. p. 576.
52. Kosaric, N. and F. Vardar-Sukan, *Potential Source of Energy and Chemical Products*, in *The Biotechnology of Ethanol*, M. Roehr, Editor. 2001, WILEY-VCH: Weinheim.
53. Lynd, L.R., et al., *Consolidated bioprocessing of cellulosic biomass: an update*. *Curr Opin Biotechnol*, 2005. **16**(5): p. 577-83.
54. Lynd, L.R., et al., *Consolidated bioprocessing of cellulosic biomass: an update*. *Current Opinion in Biotechnology*, 2005. **16**(5): p. 577-583.
55. Li, T.-H. and T.-L. Chen, *Enhancement of glucose oxidase fermentation by addition of hydrocarbons*. *Journal of Fermentation and Bioengineering*, 1994. **78**(4): p. 298-303.
56. Alriksson, B., et al., *Cellulase production from spent lignocellulose hydrolysates by recombinant *Aspergillus niger**. *Applied and Environmental Microbiology*, 2009. **75**(8): p. 2366-2374.
57. Huang, H.-J., et al., *A review of separation technologies in current and future biorefineries*. *Separation and Purification Technology*, 2007. **62**: p. 1-21.
58. Chandel, A.K., et al., *Detoxification of sugarcane bagasse hydrolysate improves ethanol production by *Candida shehatae* NCIM 3501*. *Bioresource Technology*, 2007. **98**(10): p. 1947-1950.
59. Ximenes, E., et al., *Inhibition of cellulases by phenols*. *Enzyme and Microbial Technology*, 2010. **46**(3-4): p. 170-176.
60. Bansal, P., et al., *Modeling cellulase kinetics on lignocellulosic substrates*. *Biotechnology Advances*. **27**(6): p. 833-848.
61. Scragg, A., *Environmental Biotechnology*. 2nd ed. 2005, Oxford: Oxford University Press. 447.
62. Goodenough, P.W., *Structural studies on cellulases, pectinases and xylanases*, in *Progress in Biotechnology*, J.F.R. Kwan-Hwa Park and C. Yang-Do, Editors. 1996, Elsevier. p. 83-107.
63. Kosaric, N. and F. Vardar-Sukan, *Substrates for industrial alcohol production*, in *The Biotechnology of Ethanol*, M. Roehr, Editor. 2001, WILEY-VCH: Weinheim.
64. Pointing, S.B., *Exploiting the versatile ligninolytic systems of white-rot fungi*, in *Bio-exploration of filamentous fungi*, S. Pointing and K. Hyde, B., Editors. 2001, Fungal Diversity Press: Hong Kong. p. 253-290.
65. Zaparty, M., et al., *"Hot standards" for the thermoacidophilic archaeon *Sulfolobus solfataricus**. *Extremophiles*, 2010. **14**(1): p. 119-142.
66. Verhees, C.H., et al., *The unique features of glycolytic pathways in Archaea*. *Biochem. J.*, 2003. **375**(2): p. 231-246.
67. Ward, G., Y. Hadar, and C.G. Dosoretz, *The Biodegradation of Lignocellulosic by White Rot Fungi*, in *Fungal Biotechnology in Agricultural, Food and Environmental Applications*, D.K. Arora, Editor. 2004, Marcel Dekker Inc.: New York. p. 393-407.
68. Sampedro, J. and D.J. Cosgrove, *The expansin superfamily*. Vol. 6. 2005. 242.

69. McQueen-Mason, S., D.M. Durachko, and D.J. Cosgrove, *Two Endogenous Proteins That Induce Cell Wall Extension in Plants*. The Plant Cell Online, 1992. **4**(11): p. 1425-1433.
70. Saloheimo, M., et al., *Swollenin, a Trichoderma reesei protein with sequence similarity to the plant expansins, exhibits disruption activity on cellulosic materials*. European Journal of Biochemistry, 2002. **269**(17): p. 4202-4211.
71. Sticklen, M.B., *Plant genetic engineering for biofuel production: towards affordable cellulosic ethanol*. Nat Rev Genet, 2008. **9**(6): p. 433-443.
72. Cosgrove, D.J., P. Bedinger, and D.M. Durachko, *Group I allergens of grass pollen as cell wall-loosening agents*. Proceedings of the National Academy of Science, 1997. **94**: p. 6559-6564.
73. O'Sullivan, *Cellulose: Structures slowly unravels*. Cellulose, 1997. **4**: p. 173-207.
74. Niamke, J.N. and N.S. Wang, *Cellulose Degradation by Fungi*, in *Fungal Biotechnology in Agricultural, Food and Environmental Biotechnology*, D.K. Arora, Editor. 2004, Marcel Dekker, Inc: New York. p. 363-373.
75. Penttila, M., et al., *Homology between cellulase genes of Trichoderma reesei: complete nucleotide sequence of the endoglucanase I gene*. Gene, 1986. **45**: p. 253-263.
76. Malherbe, S. and T.E. Cloete, *Lignocellulose biodegradation: fundamentals and applications*. Reviews in Environmental Science & Biotechnology 2002. **1**: p. 105-114.
77. Sternberg, D. and G.R. Mandels, *Induction of cellulolytic enzymes in Trichoderma reesei by sophorose*. J. Bacteriol., 1979. **139**(3): p. 761-769.
78. Shoemaker, S., et al., *Molecular cloning of exo-cellobiohydrolase derived from Trichoderma reesei strain L27*. Biotechnology, 1983. **1**: p. 691-696.
79. Teeri, T., et al., *Homologous domains in Trichoderma reesei cellulolytic enzymes: gene sequences and expression of cellobiohydrolase II*. Gene, 1987. **51**: p. 43-52.
80. Penttila, M., et al., *A versatile transformation system for cellulolytic filamentous fungus Trichoderma reesei*. Gene, 1987. **61**(155-164).
81. Saloheimo, M., et al., *Characterisation of secretory genes ypt1/yptA and nsf1/nsfA from two filamentous fungi: induction of secretory pathway genes of Trichoderma reesei under secretion stress conditions*. Applied and Environmental Microbiology, 2004. **70**: p. 459-467.
82. Ward, H., et al., *Cloning, sequencing and preliminary structural analysis of a small high pI endoglucanase (EGIII) from Trichoderma reesei* in Proceedings of the Second Tricel Symposium on Trichoderma cellulase and other hydrolases., P. Suominen and T. Reinikainen, Editors. 1993, Foundation for Biotechnology and Industrial Fermentation Research: Espoo, Helsinki, Finland.
83. Okada, H., et al., *Molecular characterization and heterologous expression of the gene encoding a low-molecular-mass endoglucanase from Trichoderma reesei QM9414*. Applied and Environmental Microbiology, 1998. **64**: p. 555-563.
84. Saloheimo, M., et al., *cDNA cloning of a Trichoderma reesei cellulase and demonstration of endoglucanase activity by expression in yeast*. European Journal of Biochemistry, 1997. **249**: p. 584-591.
85. Saloheimo, A., et al., *A novel, small endoglucanase gene, egl5, from Trichoderma reesei isolated by expression in yeast*. Molecular Microbiology, 1994. **13**: p. 219-228.
86. Barnett, C., R. Berka, and T. Fowler, *Cloning and amplification of the gene encoding an extracellular beta-glucosidase from Trichoderma reesei: evidence for improved rates of saccharification of cellulosic substrates*. Bio/Technology, 1991. **9**: p. 562-567.
87. Mach, R.L. and S. Zeilinge, *Genetic transformation of Trichoderma and Gliocladium in Trichoderma & Gliocladium, Basic biology, taxonomy and genetics.*, C. Kubicek and G. Harman, Editors. 1998. p. 225-242.
88. Martinez, D., et al., *Genome sequencing and analysis of the biomass-degrading fungus Trichoderma reesei (syn. Hypocrea jecorina)*. Nature Biotechnology, 2008. **26**(5): p. 553-560.

89. Miettinen-Oinonen, A., *Trichoderma reesei* strains for production of cellulases for the textile industry, in *Department of Biological and Environmental Sciences*. 2004, University of Helsinki: Helsinki. p. 96.
90. Miettinen-Oinonen, A. and P. Suominen, *Enhanced production of Trichoderma reesei Endoglucanase and Use of New Cellulase Preparations in Producing the Stonewashed Effect on Denim Fabric*. *Applied and Environmental Microbiology*, 2002. **68**(8): p. 3956-3964.
91. Sandgren, M., et al., *The X-ray crystal structure of the Trichoderma reesei family 12 Endoglucanase 3, CEL12A, at 1.9Å resolution*. *Journal of Molecular Biology*, 2001. **308**(295).
92. Hahn-Hägerdal, B. and M.F. Gorwa-Grauslund, *Biotechnology applied in the traditional process industry*, in *Science Forum at ILMAC 2007; Energy and Raw Materials - The Contributions of Chemistry and Biochemistry in the Future*. 2007: Basel, Switzerland.
93. Miettinen-Oinonen, A., et al., *Enhanced production of cellobiohydrolases in Trichoderma reesei and biofinishing of cotton fabrics with the new preparations*. *Journal of Biotechnology*, 2005. **116**(3): p. 305-317.
94. Stahlberg, J., G. Johansson, and G. Pettersson, *A New Model For Enzymatic Hydrolysis of Cellulose Based on the Two-Domain Structure of Cellobiohydrolase I*. *Nat Biotech*, 1991. **9**(3): p. 286-290.
95. Jervis, E.J., C.A. Haynes, and D.G. Kilburn, *Surface diffusion of cellulases and their isolated binding domains on cellulose*. *Journal of Biological Chemistry*, 1997. **272**: p. 24016-24023.
96. Divne, C., et al., *High-resolution crystal structures reveal how a cellulose chain is bound in the 50 Å long tunnel of cellobiohydrolase I from Trichoderma reesei*. *Journal of Molecular Biology*, 1998. **275**(2): p. 309-325.
97. Mulakala, C. and P.J. Reilly, *Hypocrea jecorina (Trichoderma reesei) Cel7A as a molecular machine: A docking study*. *Proteins: Structure, Function, and Bioinformatics*, 2005. **60**(4): p. 598-605.
98. Beckham, G.T., et al., *Applications of computational science for understanding enzymatic deconstruction of cellulose*. *Current Opinion in Biotechnology*, 2011. **22**(2): p. 231-238.
99. Nimlos, M.R., et al., *Molecular modeling suggests induced fit of Family I carbohydrate-binding modules with a broken-chain cellulose surface*. *Protein Engineering, Design and Selection*, 2007. **20**(4): p. 179-187.
100. Arantes, V. and J. Saddler, *Access to cellulose limits the efficiency of enzymatic hydrolysis: the role of amorphogenesis*. *Biotechnology for Biofuels*, 2010. **3**(1): p. 4.
101. Zhong, L., et al., *Computational simulations of the Trichoderma reesei cellobiohydrolase I acting on microcrystalline cellulose I[beta]: the enzyme-substrate complex*. *Carbohydrate Research*, 2009. **344**(15): p. 1984-1992.
102. Våljamäe, P., et al., *Synergistic cellulose hydrolysis can be described in terms of fractal-like kinetics*. *Biotechnology and Bioengineering*, 2003. **84**(2): p. 254-257.
103. Gusakov, A.V., et al., *A product inhibition study of cellulases from Trichoderma longibrachiatum using dyed cellulose*. *Journal of Biotechnology*, 1985. **3**(3): p. 167-174.
104. Liu, D., et al., *Starch composites reinforced by bamboo cellulosic crystals*. *Bioresour Technol*, 2010. **101**(7): p. 2529-36.
105. Zhao, X., et al., *Molecular simulation evidence for processive motion of Trichoderma reesei Cel7A during cellulose depolymerization*. *Chemical Physics Letters*, 2008. **460**(1-3): p. 284-288.
106. Stahlberg, J., et al., *Engineering of a glycosidase family 7 cellobiohydrolase to more alkaline pH optimum: The pH behaviour of Trichoderma reesei CEL7A and its E223S / A224H / L225V / T226A / D262G mutant*. *Journal of Biological Chemistry*, 2001. **356**(19).
107. Hong, J., et al., *Bioseparation of recombinant cellulose-binding module-proteins by affinity adsorption on an ultra-high-capacity cellulosic adsorbent*. *Anal Chim Acta*, 2008. **621**(2): p. 193-9.

108. Våljamäe, P., et al., *The initial kinetics of hydrolysis by cellobiohydrolases I and II is consistent with a cellulose surface - Erosion model*. European Journal of Biochemistry, 1998. **253**(2): p. 469-475.
109. Xu, F. and H. Ding, *A new kinetic model for heterogeneous (or spatially confined) enzymatic catalysis: Contributions from the fractal and jamming (overcrowding) effects*. Applied Catalysis A: General, 2007. **317**(1): p. 70-81.
110. Ma, A., et al., *The enzymatic hydrolysis rate of cellulose decreases with irreversible adsorption of cellobiohydrolase I*. Enzyme and Microbial Technology, 2008. **42**(7): p. 543-547.
111. Jalak, J. and P. Våljamäe, *Mechanism of initial rapid rate retardation in cellobiohydrolase catalyzed cellulose hydrolysis*. Biotechnology and Bioengineering, 2010. **106**(6): p. 871-883.
112. Nidetzky, B. and W. Steiner, *A new approach for modeling cellulase-cellulose adsorption and the kinetics of the enzymatic hydrolysis of microcrystalline cellulose*. Biotechnology and Bioengineering, 1993. **42**(4): p. 469-479.
113. Sinitsyn, A.P., et al., *Decrease in reactivity and change of physico-chemical parameters of cellulose in the course of enzymatic hydrolysis*. Carbohydrate Polymers, 1989. **10**(1): p. 1-14.
114. Puls, J. and T.M. Wood, *The degradation pattern of cellulose by extracellular cellulases of aerobic and anaerobic microorganisms*. Bioresource Technology, 1991. **36**(1): p. 15-19.
115. Ye, X., et al., *Spontaneous high-yield production of hydrogen from cellulosic materials and water catalyzed by enzyme cocktails*. ChemSusChem, 2009. **2**(2): p. 149-52.
116. Lenz, J., et al., *Changes of structure and morphology of regenerated cellulose caused by acid and enzymatic hydrolysis*. Journal of Applied Polymer Science, 1990. **41**(5-6): p. 1315-1326.
117. Ye, Z. and R.E. Berson, *Kinetic modeling of cellulose hydrolysis with first order inactivation of adsorbed cellulase*. Bioresource Technology, 2011. **102**(24): p. 11194-11199.
118. Kumarappan, S., *Biomass Supply Chains for Biofuel Production - Contracting Issues*, in *BIO World Congress*. 2009: Montreal, Canada.
119. Johnson, M.B., *Microalgal Biodiesel Production through a Novel Attached Culture System and Conversion Parameters*, in *Faculty of Virginia Polytechnic Institute and State University*. 2009, Virginia Polytechnic Institute and State University: Blacksburg.
120. NNFC, *The Biorefinery Opportunity - A North East England view 2007*, National Non-food Crops Centre.
121. Smith, W., *Mapping the development of UK biorefinery complexes*. 2007, National Non Food Crops Centre.
122. Holt, P., et al., *A bioconversion platform for biorefineries based on non-conventional yeasts in 5th Danish Conference on biotechnology and Molecular Biology - Biofuels and Biorefineries*. 2010, Danish Biotechnology Society: Hotel Munkenbjerg, Vejle, Denmark.
123. Harvey W, B., *Bioprocessing for biofuels*. Current Opinion in Biotechnology, 2011(0).
124. Cardona Alzate, C.A. and O.J. Sánchez Toro, *Energy consumption analysis of integrated flowsheets for production of fuel ethanol from lignocellulosic biomass*. Energy, 2006. **31**(13): p. 2447-2459.
125. Cardona, C.A. and Ó.J. Sánchez, *Fuel ethanol production: Process design trends and integration opportunities*. Bioresource Technology, 2007. **98**(12): p. 2415-2457.
126. Balusu, R., et al., *Production of ethanol from cellulosic biomass by Clostridium thermocellum SS19 in submerged fermentation: screening of nutrients using Plackett-Burman design*. Appl Biochem Biotechnol, 2004. **117**(3): p. 133-41.
127. Balusu, R., et al., *Optimization of critical medium components using response surface methodology for ethanol production from cellulosic biomass by Clostridium thermocellum SS19*. Process Biochemistry, 2005. **40**(9): p. 3025-3030.
128. Mabee, W.E. and J.N. Saddler, *Bioethanol from lignocellulosics: Status and perspectives in Canada*. Bioresour Technol, 2010. **101**(13): p. 4806-13.

129. Lawford, H.G. and J.D. Rousseau, *Cellulosic fuel ethanol: alternative fermentation process designs with wild-type and recombinant Zymomonas mobilis*. Appl Biochem Biotechnol, 2003. **105-108**: p. 457-69.
130. Ohgren, K., et al., *Simultaneous saccharification and co-fermentation of glucose and xylose in steam-pretreated corn stover at high fiber content with Saccharomyces cerevisiae TMB3400*. Journal of Biotechnology, 2006. **126**: p. 488-498.
131. Sonderegger, M., et al., *Fermentation performance of engineered and evolved xylose-fermenting Saccharomyces cerevisiae strains*. Biotechnology and Bioengineering, 2004. **87**(1): p. 90-98.
132. Wang, Y., et al., *Establishment of a xylose metabolic pathway in an industrial strain of Saccharomyces cerevisiae*. Biotechnology Letters, 2004. **26**: p. 885-890.
133. Sakamoto, T., et al., *Direct ethanol production from hemicellulosic materials of rice straw by use of an engineered yeast strain codisplaying three types of hemicellulolytic enzymes on the surface of xylose-utilizing Saccharomyces cerevisiae cells*. Journal of Biotechnology, 2011(0).
134. Yanase, S., et al., *Ethanol production from cellulosic materials using cellulase-expressing yeast*. Biotechnol J, 2010.
135. Lewandowicz, G., et al., *Application of membrane distillation for ethanol recovery during fuel ethanol production*. Journal of Membrane Science, 2011. **375**(1-2): p. 212-219.
136. Chen, H. and W. Qiu, *Key technologies for bioethanol production from lignocellulose*. Biotechnology Advances, 2010. **28**(5): p. 556-562.
137. Dias, M.O.S., et al., *Optimization of Bioethanol Distillation Process – Evaluation of Different Configurations of the Fermentation Process*, in *Computer Aided Chemical Engineering*, C.A.O.d.N. Rita Maria de Brito Alves and B. Evaristo Chalbaud, Editors. 2009, Elsevier. p. 1893-1898.
138. Rose, A.H., ed. *Secondary product of Metabolism*. 1 ed. *Economic Microbiology* ed. A.H. Rose. Vol. 3. 1979, Academic Press Inc. (London) LTD: London. 595.
139. Piskur, J., et al., *How did Saccharomyces evolve to become a good brewer? Trends in genetics*, 2006. **22**(4): p. 183-186.
140. Nguyen, H.-V. and C. Gaillardin, *Evolutionary relationships between the former species Saccharomyces uvarum and the hybrids Saccharomyces bayanus and Saccharomyces pastorianus; reinstatement of Saccharomyces uvarum (Beijerinck) as a distinct species*. FEMS Yeast Research, 2005. **5**(4-5): p. 471-483.
141. Masneuf-Pomarède, I., et al., *Reassessment of phenotypic traits for Saccharomyces bayanus var. uvarum wine yeast strains*. International Journal of Food Microbiology, 2010. **139**(1-2): p. 79-86.
142. Kreger-van, R., *The Yeast, a taxonomic study*. 3rd edn ed. 1984, Amsterdam: Elsevier Science Publishing.
143. Vaughan-Martini, A. and C.P. Kurtzman, *Deoxyribonucleic relatedness among species of the genus Saccharomyces sensu stricto*. International Journal of Systematic Bacteriology, 1985. **35**: p. 508-511.
144. Vaughan-Martini, A. and A. Martini, *The newly delimited species of Saccharomyces sensu stricto*. Antonie van Leeuwenhoek, 1987. **53**: p. 77-84.
145. Varnam, A.H., *The exploitation of microorganisms in the manufacture of alcoholic beverages*, in *Exploitation of Microorganisms*, D.G. Jones, Editor. 1993, University Press: Cambridge. p. 297-320.
146. Lever, M., G. Ho, and R. Cord-Ruwisch, *Ethanol from lignocellulose using crude unprocessed cellulase from solid-state fermentation*. Bioresource Technology, 2010. **101**(18): p. 7083-7087.
147. Dickinson, J.R., *Carbon Metabolism*, in *The metabolism and molecular physiology of Saccharomyces cerevisiae*, J.R. Dickinson and M. Schweizer, Editors. 1999, Taylor & Francis Ltd: London. p. 343.

148. Liu, S. and N. Qureshi, *How microbes tolerate ethanol and butanol*. New Biotechnology, 2009. **26**(3): p. 117-121.
149. D'amore, T., et al., *A Study of Ethanol Tolerance in Yeast*. Critical Reviews in Biotechnology, 1989. **9**(4): p. 287-304.
150. Szczodrak, J. and J. Fiedurek, *Technology for conversion of lignocellulosic biomass to ethanol*. Biomass and Bioenergy, 1996. **10**(5-6): p. 367-375.
151. Rosenberg, S.L., *Fermentation of pentose sugars to ethanol and other neutral products by microorganisms*. Enzyme and microbial technology, 1980. **2**: p. 185-194.
152. [www.HCRS.at](http://www.HCRS.at), *Magnetron with magnet in its mounting box - the horizontal plates aid in cooling the device by airflow from a fan*. 2005, <http://en.wikipedia.org/wiki/File:Magnetron1.jpg>.
153. Patrick, F., *Introduction to Microwaves and RF*, in *RF and Microwave Applications and Systems*. 2007, CRC Press. p. 1-1-1-12.
154. Meredith, R.J. and E. Institution of Electrical, *Engineers' handbook of industrial microwave heating*. 1998, London: Institution of Electrical Engineers.
155. Coleman, D.D. and D.A. Westcott, *CWNA certified wireless network administrator study guide*. 2009, Indianapolis, Ind.: Wiley.
156. Wikipedia.org. *ISM band*. [Webpage] 2011 18 November 2011 at 19:34 [cited 2011 24-11-2011]; [Webpage data table]. Available from: [http://en.wikipedia.org/wiki/ISM\\_band](http://en.wikipedia.org/wiki/ISM_band).
157. buzzard33, *Prevent Microwave Leakage From Your Microwave Oven*. 2008, [http://www.infobarrel.com/Media/Diagram\\_1](http://www.infobarrel.com/Media/Diagram_1). p. Prevent Microwave Leakage From Your Microwave Oven - use of image.
158. Swicord, M. and Q. Balzano, *Has Electromagnetic Energy in the Band 0.1-100 GHz Useful Medical Applications? A Review of Mechanisms and Biological Database Offers Dim Prospects*. Plasma Science, IEEE Transactions on, 2008. **36**(4): p. 1638-1649.
159. Riby, P., A. Stavrinides, Editor. 2011, None published communication: Liverpool.
160. Phipps, D.A., *SEM power/temp curves*, A. Stavrinides, Editor. 2011: Liverpool. p. 1.
161. Dressen, M.L.H.C.A., *Microwave heating in fine chemical applications; role of heterogeneity*. 2009, Technical University of Eindhoven: Eindhoven. p. 146.
162. Emerson, D.T., *The work of Jagadis Chandra Bose: 100 years of millimeter-wave research*. Microwave Theory and Techniques, IEEE Transactions on, 1997. **45**(12): p. 2267-2273.
163. Ingram, M. and L.J. Page, *The survival of microbe in modulated high-frequency voltage fields*. Journal of Applied Microbiology, 1953. **16**(1): p. 69-87.
164. Chipley, J.R., *Effects of Microwave Irradiation on Microorganisms*, in *Advances in Applied Microbiology*, D. Perlman, Editor. 1980, Academic Press. p. 129-145.
165. McLaughlin, J.T., *Tissue destruction and death from microwave radiation (radar)*. California medicine, 1957. **86**(5): p. 336-9.
166. Laurence, J.A., et al., *Biological Effects of Electromagnetic Fields—Mechanisms for the Effects of Pulsed Microwave Radiation on Protein Conformation*. Journal of Theoretical Biology, 2000. **206**(2): p. 291-298.
167. Abu-Samra, A., J.S. Morris, and S.R. Koirtyohann, *Wet ashing of some biological samples in a microwave oven*. Analytical Chemistry, 1975. **47**(8): p. 1475-1477.
168. Izquierdo, F.J., et al., *Effects of combined microwave and enzymatic treatments on the hydrolysis and immunoreactivity of dairy whey proteins*. International Dairy Journal, 2008. **18**(9): p. 918-922.
169. Mess-Elektronik, S., *Schwarzbeck BBHA 9120 D*. 2007, [http://en.wikipedia.org/wiki/File:Schwarzbeck\\_BBHA\\_9120\\_D.jpg](http://en.wikipedia.org/wiki/File:Schwarzbeck_BBHA_9120_D.jpg).
170. Richter, R.C., D. Link, and H.M.S. Kingston, *Peer Reviewed: Microwave-Enhanced Chemistry*. Analytical Chemistry, 2001. **73**(1): p. 30 A-37 A.

171. [www.Wotol.com](http://www.Wotol.com),  
[http://www.wotol.com/images/thumbs/800x800/216022\\_3c7e2601582a5fc96bf87dcaf07d94ad.jpg](http://www.wotol.com/images/thumbs/800x800/216022_3c7e2601582a5fc96bf87dcaf07d94ad.jpg). 2011.
172. [www.Sairem.com.au](http://www.Sairem.com.au). 2011.
173. Polshettiwar, V. and R.S. Varma, *Chapter 1 Fundamentals of Aqueous Microwave Chemistry*, in *Aqueous Microwave Assisted Chemistry: Synthesis and Catalysis*. 2010, The Royal Society of Chemistry. p. 1-9.
174. Zhao, H., *Microwave-assisted Enzymatic Reaction in Aqueous Media*, in *Aqueous Microwave Assisted Chemistry: Synthesis and Catalysis*, Vivek Polshettiwar and R.S. Varma, Editors. 2010, Royal Society of Chemistry Publishing: Cambridge.
175. WHO, *EMF research databases*. 2011, World Health Organisation.
176. Giombini, A., et al., *Hyperthermia induced by microwave diathermy in the management of muscle and tendon injuries*. *British Medical Bulletin*, 2007. **83**(1): p. 379-396.
177. Moulder, J., et al., *Mobile phones, mobile phone base stations and cancer: a review*. *International Journal of Radiation Biology*, 2005. **81**(3): p. 189-203.
178. Belkhode, M.L., A.M. Muc, and D.L. Johnson, *Thermal and athermal effects of 2.8 GHz microwaves on three human serum enzymes*. *Journal of Microwave Power*, 1974. **9**(1): p. 23-29.
179. Ward, T.R., J.W. Allis, and J.A. Elder, *Measure of Enzymatic Activity Coincident with 2450 MHz Microwave Exposure*. *Journal of Microwave Power*, 1975. **10**(3): p. 315-320.
180. Henderson, H.M., K. Hergenroeder, and S.S. Stuchly, *Effect of 2450 MHz Microwave Radiation on Horseradish Peroxidase*. *Journal of Microwave Power*, 1975. **10**(1): p. 27-35.
181. Olcerst, R. and J. Rabinowitz, *Studies on the interaction of microwave radiation with cholinesterase*. *Radiation and Environmental Biophysics*, 1978. **15**(3): p. 289-295.
182. Bini, M., et al., *Analysis of the Effects of Microwave Energy on Enzymatic Activity of Lactate Dehydrogenase (LDH)* *Journal of Microwave Power*, 1978. **13**(1): p. 95-100.
183. Tuengler, P., F. Keilmann, and L. Genzel, *Search for millimeter microwave effects on enzyme or protein function*. *Z. Naturforsch C.*, 1979. **34**(1): p. 60-63.
184. Galvin, M.J., D.I. McRee, and M. Lieberman, *Effects of 2.45GHz microwave radiation on embryonic quail hearts*. *Bioelectromagnetics*, 1980. **1**(4): p. 389-396.
185. Galvin, M.J., D.L. Parks, and D.I. McRee, *Influence of 2.45 GHz microwave radiation on enzyme activity*. *Radiation and Environmental Biophysics*, 1981. **19**(2): p. 149-156.
186. Millar, D.B., et al., *The effect of exposure of acetylcholinesterase to 2,450-MHz microwave radiation*. *Bioelectromagnetics*, 1984. **5**(2): p. 165-172.
187. Kabza, K.G., et al., *Effect of Microwave Radiation on Copper(II) 2,2'-Bipyridyl-Mediated Hydrolysis of Bis(p-nitrophenyl) Phosphodiester and Enzymatic Hydrolysis of Carbohydrates*. *The Journal of Organic Chemistry*, 1996. **61**(26): p. 9599-9602.
188. La Cara, F., et al., *Different effects of microwave energy and conventional heat on the activity of a thermophilic  $\beta$ -galactosidase from Bacillus acidocaldarius*. *Bioelectromagnetics*, 1999. **20**(3): p. 172-176.
189. Zhu, S., et al., *The effect of microwave irradiation on enzymatic hydrolysis of rice straw*. *Bioresource Technology*, 2006. **97**(15): p. 1964-1968.
190. Porcelli, M., et al., *Non-thermal effects of microwaves on proteins: thermophilic enzymes as model system*. *FEBS Letters*, 1997. **402**(2-3): p. 102-106.
191. Gelo-Pujic, M., E. Guibe-Jampel, and A. Loupy, *Enzymatic Glycosidations in Dry Media on Mineral Supports*. *Tetrahedron*, 1997. **53**(51): p. 17247-17252.
192. La Cara, F., et al., *Microwave exposure on a thermophilic alcohol dehydrogenase*. *Protein and Peptide Letters*, 1999. **6**(1): p. 155-162.
193. Bradoo, S., et al., *Microwave-assisted rapid characterization of lipase selectivities*. *Journal of Biochemical and Biophysical Methods*, 2002. **51**(2): p. 115-120.

194. Daniells, C., et al., *Transgenic nematodes as biomonitors of microwave-induced stress*. Mutation Research/Fundamental and Molecular Mechanisms of Mutagenesis, 1998. **399**(1): p. 55-64.
195. Zhang, Y.-H., P. and L.R. Lynd, *Toward an aggregated understanding of enzymatic hydrolysis of cellulose: noncomplexed cellulase systems*. *Biotechnology and Bioengineering*, 2004. **88**: p. 797-824.
196. Hari Krishna, S., et al., *Simultaneous saccharification and fermentation of pretreated sugar cane leaves to ethanol*. *Process Biochemistry*, 1998. **33**(8): p. 825-830.
197. Day, D.F., *Improved biorefinery for the production of ethanol, chemicals, animal feed and biomaterials from sugar cane*. 2009, Louisiana State University Agricultural Center.
198. Davidovitz, M., *A low-loss thermal isolator for waveguides and coaxial transmission lines*. *Microwave and Guided Wave Letters, IEEE*, 1996. **6**(1): p. 25-27.